

See discussions, stats, and author profiles for this publication at: <https://www.researchgate.net/publication/42542946>

Low Levels of Mutant Ubiquitin Are Degraded by the Proteasome In Vivo

ARTICLE *in* JOURNAL OF NEUROSCIENCE RESEARCH · AUGUST 2010

Impact Factor: 2.59 · DOI: 10.1002/jnr.22396 · Source: PubMed

CITATIONS

11

READS

53

5 AUTHORS, INCLUDING:



Fred W Van Leeuwen

Maastricht University

185 PUBLICATIONS 6,814 CITATIONS

SEE PROFILE

Description Thesis
File ID 115743
Filename thesis.pdf

SOURCE, OR PART OF THE FOLLOWING SOURCE:

Type Dissertation
Title The effect of mutant ubiquitin on proteasome function in relation to neurodegenerative disease
Author P. van Tijn
Faculty Faculty of Medicine
Year 2008
Pages 224

FULL BIBLIOGRAPHIC DETAILS:

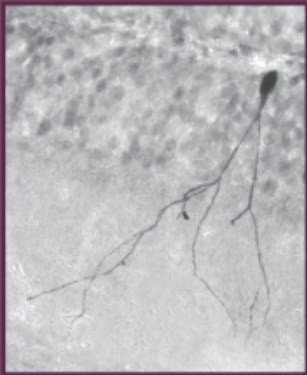
<http://dare.uva.nl/record/283599>

Copyrights

It is not permitted to download or to forward/distribute the text or part of it without the consent of the copyright holder (usually the author), other than for strictly personal, individual use.

The effect of mutant ubiquitin on proteasome function

in relation to
neurodegenerative disease



Paula van Tijn

THE EFFECT OF MUTANT UBIQUITIN ON PROTEASOME FUNCTION
IN RELATION TO NEURODEGENERATIVE DISEASE

THE EFFECT OF MUTANT UBIQUITIN ON PROTEASOME FUNCTION
IN RELATION TO NEURODEGENERATIVE DISEASE

ACADEMISCH PROEFSCHRIFT
ter verkrijging van de graad van doctor
aan de Universiteit van Amsterdam
op gezag van de Rector Magnificus
prof. dr. D.C. van den Boom
ten overstaan van een door het college
voor promoties ingestelde commissie,
in het openbaar te verdedigen
in de Agnietenkapel
op vrijdag 7 november 2008, te 12.00 uur
door

Paula van Tijn

geboren te Amsterdam

PROMOTIE COMMISSIE

Promotor: Prof. dr. D.F. Swaab

Co-promotores: Dr. D.F. Fischer

Dr. F.W. van Leeuwen

Overige leden: Prof. dr. M. Joëls

Prof. dr. M.S. Oitzl

Prof. dr. F. Baas

Prof. dr. J.P.H. Burbach

Dr. D. Jongejan-Zivkovic

Dr. N.P. Dantuma

Faculteit der Geneeskunde

The research in this thesis was conducted at the Netherlands Institute for Neuroscience, Amsterdam and was financially supported by the Internationale Stichting Alzheimer Onderzoek and Hersenstichting Nederland.

Publication of this thesis was financially supported by:

Netherlands Institute for Neuroscience

Van Leersumfonds KNAW

Stichting het Remmert Adriaan Laan Fonds

J.E. Jurriaanse Stichting

Internationale Stichting Alzheimer Onderzoek

Alzheimer Nederland

Cover illustration: UBB⁺¹ expressing neuron in the hippocampus of a UBB⁺¹ transgenic mouse

Print: Gildeprint BV, Enschede

Contents

CHAPTER I	General Introduction	7
	Scope and Outline	41
CHAPTER II	Dose-dependent inhibition of proteasome activity by a mutant ubiquitin associated with neurodegenerative disease	45
CHAPTER III	Long-term proteasome dysfunction in the mouse brain by expression of aberrant ubiquitin	65
CHAPTER IV	Low levels of mutant ubiquitin are degraded by the proteasome <i>in vivo</i>	103
CHAPTER V	Alzheimer-associated mutant ubiquitin impairs spatial reference memory	123
CHAPTER VI	Mutant ubiquitin decreases amyloid- β deposition in a transgenic mouse model of Alzheimer's disease	139
CHAPTER VII	General Discussion	155
	References	183
	Color Figures	207
	Summary	216
	Samenvatting	219
	List of Publications	222
	Dankwoord	223
	Curriculum Vitae	224

CHAPTER I

General Introduction

The neuronal ubiquitin-proteasome system:
murine models and their neurological phenotype

Progress in Neurobiology, 2008; 85(2): 176-193

Paula van Tijn, Elly M. Hol, Fred W. van Leeuwen, David F. Fischer

Contents

Introduction

The ubiquitin-proteasome pathway

- Substrate targeting by ubiquitin
- Proteasomal degradation
- UPS-related processes
- Deubiquitination

The UPS in the nervous system

The UPS in neuronal development and plasticity

UPS in neurodegenerative diseases

- Alzheimer's disease and other tauopathies
- Parkinson's disease
- Huntington's disease and other polyglutamine diseases
- Mutant ubiquitin (UBB^{+1})

Mouse models of the UPS

Mouse models of neurodegenerative disease induced by an altered UPS

Parkinson's disease mouse models

- Parkin KO mice
- UCH-Lx mutant mice
- Usp14 KO mice (ataxia mice)
- Ataxin-3 transgenic mice
- Ube3a transgenic mice
- Other UPS defective models for neurodegeneration
 - Prion disease and mahoganyd mutant mice
 - CHIP KO mice
 - Lmp2 KO mice
 - Atg KO mice

Mouse models to measure UPS activity *in vivo*

Concluding remarks

Abstract

The ubiquitin-proteasome system (UPS) is the main intracellular pathway for regulated protein turnover. This system is of vital importance for maintaining cellular homeostasis and is essential for neuronal functioning. It is therefore not surprising that impairment of this system is implicated in the pathogenesis of a variety of diseases, including neurological disorders, which are pathologically characterized by the presence of ubiquitin-positive protein aggregates. A direct correlation between intact neuronal functioning and the UPS is exemplified by a range of transgenic mouse models wherein mutations in components of the UPS lead to a neurodegenerative or neurological phenotype. These models have been proven useful in determining the role of the UPS in the nervous system in health and disease. Furthermore, recently developed *in vivo* models harbouring reporter systems to measure UPS activity could also substantially contribute to understanding the effect of neurodegeneration on UPS function. The role of the UPS in neurodegeneration *in vivo* is reviewed by discussing the currently available murine models showing a neurological phenotype induced by genetic manipulation of the UPS.

Introduction

Protein turnover plays an important role in the maintenance of cellular homeostasis and is involved in a diverse array of processes, ranging from endocytosis to signal transduction (Welchman *et al.*, 2005; Mukhopadhyay and Riezman, 2007). Protein quality control, through degradation of aberrant or misfolded proteins, also contributes to a healthy intracellular environment (Hershko and Ciechanover, 1998). Degradation of proteins can be executed by various proteolytic systems, including lysosomal degradation, chaperone-mediated autophagy, and substrate-specific degradation by the ubiquitin-proteasome system (UPS). The focus of this review is on the role of the UPS in neurodegeneration *in vivo*.

The ubiquitin-proteasome pathway

The small 76-amino-acid ubiquitin protein was first discovered over three decades ago, by Goldstein and co-workers (Goldstein *et al.*, 1975). Over the years, ubiquitin modification of substrate proteins emerged as a key regulator of many cellular processes, including protein degradation (Ciechanover *et al.*, 1980; Hershko *et al.*, 1980), and proved to be essential for cell viability *in vitro* (Finley *et al.*, 1984) and *in vivo* (Ryu *et al.*, 2007).

Substrate targeting by ubiquitin

The UPS is the main regulated intracellular proteolytic pathway and determines the stability of a broad array of proteins by a two-stage mechanism; first, substrates are tagged for degradation by covalent attachment of a chain of ubiquitin moieties, a process known as poly-ubiquitination. Subsequently, the ubiquitinated substrates are selectively targeted to the 26S proteasome, where protein degradation takes place and ubiquitin is recycled (for an extensive review of the UPS see (Glickman and Ciechanover, 2002)). Besides tagging proteins for degradation, additional roles for ubiquitin modification are currently emerging, mostly determined by the length and localization of the attached ubiquitin chain. These include regulation of chromatin structure, DNA repair and receptor endocytosis (Schwartz and Hochstrasser, 2003). Target substrates for proteasomal degradation are recognized by the enzymatic machinery of the UPS through intrinsic degradation signals (degrons, (Meinnel *et al.*, 2006)) or by association with ancillary proteins, e.g. heat-shock proteins, leading to ubiquitination of the substrate (Cyr *et al.*, 2002).

Proteasomal degradation shows a high level of substrate specificity, which is mainly achieved by the enzymatic cascade involved in substrate ubiquitination. This process employs a minimum of three different classes of enzymes performing subsequent tasks to covalently attach ubiquitin to a substrate protein. First, ubiquitin is activated by ATP-dependent cross-linking of its C-terminal glycine (G76) to the active site cysteine of ubiquitin activating enzyme E1, forming a high-energy thioester intermediate. Subsequently, the activated ubiquitin is transferred from the active site of E1 to the active site of one of the E2 ubiquitin-conjugating enzymes present in the cell. Finally, the activated ubiquitin is transferred from the E2 to the target substrate which is bound to a ubiquitin ligase (E3 enzyme) (Figure 1). Until now, only a single conserved ubiquitin E1 enzyme was identified, in contrast to E2 enzymes, of which over fifty different variants are known (Semple, 2003). Only recently two additional E1 enzymes, Uba6 and UBE1L2, both present in vertebrates, were discovered (Jin *et al.*, 2007; Pelzer *et al.*, 2007). Substrate specificity is partially defined by the different E2s, combined with a broad array of hundreds of distinct E3 enzymes, which appear to be to some extent substrate-specific (reviewed in (Glickman and Ciechanover, 2002; Pickart, 2004)).

Of the E3 enzymes, three mechanistically distinct classes are described. The HECT (Homologous to E6-associated protein C-Terminus) domain E3 enzymes bind the E2-ubiquitin complex as well as the target substrate, serving as an intermediate docking station for transfer of the ubiquitin moiety from the E2 to a lysine residue in the substrate (Figure 1). The second class of E3s is the RING-finger (Really Interesting New Gene) motif containing E3s. RING-E3s transfer the ubiquitin moiety directly from the E2 enzyme to the target substrate (Figure 1). Some RING-E3s consist of a single subunit in which the substrate recognition site and the E2-binding site are united in one subunit. Other RING-E3 enzymes consist of multiple subunits, each holding distinct properties

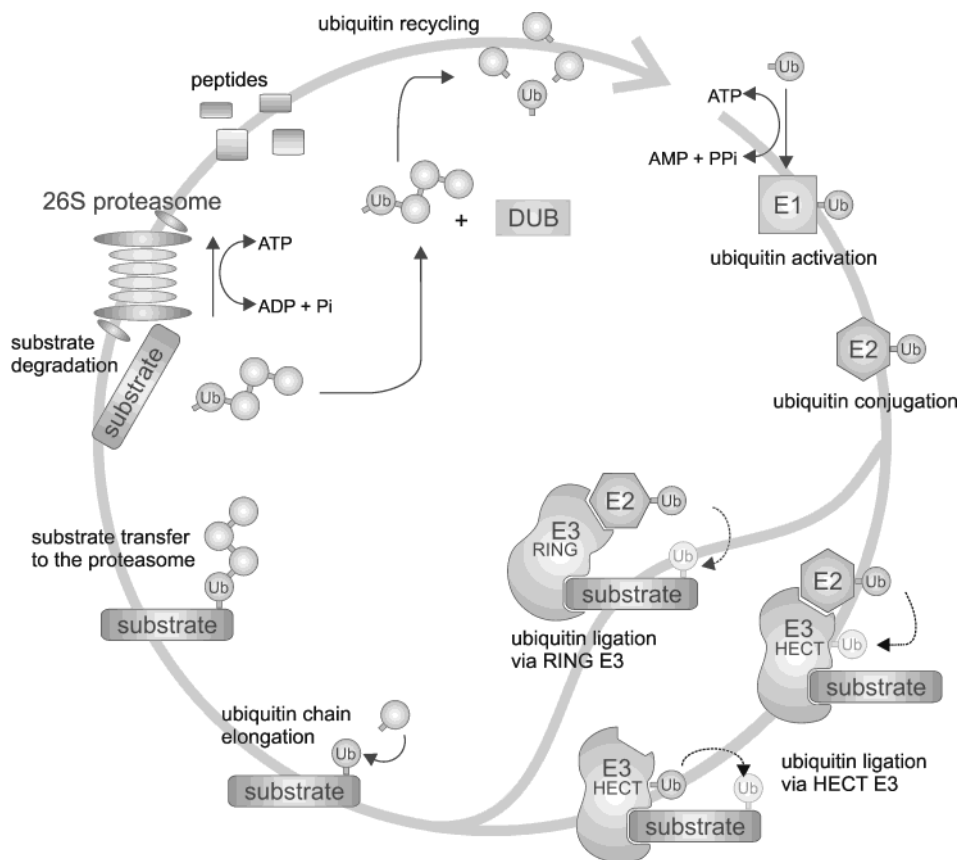


Figure 1 *Ubiquitination cascade and proteasomal degradation.* Ubiquitin (purple sphere) is activated by the E1 ubiquitin activating enzyme and transferred to a ubiquitin carrier, the E2 ubiquitin conjugating enzyme. Protein substrates to be targeted for degradation by the proteasome are recognized by one of the E3 ubiquitin ligase enzymes. In the case of RING-E3 ligases, the ubiquitin is directly transferred from the E3-bound E2 enzyme to a lysine residue in the substrate. For HECT-E3 enzymes, the ubiquitin is first transferred from the E2 to the E3 ligase and is subsequently attached to the substrate. Successive ubiquitin moieties are attached to the substrate-bound ubiquitin, forming a ubiquitin chain. With a K48-linked polyubiquitin chain of four or more ubiquitins the substrate is targeted to the 26S proteasome. Here, the ubiquitin chain is released and the substrate is degraded into small peptides by the 26S proteasome. Finally, the ubiquitin is recycled by release of free monomeric ubiquitin from the ubiquitin chain, an activity mediated by DUBs. *See color section.*

regarding substrate recognition, E2 binding and ubiquitin transfer (reviewed by (Weissman, 2001)). A third class of E3 enzymes is the U-box containing E3 enzymes (described in the next paragraph).

A ubiquitinated protein may be subjected to several subsequent rounds of ubiquitination on one or more lysine residues in the proximal ubiquitin moiety. These ubiquitin-ubiquitin linkages are made up of isopeptide bonds between an internal lysine residue in the bound ubiquitin and the C-terminal G76 of the consecutive ubiquitin moiety. Besides sequential attachment of single ubiquitin moieties to the substrate-bound ubiquitin, pre-formed ubiquitin chains can also be transferred as a whole to a substrate (Li *et al.*, 2007). In some cases, a fourth ubiquitination enzyme, known as the ubiquitin chain elongation factor E4, is necessary, together with the E1, E2 and E3 enzymes to elongate a poly-ubiquitin chain to the desired length (Koegl *et al.*, 1999). The defining motif of this E4 enzyme, designated the U-box motif, partially resembles the RING-finger domain and is also found in several other proteins which elongate ubiquitin chains. The capacity of these U-box-containing enzymes to generate ubiquitin chains in the absence of E3 enzymes indicates that they may also be addressed as a novel class of E3s (Hoppe, 2005).

Varying the ubiquitin linkage sites and chain lengths influences the fate of the ubiquitinated substrates. The ubiquitin protein contains seven conserved internal lysine residues, giving rise to numerous possible ubiquitin linkages. The minimal chain length for proteasomal targeting is a ubiquitin chain of four ubiquitins linked at the lysine at position 48 (K48) (Thrower *et al.*, 2000). *In vivo*, ubiquitin linkages can also be formed at four additional internal lysine residues (K6, K11, K29 and K63), initiating processes other than degradation. For instance, K63 linkage of ubiquitin is implicated in ribosomal function and DNA repair (Spence *et al.*, 2000).

Proteasomal degradation

Ubiquitinated substrates with a K48-linked ubiquitin chain of sufficient length are targeted to the 26S proteasome for degradation (Figure 1). The 26S proteasome is a ~2.5 MD multi-subunit protease complex, consisting of a 20S core particle flanked by at least one 19S regulatory particle. The proteolytic activity resides inside the 20S core, a barrel-shaped structure assembled of four stacked rings, with seven subunits residing in each ring. The two outer rings each contain seven α -subunits which guide substrates into the central proteolytic chamber composed of two inner rings of seven β -subunits. Three out of seven β -subunits show proteolytic active sites. The proteolytic activity can be specified into chymotrypsin-like, trypsin-like and peptidyl-glutamyl-peptide hydrolyzing activity in the β_5 , β_2 and β_1 subunits respectively. Also three alternative β subunits exist (β_{5i} , β_{2i} and β_{1i}), and incorporation of these subunits into the 20S particle gives rise to the immuno-proteasome (in addition with 20S-PA28 association) involved in antigen presentation. The 19S complex consists of a base part attached to the 20S particle (containing six ATPases of the AAA family and two additional non-ATPase subunits) and a lid on top of the base made up of at least eight different subunits (reviewed in (Pickart and Cohen,

2004; Wolf and Hilt, 2004)). The 19S proteasome particle has many specialized functions, which may be partly attributed to specific subunits, including substrate recognition and binding by the Rpt5 and Rpn10 subunits (Deveraux *et al.*, 1994; Young *et al.*, 1998; Lam *et al.*, 2002) and ubiquitin chain removal by Rpn11, after which ubiquitin is recycled (Verma *et al.*, 2002; Yao and Cohen, 2002). Presentation of substrates to the proteasome can be facilitated by proteasome-associated proteins, such as Rad23 and Dsk2, which tend to have a ubiquitin-like domain for proteasomal recognition and one or more ubiquitin-associated domains to bind to ubiquitin chains (reviewed in (Elsasser and Finley, 2005)).

UPS-related processes

An additional level of substrate selectivity (beyond E2 and E3 specificity) is achieved by spatial and temporal regulation of proteolytic degradation throughout the cell. The UPS exerts specialized functions, depending on the intracellular compartment in which it resides (e.g. at the origin of replication, mitotic spindle or synapse) or on time-dependent proteolytic regulation, the latter serving an important role in cell-cycle progression (reviewed in (Pines and Lindon, 2005)). An apparent example of a spatially regulated degradation mechanism is the endoplasmatic reticulum (ER)-associated degradation (ERAD) pathway. In the ER, proteins are glycosylated and folded before they are routed into the secretory pathway. ERAD is the main pathway for protein quality control of secretory proteins, to ensure that un- or misfolded proteins are degraded. In this system, substrates are first targeted from the ER to the ubiquitination machinery in the cytosol, where they are subsequently degraded by the 26S proteasome (reviewed by (Meusser *et al.*, 2005)).

Apart from functioning as a degradation signal, ubiquitination regulates a myriad of other processes in the cell, also dependent on the characteristics of the ubiquitin chain. Mono-ubiquitination of proteins regulates distinct cellular functions, including histone regulation, retrovirus budding, transcriptional regulation and endocytosis. Via the latter pathway substrates at the plasma membrane are modified by a single ubiquitin moiety on a lysine residue (mono-ubiquitination) or by multiple mono-ubiquitination of several internal lysine residues (multi-ubiquitination) for internalization and intracellular routing via the late endosomes (also known as multivesicular bodies) to the lysosome (reviewed in (Haglund *et al.*, 2003; Mukhopadhyay and Riezman, 2007)). Also ubiquitin-like proteins, of which the best known are NEDD8 (neuronal precursor cell expressed, developmentally down-regulated 8) and SUMO (small ubiquitin-like modifier), modify substrates by a similar cascade of E1 and E2 enzymatic activity and regulate protein function, ranging from E3-ligase activity regulation by NEDD8 to transcriptional regulation, and possibly even antagonize ubiquitination by SUMO modification of substrates (Welchman *et al.*, 2005).

Deubiquitination

Substrate ubiquitination is a reversible process and both the ubiquitination and deubiquitination processes are tightly regulated by specific enzymes. The distinct enzymatic activity which reverses ubiquitination is performed by deubiquitinating enzymes (DUBs), which serve various functions by their ability to cleave ubiquitin moieties. The approximately one hundred known DUBs belong to the family of proteases and are subdivided into five subclasses, i.e. (1) the ubiquitin C-terminal hydrolases-UCHs, (2) the ubiquitin specific proteases-USPs, (3) the ovarian tumor proteases-OTUs, (4) the Machado-Joseph Disease protein domain proteases-MJDs and (5) the JAB1/MPN/Mov34 metalloenzyme-JAMM motif proteases (Nijman *et al.*, 2005). DUBs are responsible for cleaving ubiquitin precursors, rescuing target substrates from degradation, cleaving the ubiquitin chain at the proteasome entrance, and for disassembly of unanchored ubiquitin chains generating single ubiquitin moieties. Some DUB activities are physically linked to the 26S proteasome such as ubiquitin chain release by the Rpn11 19S subunit (Verma *et al.*, 2002; Yao and Cohen, 2002). The 19S-associated DUB UCHL5 (UCH37) removes ubiquitin only from the distal end of substrate bound poly-ubiquitin chains, editing the length of the ubiquitin chain (Lam *et al.*, 1997). Other DUBs have more general functions, like recycling of ubiquitin chains to generate free ubiquitin moieties by the DUB isopeptidase-T. DUBs seem to possess (partial) substrate specificity as specific targets or involvement in specific pathways are found for an increasing number of DUBs (reviewed in (Amerik and Hochstrasser, 2004; Nijman *et al.*, 2005)).

The UPS in the nervous system

As described in the previous section, the UPS plays an important role in maintaining cellular homeostasis, determines the turnover rate of many short-lived proteins, and recent studies increasingly recognize an essential role for the UPS in cell cycle progression (Reddy *et al.*, 2007; Stegmeier *et al.*, 2007). However, the UPS also fulfills specific tasks in post-mitotic neurons, including turnover of long-lived proteins, synaptic development and maintenance of established synaptic connections (Table 1, for a detailed review of the neuronal UPS see (Yi and Ehlers, 2007)).

The UPS in neuronal development and plasticity

During development, axons have to locate to their appropriate targets in other areas of the nervous system, a process known as axon guidance. A growth cone is located at the outer end of the developing axon and determines the axonal branching pattern. In these growth cones resides an active UPS machinery, which, together with various guidance molecules,

Table 1 UPS involvement in neuronal processes

Development	Adult
axon guidance	axon regeneration after axotomy
growth cone formation	axon degeneration (axon pruning)
synapse development	synaptic connectivity (pre- and post-synaptic) dendritic spine morphology learning and memory
	neuron degeneration

regulates growth cone behavior by inducing rapid changes in local protein levels (Campbell and Holt, 2001). Also guidance receptors can be regulated via ubiquitination (Myat *et al.*, 2002) and the UPS also plays a role in formation of new growth cones and in axonal regeneration after axotomy (Verma *et al.*, 2005). In addition, modification of established axonal connections can be regulated by the UPS. This process of local degeneration of the distal ends of an axon, axon pruning, requires both the ubiquitination machinery and proteasomal activity in *Drosophila* (Watts *et al.*, 2003).

The formation of synapses also requires a tight balance between protein ubiquitination and deubiquitination. The UPS not only plays an important role in the development of synapses, it also regulates synaptic transmission and synaptic strength, for instance by regulating the levels of neurotransmitter receptors (reviewed in (Yi and Ehlers, 2007)). Turnover of many other proteins within the post-synaptic density is mediated by ubiquitin-dependent degradation and an increasing number of substrates for ubiquitination and proteasomal degradation are currently being elucidated (Ehlers, 2003). It is thus not surprising that the UPS is involved in the modulation of synaptic plasticity, first shown in *Aplysia*, where long-term facilitation was eliminated after inhibition of the proteasome (Hegde *et al.*, 1997). More recently, it was shown that a tight balance between protein synthesis and degradation determines the expression of hippocampal late long-term potentiation (LTP) (Fonseca *et al.*, 2006). Thus, as summarized in Table 1, ubiquitination and proteasomal degradation of proteins by the UPS as well as post-translational ubiquitin modification of proteins may have an influence on the development of synapses and synaptic strength on both the pre- and post-synaptic side of the synaptic cleft (reviewed in (DiAntonio and Hicke, 2004; Yi and Ehlers, 2007)).

UPS in neurodegenerative diseases

As the UPS fulfills an important role in many processes in neurons during development as well as in fully differentiated neurons, it is not surprising that a diminished function of the UPS is implicated in a broad array of neurological diseases. A direct linkage between UPS

malfunction and disease pathogenesis is the accumulation of ubiquitin conjugates and other UPS-related components in the neuropathological hallmarks of many neurodegenerative diseases, including Alzheimer's disease (AD), Parkinson's disease (PD), polyglutamine diseases, such as Huntington's disease (HD) and spinocerebellar ataxias (SCAs), amyotrophic lateral sclerosis and prion disease (reviewed by (Ciechanover and Brundin, 2003)). The discovery of familial variants of PD caused by genetic mutations in UPS-related genes (Kitada *et al.*, 1998; Leroy *et al.*, 1998) substantiated the importance of the UPS in neurodegenerative disease. However, for most diseases the precise mechanism by which (altered) UPS activity mediates disease progression is not fully understood.

There are currently two main views on the biological relevance of the ubiquitin-containing aggregates in disease: (1) they can be seen as the result of effective ubiquitination of target proteins followed by a reduced activity of the proteasome or (2) they could be a protective mechanism of the cell to confine aberrant or misfolded proteins to inert inclusions. Intracellular aggregated proteins are often sequestered into inclusion bodies (IBs), which regularly contain components of the UPS and, in some cases, molecular chaperones and intermediate filaments (reviewed in (Kopito, 2000)). In mammalian cells, aggregates can be actively transported via the microtubuli network to the aggresome, a specialized IB-like ubiquitin-rich structure at the microtubule organizing centre (Johnston *et al.*, 1998). Through sequestration into aggresomes, aggregation-prone proteins can be removed from the cell via transfer to the lysosome, possibly by an autophagic process (Taylor *et al.*, 2003). It is conceivable that not the IBs themselves but rather the early protein aggregate-intermediates (oligomers) are toxic. These oligomers are physically separated from other cellular compartments when trapped into IBs. Indeed, aggregated proteins can inhibit the UPS (Bence *et al.*, 2001; Diaz-Hernandez *et al.*, 2006) before IBs are present (Bennett *et al.*, 2005). Also, in a cell line model of HD, the formation of IBs is predictive of increased cell survival and decreases the aberrant protein load in the cell (Arrasate *et al.*, 2004). Obtaining conclusive evidence on the precise contribution of ubiquitin-containing aggregates and IB formation to disease pathogenesis will remain a challenge; the protein aggregation seems to result from UPS malfunction; however, these aggregated proteins also hold UPS inhibitory properties themselves.

General factors influencing UPS function could contribute to the pathogenesis of neurodegeneration. During aging, a main risk factor for many of these diseases, proteasome activity progressively declines in various tissue types, including nervous tissue (Keller *et al.*, 2000). Oxidative stress can influence proteasome activity levels, either by oxidative modification of the 26S proteasome itself or by increased levels of oxidative proteins which interact with the proteasome during aging (reviewed in (Carrard *et al.*, 2002; Keller *et al.*, 2002)). In turn, decreased chymotryptic proteasome activity hyper-sensitizes cells to oxidative stress, resulting in accumulation of ubiquitinated proteins (Li *et al.*, 2004). ER stress negatively influences proteasome activity and so potentially contributes to the

aberrant protein accumulation seen in neurodegenerative disorders (Menendez-Benito *et al.*, 2005). Furthermore, decreased ribosome functioning and impairments in protein synthesis are associated with early AD (Ding *et al.*, 2005), two processes which can be induced by inhibition of proteasome activity (Ding *et al.*, 2006; Stavreva *et al.*, 2006).

In the following sections, the relation between the UPS and disease pathogenesis will be briefly discussed for three types of neurodegenerative disorders: AD and other tauopathies, PD, and HD and other polyglutamine diseases.

Alzheimer's disease and other tauopathies

AD is the most common form of dementia and characterized by extracellular plaques consisting of amyloid- β (A β), and intraneuronal tangles and neuropil threads consisting of hyperphosphorylated tau (Hardy and Selkoe, 2002). Already two decades ago it was observed that neurofibrillary tangles are ubiquitin positive, as well as the dystrophic neurites surrounding the plaques (Mori *et al.*, 1987; Perry *et al.*, 1987) (Figure 2). There are now many indications that the UPS is involved in the pathogenesis of AD (reviewed by (de Vrij *et al.*, 2004; Scheper and Hol, 2005)). It has been shown that proteasome activity is diminished in affected brain areas of AD patients, such as the hippocampus and temporal cortex (Keller *et al.*, 2000) and that the enzymatic ubiquitination machinery is defective in cortical brain areas in AD (Lopez Salon *et al.*, 2000). The two predominant proteins accumulating in AD directly diminish UPS activity; i.e. paired helical filaments (tau) isolated from AD brain inhibit the proteasome via the 20S core (Keck *et al.*, 2003) and A β holds proteasome inhibitory properties in a cell-free system (Gregori *et al.*, 1995), in neuronal primary cultures (Lopez Salon *et al.*, 2003), and also in several AD transgenic mouse models (Oh *et al.*, 2005; Almeida *et al.*, 2006; Tseng *et al.*, 2007). The UPS inhibition observed in AD is not an intrinsic property of the 20S core, as purified 20S from AD brain does not show a decreased proteasome activity (Gillardon *et al.*, 2007). A β toxicity could be mediated by the E2-conjugating enzyme E2-25K, via ubiquitination of E2-25K substrates which affect proteasome activity in concert with A β (Song *et al.*, 2003). Immunisation of triple transgenic AD mice, showing A β and tau pathology, with A β antisera reverses amyloid pathology as well as early hyperphosphorylated tau pathology. This latter process was shown to be mediated through the proteasomal pathway (Oddo *et al.*, 2004), stressing the importance of this pathway in the neuropathology of AD. UCHL1, a DUB responsible for the recycling of ubiquitin, is associated with AD tangle pathology. The level of soluble UCHL1 protein is inversely correlated to the number of tangles in the brains of AD patients (Choi *et al.*, 2004). Indeed, soluble UCHL1 protein levels are reduced in the hippocampus of an AD transgenic mouse model with APP and PS mutations, accompanied by a decrease in hydrolase activity. The defects in synaptic functioning and in learning and memory present in this AD model can be reversed by exogenous neuronal

expression of UCHL1 (Gong *et al.*, 2006). For a more detailed description of the role of UCHL1 and UCHL3 in neuronal function, see section “UCH-Lx mutant mice”.

Ubiquitinated deposits can also be found in the disease hallmarks of many other diseases with tau pathology (tauopathies, (Lee *et al.*, 2001)). Ubiquitination of soluble tau occurs on three internal lysine residues and the resulting polyubiquitin chain is primarily linked via K48, indicating that tau is indeed a target for degradation by the UPS (Cripps *et al.*, 2006). Tau ubiquitination is mediated by the U-box E3/E4 CHIP (C-terminal Heat-shock protein 70 Interacting Protein), together with Hsp70. CHIP binds tau through its microtubule-binding domain, thereby allowing the ubiquitination of tau, which ultimately leads to an increase in the level of insoluble aggregated tau (Petrucelli *et al.*, 2004; Shimura *et al.*, 2004). Together, these data implicate an important role for the UPS and the chaperone-folding system in the pathogenesis of AD. The possible cross-talk between these systems might be mediated by CHIP (also see section “CHIP KO mice”).

Parkinson's disease

The main neuropathological feature of PD is degeneration of the dopaminergic neurons in the substantia nigra (SN) pars compacta, accompanied by cytoplasmic protein inclusions. These inclusions, known as Lewy bodies, contain many ubiquitinated normal and aberrant proteins, including α -synuclein, neurofilaments and components of the UPS machinery (reviewed in (Ciechanover and Brundin, 2003) (Figure 2)). A direct linkage between UPS malfunction and neurodegenerative disease is probably best exemplified by PD, as autosomal-dominant mutations in UPS enzymes appear to be causative for a percentage of PD cases. The most common form of familial PD, Autosomal Recessive-Juvenile Parkinsonism (AR-JP), results from mutations in the RING-E3 ligase parkin, which most likely leads to a decrease of function of this enzyme (Kitada *et al.*, 1998). Parkin is a RING-E3 enzyme capable of forming various types of ubiquitin linkages on substrate proteins (K48-linked, K63-linked and (multiple) mono-ubiquitination), indicating a role for this enzyme beyond substrate poly-ubiquitination routing substrates to proteasomal degradation (reviewed by (Moore, 2006)). The Pael receptor is one of the many parkin substrates (together with the E4 activity of CHIP to establish poly-ubiquitination) and defective ubiquitination induces misfolding of this receptor leading to activation of the unfolded protein response in the ER (Imai *et al.*, 2001; Imai *et al.*, 2002). Also the α -synuclein interacting protein synphilin-1 is a parkin substrate for K48- and K63-linked ubiquitination (Chung *et al.*, 2001; Lim *et al.*, 2005). Various parkin knockout (KO) mouse models have been developed, showing varying severity of PD pathology, described in section “Parkin KO mice”.

A mutation residing in the DUB UCHL1 gene leads to a diminished function of this enzyme and could be causative of autosomal dominant familial PD in one German family

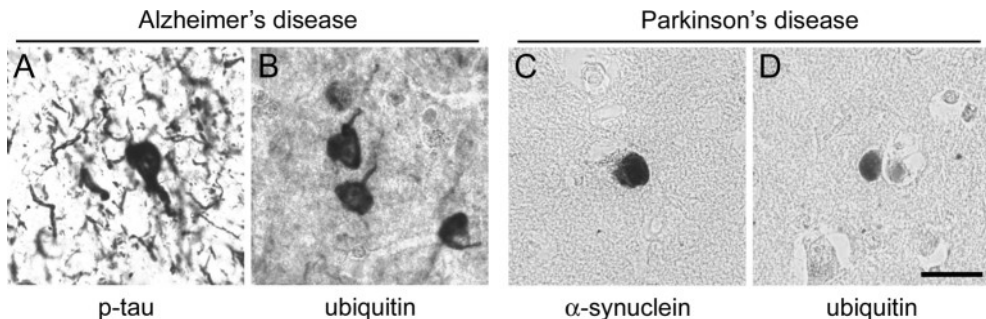


Figure 2 *Ubiquitin-positive pathology in neurodegenerative disease.* One of the neuropathological hallmarks in AD is accumulation of abnormally phosphorylated tau in the intra-neuronal tangles (A). These tangles also contain the ubiquitin protein (B). In PD patients, α -synuclein (C) and ubiquitin (D) co-localize in intra-neuronal aggregates (Lewy bodies). Immuno-stainings were performed on 200 μ m hippocampal vibratome sections of a 92-year-old female AD patient (A, B) or on 6 μ m paraffin sections of the gyrus cinguli of an 80-year-old female patient with Lewy bodies (C, D) using antibodies directed against abnormally phosphorylated tau (MC-1; Davies, P., New York, USA), ubiquitin (Z0458, Dako) and α -synuclein (clone KM51, Novacastra). Scale bar = 0.025 mm.

(Leroy *et al.*, 1998). The *in vitro* physiological function of UCHL1 is to cleave small ubiquitin C-terminal adducts (Larsen *et al.*, 1996), and also to provide single ubiquitin molecules to ubiquitinate substrate proteins (Larsen *et al.*, 1998), further described in section “UCH-Lx mutant mice”. A decrease of catalytic activity of UCHL1 through the PD mutation could putatively lead to a shortage of free ubiquitin. On the other hand, dimeric UCHL1 contains E3 activity, which enhances α -synuclein ubiquitination. A polymorphism for UCHL1, which decreases this ligase activity, has a possible protective effect on PD (Liu *et al.*, 2002). In agreement with these observations, UCHL1 protein levels are decreased in sporadic PD and the protein is a target for oxidative damage, the latter possibly interfering with its deubiquitinating activity (Choi *et al.*, 2004). As is the case in AD, in PD, the activity of the proteasome is modestly decreased in the affected brain areas (McNaught and Jenner, 2001). Also the composition of the proteasome is altered, as there is a selective substantial decrease of α -subunits and 19S regulatory particles in the dopaminergic neurons in the SN (McNaught *et al.*, 2002; McNaught *et al.*, 2003).

Huntington's disease and other polyglutamine diseases

The family of polyglutamine (polyQ) diseases is characterized by an expansion of CAG tri-nucleotide repeats in genes, such as *huntingtin* and the *ataxin* genes, leading to an extension of the encoded polyQ stretch. The best-known polyQ disease is HD, an autosomal dominant neurological disorder caused by an expanded CAG repeat in the *huntingtin*

gene. The pathological hallmarks of HD consist of nuclear and cytoplasmic huntingtin aggregates gathered into IBs. Besides mutant huntingtin, these IBs also contain many other proteins, including ubiquitin and UPS related proteins, indicating a role for the UPS in HD pathology (reviewed in (Valera *et al.*, 2005)). The current views on how huntingtin aggregates and IBs interfere with UPS function are still quite controversial. *In vitro*, polyQ aggregates, although resistant to proteasomal degradation, do not induce UPS inhibition (Verhoef *et al.*, 2002), although in other studies aggregated huntingtin does induce inhibition of the UPS (Bence *et al.*, 2001; Bennett *et al.*, 2005; Bennett *et al.*, 2007) and relocalization of proteasome components to the huntingtin aggregates leads to a decrease in UPS activity (Jana *et al.*, 2001). Also, proteasomal changes are observed in HD, resulting in a decrease of proteasome activity in the brain of HD patients (Seo *et al.*, 2004) and the induction of 20S immuno-proteasome subunits (Diaz-Hernandez *et al.*, 2003). However, total proteasome content and activity are unaltered compared to non-diseased subjects in this study. Contradicting these observations are results from transgenic mouse studies showing that UPS impairment is not necessarily connected to polyQ pathology in a SCA-7 model (Bowman *et al.*, 2005) and that proteasome activity remains unaltered in HD transgenic mice (Bett *et al.*, 2006).

CHIP is one of the proteins able to suppress polyQ toxicity, again showing a link between the UPS, the chaperone system and a neurodegenerative disease process (Miller *et al.*, 2005). Also the ubiquitin conjugating E2 enzyme E2-25K (or huntingtin interacting protein 2) interacts directly with huntingtin and may mediate ubiquitination of this protein (Kalchman *et al.*, 1996). Recently it was shown that E2-25K is involved in polyQ aggregate formation and mediates polyQ- induced cell death, depending on the C-terminal catalytic domain of the enzyme essential for ubiquitination of substrate proteins. In human postmortem brain, the E2-25K enzyme is present in a subset of the neuronal IBs found in HD and SCA3 patient material, again indicating the relevance of ubiquitination for the pathology of polyQ disease (de Pril *et al.*, 2007).

In 2006, Diaz-Hernandez *et al.* showed that the observed UPS inhibition in HD could be dissected into differential effects of aggregated huntingtin on 20S and 26S proteasome activity. Ubiquitinated filamentous huntingtin aggregates from HD transgenic mice co-localized with the 19S proteasome cap particles, resulting in 26S, but not 20S, proteasome inhibition. In addition, ubiquitin and mutant huntingtin positive filamentous aggregates isolated from human HD patients inhibited 26S proteasome activity without altering 20S activity. In contrast, intact IBs isolated from the same HD mice did not induce UPS inhibition in the 26S or 20S proteasome fraction. These data suggest that the ubiquitinated form of filamentous aggregates could be detrimental to the neuron, whereas entrapment of these aggregates into larger IBs could be cytoprotective (Diaz-Hernandez *et al.*, 2006). Ubiquitinated inclusions are also found in other polyQ diseases, indicating a general mechanism of UPS involvement in polyQ pathology. A number of SCAs are caused by

polyQ expansion in *ataxin* genes. A puzzling correlation between UPS dysfunction and polyQ disease is found in SCA-3 (Machado-Joseph disease), which results from a polyQ expansion in ataxin-3, a protein with deubiquitinating activity and able to bind ubiquitinated proteins through its ubiquitin interacting motif (UIM) (Burnett *et al.*, 2003; Burnett and Pittman, 2005). An overview of murine models harboring ataxin-3 mutations is given in section “Ataxin-3 transgenic mice”.

Mutant ubiquitin (UBB⁺¹)

Another indication of UPS malfunction in neurodegenerative disease is the occurrence of a mutant form of ubiquitin in many neurodegenerative disorders. This mutant ubiquitin (UBB⁺¹) results from a di-nucleotide deletion in the ubiquitin B mRNA. The resulting UBB⁺¹ protein has a 19 amino acid C-terminal extension, with the ubiquitin C-terminal G76, normally required for ubiquitinating substrates, mutated in Y76. UBB⁺¹ accumulates in the neuropathological hallmarks of AD and Down syndrome patients (van Leeuwen *et al.*, 1998; van Leeuwen *et al.*, 2006). Moreover, UBB⁺¹ co-localizes with huntingtin aggregates in HD and with ataxin-3 in SCA-3 (De Pril *et al.*, 2004).

UBB⁺¹ has lost the ability to ubiquitinate substrates as it lacks the C-terminal glycine. In turn, UBB⁺¹ is a ubiquitin-fusion degradation (UFD) substrate for proteolytic degradation: UBB⁺¹ is poly-ubiquitinated and directed to the 26S proteasome for degradation (De Vrij *et al.*, 2001; Lindsten *et al.*, 2002). Furthermore, ubiquitinated UBB⁺¹ is refractory to deubiquitination by the DUB isopeptidase-T (Lam *et al.*, 2000). When the protein is expressed at high levels, it is a potent inhibitor of the UPS. These dual UPS substrate/inhibitory properties of UBB⁺¹ are dose-dependent; UBB⁺¹ shifts from a proteasome substrate at low expression levels to a UPS inhibitor at high expression levels (van Tijn *et al.*, 2007). At these high expression levels, UBB⁺¹ induces cell cycle arrest, neuritic beading and mitochondrial stress, apoptotic-like cell death and a heatshock response (De Vrij *et al.*, 2001; Lindsten *et al.*, 2002; Hope *et al.*, 2003; Tan *et al.*, 2007). The frequency of UBB⁺¹ mRNA is very low (1:10⁵ to normal ubiquitin mRNA) and UBB⁺¹ mRNA levels of diseased and control patients do not differ significantly (Fischer *et al.*, 2003; Gerez *et al.*, 2005). As the UBB⁺¹ protein is only found in diseased subjects and aged subjects showing neuropathology, accumulation of the protein could reflect a downstream feature of disease pathogenesis. These data suggest that UBB⁺¹ normally is degraded and that UPS inhibition, induced by e.g. disease pathology, initiates accumulation of the protein. In human, the accumulation of UBB⁺¹ can be seen as an endogenous marker for proteasomal dysfunction (Fischer *et al.*, 2003).

It is interesting to note that UBB⁺¹ accumulation is disease-specific as the protein is present in all tauopathies studied, but it is not present in synucleinopathies such as PD (Fischer *et al.*, 2003). UBB⁺¹ was shown to accumulate occasionally in α -synuclein con-

taining neuronal aggregates in the entorhinal cortex in subjects with combined multiple system atrophy and AD (Terni *et al.*, 2007). It must be noted that in this brain area, α -synuclein pathology coexisted with tau inclusions, thus it is conceivable that UBB⁺¹ only accumulated in neurons containing both tau and α -synuclein. This discrepancy between tauopathies and synucleinopathies concerning UBB⁺¹ accumulation could reflect an intrinsic difference in the disease mechanisms; UPS inhibition might be a general disease characteristic in tauopathies leading to accumulation of many substrates, including UBB⁺¹. In the case of synucleinopathies, dysfunction of a specific UPS component, e.g. an E3 ligase, will result in a substrate-specific degradation impairment or a transient (partial) decrease of UPS activity (Fischer *et al.*, 2003; Hol *et al.*, 2005). We have generated several UBB⁺¹ transgenic mouse models to further elucidate the effect of UBB⁺¹ expression on neuronal functioning. Similar to our previous observations in cell lines, we observed that high levels of neuronal UBB⁺¹ expression led to a modest decrease in proteasome activity *in vivo*, accompanied by cognitive deficits, further indicating that intact proteasome activity is a prerequisite for proper neuronal functioning (Fischer *et al.*, 2004; van Tijn *et al.*, 2005).

Mouse models of the UPS

Recognition of the pivotal role of the UPS in many cellular pathways has led to the introduction of an array of *in vivo* models with an altered UPS. These were generated through two different approaches; (1) altered UPS function resulting from expression of (aberrant) proteins which modify UPS activity or (2) mutation of an intrinsic component of the UPS machinery, e.g. an E3 or DUB, resulting in a phenotype with disturbed UPS function. Targeting of transgene expression or protein knockdown to specific tissues make these *in vivo* models essential in understanding the mechanism of UPS action. They also provide an opportunity to test potential therapeutic agents which target the UPS *in vivo*. In this review, we will focus on mouse models with an alteration of components of the UPS machinery leading to a neurological phenotype (section “Mouse models of neurodegenerative disease induced by an altered UPS”, Table 2). In addition, we will briefly discuss the current developments in monitoring UPS activity *in vitro* and *in vivo* using UPS reporter proteins (section “Mouse models to measure UPS activity *in vivo*”, Table 3).

Mouse models of neurodegenerative disease induced by an altered UPS

Parkinson's disease mouse models

The majority of the neurodegenerative genetic mouse models for PD harbor mutations in genes which encode proteins associated with PD (e.g. α -synuclein and parkin). Most mouse models expressing PD mutations show only a partial PD phenotype; mice with

parkin mutations show pathology found in the early stages of PD, including defects in the nigrostriatal pathway without massive loss of DA neurons (reviewed in (Fleming *et al.*, 2005)). In 2004, McNaught *et al.* published a controversial PD model in rat directly linking the UPS to the development of PD pathology. Systemic injection of UPS inhibitors in adult rats induced a Parkinsonian phenotype, exemplified by gradual progressive motor deficits. In addition, these rats were reported to show PD associated DA cell loss in the SN pars compacta, as well as neuronal degeneration in other brain regions affected by PD. Lewy body-like neuronal IBs containing α -synuclein and ubiquitin were shown to be present in the affected brain areas (McNaught *et al.*, 2004). However, this promising model for PD has become increasingly controversial, as attempts by various laboratories to replicate the abovementioned results have only been partially successful (Beal and Lang, 2006). Several other studies did show that direct infusion of UPS inhibitors in the rat striatum or SN induced degeneration of nigrostriatal DA cells accompanied by neuronal inclusions resembling Lewy bodies (McNaught *et al.*, 2002; Fornai *et al.*, 2003; Miwa *et al.*, 2005).

Parkin KO mice

A subset of PD mouse models have a partial deletion of the *Park2* gene (similar to human familial autosomal recessive juvenile Parkinson (AR-JP) caused by *PARK2* mutations), leading to loss of function of the parkin RING-finger E3 protein. The pathology observed in human AR-JP closely resembles the pathology of idiopathic PD (motor impairments accompanied by DA neuron loss in the SN), but Lewy body pathology is absent.

The first two parkin KO models were engineered by deleting exon 3 of the *Park2* gene, giving rise to the absence of the parkin protein (Goldberg *et al.*, 2003; Itier *et al.*, 2003). In both models, brain morphology and cellular structure in the SN were normal without nigrostriatal DA neuron loss. Modest modifications in the DA system were present; parkin KO mice showed increased levels of extracellular DA in the striatum, as well as a decreased synaptic excitability of the striatal neurons, probably arising from a post-synaptic deficit. Parkin KO mice performed poorly in the beam transversal task, a behavioral task sensitive to nigrostriatal deficits. The levels of parkin E3 ligase substrates CDCrel-1, synphilin-1 and also levels of α -synuclein were unaltered (Goldberg *et al.*, 2003), whereas proteomic analysis of ventral midbrain tissue of these mice revealed changes in proteins involved in regulation of mitochondrial function and oxidative stress (Palacino *et al.*, 2004). In the parkin exon 3 deletion model described by Itier *et al.*, striatal levels of DA transporter protein were decreased. DA levels were increased in the limbic system, as well as DA metabolism by monoamino oxidase. Also pre-synaptic electrophysiological changes (inhibition of glutamate release) were found in the hippocampus. Compared to wild-type mice, these mice showed a decline in exploratory behavior and decreased alternation in a T-maze (Itier *et al.*, 2003). Proteomic analysis of brain tissue

from these mice revealed 12 classes of differentially regulated proteins, the main functional category being energy metabolism proteins. Also changes in protein processing pathways were present, including UPS-mediated protein degradation. Parkin E3 ligase substrates such as CDCrel-1 and synaptotagmin I were slightly up-regulated (Periquet *et al.*, 2005).

In contrast, disruption of the nigrostriatal DA system was absent in a PD model with a mutation in parkin exon 7 encoding the first RING domain (Von Coelln *et al.*, 2004). In this parkin KO model a significant reduction of catecholaminergic neurons in the locus coeruleus was observed already at 2 months of age, accompanied by a loss of noradrenalin in selective target regions of locus coeruleus axonal projections (olfactory bulb and spinal cord). This resulted in a decreased acoustic startle response, a behavioral process mediated by noradrenergic neurotransmission (Von Coelln *et al.*, 2004). The mechanism by which loss of the E3 function of parkin modulates neuron loss in the locus coeruleus is not yet understood. Analysis of known parkin substrates in these mice showed an increase in only one parkin substrate, the aminoacyl-tRNA synthetase cofactor p38/JTV-1 (Ko *et al.*, 2005). The loss of neurons in the locus coeruleus may well mimic early PD pathology, as in human sporadic PD neuron loss is more pronounced in the locus coeruleus than in the SN and pathology arises earlier in this brain region during PD progression (Braak *et al.*, 2003; Zarow *et al.*, 2003).

Several years ago, the spontaneous mouse model *quaking*^{viable} (*qk*^v) was found to harbor a ~1 Mb deletion on mouse chromosome 17 resulting in the altered splicing of the *quaking* gene. In addition, a proximal region was deleted containing the first five coding exons of *Park2*, the Park2 co-regulated gene (*Pacrg*) and the joint *Park2/Pacrg* promoter region. This deletion resulted in the absence of *Park2* and *Pacrg* mRNA as well as the absence of the resulting proteins in homozygous *qk*^v mice (Lockhart *et al.*, 2004). The main phenotype of *qk*^v mice consists of demyelination of the central nervous system in combination with locomotor deficiencies and tremor of the hind limbs (Sidman *et al.*, 1964). Together with the previously described parkin KO models, these mice also showed an altered DA regulation resulting in an increased DA metabolism, but without changes in the DA levels in the nigrostriatal and mesolimbic systems (Nikulina *et al.*, 1995). Contrary to the neuron loss in the locus coeruleus in the exon 7 parkin KO mice, *qk*^v mice showed an increased noradrenergic neuron count in the locus coeruleus (Le Saux *et al.*, 2002).

In contrast to the earlier observations in parkin-deficient mice, an exon 2 parkin KO model with a deleted ubiquitin-like domain did not exhibit a Parkinsonian phenotype even though functional parkin protein could not be detected (Perez and Palmiter, 2005). This discrepancy may originate in the different genetic backgrounds, which influences e.g. behavioral performance. Varying types of parkin mutations could also induce different splicing patterns of the parkin gene. A possible explanation for the absence of a PD phe-

notype in the parkin exon 2 KO mice could be a redundancy between E3 ligases present in the mouse brain, which compensates for the loss of parkin E3 ligase activity (Perez and Palmiter, 2005). Already in the parkin KO models which do show a Parkinsonian phenotype, contrasting observations indicate a variable effect of the parkin E3 deletion, such as the decrease in neurons in the locus coeruleus in the exon 7 mutant (Von Coelln *et al.*, 2004), as opposed to the increase in locus coeruleus neurons in the *qk^v* mice (Le Saux *et al.*, 2002). It remains to be investigated whether loss of parkin activity has an effect on proteasome function *in vivo*, as does the precise mechanism by which loss of an E3 ligase induces a partial PD phenotype.

UCH-Lx mutant mice

At approximately 6 months of age, the spontaneous autosomal recessive mutant gracile axonal dystrophy (*gad*) mice develop sensory ataxia, followed by tremor, moving difficulties and hind-limb muscle atrophy, leading to premature death (Yamazaki *et al.*, 1988). On a neuropathological level, the primary defects in the *gad* mice include axonal dystrophy of the gracile tract and degeneration of the gracile nucleus in the medulla. The axons show a “dying back” degenerative phenotype and spheroid body formation occurs in the nerve terminals of the axons in the gracile nucleus surrounded by projections of reactive astrocytes (reviewed in (Kwon and Wada, 2006)). A decade later, it was shown that this phenotype resulted from an in-frame deletion of exons 7 and 8 of the *Uchl1* gene, coding for the ubiquitin C-terminal hydrolase Uchl1 (Saigoh *et al.*, 1999).

This mouse model was the first to link a defective ubiquitination machinery to a neurodegenerative phenotype *in vivo*. The deletion in the *Uchl1* gene resulted in the formation of Uchl1 protein lacking the catalytic site residue. However, the phenotype of *gad* mice does not resemble a Parkinsonian phenotype, as might be expected since a UCHL1 mutation in human has been identified in one PD family. Interestingly, abnormal accumulation of proteins did occur in this model, such as a diffuse intracellular accumulation of amyloid precursor protein, and probably also A β . To some extent this resembles AD pathogenesis, where A β deposition in fibrillary and dense-core plaques takes place accompanied by axonal degeneration and glial cell activation (Ichihara *et al.*, 1995). In addition, ubiquitinated “dot-like” structures and increased proteasome immunoreactivity were observed in the affected brain regions in the *gad* mouse, further connecting malfunctioning of the UPS to this model (Wu *et al.*, 1996; Saigoh *et al.*, 1999). The small DUB Uchl1 is normally involved in generating monomeric ubiquitin (Larsen *et al.*, 1998) and associates with mono-ubiquitin *in vivo*, preventing its degradation by extending the half-life of the protein (Osaka *et al.*, 2003). In line with these observations, loss of Uchl1 function in *gad* mice induced a 20-30% decrease in neuronal mono-ubiquitin levels. In mice overexpressing Uchl1, the opposite effect was found, i.e. an increase in free mono-ubiquitin levels. It is possible that these decreased levels of free ubiquitin affect the ubiquitination of substrates

and initiate accumulation of proteins which would normally be degraded by the UPS (Osaka *et al.*, 2003).

When a mutant form of human UCHL1, found in familial PD patients (UCHL1 I93M), is expressed in a transgenic model, a different phenotype emerges. High expression levels of UCHL1 I93M led to a 30% reduction in TH-positive DA neurons in the SN at 20 weeks of age and also to a decrease in DA levels in the striatum, accompanied by neuro-pathological features, such as cytoplasmic inclusions positive for UCHL1 and ubiquitin and dense-core vesicles in neurons of the SN. Unlike Lewy bodies, the ubiquitin-positive inclusions were not eosinophilic and did not stain for α -synuclein. These mice showed a mild behavioral defect in spontaneous voluntary movement. This model is the first mouse model for familial PD which shows DA cell loss in the SN. However, the 30% decrease in DA cell number appears to be insufficient to induce a complete PD phenotype in these mice (Setsuie *et al.*, 2007).

The ubiquitin C-terminal hydrolases UCHL1 and UCHL3 display 52% sequence identity and are probably functionally redundant to some extent. However, the expression patterns differ; the *Uchl3* transcript is widely present, whereas *Uchl1* expression is confined to brain and testis. As *Uchl1* deficient mice (*gad* mice) show a neurological phenotype, it could be expected that loss of *Uchl3* also induces a phenotype. However, mice lacking functional *Uchl3*, due to a deletion of exons 3-7 in the *Uchl3* gene, did not show an overt developmental or adult phenotype and no histological defects were found in any of the tissues studied, including brain tissue (Kurihara *et al.*, 2000). Further analysis did show a small defect in the dorsal root ganglion cell bodies and dystrophic axons were found in the nucleus tractus solitarius and area postrema (Kurihara *et al.*, 2001). When these *Uchl3^{Δ3-7}* mice were crossed with *gad* mice, the neurodegenerative phenotype of the *gad* mice was enhanced and accompanied by an increased weight loss, probably due to dysphagia. A loss of function of either *Uchl1* or *Uchl3* thus led to a distinct phenotype, showing that these DUBs have specific functions. In a double knockout, these phenotypes were enhanced, hinting that *Uchl1* and *Uchl3* also have overlapping functions in maintaining neuronal homeostasis in specific areas of the brain (Kurihara *et al.*, 2001).

Ap-uch, the *Aplysia* orthologue of *Uchl3*, is required for long-term facilitation in *Aplysia*, showing a direct connection between the ubiquitin pathway and memory formation (Hegde *et al.*, 1997). Using several learning and memory paradigms, Wood *et al.* investigated if murine *Uchl3* also plays a role in this process. Indeed, *Uchl3^{Δ3-7}* mice showed a significant learning deficit and impaired spatial reference memory in a watermaze, as well as impaired working memory coupled to a slightly impaired reference memory in a radial maze without deficits in long-term potentiation. The direct relation between loss of *Uchl3* and defective learning and memory is not clear. A decreased availability of ubiquitin due to defective deubiquitination could affect processes regulated by mono-ubiquitination, and alter proteasomal turnover of as yet undefined substrates of *Uchl3* (Wood *et al.*, 2005).

Although a direct correlation between Uchl1 and learning and memory has not been established in the gad mice, it is known that inhibition of Uchl1 activity in mice inhibits hippocampal LTP and that transduction of Uchl1 protein can reverse synaptic defects and contextual memory deficits in AD transgenic mice (Gong *et al.*, 2006). These observations further establish a role for the UCHs in cognitive function.

Usp14 KO mice (ataxia mice)

The spontaneous recessive mouse mutant *ataxia* has provided new insights in the relation of the UPS to synapse function. In these *ataxia* mice (ax^J), an insertion was found in intron 5 of the *Usp14* gene, resulting in a decrease of *Usp14* gene expression in the brain of mice to 5% of the *Usp14* expression levels in wild-type mice (Wilson *et al.*, 2002). This is reflected in greatly reduced levels (90%-100%) of Usp14 protein expression in brain extracts from homozygous mutants (Wilson *et al.*, 2002; Anderson *et al.*, 2005). ax^J/ax^J mice showed neurological deficits starting with tremors, followed by paralysis of the hind limbs and by death at ~10 weeks of age. Only mild developmental defects were found in the CNS, including under-development of the corpus callosum, hippocampus, dentate gyrus and some regions in the brainstem (D'Amato and Hicks, 1965; Burt, 1980). ax^J/ax^J mice showed no overt neuropathology, including absence of neuronal cell loss and ubiquitin-positive pathology. Wilson *et al.* demonstrated that ax^J/ax^J mice showed pre-synaptic defects in synaptic transmission at the NMJ, indicative of defective neurotransmitter release. In addition, these mice showed alterations in short-term plasticity in the CA1-CA3 circuit of the hippocampus, also pointing to a pre-synaptic defect (Wilson *et al.*, 2002).

The deficits found in ax^J mice could give more information about the role of the UPS in synaptic transmission in the normal as well as the diseased brain, as synaptic deficits are an early pre-clinical event in e.g. AD (Coleman *et al.*, 2004). USP14 normally functions as a proteasome-associated DUB (Borodovsky *et al.*, 2001). Ubp6 (the yeast homologue of Usp14) appears to have a dual role in proteasome function; it delays substrate degradation by partial inhibition of the proteasome, whilst simultaneously deubiquitinating the same substrate (Hanna *et al.*, 2006). It is not yet understood to what extent the deubiquitinating activity or the proteasome inhibitory activity of Usp14 contributes to the neurological phenotype of these mice. It is conceivable that Usp14 regulates local turnover of substrates involved in synaptic transmission and so induces the synaptic deficits; possible target proteins could be related to synaptic vesicle trafficking and sorting, vesicle docking or endocytosis (Wilson *et al.*, 2002).

In the brain of ax^J/ax^J mice, the levels of monomeric ubiquitin were decreased by 30-40%, indicating that Usp14 is required for maintaining a pool of free ubiquitin (Anderson *et al.*, 2005). Usp14 normally associates with proteasomes extracted from brain tissue in wild-type mice. This association was lost in ax^J mice, most likely attributable to the very

low levels of Usp14 protein. However, this did not affect the proteolytic activity of the proteasome measured with fluorogenic 20S proteasome substrates. In contrast to the observations in yeast, where Usp14 homologue Ubp6 represents the predominant ubiquitin-hydrolyzing activity of the proteasome (Leggett *et al.*, 2002), only a small decrease was found in the ubiquitin hydrolyzing activity in *ax^J* mice (Anderson *et al.*, 2005). It is thus conceivable that other DUBs, such as the proteasome-associated DUB Uchl5 (synonym UCH37), compensate for the decreased Usp14 levels to maintain ubiquitin hydrolysis at the proteasome. The ataxia phenotype of *ax^J* mice, including the decreased levels of monomeric ubiquitin and motor deficits, could be rescued by transgenic neuronal expression of recombinant Usp14 (Crimmins *et al.*, 2006).

Ataxin-3 transgenic mice

One of the polyQ diseases with a direct link to the UPS is Machado-Joseph disease, also known as SCA-3. This disease is characterized by progressive motor problems due to motor neuron defects. This most common autosomal dominant ataxia is caused by an expansion of the polyQ repeat in the ataxin-3 (*ATXN3*) gene. Neuropathologically, neuron loss is present in the spinal cord and in several brain regions, such as the brainstem and basal ganglia. IBs are found in the surviving neurons, containing aggregated mutant polyQ protein and UPS associated proteins including ubiquitin (reviewed in (Zoghbi and Orr, 2000)). The normal ataxin-3 protein (with a polyQ repeat length of 12-41) was identified as a protein which binds to ubiquitin through UIM domains (Donaldson *et al.*, 2003) and shows DUB activity, possibly in the N-terminal Josephin domain (Burnett *et al.*, 2003). Mutant ataxin-3 has a polyQ repeat of 62-84 repeats. Due to alternative splicing, different isoforms of mutant ataxin-3 are formed (Ichikawa *et al.*, 2001), including mjd1a (Kawaguchi *et al.*, 1994) and ataxin-3c (Schmidt *et al.*, 1998).

In the first SCA-3 mouse models, expression of an mjd1a cleavage fragment containing an expanded polyQ stretch (Q79) induced motor deficiencies, including an ataxic phenotype and gait disturbance starting at 4 weeks of age, whereas expression of a control Q35 fragment as well as full-length mjd-Q79 did not induce any phenotype (Ikeda *et al.*, 1996). In the affected mice, the cerebellum was severely atrophic and neuronal Purkinje cell loss was observed, while the cortex morphology appeared normal without neuropathology. It should be noted that in this model transgene expression was driven by the L7 promoter, giving rise to high expression levels in cerebellar Purkinje cells (Ikeda *et al.*, 1996). However, in human SCA-3 pathology the affected cerebellar cells are mainly located in the dentate nuclei (Koeppen, 2005) and no neuronal IBs are found in Purkinje cells (Koyano *et al.*, 2002).

This mjd1a cleavage fragment was not found in a transgenic model expressing a YAC construct encoding the full-length *ATXN3* gene with an expanded polyQ stretch and flank-

ing genomic DNA sequences (Cemal *et al.*, 2002). In diseased mice, the normally predominantly cytoplasmic ataxin-3 protein was relocated to neuronal ubiquitinated intranuclear IBs in the pontine and dentate nucleus, two areas affected by SCA-3. Areas not implicated in SCA-3 pathology (e.g. hippocampus and striatum) were devoid of IBs. In the mice with an expanded polyQ stretch, motor deficiencies were accompanied by degeneration of the dentate and pontine nuclei and slight atrophy of the Purkinje cell layer (Cemal *et al.*, 2002). Generally, the phenotype in this model was milder and showed slower progression than in the mjd1a-Q79 cleavage model.

More recently a third transgenic model for SCA-3 was presented that expressed high levels of normal (Q20) or expanded (Q71) full length human mjd1a in the brain and spinal cord (Goti *et al.*, 2004). The mjd1a-Q71 mice showed SCA-3-like pathology, including motor deficits, neuronal intranuclear inclusions and cell loss in the SN. These mice also showed weight loss accompanied by a decreased life-span. An ataxin-3 mjd1a cleavage fragment still containing the polyQ stretch was detected in the brains of the mjd1a-Q71 mice. Notably, there was an abundance of the cleavage fragment in affected mjd1a-Q71 transgenic mice compared to mjd1a-Q71 mice with a normal phenotype (Goti *et al.*, 2004), which showed the toxicity of the fragment. It could be that this cleavage fragment recruits the full-length protein into the aggregates *in vivo* the same way it does *in vitro* (Haacke *et al.*, 2006). The normal ataxin-3 protein is ubiquitinated and degraded by the UPS (Matsumoto *et al.*, 2004; Berke *et al.*, 2005) and has two or three functional UIMs mediating binding of the protein to ubiquitin chains. These UIMs are required and sufficient to localize ataxin-3 into aggregates *in vitro* (Donaldson *et al.*, 2003). In *Drosophila*, the normal ataxin-3 function paradoxically protects against polyQ-induced neurodegeneration by diminishing the aggregation of the mutant ataxin-3 protein. This process requires an intact protease domain and UIMs of ataxin-3 and depends on normal proteasome function, indicating that the UPS mediates this protective effect (Warrick *et al.*, 2005).

Ube3a transgenic mice

The *UBE3A* gene encodes for one of the first E3 ubiquitin ligases discovered, the ubiquitin-protein ligase E3A (E6-AP), which promotes degradation of several proteins including the p53 tumor suppressor protein in complex with the E6 viral protein (reviewed in (Glickman and Ciechanover, 2002)). In Angelman Syndrome (AS), a neurological disorder associated with severe mental retardation, motor problems and seizures, the human *UBE3A* locus is mutated (by a maternal deletion) (Kishino *et al.*, 1997). The chromosomal region where the *UBE3A* gene resides is subject to genomic imprinting, i.e. specific expression of the gene according to parental origin. In mice, this mechanism leads to expression of primarily the maternal allele in several brain regions, including the hippocampal neurons and Purkinje cells (Albrecht *et al.*, 1997).

The two best-characterized mouse models with an AS phenotype are maternally deficient (m-/p+) for *Ube3a*. In the AS model developed by Jiang *et al.*, the m-/p+ mice did not show gross phenotypic abnormalities, but displayed motor dysfunction with varying severity (Jiang *et al.*, 1998). Also seizures were more readily induced in the m-/p+ mice or in mice with a total deficiency of *Ube3a*, as well as continuous abnormalities in EEG recordings in awake active mice. *Ube3a* protein expression was absent from the hippocampal neurons and Purkinje cells in m-/p+ mice, where this was not the case in wild-type or m+/p- mice, indicating that, indeed, the maternal allele is essential for expression in these brain regions. The hippocampus is important in learning and memory formation; therefore, context-dependent memory and LTP were measured in these mice (Jiang *et al.*, 1998). Indeed, the m-/p+ mice were deficient in a fear-conditioning paradigm for context-dependent memory and showed a defective LTP response, possibly through increased phosphorylation of the calcium/calmodulin-dependent protein kinase II, a protein involved in calcium-dependent signal transduction pathways needed for LTP induction (Weeber *et al.*, 2003). This is also exemplified by the rescue of the AS phenotype in *Ube3a* m-/p+ mice by introducing a mutation preventing the increased inhibitory phosphorylation of CamKIIα (van Woerden *et al.*, 2007). In addition, the ubiquitination substrate for E6-AP, p53, was increased in the cytoplasm of hippocampal and cerebellar neurons (Jiang *et al.*, 1998).

Similar results were found in a *Ube3a* maternal deficient AS model by Miura *et al.*; these mice also showed learning deficits, EEG abnormalities and motor dysfunction (Miura *et al.*, 2002), as well as sleep disturbances in baseline conditions or after sleep deprivation (Colas *et al.*, 2005) and altered Purkinje cell firing (Cheron *et al.*, 2005). The only discrepancy between these two mouse models is the absence of p53 accumulation in the model by Miura *et al.* The origin of this difference is not yet fully understood, although it indicates that p53 degradation is not essential to the AS phenotype (Miura *et al.*, 2002). The AS mouse models show that the UPS plays an important role in learning and memory, and in LTP formation in mice. Due to *Ube3a* loss of function, ubiquitination and subsequent degradation of as yet unidentified *Ube3a* substrates might be defective, as was shown for p53, which could influence learning and memory.

Other UPS defective models for neurodegeneration

Prion disease and mahogany mutant mice

Mutations in the prion protein gene are causative for several forms of spongiform neurodegeneration, including Creutzfeld-Jacob disease. The mutations cause conformational changes in the prion protein (PrP), leading to the misfolded PrP-scrapie variant (PrPsc), accumulating in extracellular prion-amyloid aggregates, accompanied by neuronal death, spongiform vacuolation and astrogliosis. There are several indications that the pathogene-

sis of prion disease is modulated by the UPS: (1) PrP can be ubiquitinated and is possibly an ERAD substrate (Yedidia *et al.*, 2001), (2) UPS inhibition promotes aggregation of mutant PrP and also (3) promotes a cytosolic conversion of wild-type PrP to mutant PrP *in vitro* (Ma and Lindquist, 2002; Ma *et al.*, 2002). In addition, (4) prion infection reduces proteasome activity *in vitro* and *in vivo* (Kristiansen *et al.*, 2007).

A null-mutation in the mouse *Mgrn1* gene, responsible for the coat color mutation *mahoganoid*, leads to a phenotype resembling prion disease neuropathology, including progressive spongiform neurodegeneration starting from 2 months of age. Vacuolation of the grey matter and astrogliosis begin around 11-12 months. No accumulation of PrPsc was observed in these mice. The *Mgrn1* (mahogunin) mRNA has 4 isoforms which express a RING domain, possibly identifying mahogunin as a RING-E3 ubiquitin ligase. Indeed, mahogunin exhibits E3 ligase activity *in vitro*, suggesting that defective substrate ubiquitination might underlie the prion disease phenotype *in vivo* (He *et al.*, 2003). When these *Mgrn1* null mutant mice were analyzed for changes in protein expression, many mitochondrial proteins showed reduced expression levels. Indeed, mitochondrial activity was decreased, leading to mitochondrial dysfunction in animals by 1 month of age. Several other proteins were upregulated in the brain of these mutant mice. Possibly these proteins are normally targets for *Mgrn1*-mediated ubiquitination and subsequent proteasomal degradation (Sun *et al.*, 2007).

CHIP KO mice

The CHIP protein directly connects the chaperone system and the UPS with neurodegeneration. CHIP facilitates proteasomal degradation of Hsp70 bound phospho-tau through its E3 ligase activity (Petruccielli *et al.*, 2004). The majority of CHIP KO mice (Dai *et al.*, 2003) showed a motor deficit, were smaller than wild-type littermates and died prematurely on day 30-35 (Dickey *et al.*, 2006). In these symptomatic CHIP KO mice the Hsp70 levels were decreased. The levels of soluble phospho-tau and total tau were significantly increased, confirming a role for CHIP in turnover of tau protein. Poly-ubiquitinated tau was absent in the CHIP KO model, even though the phospho-tau levels were high. Abnormal tau accumulation consisted of phospho-tau species, but not the conformationally altered tau which is seen in, for instance, AD.

In this model, CHIP proved to be essential for ubiquitination and degradation of phospho-tau. This model could be useful to dissect the role of the chaperone system in tau-related neurodegeneration in human, where the balance between phosphorylation of tau and ubiquitin-dependent degradation of phospho-tau is possibly regulated by CHIP. In disease, a diminished UPS function or increased levels of abnormally phosphorylated tau could disturb this balance. The levels of ubiquitinated phospho-tau then exceed the proteasome capacity for degradation, and ubiquitination of phospho-tau by CHIP will now mediate the aggregation of these tau species into ubiquitin-positive stable aggregates. The

latter mechanism might protect neuronal cells against the excess of possibly toxic soluble (hyper-) phospho-tau species (Dickey *et al.*, 2006).

Lmp2 KO mice

In a mouse model lacking functional expression of the low mass protein 2 (*Lmp2*, *Psmb9*) β 1i subunit of the immuno-proteasome, no substantial abnormalities were found. Proteasome activity levels in the brain remained unchanged, although changes in activity were observed in peripheral tissues (Van Kaer *et al.*, 1994). Recently, proteasomal activity of *Lmp2* KO brain tissue was studied in more detail, showing a lower chymotrypsin and peptidyl-glutamyl-peptide hydrolyzing activity at 4 months of age, as well as a more robust age-related decline in 20S and 26S proteasome activity at 12 months of age (Ding *et al.*, 2006). At 3-4 months, these mice showed enhanced motor function accompanied by an increase in body weight. A direct correlation between loss of the *Lmp2* proteasome sub-unit and the increase in motor function remains unclear (Martin *et al.*, 2004).

Atg KO mice

Recently it was shown that disturbance of the autophagy system can also induce a neurodegenerative phenotype. Autophagy is a process involved in bulk protein turnover and is especially important for nutrient supply during starvation. Constitutive basal autophagy also plays a role in degradation of cytosolic proteins, as does the UPS, and declined macro-autophagy as well as chaperone mediated autophagy are implicated in neurodegenerative disease (reviewed by (Nixon, 2006)). In mice deficient for neuronal autophagy-related 7 protein (*Atg7*, (Komatsu *et al.*, 2006)) or autophagy-related 5 (*Atg5*, (Hara *et al.*, 2006)) autophagy was impaired in cells of neural lineage. These mice showed a neurodegenerative phenotype, including motor deficits and massive neuron loss in several brain areas. Strikingly, in both the *Atg7* and the *Atg5* KO mice IBs containing ubiquitinated proteins appeared in a time-dependent manner, preceded by accumulation of ubiquitinated diffuse abnormal proteins in the *Atg5* KO mice and without altering proteasome function in the *Atg7* KO mice.

These two mouse models show that the autophagic pathway is important for maintaining intracellular homeostasis and that age-dependent accumulation of ubiquitinated proteins occurs even when the UPS is fully functional. Currently it is still undetermined if the UPS and autophagy operate separately or cooperatively in removing proteins from the intracellular environment in these mice (Hara *et al.*, 2006; Komatsu *et al.*, 2006). Conversely, UPS inhibition can induce autophagy in cell culture and also in *Drosophila*, possibly to alleviate ER stress induced by proteasome impairment (Ding *et al.*, 2007; Pandey *et al.*, 2007). In addition, autophagy was shown to be the compensatory degradation system for UPS impairment in a *Drosophila* model for the neurodegenerative disease spinobulbar muscular atrophy (Pandey *et al.*, 2007).

Table 2 Mouse models for neurodegeneration with a defective UPS

Model	Mutation	Function	Neuropathology	Reference(s)
parkin KO	parkin Δexon 3	RING-E3	striatal DA level ↑, striatal synaptic excitability ↓, motorfunction ↓, levels of parkin substrates unaltered decreased mitochondrial function	(Goldberg <i>et al.</i> , 2003) (Palacino <i>et al.</i> , 2004)
	parkin Δexon 3	RING-E3	limbic DA level ↑, limbic DA metabolism ↑, striatal DA transporter levels ↓, hippoc. glutamate release inhibited, motorfunct. ↓ protein levels of parkin substrates ↑, altered levels of UPS proteins	(Itier <i>et al.</i> , 2003) (Periquet <i>et al.</i> , 2005)
	parkin Δexon 7	RING-E3	noradrenalin in spinal cord & olf bulb ↓, acoustic startle response ↓, catecholaminergic neuron loss in locus coeruleus levels of parkin substrate p38/JTV-1 ↑, other substrates unaltered	(Von Coelln <i>et al.</i> , 2004) (Ko <i>et al.</i> , 2005)
	parkin Δexon 2	RING-E3	no DA or behavioral phenotype	(Perez and Palmiter, 2005)
	<i>quaking</i> ¹	RING-E3	demyelinisation of CNS striatal DA receptor level ↑, DA metabolism ↑, motorfunction ↓ noradrenergic neurons in locus coeruleus ↑	(Sidman <i>et al.</i> , 1964) (Nikulina <i>et al.</i> , 1995) (Le Saux <i>et al.</i> , 2002)
Uchl1 KO	<i>gad</i> ¹ , Uchl1 Δexon 7-8	DUB	sensory ataxia, locomotor deficits, premature death (6 months), axonal dystrophy of the gracile tract, gracile nucleus degeneration diffuse APP and Aβ accumulation ubiquitin dot-like inclusions proteasome immunoreactivity ↑ mono-ubiquitin levels ↓	(Yamazaki <i>et al.</i> , 1988) (Ichihara <i>et al.</i> , 1995) (Wu <i>et al.</i> , 1996) (Saigoh <i>et al.</i> , 1999) (Osaka <i>et al.</i> , 2003)
UCHL1 mutant	UCHL1 193M	DUB	DA neuron loss in SN, striatal DA levels ↓, ubiquitin/UCHL1 positive inclusions, motorfunction ↓	(Setsuie <i>et al.</i> , 2007)
Uchl3 KO	Uchl3 Δexon 3-7	DUB	no gross phenotypic abnormalities abnormal dorsal root ganglion cells, dystrophic axons spatial learning and memory deficits	(Kurihara <i>et al.</i> , 2000) (Kurihara <i>et al.</i> , 2001) (Wood <i>et al.</i> , 2005)
Usp14 KO	<i>ataxia</i> ¹ , Usp14 IAP exon 5	DUB	neurological deficits; tremor, paralysis, premature death (6-10 weeks), slight abnormalities CNS morphology synaptic transmission NMJ and hippoc. ↓ mono-ubiquitin levels ↓	(D'Amato and Hicks, 1965) (Wilson <i>et al.</i> , 2002) (Anderson <i>et al.</i> , 2005)

Table 2 Mouse models for neurodegeneration with a defective UPS (continued)

Model	Mutation	Function	Neuropathology	Reference(s)
ataxin3 mutant	mjd1a-Q79 fragment	DUB	motorfunction ↓, cerebellar atrophy, Purkinje cell loss	(Ikeda <i>et al.</i> , 1996)
	ataxin-3 polyQ YAC	DUB	motorfunction slightly ↓, pontine & dentate nucleus atrophy, ubiquitin positive inclusions	(Cemal <i>et al.</i> , 2002)
	mjd1a-Q71	DUB	motorfunction ↓, ubiquitin positive inclusions, neuron loss in SN, premature death, mjd1a cleavage fragment detected	(Goti <i>et al.</i> , 2004)
Ube3a KO	Ube3a Δexon 2 (maternal)	HECT-E3	motorfunction ↓, inducible seizures, EEG abnormalities, protein levels of Ube3a substrate p53↑, learning and memory deficits, LTP↓ misregulation of hippocampal CamKIIα	(Jiang <i>et al.</i> , 1998) (Weeber <i>et al.</i> , 2003)
	Ube3a Δexon 15-16 (maternal)	HECT-E3	motorfunction ↓, EEG abnormalities, unaltered protein levels of Ube3a substrate p53, learning and memory deficits sleep disturbances altered Purkinje cell firing	(Miura <i>et al.</i> , 2002) (Colas <i>et al.</i> , 2005) (Cheron <i>et al.</i> , 2005)
Mgrn1 KO	<i>mahogany</i> non-agouti curly ¹ , Mgrn1 mutation intron 9	RING-E3	progressive spongiform neurodegeneration, vacuolation of gray matter, astrogliosis from 11-12 months mitochondrial dysfunction	(He <i>et al.</i> , 2003) (Sun <i>et al.</i> , 2007)
CHIP KO	CHIP Δexon 1-3	U-box E3	premature death (5 weeks), motorfunction ↓, soluble phospho-tau and total tau ↑, absence of poly-ubiquitinated tau	(Dickey <i>et al.</i> , 2006)
Lmp2 KO	Lmp2 Δexon 2 / intron 2 (partial)	20S β1-immuno subunit	proteasome activity ↓, protein oxidation ↑ motor function ↑	(Ding <i>et al.</i> , 2006) (Martin <i>et al.</i> , 2004)
Atg5 KO	Atg5 Δexon 3	autoph. enzyme	motorfunction ↓, massive neuron loss, ubiquitin positive inclusions, diffuse accumulation of ubiquitinated proteins	(Hara <i>et al.</i> , 2006)
Atg7 KO	Atg7 mutation exon 14	autoph. enzyme	motorfunction ↓, massive neuron loss, ubiquitin positive inclusions	(Komatsu <i>et al.</i> , 2006)

¹ spontaneous mutant

Mouse models to measure UPS activity in vivo

Correlation of proteasome activity with genetic or pharmacological manipulation in mouse models for neurological diseases can also specify the role of the UPS. The activity of the UPS may be monitored using fluorescent substrates, e.g. by monitoring proteolytic cleavage of small fluorogenic substrates. Various probes have been developed for the three different catalytic activities of the proteasome. Most of these substrates are directly processed by the 20S core, without the necessity of the 19S particle and do not require ubiquitination for degradation. The total proteasome content of a sample may also influence the level of measured activity. A second method of measuring UPS activity is monitoring the turnover of well-defined endogenous substrates of the UPS. In this case, the proteasome has to be fully assembled to degrade these substrates. It should be taken into account that proteasome activity is time and cell type-specific and also depends on the ubiquitination capacity (reviewed in (Lindsten and Dantuma, 2003)). Another caveat is that these substrates should be properly ubiquitinated and that they are translation dependent. There are indications that inhibition of the proteasome also affects protein synthesis (Ding *et al.*, 2006), possibly affecting turnover of these substrates.

Vast progress was made in measuring UPS activity by the development of fluorescently tagged UPS reporter substrates (reviewed by (Neefjes and Dantuma, 2004)). These short-lived substrate proteins contain an artificial degron and are degraded by the proteasome. When the UPS is inhibited, these fluorescent substrates will accumulate and may be directly visualized and quantitatively analyzed (Table 3). Dantuma *et al.* developed various fluorescent reporter substrates by generating ubiquitin-green fluorescent protein (GFP) fusion proteins with a short half-life, which are based on the N-end rule degron. A UFD substrate was developed as well, by attaching an uncleavable ubiquitin moiety to GFP. In this case, the ubiquitin acts as an acceptor for additional ubiquitin moieties forming a K48 linked chain, after which the whole construct, including the GFP, is efficiently targeted for proteasomal degradation. These substrates (e.g. Ub-R-GFP and Ub^{G76V}-GFP) give very low background fluorescence in living cells and accumulate readily after treatment with UPS inhibitors (Dantuma *et al.*, 2000). Analogous to these GFP-based substrates, various types of substrates with a yellow fluorescent protein (YFP) tag have also been developed, including a YFP-tagged ERAD substrate based on the T-cell receptor subunit CD3δ, an N-end rule substrate, a UFD substrate and a substrate containing a CL-1 degron (Menendez-Benito *et al.*, 2005), based on the previously described GFP-CL1 (Bence *et al.*, 2001). By developing a transgenic mouse line ubiquitously expressing the Ub^{G76V}-GFP construct, it also became feasible to monitor UPS activity *in vivo*. Transgene expression was confirmed in many tissues ranging from heart to brain tissue, the latter shown by accumulation of the reporter in cultured primary neurons after treatment with proteasome inhibitor and after infection with UBB⁺¹ (Lindsten *et al.*, 2003); this also occurred in cortical organotypic cultures of these transgenic mice (van Tijn *et al.*, 2007).

Table 3 UPS reporter constructs

UPS Reporter Construct	Degradation Signal	Reporter Molecule	Tg Line	Comments	Reference(s)
Ub-R-GFP; Ub-L-GFP	N-end rule	GFP			(Dantuma <i>et al.</i> 2000)
Ub-P-GFP; Ub ^{G76V} -GFP	UFD	GFP	yes		(Dantuma <i>et al.</i> 2000); (Lindsten <i>et al.</i> 2003)
Ub-R-YFP	N-end rule	YFP			(Menendez-Benito <i>et al.</i> 2005)
Ub ^{G76V} -YFP	UFD	YFP			(Menendez-Benito <i>et al.</i> 2005)
CD3δ-YFP	ERAD substrate	YFP			(Menendez-Benito <i>et al.</i> 2005)
YFP-CL1	C-terminal CL1-degron	YFP			(Menendez-Benito <i>et al.</i> 2005)
polyUb-β-lactamase	UFD	β-lactamase-CCF2			(Stack <i>et al.</i> 2000)
Ub-FL	UFD	firefly luciferase		<i>in vivo</i> UPS imaging	(Luker <i>et al.</i> 2003)
GFP ^u	C-terminal CL1-degron	GFP			(Bence <i>et al.</i> 2001)
GFPdgn	C-terminal CL1-degron	GFP	yes		(Kumarapeli <i>et al.</i> 2005)
EGFP-HC (GFP-HLA-A2)	ERAD	GFP		when co-expressed with viral US11	(Kessler <i>et al.</i> 2001); (Fiebiger <i>et al.</i> 2002)
6xHisUb/GFP	-		yes		(Tsirigotis <i>et al.</i> 2001)
6xHisUb ^{K48R} /GFP	-	GFP, histidine	yes	for monitoring ubiquitination	(Zhang <i>et al.</i> 2003)
6xHisUb ^{K63R} /GFP	-		yes		(Zhang <i>et al.</i> 2003)

Using this transgenic model, the role of the UPS can be analyzed *in vivo* and further elucidated by cross breeding this line with neurodegenerative mouse models. One of the first examples hereof is a study by Bowman *et al.*, in which the Ub^{G76V}-GFP mice were crossed with a transgenic model for SCA-7, showing that in Ub^{G76V}-GFPxSCA7 mice, IBs were not directly linked to UPS inhibition (Bowman *et al.*, 2005).

Another reporter based on the UFD degradation signal is a β-lactamase fused to two Ub^{G76V} moieties. This reporter has an *in vitro* half-life of less than 10 minutes, which decreases even further when more uncleavable ubiquitins are added to the construct (Stack *et al.*, 2000). This mechanism of creating a degradation signal by fusing Ub^{G76V} moieties to a substrate was also true for GFP and pro-caspase-3, making this poly-ubiquitin signal a

general applicable mechanism to tag proteins for degradation (Stack *et al.*, 2000). A similar model involving this principle employs a firefly luciferase-based reporter (Ub-FL) of which the N-terminus is fused to four Ub^{G76V} moieties (Luker *et al.*, 2003). Luker et al. showed that this reporter is degraded in cell lines, unless the UPS was inhibited. In Ub-FL xenografts re-implanted in mice, the background fluorescence was nearly undetectable. After treatment with clinically relevant doses of the UPS inhibitor bortezomib (used to treat multiple myeloma) UPS inhibition was visualized *in vivo* by measuring the bioluminescence of the Ub-FL xenografts. This approach also allowed multiple measurements of UPS activity over time (Luker *et al.*, 2003), since the measurement can be performed with a lumino-scanner in living animals.

Besides these N-end rule and UFD based UPS reporters, also other UPS reporter constructs have been developed, such as the GFP-tagged ERAD substrate MHC class 1 heavy chain, when co-expressed with the human cytomegalovirus proteins US2 or US11 (Kessler *et al.*, 2001; Fiebiger *et al.*, 2002) and the UPS reporters based on the 16 amino acid long CL-1 degron fused to the C-terminus of GFP (Bence *et al.*, 2001; Kumarapeli *et al.*, 2005). Using this latter CL-1 reporter (GFP-unstable; GFP^u), which has a protein half-life of 20-30 minutes, it was shown that protein aggregation induced by expression of a huntingtin fragment with an expanded polyQ repeat or a folding mutant involved in cystic fibrosis lead to accumulation of the GFP^u reporter, indicating impairment of the proteasome (Bence *et al.*, 2001). On the other hand, it was shown in a different study, using the previously mentioned Ub^{G76V}-GFP and Ub-R-GFP reporters, that aggregate formation of polyQ proteins did not induce accumulation of these reporters (Verhoef *et al.*, 2002). This discrepancy between the two reporter systems indicates that both might respond to a blockade of different components of the UPS pathway. Using GFP^u it was also shown that, in cell lines, overexpression of PD-related mutant α -synuclein decreased UPS activity and increased the sensitivity to proteasome inhibition, an effect rescued by the E3 parkin (Petrucelli *et al.*, 2002). In a transgenic line expressing a similar GFP reporter (GFPdgn), accumulation of GFP was present in many tissues after intravenous and intraperitoneal injection with the UPS inhibitor MG262. However, in contrast to the Ub^{G76V}-GFP transgenic mice, a significant level of background baseline fluorescence was detected. This makes it possible to study not only UPS impairment by measuring accumulation of GFP, but also activation of the UPS, by observing decreases in GFP levels (Kumarapeli *et al.*, 2005).

Furthermore, models have been engineered for monitoring the ubiquitination process. Tsirigotis et al. developed a mouse model expressing a 6xHis-Ub/GFP fusion protein under the UbC promoter to monitor protein ubiquitination. By analyzing epitope-tagged ubiquitin patterns and identifying the ubiquitinated proteins, more can be learned about general ubiquitination *in vivo* (Tsirigotis *et al.*, 2001). In a similar fashion, transgenic lines were designed with 6xHisUb^{K48R}/GFP or 6xHisUb^{K63R}/GFP fusion constructs to study

defective K48 or K63 ubiquitination. Overexpressing Ub^{K48R} mediated a protective effect against viral insults (Zhang *et al.*, 2003) and other cellular stressors (Gray *et al.*, 2004), and delayed the onset of neurological disease symptoms in a familial amyotrophic lateral sclerosis mouse model (Gilchrist *et al.*, 2005) and in a transgenic mouse model for SCA-1 (Tsirigotis *et al.*, 2006).

Concluding remarks

Evidently, the UPS fulfills an important role in maintaining neuronal homeostasis by regulating a variety of processes and by serving as a protein quality control mechanism to rid the cell of aberrant or misfolded proteins. The latter is of especial importance for the pathogenesis of neurodegenerative disease, where abnormal accumulation of proteins can be found in the disease hallmarks. In many of these proteinaceous aggregates, components of the UPS machinery and chaperone proteins are present, indicating a direct link between the UPS and disease. Furthermore, the decreases in proteasome activity, found in, for instance, AD and PD, and the increasing evidence for ubiquitin modification of disease-related proteins, point to an important role for this system in neuropathogenesis. In sporadic forms of neurodegenerative disease it is not yet fully understood if malfunctioning of the UPS is a result of the disease progression or if it is an initial factor in disease onset. This issue is further complicated by the fact that many disease-related proteins are also ubiquitin-modified in a non-diseased state to exert their normal function or to regulate their half-life. The diversity of possible ubiquitin linkages on substrates, including (multiple) mono-ubiquitination and K48-linked and K63-linked poly-ubiquitination, also adds to the complexity of the role of the UPS in neurodegenerative disease.

The current advancements towards resolving the fundamental mechanisms of proteasomal degradation *in vivo*, using the increasing diversity of UPS model systems, will contribute to unraveling the role of the UPS in neuropathogenesis and in the pathogenesis of many other diseases. Further research could also elucidate if there are means by which altering the UPS with chemical compounds, such as UPS inhibitors, or by silencing specific components of the UPS machinery, might alter disease progression in a favorable way (Hol *et al.*, 2006).

Acknowledgements

We thank The Netherlands Brain Bank, Amsterdam and R.A.I. de Vos, Laboratory of Pathology Oost Nederland for supply of the brain material of an AD and Lewy body disease patient, and B. Hobo for providing technical assistance with immunostainings. Wilma Verweij provided text suggestions. This research was supported by the ISAO

CHAPTER I

#01504 and #06502, Hersenstichting Nederland #12F04.01, #15F07.48 and #H00.06 and NWO GPD #970-10-029 and #903-51-192.

CHAPTER I

Scope and Outline

Scope and outline of this thesis

The ubiquitin-proteasome system (UPS) is of vital importance for maintaining intracellular homeostasis, as it is the main regulated pathway for degradation of aberrant, misfolded and short-lived proteins. Increasing evidence suggests that impairment of this pathway is involved in the pathogenesis of a broad array of neurodegenerative disorders, which are characterized by ubiquitin-positive protein aggregates. This is further exemplified by a range of murine models, wherein mutations in components of the UPS can induce a neurological phenotype, reviewed in **Chapter 1**.

Another compelling indication for malfunctioning of the UPS in neurodegenerative disease is the accumulation of a mutant ubiquitin, UBB⁺¹, in the neuropathological hallmarks of tauopathies, including Alzheimer's disease (AD), and in the hallmarks of Huntington's disease. The aim of this thesis is to dissect the effects of UBB⁺¹ on UPS function and relate this to neurodegenerative disease *in vitro* and *in vivo*.

In **Chapter 2**, we characterize the *in vitro* properties of UBB⁺¹ regarding proteasome activity in cell lines and in organotypic cortex cultures. We demonstrate in a human cell line, using a green fluorescent based reporter for proteasome activity, that UBB⁺¹ properties shift from proteasome substrate to a (reversible) proteasome inhibitor in a dose-dependent manner. Also in mouse organotypic cortex slices, UBB⁺¹ accumulation and subsequent UPS inhibition is present only at high expression levels.

These findings are further corroborated *in vivo* in **Chapter 3** and **Chapter 4**, where we describe the generation and characterization of transgenic mouse models neuronally expressing varying levels of UBB⁺¹. We generated the high expression UBB⁺¹ transgenic lines 3413 and 8630, showing accumulation of the UBB⁺¹ protein mainly in the cortex, hippocampus and striatum, as described in **Chapter 3**. Although no overt neuropathology is present in these mice, line 3413 transgenic mice do show decreased cortical proteasome activity, accompanied by accumulation of ubiquitinated proteins and alterations in proteins involved in energy metabolism or organization of the cytoskeleton. UBB⁺¹ induced proteasome inhibition also gives rise to a moderate spatial memory deficit in the Morris watermaze and in Pavlovian fear conditioning at the age of 9 months.

In **Chapter 4**, we describe the transgenic mouse line 6663, expressing low levels of UBB⁺¹. Similar to our previous observations *in vitro* in Chapter 2, the UBB⁺¹ protein is a substrate for proteasomal degradation at low expression levels *in vivo* and therefore, the UBB⁺¹ protein is scarcely detectable in the brains of line 6663 transgenic mice. UBB⁺¹ accumulates only after intracranial administration of proteasome inhibitors. Using this transgenic line 6663, we also provide *in vivo* confirmation that UBB⁺¹ accumulation serves as an endogenous marker for proteasome inhibition.

The relation between UPS inhibition and cognitive behavior is further studied in **Chapter 5**. We show that the defect in spatial memory in the watermaze at 9 months of

age, described in Chapter 3, persists up to the age of 15 months. This defect is not accompanied by other gross neurological defects. Also motor coordination, assessed using the rotarod paradigm, is not affected in the 3413 UBB⁺¹ transgenic mice up to the age of 15 months.

In **Chapter 6**, we study the effect of UBB⁺¹ induced UPS inhibition on AD pathogenesis. Therefore, we crossed the 3413 transgenic mice with a transgenic mouse model for AD, expressing mutant amyloid precursor protein and mutant presenilin 1, showing cerebral amyloid deposition. By measuring the plaque burden in UBB⁺¹/AD triple transgenic mice during aging, we demonstrate that UBB⁺¹ induced proteasome inhibition significantly decreases the plaque load in the cortex and dentate gyrus at 6 months of age compared to AD control mice, without affecting the levels of UBB⁺¹ accumulation.

In **Chapter 7**, we critically discuss the results presented in this thesis and provide possible mechanisms for UBB⁺¹ induced proteasome inhibition. In addition, pathways underlying the cognitive deficits of the UBB⁺¹ transgenic mice are further addressed. Finally, the role of UBB⁺¹ accumulation and concomitant proteasome inhibition is discussed in relation to human neurodegenerative disease and suggestions for future research are provided.

CHAPTER II

Dose-dependent inhibition
of proteasome activity by a mutant ubiquitin
associated with neurodegenerative disease

Journal of Cell Science, 2007; 120(Pt 9): 1615-1623

Paula van Tijn*, Femke M.S. de Vrij*, Karianne G. Schuurman,
Nico P. Dantuma, David F. Fischer, Fred W. van Leeuwen, Elly M. Hol

* *these authors contributed equally*

Summary

The ubiquitin-proteasome system is the main regulated intracellular proteolytic pathway. Increasing evidence implicates impairment of this system in the pathogenesis of diseases with ubiquitin-positive pathology. A mutant ubiquitin, UBB⁺¹, accumulates in the pathological hallmarks of (i) tauopathies, including Alzheimer's disease, (ii) polyglutamine diseases, (iii) liver disease and (iv) muscle disease and serves as an endogenous reporter for proteasomal dysfunction in these diseases. UBB⁺¹ is a substrate for proteasomal degradation, however it can also inhibit the proteasome. Here, we show that UBB⁺¹ properties shift from substrate to inhibitor in a dose-dependent manner in cell culture using an inducible UBB⁺¹ expression system. At low expression levels, UBB⁺¹ was efficiently degraded by the proteasome. At high levels, the proteasome failed to degrade UBB⁺¹, causing accumulation of UBB⁺¹ which subsequently induced a reversible functional impairment of the ubiquitin-proteasome system. Also in brain slice cultures, UBB⁺¹ accumulation and concomitant proteasome inhibition was only induced at high expression levels. Our findings show that by varying UBB⁺¹ expression levels, the dual proteasome substrate/inhibitory properties can be optimally employed to serve as research tool to study the ubiquitin-proteasome system and to further elucidate the role of aberrations of this pathway in disease.

Introduction

The main function of the ubiquitin-proteasome system (UPS) is proteolytic degradation of target substrates, including aberrant and misfolded proteins, to maintain cellular homeostasis (Glickman and Ciechanover, 2002). UPS-mediated post-translational regulation is also involved in many other cellular pathways such as transcription, DNA repair and endocytosis (Welchman *et al.*, 2005). Ubiquitin (Ub) tags proteins for degradation through an enzymatic cascade, consisting of Ub activating (E1), Ub conjugating (E2) and Ub ligating (E3) enzymes. Via this pathway, a Ub is conjugated to internal lysine residues in substrate proteins. Through the sequential addition of Ub molecules to the substrate-bound Ub, a poly-Ub tree is formed which targets the substrate protein for degradation by the 26S proteasome (Glickman and Ciechanover, 2002; Pickart and Cohen, 2004).

As the UPS is important for maintaining intracellular homeostasis, it is not surprising that impairment of the UPS has been observed to occur in the pathogenesis of numerous diseases, often demonstrated by the accumulation of Ub conjugates or other components of the UPS machinery in protein aggregates (Ciechanover and Brundin, 2003). One of the disease-specific proteins which accumulates is ubiquitin-B⁺¹ (UBB⁺¹), a mutant form of Ub formed by a di-nucleotide deletion in the mRNA of the ubiquitin B gene (van Leeuwen *et al.*, 1998). Previous *in vitro* results showed that UBB⁺¹ is ubiquitinated and appears

to be a protein with dual properties; on one hand it acts as a ubiquitin-fusion-degradation (UFD) substrate for the proteasome, on the other hand, it acts as a specific inhibitor of the proteasome (Lam *et al.*, 2000; Lindsten *et al.*, 2002). UBB⁺¹ accumulation eventually leads to apoptotic cell death (De Vrij *et al.*, 2001; De Pril *et al.*, 2004) and induces expression of heat-shock proteins (Hope *et al.*, 2003).

In the diseased brain, UBB⁺¹ accumulates in the neuropathological hallmarks of tauopathies; e.g. in neuronal tangles in Alzheimer's disease (AD), but also in astrocytes in progressive supranuclear palsy (Fischer *et al.*, 2003; van Leeuwen *et al.*, 2006). UBB⁺¹ is also found in intranuclear inclusions characteristic for polyglutamine diseases (De Pril *et al.*, 2004). Outside the nervous system, UBB⁺¹ accumulates in the inclusion bodies of the muscle disease inclusion-body myositis (Fratta *et al.*, 2004) and in Mallory bodies of chronic liver disease (McPhaul *et al.*, 2002). We reported that *UBB*⁺¹ mRNA is present in equal levels in non-demented control individuals compared to AD patients (Fischer *et al.*, 2003; Gerez *et al.*, 2005). This suggests that the *UBB*⁺¹ mRNA transcript is always present. The UBB⁺¹ protein, however, seems to be efficiently degraded in healthy control subjects. Through a decline in UPS activity, for example by aging or disease related processes, the degradation of the UBB⁺¹ protein might be affected to such an extent that accumulation of the protein commences. Therefore we have proposed that UBB⁺¹ accumulation can serve as an endogenous reporter for a decreased UPS activity (Fischer *et al.*, 2003). Once accumulated, UBB⁺¹ can contribute to disease pathogenesis by inhibiting the UPS (e.g. (Hol *et al.*, 2005)). It is conceivable that this accumulation of UBB⁺¹ will only occur after exceeding a threshold level, causing a shift in the protein properties from proteasome substrate to proteasome inhibitor.

Indeed, results from the present study show that in human cell lines expressing inducible UBB⁺¹ levels, the UBB⁺¹ protein is degraded by the 26S proteasome at low expression levels and accumulates only after exceeding a threshold level of expression. In addition, we show that UBB⁺¹ exhibits dose-dependent UPS inhibitory properties. Our experiments show that UBB⁺¹ accumulation and subsequent UPS inhibition are both reversible processes. We further broadened the scope of these novel findings in cell lines to mouse organotypic cortex cultures, which closer resemble the human brain. In agreement with our *in vitro* results, UBB⁺¹ accumulation leads to successive inhibition of the UPS in these organotypic cultures only after surpassing a threshold level of expression. In conclusion, UBB⁺¹ is a protein which can be used as reporter for UPS activity as well as a highly selective dose-dependent UPS inhibitor by differentiating the levels of expression using (inducible) vectors with varying promoter constructs.

Materials and methods

Plasmid construction and viral constructs

Ub, UBB⁺¹ and UBB^{+1K29,48R} open reading frames were cloned in pcDNA3 (Invitrogen) as described earlier (Lindsten *et al.*, 2002). For the Tet-off inducible expression system the UBB⁺¹ open reading frame was cloned downstream of the TRE-minimal cytomegalovirus immediate early (CMV) sequence of a Tet-off expression vector (pRevTRE; Clontech) into pcDNA3 and co-transfected with pRevTet-Off (Clontech). First generation recombinant adenoviral vectors Ad-UBB⁺¹ and Ad-Ub were generated, purified and titered as described elsewhere (Hermens *et al.*, 1997; De Vrij *et al.*, 2001). Adenoviral vectors were based on the Ad5 mutant *dl309* (Jones and Shenk, 1979) and employed the CMV promoter to drive transgene expression. Titration of double CsCl gradient-purified Ad-CMV-UBB⁺¹ and Ad-CMV-Ub on the permissive cell line 911 (Fallaux *et al.*, 1996) revealed titres of 1×10^9 plaque forming units/ml. Lentiviral vectors were generated by cloning DNA encoding Ub-M-GFP, Ub^{G76V}-GFP, UBB⁺¹ or UBB^{+1K29,48R} into the lentiviral transfer plasmid pRRRLsin-ppThCMV. Lentivirus was produced according to Naldini *et al.* (Naldini *et al.*, 1996) and harvested and titered as described previously using a HIV-1 p24 coat protein ELISA (NEN Research, Boston, USA) (De Pril *et al.*, 2004). Virus titres were correlated to titres determined by counting GFP fluorescent cells of an LV-Ub-M-GFP stock. In this way titres of adenoviral and lentiviral stocks could be correlated.

Cell lines and transfections

The human cervical epithelial carcinoma cell line HeLa stably transfected with Ub^{G76V}-GFP (Dantuma *et al.*, 2000) was cultured in high-glucose Dulbecco's modified Eagle medium, containing 10% FCS, supplemented with 100 U/ml penicillin and 100 µg/ml streptomycin (all Gibco). Stable cell line HeLa Ub^{G76V}-GFP was maintained on 60 µg/ml geneticin (G418; Gibco) selection. For Western blot and flow cytometry, HeLa Ub^{G76V}-GFP cells were plated on 6 or 12-wells plates with 1×10^5 cells/well or 0.5×10^4 cells/well respectively one day prior to transfection. Cells were transiently transfected with the calcium-phosphate method using 1 µg/ml DNA per vector. Where mentioned doxycycline (Sigma-Aldrich) treatment was applied 16 hours after transfection. Samples were harvested 48 hours after continuous doxycycline treatment, unless stated otherwise. Where indicated cells were additionally treated with the proteasome inhibitors MG132 (1 µM; Affiniti Research) or epoxomicin (100 nM; Affiniti Research) for 16 hours before samples were taken.

Western blotting

For Western blotting, cells pellets were resuspended in suspension buffer (0.1 M NaCl, 0.01 M Tris-HCl pH7.6, 1 mM EDTA, 1 mM PMSF, 10 µg/ml leupeptin) and lysed by 2 x 20 s sonification. Total protein content was quantified by Bradford measurement, equal protein amounts were fractionated by SDS-PAGE and blotted semi-dry to nitrocellulose filter (Schleicher and Schuell, Germany). UBB⁺¹ was detected using rabbit polyclonal anti-UBB⁺¹ antibody (Ub3 serum; 05/08/97; 1:1000 overnight (De Vrij *et al.*, 2001)) and secondary swine anti-rabbit HRP (Dako; 1:1000) diluted in Supermix (0.05 M Tris-HCl, 0.9% NaCl, 0.25% gelatine and 0.5% Triton-X-100, pH7.4). Blots were developed by enhanced chemoluminescence (Lumilight ECL, Perkin Elmer, USA).

Flow cytometry

For flow cytometry, cell suspensions were fixed in 4% formalin in PBS, and resuspended in PBS-0.5% bovine serum albumin (Roche). GFP could be directly visualized, for UBB⁺¹ cytometry cells were stained with primary antibody anti-UBB⁺¹ (Ub3 serum; 1:500) and secondary antibody anti-rabbit Cy5 (Jackson ImmunoResearch; 1:400). Analysis was performed on at least 10000 cells per sample with a flow cytometer (FACSCalibur, Becton Dickinson Biosciences); data were analyzed using CellQuest software (Becton Dickinson Biosciences).

Organotypic cortex slice cultures

C57Bl/6 or C57Bl/6 Ub^{G76V}-GFP/2 tg mice (Lindsten *et al.*, 2003) were decapitated at post-natal day 5; the brain was transferred to ice cold Gey's Balanced Salt Solution (Sigma-Aldrich) containing 5.4 mg/ml glucose, 100 U/ml penicillin and 100 µg/ml streptomycin (all Gibco). After removal of the meninges, the fronto-parietal part was sliced into 300 µm coronal sections per hemisphere using a tissue chopper (McIlwain). The first four slices were discarded. Slices were cultured on an air-fluid interface on culture plate inserts (Millipore; 0.4 µm pore; 30 mm diameter; 3 cultures per insert) on medium containing 50% Minimum Essential Medium alpha, 25% HBSS, 25% horse serum, 6.5 mg/ml glucose, 2 mM glutamine (all Gibco) and penicillin/streptomycin (100 U/ml, 100 µg/ml). Viral transduction of cultures was achieved by applying 1x10⁶ transducing units of virus in a 10 µl droplet of culture medium on top of the slices. Treatment with epoxomicin (1 µM; Affiniti Research) or MG132 (10 µM; Affiniti Research) was performed in the same manner. Inhibitors were applied for 6 hours and subsequently left on or washed out overnight. Slices were stained free floating with rabbit polyclonal anti-UBB⁺¹ (Ub3 serum; 1:1000), rabbit polyclonal anti-GFAP (DAKO; 1:4000), monoclonal anti-GFP (Chemicon; 1:500) and monoclonal NeuN (Chemicon; 1:400) diluted in Supermix, followed by Cy2

and Cy3 staining (Jackson ImmunoResearch; 1:800) Nuclei were visualised with TO-PRO-3 (Molecular Probes; 1:1000). Subsequently, slices were mounted in mowiol (0.1 M Tris-HCl pH8.5, 25% glycerol, 10% w/v Mowiol 4-88) images were acquired using confocal laser scanning microscopy (Zeiss 510) and accompanying software (Zeiss LSM Image Browser).

Results

UBB⁺¹ accumulates at high expression levels

We hypothesized that the previously described opposing properties of UBB⁺¹ (Lindsten *et al.*, 2002; Hol *et al.*, 2005) can be explained by a dose-dependent shift from UPS substrate to inhibitor. In this study we quantified this effect in living cells using a HeLa cell-line stably expressing the Ub^{G76V}-GFP UPS reporter (Dantuma *et al.*, 2000). Inducible levels of UBB⁺¹ expression were achieved using the Tet-off gene-expression system. UBB⁺¹ protein expression levels were analyzed with Western blot (Fig. 1) and Ub^{G76V}-GFP reporter accumulation was measured in the same sample using flow cytometry (Fig. 2). HeLa cells were transiently transfected with the UBB⁺¹ Tet-off constructs and after 16 hours, doxycycline (dox) was added to the culture medium for 48 hours to regulate UBB⁺¹ expression. Western blot analysis on cell lysates showed that UBB⁺¹ protein accumulation was present only at high expression levels induced by absence of dox (maximal expression) or low dox concentrations ranging from 0 to 0.01 ng/ml (Fig. 1A). In addition, ubiquitination of UBB⁺¹ (Ub-UBB⁺¹) was present in cells which showed UBB⁺¹ accumulation and in cells transiently transfected with a CMV-UBB⁺¹ pcDNA3 high expression control plasmid, as expected (Lindsten *et al.*, 2002) (Fig. 1A). Ubiquitination of UBB⁺¹ is essential for targeting UBB⁺¹ to the proteasome. A double lysine mutant of UBB⁺¹, UBB^{+1K29,48R}, cannot be ubiquitinated and is not targeted to the proteasome (Lindsten *et al.*, 2002). Transient transfection with a CMV-UBB^{+1K29,48R} pcDNA3 plasmid indeed showed an increased accumulation of the non-ubiquitinated form of this protein compared to CMV-UBB⁺¹ pcDNA3 (not shown).

Proteasomal degradation of UBB⁺¹ could explain the absence of accumulation at lower expression levels. Therefore, we treated the UBB⁺¹ Tet-off transfected cells with dox for 48 hours and simultaneously with the reversible proteasome inhibitor MG132 (1 µM) during the final 16 hours before sampling. Indeed, MG132 treatment shifted the regulated expression level at which UBB⁺¹ accumulation could be observed to a lower level (Fig. 1B, lanes marked with arrowheads). From these experiments, we conclude that UBB⁺¹ is degraded by the UPS at sub-maximal expression levels. However, the UPS fails to degrade UBB⁺¹ sufficiently after exceeding a threshold level of expression, leading to stabilization of the UBB⁺¹ protein.

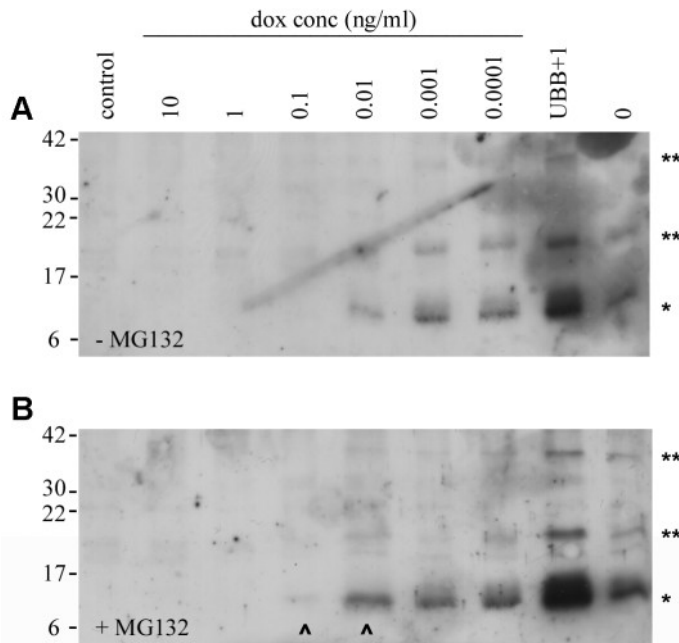


Figure 1 *UBB⁺¹* is degraded by the UPS at low expression levels. A, B: Western blot of cell lysates of HeLa cells transiently transfected with inducible Tet-off CMV-*UBB⁺¹* vectors treated with decreasing dox concentrations. *UBB⁺¹* was detected with anti-*UBB⁺¹* antibody (Ub3 (De Vrij et al., 2001)) in cells without proteasome inhibitor treatment (A) or in cells treated overnight with 1 μ M proteasome inhibitor MG132 (B). CMV-*UBB⁺¹* pcDNA3 (*UBB+1*) and empty pcDNA3 vector (control) transfections served as controls. Arrows in B indicate additional *UBB⁺¹* expression after proteasome inhibitor treatment. Protein input was equal in all lanes determined by Bradford protein measurement (not shown); this is a representative experiment of two duplicate experiments. Molecular mass in kDa is indicated on the left, * *UBB⁺¹*, ** Ub-*UBB⁺¹*.

UBB⁺¹ induces dose-dependent UPS inhibition

Our previous work showed that *UBB⁺¹* can act as a proteasome inhibitor (Lindsten *et al.*, 2002). Thus, we next determined the expression level at which inducible *UBB⁺¹* inhibited the proteasome and if this proteasome inhibition was dose-dependent. Therefore, we transfected stable HeLa *Ub^{G76V}-GFP* cells with the inducible Tet-off *UBB⁺¹* vectors as described in Fig 1. General inhibition of the proteasome leads to accumulation of GFP in this *Ub^{G76V}-GFP* HeLa cell line, a reporter cell line for UPS activity (Dantuma *et al.*, 2000). Indeed, flow cytometric analysis of HeLa *Ub^{G76V}-GFP* cells treated overnight with proteasome inhibitors epoxomicin (irreversible inhibitor, 100nM) or MG132 (reversible inhibitor, 1 μ M) showed a large increase in the percentage of GFP positive cells to ~90% (Fig. 2A). Transient transfection with CMV-*UBB⁺¹* pcDNA3 resulted in significant accu-

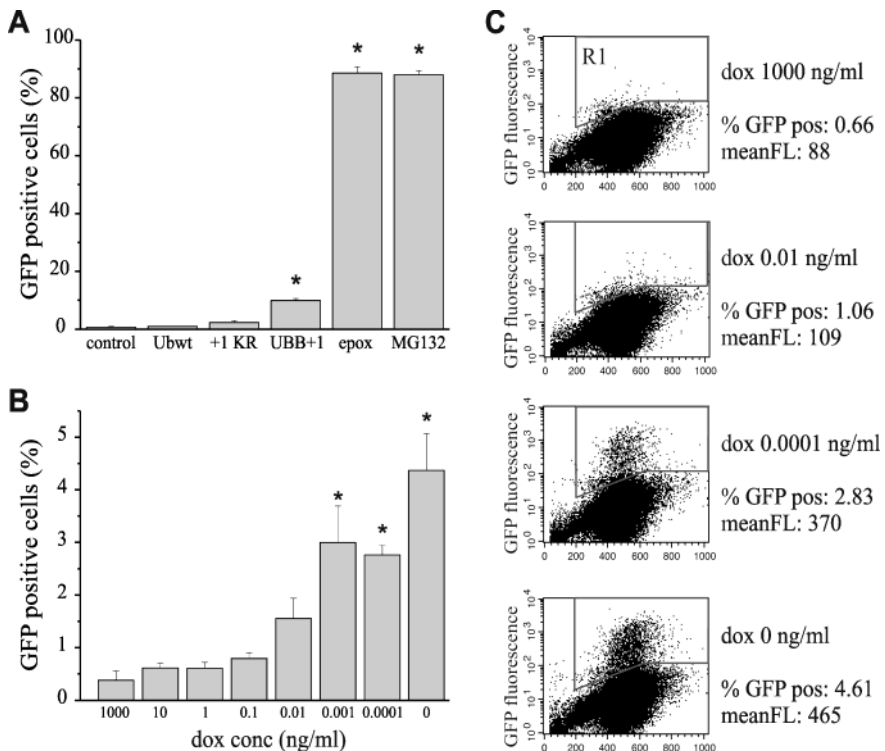


Figure 2 High levels of UBB⁺¹ inhibit the proteasome. Flow cytometric analysis of Ub^{G76V}-GFP HeLa cells for GFP fluorescence as indication of UPS inhibition (% GFP positive cells of total living cells). A: Cells were transiently transfected with empty pcDNA3 vector (control), CMV-Ub wildtype pcDNA3 (Ubwt), CMV-UBB^{+1K29,48R} pcDNA3 (+1KR) or CMV-UBB⁺¹ pcDNA3 (UBB+1) or treated with 100 nM epoxomicin (epox) or 1 μ M MG132. Significant accumulation of GFP compared to empty vector control is marked by an asterisk (* p<0.005, ANOVA Bonferroni). B: Ub^{G76V}-GFP cells were transiently transfected with the inducible Tet-off UBB⁺¹ expression system and treated with decreasing concentrations of dox. Significant increase in percentage of GFP positive cells, compared with levels in cells treated with 1000 ng/ml dox is marked by an asterisk (* p<0.05, ANOVA Bonferroni). Results are the means \pm s.e.m. of three or four independent duplicate experiments. C: Representative flow cytometric scatter plots of UBB⁺¹ Tet-off transfected cells treated with 1000, 0.01, 0.0001 and 0 ng/ml dox as shown in B. GFP positive cells were detected in the region set as R1. The mean GFP fluorescence and the percentage GFP positive living cells in each plot are indicated on the right.

mulation of the GFP reporter in ~10% of the living cells (Fig. 2A), reaffirming our previous observations that UBB⁺¹ acts as a proteasome inhibitor (Lindsten *et al.*, 2002). The discrepancy between the high levels of UPS inhibition achieved with classical inhibitors (~90% GFP positive) compared to UBB⁺¹ (~10% GFP positive) is partially due to the transfection efficiency of UBB⁺¹, which is routinely ~40% in this cell line (data not

shown) and probably also due to the fact that not all UBB⁺¹ positive cells have built up enough expression to surpass the threshold level for UPS inhibition, corroborating our hypothesis that a critical level of UBB⁺¹ must be reached before the protein is stabilized. As expected, transient transfection with CMV-UBB^{+1K29,48R} pcDNA3, which is not directed to the UPS, did not lead to significant UPS inhibition (Fig. 2A). Also transfection of wildtype Ub (CMV-Ub pcDNA3) did not lead to significant accumulation of the GFP reporter (Fig. 2A).

We determined if the proteasome inhibition induced by UBB⁺¹ was dose-dependent by transfecting HeLa Ub^{G76V}-GFP cells with the inducible Tet-off UBB⁺¹ vectors. Maximal UBB⁺¹ expression (absence of dox) was sufficient to induce UPS inhibition, shown by significant accumulation of the GFP reporter, although the percentage of GFP positive cells (4.4%) was lower than after transient transfection with CMV-UBB⁺¹ pcDNA3 (Fig. 2B). Furthermore, increasing GFP reporter accumulation was visible in a range from 0.01 to 0.0001 ng/ml dox, reaching significance at dox concentrations of 0.001 and 0.0001 ng/ml (Fig. 2B). This increase in the percentage of GFP positive cells and in the mean GFP fluorescence intensity is visualised in representative plots in Fig. 2C. These results indicate that UBB⁺¹ inhibited the proteasome in a dose-dependent manner, starting from expression levels at which UBB⁺¹ accumulation commenced.

Accumulation of UBB⁺¹ and UPS inhibition is reversible in living cells

The previous results showed that increasing UBB⁺¹ expression gave rise to dose-dependent UPS inhibition. It is conceivable that this UPS inhibition is irreversible, causing a defective degradation of previously accumulated UBB⁺¹ even after UBB⁺¹ expression is shut down. To verify this we measured the percentage of remaining UBB⁺¹ positive cells after shutting down UBB⁺¹ expression. Ub^{G76V}-GFP HeLa cells were transiently transfected with the Tet-off UBB⁺¹ vectors and expressed high levels of UBB⁺¹ for 64 hours, after which a baseline sample was taken (timepoint 0 hours). UBB⁺¹ expression was continued at high levels and additional samples were taken at 12 hours and 36 hours after the baseline measurement. Alternatively, UBB⁺¹ expression was shut down by adding 10 ng/ml dox and samples were taken at similar timepoints. The percentages of UBB⁺¹ (Fig. 3A) positive cells and GFP/UBB⁺¹ double positive cells indicative for UPS inhibition (Fig. 3B) were determined for every timepoint using flow cytometry (minimal 10000 cells counted per sample).

At the baseline measurement (0 hours), maximal UBB⁺¹ levels were present resulting in 5.3% UBB⁺¹ positive cells (Fig. 3A) leading to 1.3% UBB⁺¹/GFP double positive cells (Fig. 3B). Thus ~25% of the UBB⁺¹ positive cell population also accumulated the GFP reporter, indicating that UBB⁺¹ accumulation preceded inhibition of the UPS, which is in agreement with earlier observations in a different setup (Lindsten *et al.*, 2002). After 12

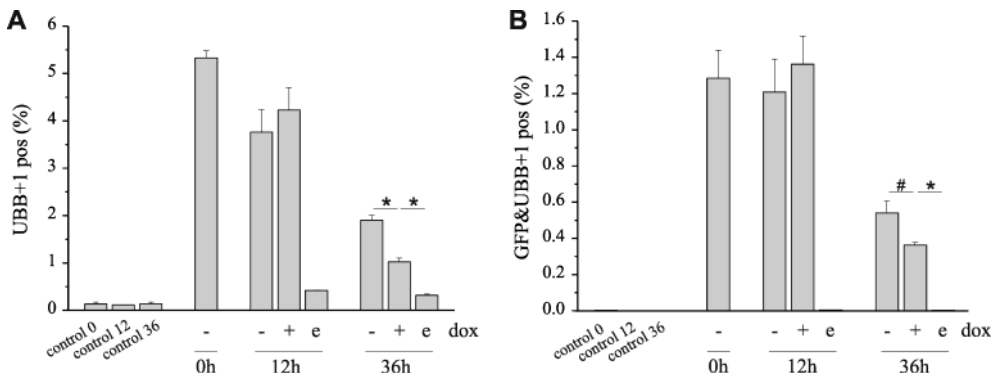


Figure 3 *Accumulation of UBB⁺¹ is reversible after shutting off expression.* Flow cytometric analysis of the percentage of UBB⁺¹ (A) or UBB⁺¹/GFP (B) positive cells at 0 hours, 12 hours and 36 hours after shutting down maximal UBB⁺¹ expression. Ub^{G76V}-GFP HeLa cells were not transfected (control), transfected with empty pcDNA3 vector (e) or transfected with the UBB⁺¹ Tet-off vectors. After 64 hours of maximal expression (absence of dox) a baseline sample was taken (0 hours). UBB⁺¹ expression was continued at maximal levels (dox-) or shut down by addition of 10 ng/ml dox (dox+) and samples were analyzed after 12 hours and 36 hours of dox treatment. Results are the means \pm s.e.m. of two or three independent duplicate experiments. * p<0.01, # p=0.099 ANOVA within timegroup.

hours, continuous UBB⁺¹ expression (dox-) or shutting down expression (dox+) both gave rise to equal slight decreases in UBB⁺¹ protein levels. However, constant UBB⁺¹ expression (dox-) induced a ~50% decrease in the number of UBB⁺¹ positive cells from 3.8% to 1.9% at 36 hours compared to 12 hours after baseline measurement (Fig. 3A). This is presumably caused by either loss of the expression plasmid after transient transfection, or by loss of UBB⁺¹ due to UBB⁺¹ induced cell death as seen in previous experiments (De Vrij et al., 2001). In the condition where the expression of UBB⁺¹ was shut down (dox+) for 36 hours, the percentage of UBB⁺¹ positive cells dropped with ~75% compared with levels 12 hours after dox treatment from 4.2% to 1.0%. This remaining percentage of UBB⁺¹ positive cells (1.0%) was significantly lower than when the cells had continuous UBB⁺¹ expression (1.9%). This indicated that UBB⁺¹ accumulation was reversible at 36 hours after shutting down expression, although the remaining UBB⁺¹ accumulation stayed significantly elevated compared to a transfection control sample (0.3%) (Fig. 3A).

The percentage of UBB⁺¹/GFP double positive cells remained stable after 12 hours in both the dox treated and untreated condition (Fig. 3B). After 36 hours, this population of cells decreased in both the continuous UBB⁺¹ expression condition (dox-) and after shutting down expression (dox+). However, similar to the results for UBB⁺¹ accumulation, the UBB⁺¹/GFP positive cell population was lower in the dox treated condition (dox+) than in the condition with constant UBB⁺¹ expression (dox-), although this effect was not significant (Fig. 3B). This lower amount of GFP reporter accumulation in the condition where

UBB^{+1} expression has been shut down for 36 hours indicated that the UPS inhibition induced by UBB^{+1} was a reversible process. Moreover, possible UBB^{+1} induced cell death should be lower when UBB^{+1} expression is shut down, so the decrease in GFP accumulation can then only be attributed to the reversal of UPS inhibition.

To corroborate these data, we also used a experimental setup where high levels of UBB^{+1} expression were induced with lentiviral (LV) vectors in a human neuroblastoma cell line (SH-SY5Y). By using LV transduction, the UBB^{+1} cDNA integrated in the cellular DNA, leading to stable expression of the protein. With this high continuous LV- UBB^{+1} expression, experiments could be done in a shorter time span in which UBB^{+1} induced cell death did not occur yet. In this setup, LV- UBB^{+1} transduction induced UBB^{+1} accumulation which further increased after overnight inhibition of the UPS with the reversible inhibitor MG132. After restoring proteasome activity by removing MG132, the percentage of UBB^{+1} positive cells decreased significantly compared to the condition in which MG132 was not removed (data not shown), indicating that UBB^{+1} accumulation is a reversible process. The percentage of UBB^{+1} positive cells in the condition with maximal UBB^{+1} expression was comparable to the percentage of positive cells after a control LV- $\text{UBB}^{+1\text{K29,48R}}$ infection. It is known from previous experiments that this control LV-

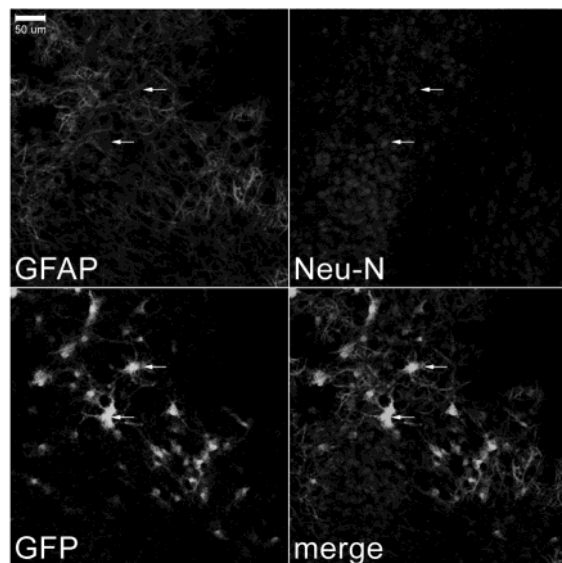


Figure 4 Lentiviral transduction targets a heterogeneous cell population in cortex slice cultures. GFAP (red) and NeuN (blue) double staining on LV-Ub-M-GFP transduced organotypic cortex slice cultures of C57Bl/6 mice revealed mostly GFAP labelled GFP positive glia, but also GFP positive neurons. Arrows indicate transduced neurons, positive for both GFP and NeuN. Bar, 50 μm . See color section.

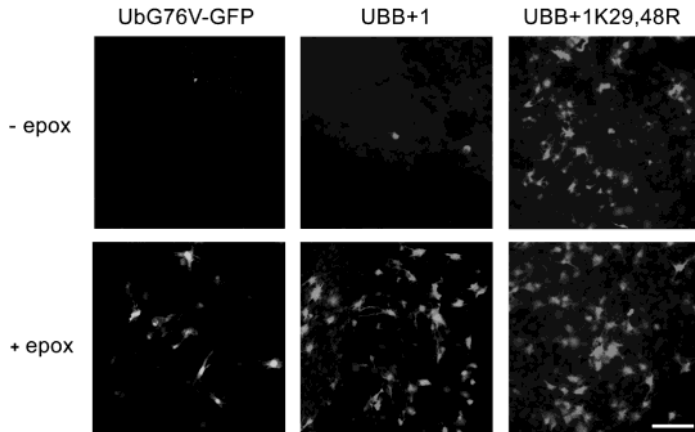


Figure 5 *UBB⁺¹* is degraded by the proteasome in cortex slice cultures. Organotypic cortex slices of C57Bl/6 mice were transduced with LV-Ub^{G76V}-GFP, LV-UBB⁺¹ or LV-UBB^{+1K29,48R}. Both the UPS reporter protein Ub^{G76V}-GFP (green) and UBB⁺¹ (red) are efficiently degraded by the 26S proteasome and only accumulate after treatment with proteasome inhibitor. The lysine mutant of UBB⁺¹, UBB^{+1K29,48R}, is not degraded by the proteasome and accumulates already without inhibitor treatment; - epox: not treated with epoxomicin, + epox: treated overnight with 1 μ M epoxomicin. Bar, 100 μ m. See color section.

UBB^{+1K29,48R} construct does not induce cell death (De Pril *et al.*, 2004), thereby ruling out the possibility that UBB⁺¹ induced cell death affected the reversibility of UBB⁺¹ accumulation in this setup.

Degradation of UPS substrates in organotypic cortex cultures

We then investigated if these results in cell lines also hold true in primary (neuronal) cultures using mouse organotypic cortex slice cultures, so that we could extrapolate our data to neurodegenerative disease conditions. First, we verified that transduction of cells was possible in this setup using LV vectors. Cortex slice cultures of C57Bl/6 mice were infected with Ub-M-GFP, a ubiquitin fusion protein that results in a stable form of GFP (Dantuma *et al.*, 2000). This gave rise to many GFP immuno-positive cells two days after transduction (Fig. 4). The transduced cell population consisted mainly of astrocytes, although also a substantial amount of GFP positive neurons was present in the slice, as demonstrated by double-staining with neuronal (NeuN) and glial (glial fibrillary acidic protein (GFAP)) markers (Fig. 4).

To assess general UPS function in the cortex culture system, slices were LV transduced with the UPS reporter construct Ub^{G76V}-GFP. As shown in Figure 5, Ub^{G76V}-GFP was efficiently degraded by the proteasome and GFP accumulation was only present after

treatment with proteasome inhibitor (1 μ M epoxomicin) (Fig. 5). Transduction of cortex cultures with LV-UBB⁺¹ also did not lead to accumulation of the protein (Fig. 5), in contrast to the neuronal cell cultures. Apparently, the UBB⁺¹ protein was efficiently degraded by the 26S proteasome in cortex slice cultures, as demonstrated by the accumulation of UBB⁺¹ after overnight proteasome inhibition by 1 μ M epoxomicin (Fig. 5). These results indicate that LV-UBB⁺¹ expression leads to sub-threshold expression in this cortex slice system at which the protein does not accumulate. The LV-UBB^{+1K29,48R} mutant showed accumulation of the protein regardless of proteasome inhibition, as expected (Fig. 5).

UBB⁺¹ accumulation is not reversible in cortex cultures

We made use of the reversible proteasome inhibitor MG132 to study if accumulation of UBB⁺¹ in cortex cultures also decreased after wash out of the proteasome inhibitor as we observed in the neuroblastoma cell line experiments. Consistent with results obtained with epoxomicin treatment as shown above, applying MG132 overnight to LV transduced cultures resulted in strong accumulation of both Ub^{G76V}-GFP and UBB⁺¹ (Fig. 6). When MG132 treated cultures were rinsed and allowed to recover, proteasome activity was restored, as demonstrated by the regained capacity to completely degrade the GFP reporter

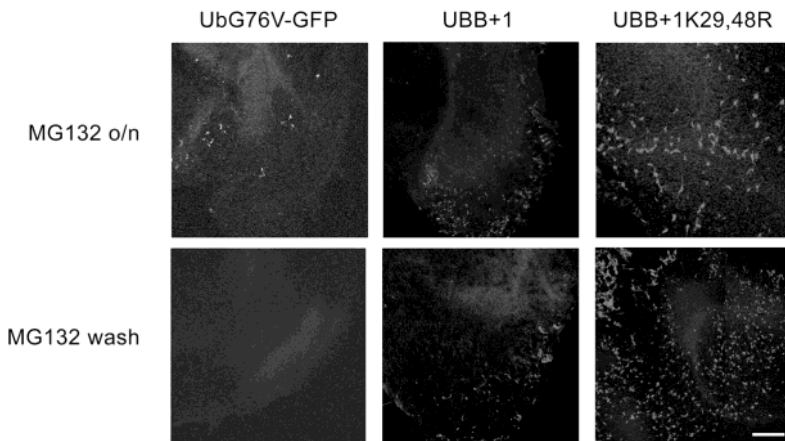


Figure 6 *UBB⁺¹ remains present after washout of inhibitor in cortex slice cultures.* Overnight incubation of cortex cultures transduced with LV-Ub^{G76V}-GFP or LV-UBB⁺¹ with the reversible proteasome inhibitor MG132 (10 μ M) resulted in accumulation of both proteins. Washing out the reversible inhibitor reactivated the proteasome, as shown by the degradation of the proteasome reporter substrate Ub^{G76V}-GFP. However, UBB⁺¹ remained accumulated in a considerable amount of cells after reactivation of the proteasome. Transduction with the LV- UBB^{+1K29,48R} control construct gave rise to accumulation of the UBB⁺¹ protein regardless of proteasome inhibitor treatment. Ub^{G76V}-GFP is depicted in green, UBB⁺¹ in red and the nuclear staining (TO-PRO) in blue. Bar, 500 μ m. See color section.

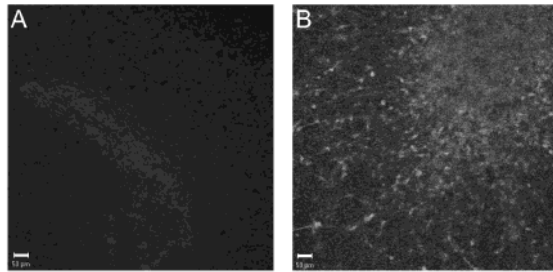


Figure 7 The UPS reporter system in cortex cultures of Ub^{G76V} -GFP transgenic mice. A: Ub^{G76V} -GFP tg organotypic cortex cultures without treatment with proteasome inhibitors. B: Ub^{G76V} -GFP tg cortex cultures treated with 1 μ M epoxomicin. The GFP-reporter substrate only accumulated after proteasome inhibition. Bars, 50 μ m. See color section.

protein (Fig. 6). This restored proteasome activity did not seem capable of degrading accumulated UBB⁺¹ under these washout conditions, as the number of cells containing accumulated UBB⁺¹ after washout of the inhibitor was similar to the number of UBB⁺¹ positive cells after initial transduction (Fig. 6). This indicated that, in contrast the results obtained in cell lines, UBB⁺¹ accumulation in cortex cultures remained present after washout of the proteasome inhibitor, which might be due to the recovery time needed after washout to degrade UBB⁺¹.

Accumulated UBB⁺¹ inhibits the UPS in cortex cultures

In vitro, UBB⁺¹ inhibits the UPS after exceeding a threshold as shown in a Ub^{G76V} -GFP stable HeLa cell line. We employed a Ub^{G76V} -GFP transgenic (tg) mouse line (Ub^{G76V} -GFP/2) to translate these results to our cortex culture setup. In this mouse model, the UPS reporter is ubiquitously expressed and similar to the HeLa cell line, GFP accumulates only after proteasome inhibition (Lindsten *et al.*, 2003). To verify the GFP proteasome reporter system in organotypic cortex slices of Ub^{G76V} -GFP/2 tg mice, the cortex slices were cultured and treated with 1 μ M epoxomicin. Indeed, the GFP reporter only accumulated in the cortex slice cultures after treatment with proteasome inhibitor (Fig. 7). Similar to cortex slices from non-tg mice, in the Ub^{G76V} -GFP/2 cortex slices, LV-UBB⁺¹ transduction did not lead to UBB⁺¹ accumulation (Fig. 8B) unless additional proteasome inhibitors were applied (not shown). This additional proteasome inhibitor treatment led to GFP reporter accumulation in the tg cultures regardless of UBB⁺¹ expression, making it impossible to distinguish proteasome inhibition by the inhibitor or by UBB⁺¹. Therefore, we used adenoviral (Ad) instead of LV transduction of UBB⁺¹ to induce higher expression levels, which might exceed the accumulation threshold. We confirmed the increased expression

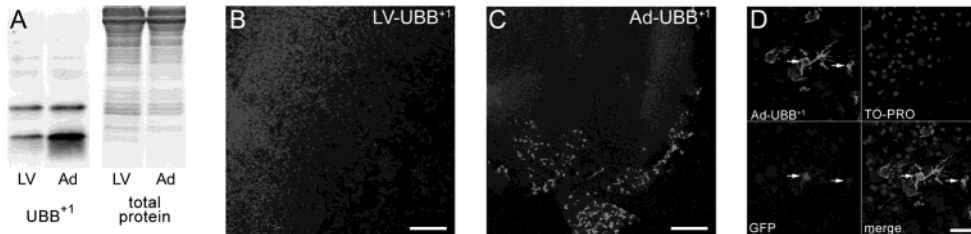


Figure 8 *High Ad-UBB⁺¹ expression causes proteasome inhibition in cortex cultures.* High levels of UBB⁺¹ expression with Ad-UBB⁺¹ lead to accumulation of UBB⁺¹ without inhibitor treatment. A: Representative Western blot of HEK293 cell lysates transduced with equal MOI of LV-UBB⁺¹ (left lane) or Ad-UBB⁺¹ (right lane). Equal amounts of protein were loaded per lane, as confirmed by Coomassie staining of total protein load of the same lanes shown on the right. The blot was stained with anti-UBB⁺¹ antibody Ub3 and quantified with Imagepro software (quantification not shown). B, C: Organotypic cortex slice cultures of Ub^{G76V}-GFP tg mice were transduced with LV-UBB⁺¹, which did not induce UBB⁺¹ accumulation (B) or Ad-UBB⁺¹, which did result in many UBB⁺¹ immuno-positive cells (C). D: UBB⁺¹ accumulation after adenoviral transduction lead to accumulation of Ub^{G76V}-GFP (arrows). Bars, 250 μ m (B), 500 μ m (C), 50 μ m (D). See color section.

of Ad-UBB⁺¹ (right lane, Fig. 8A) compared to LV-UBB⁺¹ (left lane, Fig. 8A) in HEK293 cells, showing that Ad-UBB⁺¹ transduction resulted in 4- to 5-fold higher expression of UBB⁺¹ compared to LV transduction (Fig. 8A). Transduction of Ub^{G76V}-GFP tg cortex cultures with Ad-UBB⁺¹ indeed resulted in accumulation of UBB⁺¹ in many cells (Fig. 8C), in contrast to LV-UBB⁺¹ transduction (Fig. 8B). The majority of cells that were positive for UBB⁺¹ after Ad-UBB⁺¹ transduction clearly accumulated the GFP reporter (Fig. 8D). UBB⁺¹ accumulation was observed mainly in the cytosol, whereas the GFP reporter accumulation was present in the cytosol as well as in the nucleus. Similar to the *in vitro* results, inducing a high level of UBB⁺¹ expression in organotypic cortex slice resulted in surpassing the accumulation threshold and subsequent inhibition of the proteasome.

Discussion

Our previous results indicated that UBB⁺¹ behaves both as a substrate as well as an inhibitor of the UPS (Lindsten *et al.*, 2002; Fischer *et al.*, 2003). In this study we further explored the dual UPS substrate/UPS inhibitor properties of UBB⁺¹, using novel tet-off inducible UBB⁺¹ expression vectors. Varying levels of UBB⁺¹ expression. We show here that a concentration-dependent shift in UBB⁺¹ properties from UPS substrate to inhibitor takes place with increasing expression levels. UBB⁺¹ accumulation commenced only at high expression levels and preceded the induction of UPS inhibition. In addition, we show in this study that both UBB⁺¹ accumulation and UPS inhibition were partially reversible after

ceasing UBB⁺¹ expression. We further studied UBB⁺¹ characteristics in organotypic cortex slice cultures, a system which reflects a multi-cellular environment in which neuronal connectivity and neuron-glia interactions are preserved (Sundstrom *et al.*, 2005). This study is, to our knowledge, the first employing organotypic cultures to assess UBB⁺¹ properties. In these cultures, UBB⁺¹ accumulation and subsequent UPS inhibition only occurred at high levels of expression, similar to the results obtained in cell lines. In summary, the current study shows that UBB⁺¹ properties dose-dependently shift from a proteasome substrate to a partially reversible proteasome inhibitor after a critical level of accumulation is reached.

We hypothesized that UBB⁺¹ might be able to irreversibly sustain or even increase its own accumulation through a “feedback loop” of UBB⁺¹-induced UPS inhibition. Surprisingly, a clear decrease was observed in the percentage of UBB⁺¹ positive cells after shutting down expression of UBB⁺¹ (Fig. 3A) or recovery after UPS inhibition, although UBB⁺¹ levels remained elevated compared to the levels before treatment. It is conceivable that this decline of UBB⁺¹ accumulation continues over time, clearing the remaining accumulation after a longer period of recovery. This reversible accumulation was not as clear in cortex slices; many UBB⁺¹ positive cells remained present after recovery of proteasomal inhibition in a setup where full degradation of the UPS reporter Ub^{G76V}-GFP was observed (Fig. 6). In these slices, 16 hours of UPS recovery might not be sufficient to observe a clear UBB⁺¹ degradation. These results indicate that the UBB⁺¹ protein likely has a longer half-life than Ub^{G76V}-GFP in cortex slices, corresponding to previous cell line observations regarding the half-life of UBB⁺¹ compared to Ub^{G76V}-GFP (Lindsten *et al.*, 2002). Also, a slight decrease in UBB⁺¹ intensity or number of UBB⁺¹ positive cells might not be detectable in cortex slices as an exact quantification is not feasible due to variation. Alternatively, primary neurons and astrocytes might respond differently to the inhibition of the UPS compared to tumour cell lines.

A point of interest is that LV vectors are known to efficiently transduce neuronal cells in culture (Ehrengruber *et al.*, 2001). In our organotypic slices we observed that the majority of the infected population consisted of GFAP positive glial cells, although neuronal cells were also transduced (Fig. 4). In this respect it is important to note that in the human brain, UBB⁺¹ not only accumulates in neurons in for instance AD, but also in glial cells of white matter in e.g. progressive supranuclear palsy (Fischer *et al.*, 2003). The UBB⁺¹ protein was mainly localized in the cytosol of the transfected cells in the slices. Surprisingly, UBB⁺¹ positive cells showed accumulation of the Ub^{G76V}-GFP reporter in both the cytosol and in the nucleus (Fig. 8D). Intranuclear localisation of the GFP reporter was also seen in Ub^{G76V}-GFP tg cortex cultures (Fig. 4) and in neuronal cultures from a comparable Ub^{G76V}-GFP tg line (Lindsten *et al.*, 2003) treated solely with proteasome inhibitor, indicating that general UPS inhibition results in both cytosolic and nuclear accumulation of the GFP-reporter.

Besides the UBB⁺¹ protein, shown in this study to be a dose-dependent reversible UPS inhibitor, many other compounds are known that inhibit the proteolytic activity of the 26S proteasome. These inhibitors can be divided into several major classes such as the synthetic peptide aldehydes, which act upon reversible binding (e.g. MG132, MG115 and PSI), the peptide boronates, a class of highly selective reversible inhibitors which have a slow on-off rate (e.g. MG262 and PS-341) and peptide vinyl-sulfones which bind irreversibly to the 20S core. Lactacystin and the specific 26S proteasome inhibitor epoxomicin are natural non-peptide irreversible proteasome inhibitors (reviewed in (Kisselev and Goldberg, 2001; Myung *et al.*, 2001)). In this respect, UBB⁺¹ can be classified as an endogenously encoded inhibitor of the UPS, which induces dose-dependent reversible UPS inhibition (Fig. 1B). UPS inhibition by UBB⁺¹ is a specific effect of UBB⁺¹ and not due to overloading the UPS by over-expressing a UPS substrate, as comparable expression of other UPS substrates such as ^{FLAG}Ub^{G76V}-nfGFP, ^{FLAG}Ub-R-nfGFP or ^{FLAG}p53 did not inhibit the UPS (Lindsten *et al.*, 2002). Through the possibility to vary UBB⁺¹ expression levels in different models systems (e.g. cell lines, primary cultures and transgenic animal models) using inducible vectors, the dual UPS substrate and UPS inhibitory properties of this protein can be optimally employed.

In this study we further validate our hypothesis that the presence of UBB⁺¹ serves as a marker for proteasomal dysfunction in human neurodegenerative disease (Fischer *et al.*, 2003; Hol *et al.*, 2005), showing in human cell lines and neuronal slice cultures that inhibition of the proteasome using proteasome inhibitors can induce the accumulation of UBB⁺¹, even if at these specific expression levels UBB⁺¹ is normally degraded. Accordingly, UBB⁺¹ accumulation in human pathology can serve as an endogenous marker for UPS inhibition, which holds UPS inhibitory properties itself (Fig. 9). Recently, it was shown that a decline in proteasome activity induced by classical proteasome inhibitors impaired protein synthesis in neuronal cells (Ding *et al.*, 2006) and disrupted multiple processes in ribosome biogenesis (Stavreva *et al.*, 2006). After washout of the reversible proteasome inhibitor MG262, levels of protein synthesis were restored (Ding *et al.*, 2006). As UBB⁺¹ is also an inhibitor of the proteasome, it is possible that we underestimated the extent of UBB⁺¹ accumulation in our experiments due to a decreased UBB⁺¹ synthesis. Also the protein synthesis levels of the GFP-reporter might be decreased. Conversely, the reversal of UBB⁺¹ accumulation after shutting down UBB⁺¹ expression might be influenced by an increased level of protein synthesis, possibly slowing the process of accumulation reversal. Decreases in ribosome function and protein synthesis are also associated with aging (reviewed by (Rattan, 1996)) and neurodegenerative disease (Ding *et al.*, 2005). Possibly, the accumulated UBB⁺¹ in the neurodegenerative disease hallmarks further contributes to these processes via its UPS inhibitory properties. Future experiments could further clarify this issue.

- 1) UBB⁺¹ translation equals UBB⁺¹ degradation

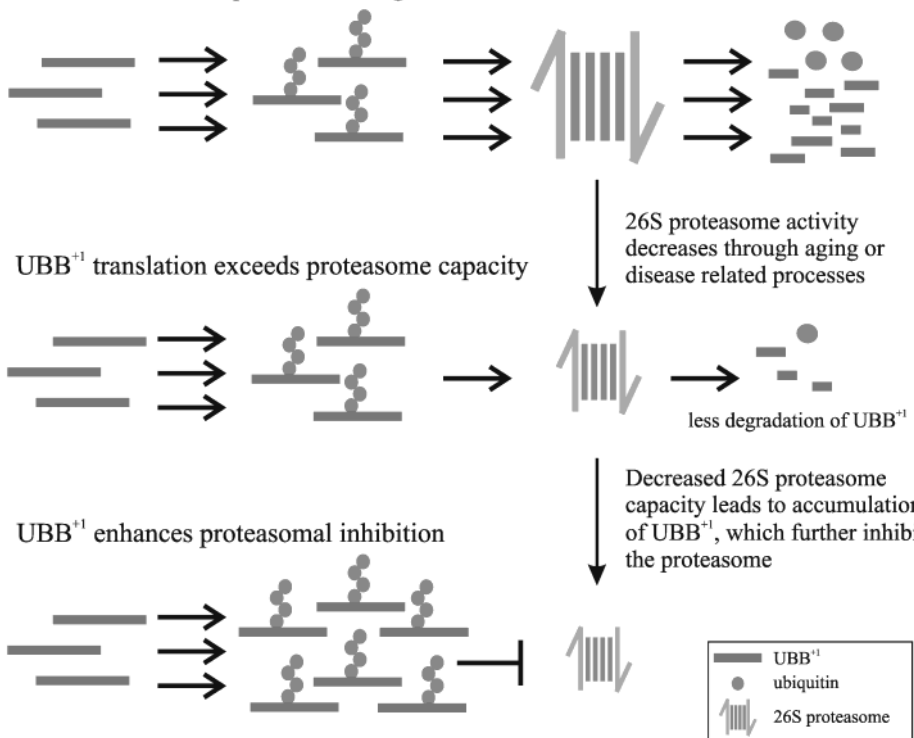


Figure 9 *UBB⁺¹ properties shift from UPS substrate to inhibitor.* (1) UBB⁺¹ mRNA and translation levels are constant throughout life (Fischer *et al.*, 2003; Gerez *et al.*, 2005). In non-diseased tissue, the 26S proteasome is capable of degrading all the translated UBB⁺¹ and accumulation of UBB⁺¹ is not present. (2) Due to various causes such as disease or aging the efficiency of proteasomal degradation can decrease, leading to a diminished degradation of UBB⁺¹. (3) The levels of translated UBB⁺¹ exceed the degradation capacity of the proteasome and surpasses the accumulation threshold. Accumulated UBB⁺¹ now holds UPS inhibitory properties itself, which can aggravate the initial decrease in UPS activity. See color section.

The reversible inhibitory properties of UBB⁺¹ can prove to be useful in many research fields besides neurobiology. The UPS is most well-known in its function in protein quality control, but increasing significance is attributed to its role in development, endocytosis, DNA repair and transcriptional regulation (Welchman *et al.*, 2005). In this respect, the role of UPS regulated protein turnover in cell cycle progression has become of major importance in cancer research, as oncogenic mutations can be found which perturb ubiquitination of cell cycle proteins and induce the disruption of intracellular balance between cell growth and death characteristic for cancer cells (Mani and Gelmann, 2005). Therefore it is not surprising that proteasome inhibitors have emerged as attractive drug targets for

e.g. cancer therapy (Hol *et al.*, 2006; Nalepa *et al.*, 2006). The first clinically approved anti-cancer drug in this respect is bortezomib (Velcade ®), a small-molecule UPS inhibitor used to treat malignant multiple myeloma (reviewed in (Rajkumar *et al.*, 2005)), which can induce apoptosis in tumour cells (Adams, 2004). As UBB⁺¹ is an endogenously encoded UPS inhibitor which induces apoptosis, it is possible to mediate tissue-specific gene delivery by viral vectors. This unique combination makes it worthwhile to further explore the potential of UBB⁺¹ as a tissue specific UPS inhibitor in disease.

Acknowledgements

We would like to thank L. Naldini (University of Torino, Torino, Italy) for the lentiviral constructs and K. Lindsten and V. Menéndez-Benito (Karolinska Institute, Stockholm, Sweden) for assistance with the work on the Ub^{G76V}-GFP transgenic mice. This research was supported by HFSPO grant RG0148/1999B, Hersenstichting Nederland H00.06 and 12F04.01, ISAO 01504, 04507 and 04830, MW-NWO/Swedish MRC 910-32-401 and Stichting “De drie lichten” 00/56.

CHAPTER III

Long-term proteasome dysfunction in the mouse brain
by expression of aberrant ubiquitin

Neurobiology of Aging, 2008; in press

David F. Fischer*, Renske van Dijk*, Paula van Tijn*,
Barbara Hobo, Marian C. Verhage, Roel C. van der Schors,
Ka Wan Li, Jan van Minnen, Elly M. Hol, Fred W. van Leeuwen

* *these authors contributed equally*

Abstract

Many neurodegenerative diseases are characterized by deposits of ubiquitinated and aberrant proteins, suggesting a failure of the ubiquitin-proteasome system (UPS). The aberrant ubiquitin UBB⁺¹ is one of the ubiquitinated proteins accumulating in tauopathies such as Alzheimer's disease (AD) and polyglutamine diseases such as Huntington's disease. We have generated UBB⁺¹ transgenic mouse lines with post-natal neuronal expression of UBB⁺¹, resulting in increased levels of ubiquitinated proteins in the cortex. Moreover, by proteomic analysis, we identified expression changes in proteins involved in energy metabolism or organization of the cytoskeleton. These changes show a striking resemblance to the proteomic profiles of both AD brain and several AD mouse models. Moreover, UBB⁺¹ transgenic mice show a deficit in contextual memory in both watermaze and fear conditioning paradigms. Although UBB⁺¹ partially inhibits the UPS in the cortex, these mice do not have an overt neurological phenotype. These mouse models do not replicate the full spectrum of AD-related changes, yet provide a tool to understand how the UPS is involved in AD pathological changes and in memory formation.

Introduction

A balance between protein synthesis and ubiquitin-mediated proteasomal degradation contributes to normal neuronal function (Fonseca *et al.*, 2006; van Tijn *et al.*, 2008). Ubiquitin is tagged to proteins via its C-terminal glycine residue, after which the target protein is degraded by the proteasome (reviewed in (Pickart, 2001)). Aberrations of the ubiquitin-proteasome system (UPS) have been implicated in the pathogenesis of neurodegenerative diseases (reviewed in (Ciechanover and Brundin, 2003; de Vrij *et al.*, 2004)). Ubiquitinated proteins accumulate in neurodegenerative disease hallmarks (Mori *et al.*, 1987) and an age- and disease-related decline of UPS activity has been reported (Keller *et al.*, 2000; Keck *et al.*, 2003; Bennett *et al.*, 2007). Furthermore, it was reported that impairment of the UPS can be mediated by protein aggregation (Bence *et al.*, 2001; Bennett *et al.*, 2005), oxidative stress or oxidized proteins (Okada *et al.*, 1999; Hyun *et al.*, 2002) and amyloid-beta (Aβ) (Gregori *et al.*, 1995; Oh *et al.*, 2005; Kristiansen *et al.*, 2007), leading to e.g. accumulation of tau (Song *et al.*, 2003; Oddo *et al.*, 2004).

We have reported on the occurrence of an aberrant ubiquitin B⁺¹ (UBB⁺¹) that selectively accumulates in neurodegenerative diseases such as the tauopathies like Alzheimer's disease (AD) and the polyglutamine disease Huntington's disease (HD) (van Leeuwen *et al.*, 1998; Fischer *et al.*, 2003; De Pril *et al.*, 2004). UBB⁺¹ is translated from an aberrant mRNA that is present at low frequency both in the brains of control subjects as well as in patients with neurodegenerative diseases (Fischer *et al.*, 2003; Gerez *et al.*, 2005). UBB⁺¹ has lost the ability to ubiquitinate proteins (De Vrij *et al.*, 2001), but is ubiquitinated itself

and is both a substrate (Lindsten *et al.*, 2002), and an inhibitor of the UPS (Lam *et al.*, 2000). High levels of prolonged UBB⁺¹ expression with viral vectors eventually lead to apoptosis in neuroblastoma cell lines (De Vrij *et al.*, 2001; De Pril *et al.*, 2004). The dual substrate/inhibitor property of UBB⁺¹ has provided us with a tool to chronically inhibit the activity of the UPS (Hol *et al.*, 2005; van Tijn *et al.*, 2007).

We have generated several lines of transgenic mice expressing UBB⁺¹ in neurons and analyzed these mice for gross neuropathology and changes in lifespan. We identified a reduction in proteasome activity in the brains of these mice. By two-dimensional (2D) gel electrophoresis followed by mass spectrometry we identified proteins that are mis-regulated or proteins that are post-translationally modified as a result of the transgene expression and the subsequent chronic proteasome inhibition. Furthermore, we analyzed the impact of chronic proteasome inhibition on learning and memory, which is one of the salient features of AD. To our knowledge, no studies on chronic impairment of the *in vivo* proteasome and consequent proteomic changes have been published so far. Hence, this study gives the first insights into the consequences of long-term proteasome inhibition in a transgenic mouse model harbouring a mutation relevant to neurodegeneration, and reveals some of the pathways that are affected as a consequence.

Materials and Methods

Generation of transgenic mice

Two different promoters were used to drive expression in transgenic mice: the murine Thy-1.2 promoter (Caroni, 1997) and the murine CamKIIα promoter (Mayford *et al.*, 1996). The *UBB*⁺¹ cDNA, encoded by the first ubiquitin sequence and the C-terminus in the +1 reading frame (van Leeuwen *et al.*, 1998) was either cloned directly in the Thy-1.2 cassette with XhoI, or with a flanking 5' intron (Choi *et al.*, 1991) and 3' polyadenylation site (bovine growth hormone) in the CamKIIα cassette by NotI (Figure 1). Before injection, inserts were excised from the plasmid, purified from gel by electro-elution and ethanol precipitated. Constructs were injected into fertilized oocytes of FVB/N (line 8630) or C57Bl/6 (line 3413) mice. The lines were maintained on their respective genetic background by breeding hemizygous mice to wild-type mice. The founder of line 8630 was highly mosaic (1/104 F1 screened), F1 mice from line 3413 were generated by *in vitro* fertilization. From F2 onwards Mendelian ratios were observed in the offspring. Mice were kept in group housing on a 12/12 h light-dark cycle with food and water ad libitum in specific pathogen free conditions (Nicklas *et al.*, 2002). Mice were genotyped on DNA isolated from ear-snips using the QIAamp DNA mini kit (Qiagen), primers are listed in Supplementary information. The copy-number of the transgene (3413: 13 copies, 8630: 2 copies) was determined by Southern blotting and analysis on a Storm 860 phosphorimager

(Molecular Dynamics). All animal experiments were performed conforming to national animal welfare law and under guidance of the animal welfare committee of the Royal Netherlands Academy of Arts and Sciences.

RNA isolation and qPCR

Mice were euthanized by carbon dioxide asphyxiation, the brain was immediately dissected and hemispheres were frozen in liquid nitrogen. RNA was isolated using Trizol (Invitrogen) and an Ultraturrax homogenizer and stored at -20°C. cDNA was synthesized from 2 µg of RNA using superscript II (Invitrogen). Real-time quantitative PCR was performed with SYBR-green mastermix (Applied Biosystems) on an ABI5700 (Applied Biosystems) as described previously (Hope *et al.*, 2003). Primers are listed in Table S3 in the Supplementary data file. The primer-set for the *ubiquitin-B* (*UBB*) target recognizes both the endogenous UBB mRNA and the transgene, the bovine growth hormone polyA set recognizes the CamKIIα transgene, three house-keeping genes were used as normalizers (*EF1α*, *Ube2d2* and *rS27a* (Warrington *et al.*, 2000; Lee *et al.*, 2002)). Statistics was performed with a Mann-Whitney U-test in SPSS 11 for Mac.

Radioimmunoassay

Mice were euthanized by carbon dioxide asphyxiation, after which the brain was immediately dissected and hemispheres were frozen in liquid nitrogen. A hemisphere was homogenized in suspension buffer: 100 mM NaCl, 50 mM Tris pH7.6, 1 mM EDTA pH8.0, 0.1% Triton-X-100, 10 mM DTT and protease inhibitors (Complete, Roche), samples were stored at -80°C. Total protein concentration was determined by means of a Bradford assay (Bradford, 1976). UBB⁺¹ protein levels were measured in a radioimmunoassay (RIA) as described previously (Hol *et al.*, 2003) with Ubi3 peptide and Ubi3 antiserum (5/08/97, final dilution 1:24000) (De Vrij *et al.*, 2001).

Immunohistochemistry

Animals were given deep pentobarbital anaesthesia (i.p.) and were perfused intra-cardially with phosphate-buffered saline (PBS) followed by PBS containing 4% (w/v) paraformaldehyde. Brains were cut either on a sectioning vibratome in 50 micron thick sections or after 30% sucrose protection on a cryostat in 10 micron sections. Sections were stained with anti UBB⁺¹ (Ubi3 5/08/97, final dilution 1:1000) (Fischer *et al.*, 2003), non neuronal enolase (6880-1004, Biotrend Chemikalien GmbH, Keln, Germany (1:250) (Day and Thompson, 1984)), a mouse monoclonal antibody against glutamine synthetase (MAB302, Chemicon, Temecula, CA, USA (1:250), a rabbit polyclonal raised against

bovine glial fibrillary acidic protein (GFAP) (DAKO, Carpinteria, CA, USA) for GFAP or a mouse monoclonal AT8 against hyper-phosphorylated tau. Primary antibodies were followed by a peroxidase-anti-peroxidase sandwich (Sternberger *et al.*, 1970) or followed by avidin-biotin-peroxidase and 3,3'-diaminobenzidine (DAB) color reaction intensified by 0.2% nickel ammonium sulphate. The neuropathological Gallyas staining is described in (Braak *et al.*, 2003).

Measurement of proteasome activity

Mice of line 3413 and 8630 (8 months old) were euthanized by carbon dioxide asphyxiation, after which cerebral cortices were immediately dissected. Cortices were homogenized at 4°C in 2 ml 50 mM Hepes-KOH pH7.5, 5 mM MgCl₂, 2 mM ATP, 250 mM sucrose using a Potter tube and centrifuged as described (Gaczynska *et al.*, 1994). Samples were stored in 200 µl 50 mM Hepes-KOH pH7.5, 5 mM MgCl₂, 2 mM ATP, 20% glycerol at -80°C. Protein concentration was measured with a Bradford assay. Five µg of protein was added to 200 µl of 50 mM Hepes-KOH pH7.5, 50 µM Suc-LLVY-AMC (BIOMOL International LP, Exeter, UK) and incubated for 60 min at 37°C. The sample was diluted with water to 1 ml and cleavage of the fluorogenic peptide was measured in a LS50 luminescence spectrometer (PerkinElmer) with the following settings: excitation at 380 nm with a 5 nm slit, emission at 440 nm with a 10 nm slit, integration over 4 s.

Watermaze

All mice were male and were housed solitary during the experiment. The experimenter was blind to the genotype of the mice. The maze consisted of a circular pool of 1.22 m in diameter filled with water at 26 ± 1°C, made opaque by addition of white non-toxic latex paint. Training commenced with a free-swim trial of 120 s on day 1. Hidden platform training was conducted for four consecutive days (4 trials per day, ~30 min intertrial interval). Mice were allowed to search for a hidden circular platform (11 cm diameter) submerged 0.5 cm under the water surface for 60 s. The platform location remained constant during the trials (NW), the inlet position was chosen pseudorandomly (N, E, S, W) every trial. When unable to find the hidden platform, mice were guided to the platform using a plastic scoop. Mice were allowed to remain on the platform for 20 s. Memory retention was tested three days after acquisition training in a 60 s probe trial, in which the submerged platform was removed. Inlet position was chosen in the opposite quadrant of the former platform position.

In the visual platform test, both the platform location and the inlet location were pseudorandomised. Visual training consisted of three trials wherein the platform was elevated 0.5 cm above the water surface and marked with a black and white striped pole and flag.

All trials were monitored by a camera, recorded and analyzed using a computerized tracking system (Ethovision, Noldus, The Netherlands).

Fear conditioning

All mice were male and housed solitary during the fear conditioning experiment. Conditioning took place on day 1 in a conditioning chamber with transparent walls and a stainless-steel grid floor connected to a shock delivery module (Med Associates Inc., Vermont), cleaned with a 70% ethanol solution for a distinctive odor. Following a 192 s baseline period, mice received a 70 dB/8 kHz tone (conditioned stimulus, CS) for 20 s coupled to a 1 mA scrambled footshock (unconditioned stimulus, US). The US was presented during the last 2 s of the CS. This procedure was repeated three times with an interval of 64 s. After the last US the mice remained in the chamber for 64 s after which they were returned to their home cage. Two separate groups of mice were trained and tested on day 2 as well as day 8; one group for context-dependent conditioning and one group for novel context and tone-dependent conditioning. For context-dependent conditioning, the mice were placed into the conditionings chamber as used on day 1 (no CS or US) for 300 s. For novel context, mice were placed in a different chamber with non-transparent black walls and a solid plastic white floor, cleaned with a 2% acidic acid solution and an alternate position in the testing room compared to day 1. Following an initial 192 s period without cues (novel context), the CS was presented for 300 s (tone conditioning). Freezing per 2 s intervals was manually scored by two independent observers as a measure of fear and averaged per condition or over 32 s time bins for analysis.

2D-gel electrophoresis

After sedation of the mice with O₂/CO₂, followed by decapitation, the cortex of the mice (for details on genotype and age, see Supplementary information) was dissected from the brain and immediately homogenized in lysis buffer (9 M urea, 3% CHAPS, 10 mM Tris, 0.5% (32.5 mM) dithiothreitol (DTT), 0.5% immobilized pH gradient (IPG) buffer, non linear gradient of pH3-10 (Amersham Pharmacia Biotech, Piscataway, NJ, USA), 0.1% bromo-phenol-blue). The RC DC Protein Assay (Bio-Rad Laboratories, Hercules, CA, USA) was used to determine the protein concentration of the samples. For silver staining and for blotting, 250 µg protein was subjected to 2D gel electrophoresis. 350 µl of the protein samples (consisting of 250 µg protein) were loaded on 18 cm immobilized pH gradient gels (IPG strip, Immobiline DryStrip, pH range 3-10-non-linear, Amersham Pharmacia Biotech). Rehydration of the IPG strips was performed for 12 h at 30 V, after which proteins were focused overnight (65 kVh, 20°C) using an IPG-Phor (Amersham Pharmacia Biotech). Prior to the second dimension, IPG strips were equilibrated in 1%

(65 mM DTT, 50 mM Tris-Cl pH8.8, 6 M urea, 30% glycerol, 2% sodium dodecyl sulphate (SDS) for 15 min. followed by 2.5% (260 mM) iodoacetamide, 50 mM Tris-Cl pH8.8, 6 M urea, 30% glycerol, 2% SDS for 15 min. The SDS polyacrylamide gel electrophoresis as the second dimension separation was carried out using the Isodalt System (Amersham Pharmacia Biotech) in 1.5 mm 12% Laemmli gels (Duracryl, Genomic solutions, Ann Arbor, MI, USA) and run for at least 16 h at 85 V at 16°C. Immediately after electrophoresis, gels were fixed in 50% methanol, 5% acetic acid for 20 min and then stained with a silver staining procedure that is compatible with mass spectrometric analysis (Shevchenko *et al.*, 1996). Silver stained gels were scanned (GS-800 Calibrated Densitometer, BioRad, Hemel, Hamstead, UK) and data were analyzed by PD-Quest software (Bio-Rad Laboratories).

Immunoblotting

For blotting of the proteins on nitrocellulose membranes, gels were first incubated in blot buffer (25 mM Tris, 192 mM glycine, 0.1% SDS, 15% methanol) for 15 min. Then the proteins were electroblotted to nitrocellulose membranes (pore size 0.45 µm) using the Isodalt System containing the blot buffer at 400 mA for 5 h. The membranes were incubated after blotting in a mixture of two polyclonal antibodies against ubiquitin (#Z0458, DAKO, Glostrup, Denmark (1:300) and #U5379 Sigma, St. Louis, MO, USA (1:100)) or the monoclonal MCP 231 (Hendil *et al.*, 1995) (PW8195, Affinity Research Products Ltd, Mamhead, Exeter, UK (1:2000)) against 20S proteasome subunits $\alpha_{1, 2, 3, 5, 6, 7}$. After overnight incubation with the primary antibody at 4°C, the blots were washed with Tris-buffered saline-Tween (65 mM Tris-HCl pH7.5, 150 mM NaCl, 0.05% Tween 20) and incubated with secondary rabbit or mouse polyclonal antibodies (DAKO (1:2000)) conjugated to horseradish peroxidase in Supermix (50 mM Tris, 150 mM NaCl, 0.25% gelatin and 0.5% Triton X-100, pH7.4). Labeled proteins were visualized using the enhanced chemiluminescence detection kit (Lumilight ECL, Roche Diagnostics, Mannheim, Germany). All blots were treated equally, i.e. identical exposure, film development and fixation times.

Protein identification by mass spectrometry

Protein spots were manually excised from the gel, washed, dehydrated and in-gel digested by trypsin (at 10 µg/ml in 50 mM ammonium bicarbonate buffer, overnight at 37°C) as described (Shevchenko *et al.*, 1996), with some minor modifications. Tryptic peptides were extracted from the gel with 25 mM ammonium bicarbonate buffer followed by two extractions with two volumes of 1% formic acid, 50% acetonitrile. The three extraction volumes were combined in the same tube and lyophilized to about 30 µl. Protein spots 1

to 11 were analyzed by an electrospray (ESI) Q-TOF tandem mass spectrometer (Micromass Inc., Manchester, UK) as described previously (Nagle *et al.*, 2001; Li *et al.*, 2004). In brief, the extract was loaded into a homemade poros microtip extraction column, and the bound tryptic peptides were eluted with 10 µl 50% acetonitrile, 5% formic acid. The eluent was loaded into a nano-electrospray capillary, which was pulled from borosilicate glass capillary GC 100F-10 with a microcapillary puller. The samples 12 to 16 were analyzed by an Applied Biosystems 4700 Proteomics Analyzer with TOF/TOF™ Optics as described by Li *et al.* (Li *et al.*, 2004). In brief, 0.5 µl of the incubation buffer was pipetted to the MALDI plate and mixed with 1 µl of a-cyano-4-hydroxycinnamic acid, which was directly deposited onto the MALDI plate. The a-cyano-4-hydroxycinnamic acid matrix concentration was 5 mg/ml in 50% acetonitrile/50% water containing 0.1% trifluoroacetic acid. Mass spectra were searched against NCBI database using mascot software from Matrix Science.

Results

Generation of UBB⁺¹ transgenic mice

We have generated two transgenic mouse lines expressing UBB⁺¹ in the post-natal brain: line 3413 with expression driven by the CamKIIα promoter, and line 8630 by the Thy-1.2 promoter (Figure 1). UBB⁺¹ mRNA in these lines was expressed at 49% and 67% of endogenous UBB mRNA levels in the 3413 and 8630 line respectively, UBB⁺¹ protein levels reached approximately 1 µg/g and 1.5 µg/g total brain content respectively (Figure 1). These levels are several orders of magnitude lower than those reported for free Ub protein

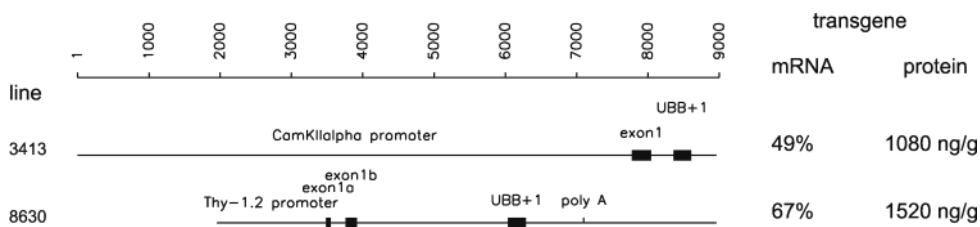


Figure 1 Transgene expression on mRNA and protein level. Two different constructs used to generate transgenic mice. The first non-coding exon in both Thy-1.2 and CamKIIα promoter constructs is derived from Thy-1.2 or CamKIIα respectively. UBB⁺¹ mRNA expression in the brain of mice (n=4 per genotype) was determined by qPCR. Transgene expression was measured with primers recognizing both the transgene and the endogenous UBB mRNA. Expression is relative to UBB levels of wild-type littermates (averages shown). UBB⁺¹ protein expression in the brain of mice (n=4 per genotype) was measured with a radioimmunoassay, and is expressed at ng/g total protein content.

(1-2,5 mg/g) and total ubiquitin levels (approximately 10 mg/g) in cell lines (Takada *et al.*, 1996; Ponelies *et al.*, 2005). The differential expression of UBB⁺¹ on mRNA and protein levels suggests that either translation of UBB⁺¹ is sub-optimal, or more likely, that a significant fraction of UBB⁺¹ protein is degraded through the UPS (Lindsten *et al.*, 2002; Fischer *et al.*, 2003). In line 3413, UBB⁺¹ mRNA and protein are expressed at maximal levels from p22 onwards, with 50% levels at p11 and 20% levels at birth (Figure S3 in Supplementary material). In line 3413, the protein is expressed in neurons in the cortex, hippocampus, amygdala and striatum (Figure 2A and 2C), which is very similar to other mouse lines carrying a CamkIIα transgene (Mayford *et al.*, 1996). In line 8630, the transgene is expressed in neurons in the cortex and the hippocampus (Figure 2A), but also in motor neurons in the spinal cord (Figure 2B), similar to other Thy-1.2 transgenic mouse lines (Caroni, 1997; Feng *et al.*, 2000).

Lack of overt neuropathology and neurological phenotype

The life-span of the transgenic mice from both lines was similar to that of their non-transgenic littermates. We have analyzed the brains of mice from both lines at different ages (up to 21 months) for gross neuropathology by staining with antibodies against aberrant tau to detect tangles (Bi *et al.*, 2001; Frasier *et al.*, 2005), antibodies against GFAP to detect astrogliosis and by Gallyas silver staining to detect general pathology. We did not observe any neuropathology in these mice (Figure 3 and Figure S1 in Supplementary material). When 8630 mice were cross-bred, homozygotes were born at the expected Mendelian frequency, and had a life-span comparable to their non-transgenic and heterozygote littermates. No gross morphological changes were observed in the brains of the homozygous 8630 mice (Figure S2 in Supplementary material). All subsequent experiments were performed with heterozygote UBB⁺¹ transgenic mice. These data suggest that long-term neuronal UBB⁺¹ expression does not compromise life-span in the mouse, nor does it cause overt pathology of the Alzheimer or Parkinson type.

Inhibition of the proteasome in UBB⁺¹ transgenic mice

As we previously reported that UBB⁺¹ inhibits the UPS *in vitro*, when expressed at high levels (Lindsten *et al.*, 2002), we now investigated whether UPS activity was also decreased in UBB⁺¹ transgenic mice. We measured a significant ($p<0.05$) reduction of chymotryptic activity in partially purified 26S proteasomes from UBB⁺¹ transgenic mouse line 3413 cortex to 82% of wild-type levels (Figure 4). In line 8630, we observed a similar trend that failed to reach statistical significance ($p>0.05$). This activity was sensitive to epoxomicin, showing that the proteolytic activity we measured is indeed proteasome activity (Meng *et al.*, 1999). These data indicate that proteasome activity in the brain of

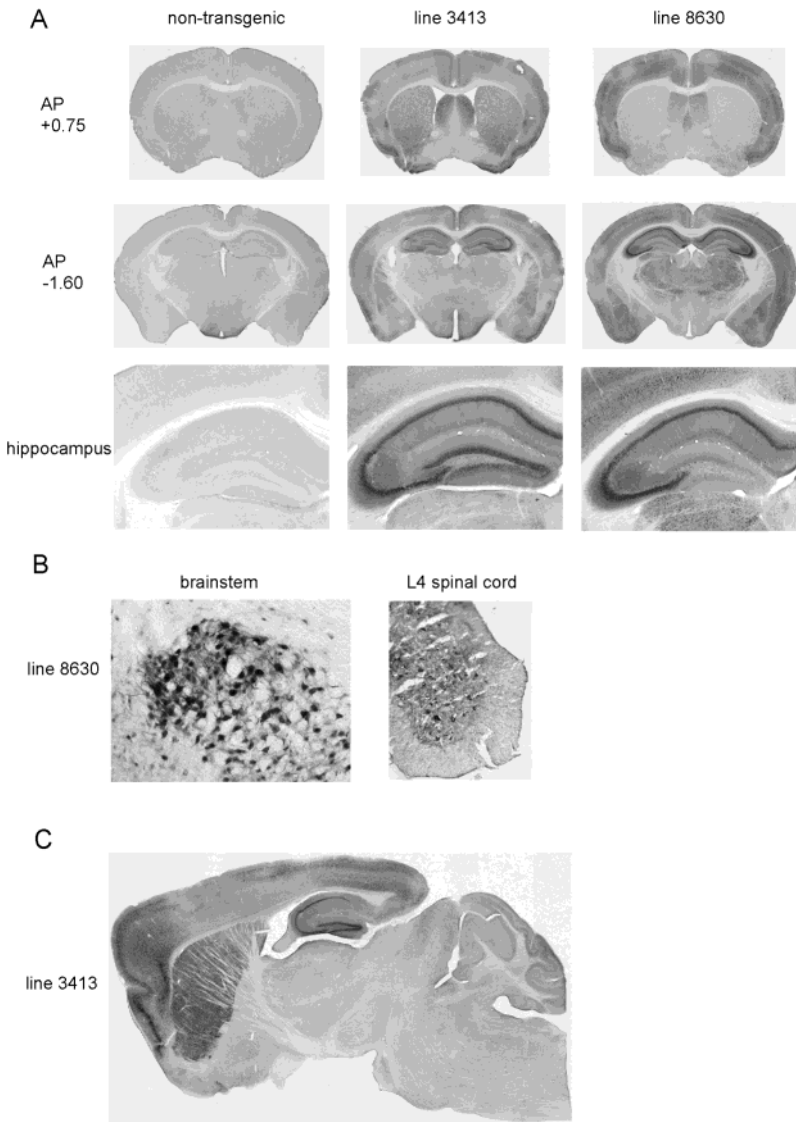


Figure 2 Transgene expression in the brains of 1-year-old male UBB⁺¹ transgenic mice. A. Vibratome sections were stained with Ubi3 antibody against the unique C-terminus of UBB⁺¹, coronal sections in the frontal area (AP +0.75 mm relative to bregma) and at the hippocampal formation (AP -1.6 mm) are shown, as well as a magnification of the hippocampus. Note the absence of expression in the dentate gyrus in line 8630. Line 3413 also shows expression in striatum and amygdala. B. UBB⁺¹ expression in line 8630 in motor neurons of the brainstem and spinal cord (L4). Vibratome sections (brainstem) or cryosections (spinal cord) were stained with Ubi3 antibody. C. Sagittal section of the brain of a line 3413 UBB⁺¹ transgenic mouse. Note the strong staining in the striatum.

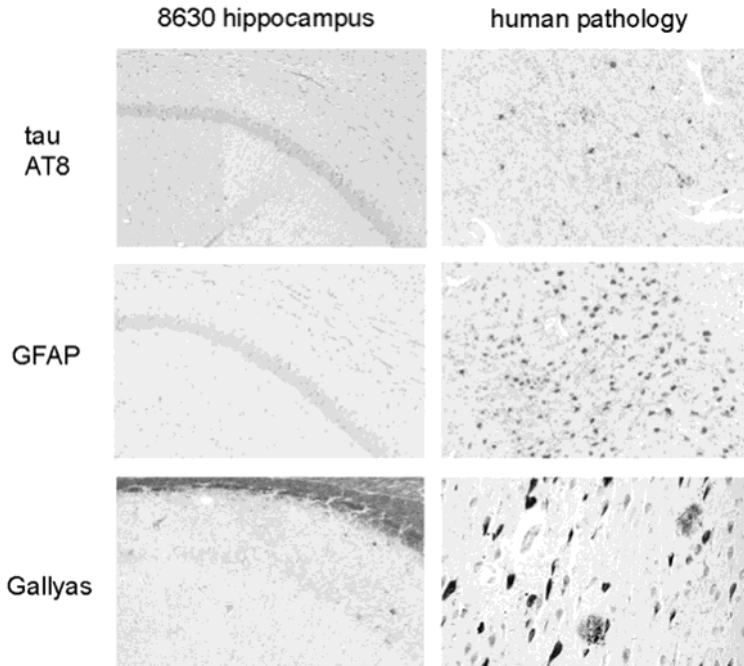


Figure 3 *Neuropathological staining in UBB^{+1} transgenic mouse line 8630.* Brains (n=2) of 21 month old transgenic mice of line 8630 were analyzed for the presence of neuropathology. Neuropathological staining was employed with antibodies against hyperphosphorylated tau and GFAP or by Gallyas silver iodide staining. Counterstaining was performed with haematoxylin (not for Gallyas). The left-hand panels show a magnification of area CA1 of the transgenic mouse hippocampus. The right-hand panels show positive controls for each staining: the CA1-subiculum region of an Alzheimer patient. Note the lack of neuropathology in the UBB^{+1} transgenic mouse brain.

UBB^{+1} transgenic mice is significantly reduced. This decrease in proteasome activity is underestimated, since a total brain homogenate was prepared wherein only the neurons express UBB^{+1} and therefore only the neurons suffer from an impaired UPS.

Such a reduction in proteasome activity is likely to lead to an increase in ubiquitinated proteins. Figure 5 shows two representative examples of 2D immunoblots of a UBB^{+1} transgenic mouse of line 8630 (Figure 5A) and a control mouse (Figure 5B). The total level of ubiquitinated proteins is indeed increased in the cortex of UBB^{+1} transgenic mice compared with control mice. Similar results were obtained with 3413 transgenic mice (data not shown). This implies that UBB^{+1} is not only capable of inhibiting the UPS *in vivo*, but that UBB^{+1} expression also results in an apparent increase in ubiquitinated proteins in the cortex of UBB^{+1} transgenic mice.

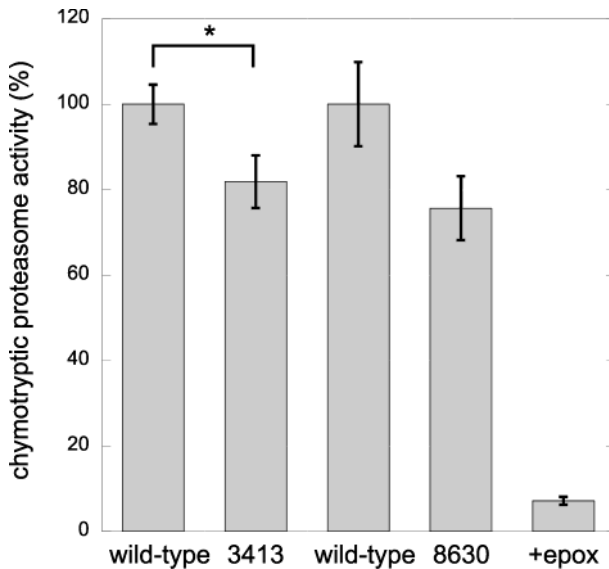


Figure 4 Proteasome activity in cerebral cortex homogenates of line 3413 and line 8630. Chymotryptic activity was measured on 26S proteasomes prepared from the cortex of wild-type mice, or transgenic mice (n=7 per group). As a control for activity of the proteasome, the specific proteasome inhibitor epoxomicin (+epox) (Meng *et al.*, 1999) was added to the reaction in a final concentration of 2 μ M. The activity is plotted relative to wild-type, error bars indicate S.E.M. The asterisk denotes statistical significance ($p=0.043$).

Protein expression profile of α subunits of the proteasome

To further address the role of UBB⁺¹ in proteasome function, we used the monoclonal antibody MCP 231 (Hendil *et al.*, 1995) against subunits $\alpha_{1, 2, 3, 5, 6}$ and α_7 of the 20S proteasome core on the same immunoblots as described for detection of ubiquitinated proteins. This antibody recognizes six different subunits whose 2D pattern is already known (Hendil *et al.*, 1995). Post-translational modifications of the proteasome subunits or a change in subunit expression could indicate that proteasome core is altered, and therefore is likely to have a direct effect on the function of the proteasome. However, we did not observe significant differences in protein expression patterns of these subunits between the cortex of UBB⁺¹ transgenic mice (Figure 5G) and control mice (Figure 5H). This implies that the decrease in proteasome activity and the increase in ubiquitinated proteins that we found in UBB⁺¹ transgenic mice do not involve changes in expression or post-translational modifications of the $\alpha_{1, 2, 3, 5, 6}$ and α_7 20S subunits.

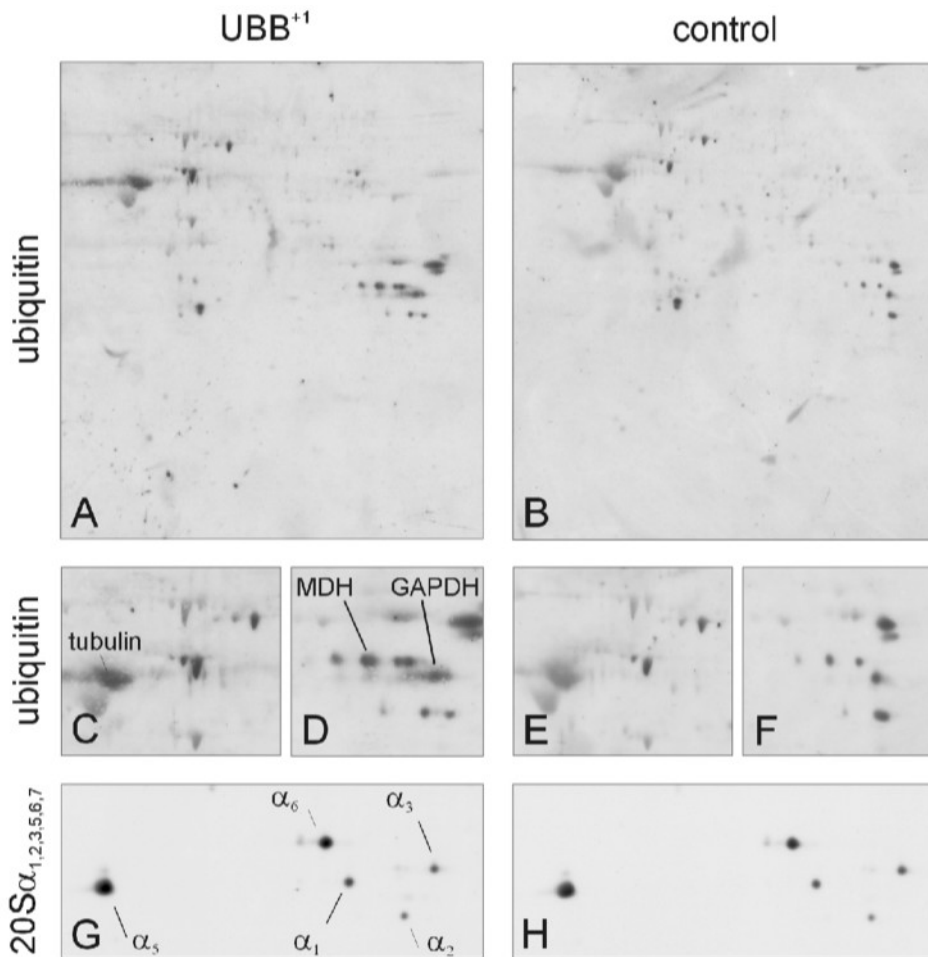


Figure 5 *Accumulation of ubiquitinated proteins in UBB^{+1} transgenic mice.* 2D immunoblots of ubiquitinated proteins and $20S \alpha$ subunits in the cortex of UBB^{+1} transgenic and control mice (littermates). A and B are 2D immunoblot images of cortex proteins from a line 8630 transgenic (Supplementary Table S2 #6) and a control mouse (Supplementary Table S2 #5) respectively, immunostained for ubiquitin. Panels C and D are magnifications of two areas in A that are immunopositive for ubiquitinated proteins, and E and F of the same areas in B (MDH: malate dehydrogenase; GAPDH: glyceraldehyde 3-phosphate dehydrogenase). Note that not only the amount of proteins positive for ubiquitin is higher in transgenic mice, but that also modifications of proteins can be observed as some spots show a pI shift (compare D and F). G and H are expanded 2D immunoblot images of cortex proteins from a transgenic (Supplementary Table S2 #8) and a control mice (Supplementary Table S2 #7) respectively, immunostained for the $20S \alpha_{1,2,3,5,6}$ and α_7 subunits of the proteasome (indicated in G). No differences between a transgenic and a control mouse were observed in levels or possible modifications of $20S \alpha$ subunits. Note that the α_7 subunit is not detected with this antibody.

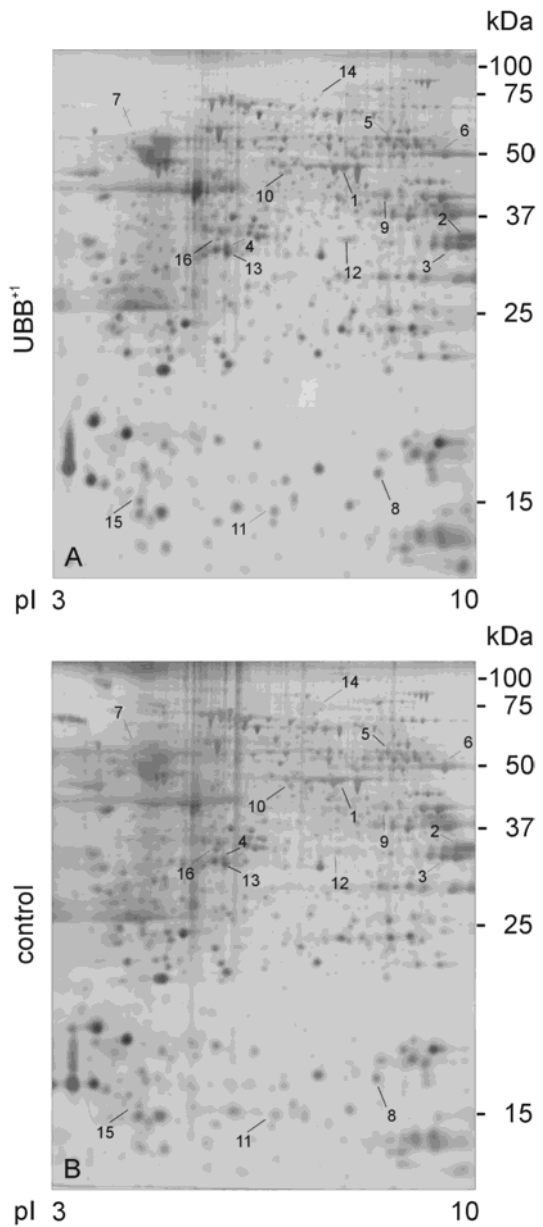


Figure 6 Comparative proteome analysis of the cortex of UBB⁺¹ transgenic and control mice. Silver stained 2D gel images of mice cortex proteins. Upper image is from a UBB⁺¹ transgenic line 8630 mouse (Supplementary Table S2 #6) and the gel on the bottom from a control littermate (Supplementary Table S2 #5). Indicated (by lines and numbers) are the proteins that are either differentially expressed or post-translationally modified.

Protein expression profile of cortex of UBB⁺¹ transgenic mice

We reported earlier that expression of UBB⁺¹ in neuroblastoma results in induction of heat shock proteins on mRNA and protein level (Hope *et al.*, 2003). We examined the expression levels of hsp40, hsp70c, hsp90 and $\alpha\beta$ -crystallin in the cortex of UBB⁺¹ transgenic mice, but did not find a significant difference in expression between transgenic and wild-type littermates (Figure S4 in Supplementary material). These data suggest that the acute response to proteasome inhibition is markedly different from that to prolonged low-level inhibition (Hope *et al.*, 2003). Furthermore, this implies that in our model the proteasome is chronically inhibited without the a-specific massive cell death caused by the induction of a stress response. Therefore, this model faithfully mimics the gradual and chronic proteasome inhibition in aging and neurodegenerative diseases. By identifying proteins that are differentially expressed in the cortex of UBB⁺¹ transgenic mice we expected to provide insights in the pathways that are affected as a result of diminished proteasome activity. Cortex proteins of five UBB⁺¹ transgenic mice and five control mice (see also Table S2 in Supplementary material) were individually separated by 2D gel electrophoresis (one gel per animal). Silver stained gels were analyzed for changes in expression and post-translational modifications of proteins.

We identified a total of 16 differentially expressed protein spots between UBB⁺¹ transgenic mice (differentially expressed both in line 3413 and line 8630) and wild-type controls, indicated by numbers 1 to 16 in Figure 6. Six spots (of which one spot was not statistically significant) differed by at least a factor of 1.5 in intensity and nine spots were post-translationally modified (Table 1 and Table S1 in Supplementary information). This modification could either be a shift towards the acidic or basic end of the gel (e.g. by (de)-phosphorylation or oxidative modification) or ubiquitination of the protein. The latter was determined by immunoblotting with antibodies against ubiquitin (Figure 5). Three out of nine post-translationally modified protein spots showed a change in acidity, three spots were immunoreactive for ubiquitin and three spots revealed both a shift and ubiquitination (Table 1).

Identification of differentially expressed proteins

Table 1 lists the identity of 16 proteins that reproducibly were either up or down regulated by at least a factor of 1.5 or modified in the cerebral cortex of UBB⁺¹ transgenic mice (observed in both lines 8630 and 3413). Detailed information on these proteins, including statistical analysis can be found in the Supplementary data (Table S1 and Figure S5). Gene ontology showed that nine of the identified proteins were metabolic enzymes of which six are involved in energy metabolism. Furthermore, we identified four proteins that can be categorized as cytoskeletal proteins. Two remaining proteins we identified could not be assigned to any of the above categories (parvalbumin alpha and mu crystallin). Compari-

son with published proteomic profiles of brains of several mouse models for AD (van Leuven, 2000) and of human AD brain tissue samples (Tsugita *et al.*, 2000; Schonberger *et al.*, 2001; Castegna *et al.*, 2002; Castegna *et al.*, 2002; Kim *et al.*, 2002; Tilleman *et al.*, 2002; Tilleman *et al.*, 2002; Tsuji *et al.*, 2002; Castegna *et al.*, 2003; Choi *et al.*, 2004; Shin *et al.*, 2004; Wang *et al.*, 2005) showed that for 5 out of these 16 proteins, similar changes were observed in either human Alzheimer brain tissue or in one or more AD mouse models (Table 1). These findings suggest that the UBB⁺¹ transgenic mouse models may replicate some of the endophenotypes of AD.

Table 1 Identified proteins that are up or down regulated or post-translationally modified in the cortex of UBB⁺¹ transgenic mice (both present in line 3413 and in line 8630). Spot numbers correspond to the numbers in Figure 6. Quantification of spots and statistical analyses was carried out using PD-Quest software. Significance of difference in abundance was determined by a paired Student's *t*-test (*p* value) between three control mouse gels and three UBB⁺¹ gels. Published proteomics data from AD brain, APP transgenic mouse model Tg2576 or other AD mouse models (tau, APOE, GSK-3 β) is presented as a comparison with references.

Spot	Protein Name	UBB ⁺¹ Tg	AD Brain	APP Tg	Other AD Tgx
<i>Energy metabolism-related enzymes</i>					
1	Alpha enolase	modified ^a	modified/increased (Schonberger <i>et al.</i> , 2001; Castegna <i>et al.</i> , 2002; Castegna <i>et al.</i> , 2003; Sultana <i>et al.</i> , 2007)	oxidized/ nitrated/ increased (Shin <i>et al.</i> , 2004)	Increased (Tilleman <i>et al.</i> , 2002)
2	Malate dehydrogenase, mitochondrial	modified and ubiquitinated ^b	N/A	decreased (Shin <i>et al.</i> , 2004)	N/A
3	Glyceraldehyde 3-phosphate dehydrogenase	modified and ubiquitinated	increased (Schonberger <i>et al.</i> , 2001; Wang <i>et al.</i> , 2005; Sultana <i>et al.</i> , 2007)	increased (Shin <i>et al.</i> , 2004)	N/A
4	Pyruvate dehydrogenase (Lipoamide) beta	ubiquitinated	N/A	N/A	N/A
5	Dihydrolipoamide dehydrogenase, mitochondrial	increased (1.82-fold, <i>p</i> <0.05)	N/A	N/A	increased (Tilleman <i>et al.</i> , 2002)
6	ATP synthase alpha chain, mitochondrial	modified and ubiquitinated	decreased (Tsuji <i>et al.</i> , 2002)	decreased (Shin <i>et al.</i> , 2004)	increased (Tilleman <i>et al.</i> , 2002)

Table 1 Identified proteins that are up or down regulated or post-translationally modified in the cortex of UBB⁺¹ transgenic mice (continued).

Spot	Protein Name	UBB ⁺¹ Tg	AD Brain	APP Tg	Other AD Tgx
<i>Other metabolic enzymes</i>					
7 ^c	Protein disulfide isomerase	decreased	N/A	N/A	oxidized (Choi et al., 2004)
8	Nucleoside-diphosphate kinase B	increased (1.54-fold, p<0.001) ^d	decreased (Kim et al., 2002)	N/A	increased (Tilleman et al., 2002)
9	Glutamine synthetase	increased (2.00-fold, p<0.01)	oxidized (Castegna et al., 2002)	N/A	increased (Tilleman et al., 2002)
<i>Cytoskeleton-related proteins</i>					
10	Tubulin alpha-1 chain	ubiquitinated	N/A	N/A	decreased (Tilleman et al., 2002)
7 ^c	Tubulin alpha-2 chain	decreased	N/A	N/A	decreased (Tilleman et al., 2002)
11	Profilin II	modified	decreased (Schonberger et al., 2001)	N/A	N/A
12	LIM and SH3 protein 1	modified	N/A	N/A	increased (Tilleman et al., 2002)
<i>Signal transduction proteins</i>					
13	Guanine nucleotide-binding protein beta subunit 4	ubiquitinated	N/A	N/A	N/A
14	Dihydro-pyrimidinase related protein -2	decreased (2.17-fold, p=0.24)	decreased/oxidized (Schonberger et al., 2001; Castegna et al., 2002; Tsuji et al., 2002)	increased (Shin et al., 2004)	oxidized/increased (Tilleman et al., 2002; Choi et al., 2004; David et al., 2006)
<i>Others</i>					
15	Parvalbumin alpha	increased (3.51-fold, p=0.02)	N/A	N/A	N/A
16	Mu-crystallin homolog	decreased (2.15-fold, p<0.05)	N/A	N/A	N/A

^a a shift in pI (e.g. by (de-)phosphorylation) ^b increased in ubiquitination ^c two proteins were identified in one spot ^d n=6

High expression of UBB⁺¹ affects spatial memory

To investigate the behavioral effects of prolonged expression of UBB⁺¹ in the brain, and the concomitant decrease in UPS activity, we measured acquisition of spatial learning and memory in a Morris watermaze in 9-month-old male UBB⁺¹ transgenic mice. For this task, we selected line 3413, as the genetic background (C57Bl/6) is compatible with such experiments (Crawley *et al.*, 1997; Silva *et al.*, 1997). A visual platform task was performed to identify possible sensory-motor deficits. Four out of thirteen 3413 transgenic mice and one out of fifteen wild-type mice were excluded from further analysis due to poor performance on this task. Both transgenic ($n=9$) and wild-type ($n=14$) mice displayed significant task acquisition over three consecutive visual trials (repeated measures ANOVA, effect of trial $p=0.024$) (Figure 7F). Furthermore, no significant differences were present between the two groups.

During acquisition, mice were trained to find a hidden platform in the north-west (NW) quadrant of the maze and escape latencies were analyzed to assess acquisition of the task. Repeated measures ANOVA of the mean escape latencies over acquisition days 1-4 revealed a significant effect of training day ($p<0.001$), indicating a general learning effect in both groups. However, there was no significant effect of genotype or interaction between day and genotype during acquisition (Figure 7A). A direct comparison of mean escape latencies per day also did not reveal significant differences between the 3413 transgenic and wild-type mice (Figure 7A). Similar results were obtained when the acquisition trials were analyzed separately (Figure 7B). We did observe a significant slight decrease in swimming speed in the 3413 transgenic group during the acquisition trials ($p<0.001$), but this difference was not significant during the probe trial (Figure 7C).

Spatial reference memory was assessed in a 60 s probe trial one week after training commenced. Results revealed that the 3413 transgenic mice show significantly poorer performance than wild-type mice. The wild-type mice demonstrate a preference for the former hidden-platform quadrant NW (NW versus NE, SE, SW; ANOVA Bonferroni, $p<0.02$ or higher level of significance for each quadrant comparison), whereas this preference was not present in 3413 transgenic mice (Figure 7D). Also the average distance to the former platform location was significantly decreased in the wild-type mice (39.3 ± 2.5 cm) compared to the 3413 transgenic mice (49.2 ± 2.6 cm) ($p=0.016$; Figure 7E).

To corroborate the results obtained in the Morris maze, we assessed memory retention in 9-month-old naive 3413 UBB⁺¹ transgenic mice and wild-type littermates in a fear conditioning paradigm. The mice were trained in a defined context with three mild foot-shocks coupled to an auditory cue on day 1. The freezing response of the mice was used as an index for tone- or context-related fear conditioning and was scored on day 2 and day 8. Baseline scores of freezing behavior were negligible in the 3413 transgenic as well as the wild-type mice (Figure 8A). When placed in a novel context 2 or 8 days after training, freezing behavior was significantly elevated compared to baseline in the 3413 transgenic

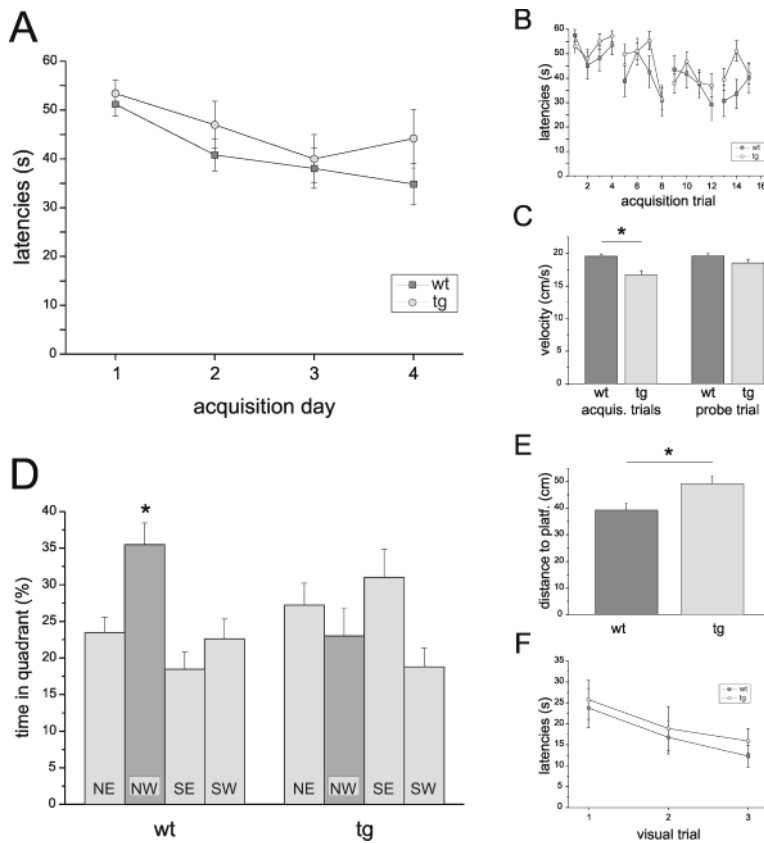


Figure 7 Impaired spatial reference memory in 3413 transgenic mice in the Morris watermaze. A. Performance on the acquisition phase of the watermaze task was measured by analyzing mean escape latencies (s) to find the hidden platform averaged per acquisition day of 3413 transgenic (tg) mice (n=9, open circles) and wild-type (wt) control mice (n=14, filled squares). A significant effect of day was present (repeated measures ANOVA, $p<0.001$), although no significant effect of genotype or interaction between day and genotype could be observed. B. The mean escape latencies averaged per acquisition trial also showed a main effect of day (repeated measures ANOVA, $p<0.001$), with no effect of genotype or interaction between day and genotype. C. The average swimming speed (cm/s) displayed in the acquisition trials showed a significant difference between the 3413 transgenic and wild-type mice (Students t-test, $p<0.001$). During the probe trial the average velocity of the two groups was similar. D. During the 60 s probe trial of the hidden platform task, total time spent in each quadrant was compared as a measure of spatial reference memory. Wild-type mice showed acquisition of the former platform position in the NW quadrant (ANOVA, $p<0.02$), in contrast to the 3413 transgenic mice which showed no preference for the former platform quadrant. E. The average distance to the former platform position was increased in the 3413 transgenic mice compared to the wild-type mice (Students t-test, $p=0.016$). F. Wild-type and 3413 transgenic mice show a significant acquisition of the visual task, shown by decreasing escape latencies per trial (repeated measures ANOVA, trial effect $p=0.024$). There were no effects of genotype on the ability to find the visible platform. All data are presented as average \pm S.E.M.

and wild-type mice (Figure 8A). During the tone-related conditioning, which is mainly amygdala-dependent (reviewed in (Maren, 2001)), a robust freezing response occurred up to ~80% of the time during the tone presentation. No significant differences were present between the two groups at day 2 or day 8 (Figure 8A). However, in the context-related conditioning, which is amygdala-dependent as well as hippocampus-dependent (Maren, 2001), the 3413 transgenic mice showed a significantly decreased freezing response compared to the wild-type mice on day 8 after training ($p=0.044$; Figure 8A). When the averaged freezing results of the contextual test at day 8 were separated over 32 s time bins, it was evident that the 3413 transgenic mice performed more poorly than wild-type mice, reaching significance at time bins 3 and 4 ($p=0.04$, $p=0.032$; Figure 8B). These results show that 9-month-old 3413 transgenic mice, in addition to a deficit in spatial memory retention in the Morris maze, also show a deficit in context-dependent fear conditioning.

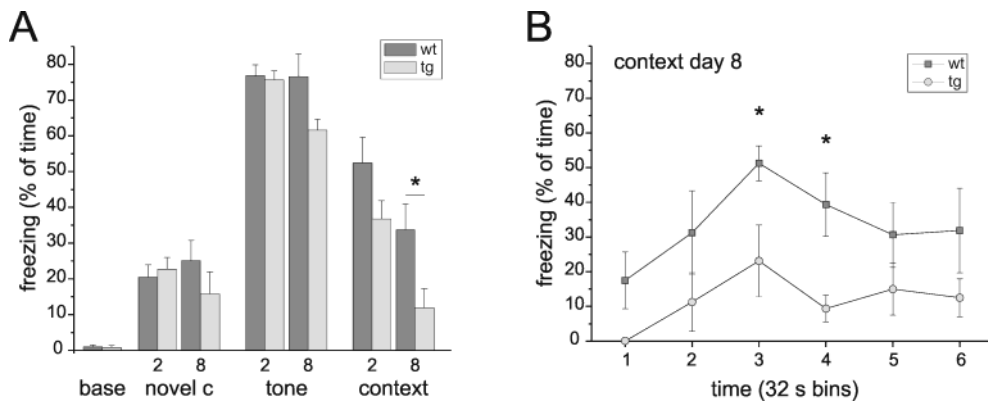


Figure 8 3413 transgenic mice show an impaired contextual fear conditioning. A. Freezing behavior (% of time) was plotted as a measure of fear conditioning. There was no significant difference between 3413 transgenic mice ($n=4$) and wild-type littermates ($n=5$) in the novel context and tone retention. In the context related conditioning, the 3413 transgenic mice ($n=5$) performed significantly poorer than the wild-type mice ($n=5$) on day 8 (Student's t-test, $p=0.044$). B. Freezing behavior of the 3413 transgenic mice (open circles) and the wild-type littermates (filled squares) was plotted for the context retention test on day 8. Freezing over the first 6 time bins of the task of 32 s per time bin showed a significantly higher freezing response in the wild-type mice over all 6 time bins, reaching significance at the 3rd and 4th time bin ($p<0.05$). All data represent average \pm S.E.M.

Discussion

Lack of overt neuropathology

The aberrant ubiquitin UBB⁺¹ has been first identified in AD (van Leeuwen *et al.*, 1998). Subsequently, accumulation of this protein was shown in other tauopathies (Fischer *et al.*, 2003; van Leeuwen *et al.*, 2006), HD (De Pril *et al.*, 2004), alcoholic liver Mallory bodies (McPhaul *et al.*, 2002) and inclusion body myositis (Fratta *et al.*, 2004). We surmised that the disease-specific accumulation of UBB⁺¹ was due to disease-specific inhibition of the UPS (Fischer *et al.*, 2003). We have generated transgenic mice that postnatally express UBB⁺¹ in neurons to mimic the expression of UBB⁺¹ as found in neuropathology. Indeed, UBB⁺¹ causes chronic inhibition of the proteasome, accompanied by increased levels of ubiquitinated proteins. Because the transgene is not targeted to glial cells and only a sub-population of neurons expresses UBB⁺¹, we suppose that we are underestimating the inhibition of the UPS in neurons.

Surprisingly, none of the UBB⁺¹ transgenic mouse showed a reduced life-span or overt neuropathology (e.g. aberrant tau, A β , Lewy body pathology, reactive astrocytes). At two years of age, these mice still express UBB⁺¹ in the same neuronal populations, and without apparent cell loss (Figure S1 in Supplementary data). Thus, the neuronal UPS in the mouse is capable of maintaining cell survival under mutant ubiquitin load. This is somewhat unexpected, as we reported previously that high levels of UBB⁺¹ lead to apoptosis (De Vrij *et al.*, 2001; De Pril *et al.*, 2004). However, in those experiments viral vectors were used to transduce neuroblastoma cells, resulting in very high expression levels. It is likely that lower expression levels in the transgenic mice allow long-term expression of UBB⁺¹, without leading to a stress response and programmed cell death. Cell lines are also capable of survival under long-term low-level pharmacological proteasome inhibition (Ding *et al.*, 2003). Small changes in proteasome activity can however be relevant to a neurodegenerative disease such as amyotrophic lateral sclerosis (ALS) (Puttaparthi *et al.*, 2003; Gilchrist *et al.*, 2005).

Mechanism of proteasome inhibition

Several mechanisms may underlie a diminished activity of the proteasome, i.e. alterations in levels of free ubiquitin, proteasome subunits, post-translational modifications of proteasome subunits (e.g. phosphorylation or oxidative modifications) or inhibition by damaged proteins (e.g. 4-hydroxynonenal bound proteins). It is unlikely that the expression of UBB⁺¹ causes changes in the levels of free Ub in this mouse model, as we did not detect changes in mouse UBB mRNA expression (Figure S4 in Supplementary data). Furthermore, the levels of UBB⁺¹ protein are several orders of magnitude lower than those reported for free and total Ub (Takada *et al.*, 1996; Ponelies *et al.*, 2005), although mRNA

levels for the transgene are approximately half that of the mouse UBB mRNA. These findings suggest that the majority of UBB⁺¹ protein in the transgenic mouse brain is degraded by the proteasome (Fischer *et al.*, 2003), but that it causes a concomitant chronic inhibition of the proteasome (van Tijn *et al.*, 2007). In the AD brain it was shown that a loss of proteasome activity was not associated with a decrease in proteasome subunit expression (Keller *et al.*, 2000). UBB⁺¹ expression also does not seem to alter the expression or relative levels of α subunits of the catalytic core of the 20S proteasome (Figure 5). This could imply that chronic impaired proteasome activity in UBB⁺¹ transgenic mice occurs through a ‘direct’ inhibition of ubiquitinated UBB⁺¹ on one or more of the proteasome subunits, thereby acting as an endogenous inhibitor without affecting the expression of the complex itself. This notion is further supported by the work of the group of Cecile Pickart, which showed in that ubiquitinated UBB⁺¹ is particularly stable a cell free system and potently inhibits the degradation of a polyubiquitinated substrate by purified proteasomes (Lam *et al.*, 2000), indicating that no transcriptional alterations are required for this blockade. The diminished proteasome activity in UBB⁺¹ transgenic mice could for instance be explained by a steric interference to the pore or 19S cap of the complex by stable forms of ubiquitinated UBB⁺¹. As UBB⁺¹ over-expression results in an increase in ubiquitinated proteins (Figure 5), this aberrant ubiquitin protein most likely interferes with ubiquitin-dependent proteasomal degradation. Considering the reported heterogeneity of proteasome complex within a tissue (Dahlmann *et al.*, 2000; Drews *et al.*, 2007), inhibition of proteasomes by UBB⁺¹ could affect only those proteasomes dedicated to ubiquitin-dependent proteolysis, leaving other complexes unaffected. Indeed, a number of proteasome substrates have been reported to be degraded in an ubiquitin-independent fashion (David *et al.*, 2002; Grune *et al.*, 2003; Shringarpure *et al.*, 2003). The most notable of these, tau, indeed does not accumulate in our mouse model (Figure 3), whereas infusion of a 20S core proteasome inhibitor, epoxomicin in the mouse brain does result in tau accumulation (Oddo *et al.*, 2004). The different mechanisms of proteasome inhibition by chemical inhibitors compared by UBB⁺¹ could explain the relatively mild phenotype of the mouse lines reported here.

Proteomic profile upon chronic ubiquitin-proteasome system inhibition

We furthermore investigated the implications of long-term proteasome inhibition by UBB⁺¹ expression on the mouse cortex proteome. We examined the proteome profiles from pairs of transgenics and wild-type littermates over a range of ages (Table S2 in the Supplementary data), but found no age-specific changes and only genotype-specific changes. This is in line with a lack of change in UBB⁺¹ expression in adult to old mice (see Figure S1 in the Supplementary data). Each of the changes reported in Table 1 was consistent between the two lines of UBB⁺¹ transgenics (in both FVB/N or C57Bl/6 back-

ground).

We here found that the levels of cortical ubiquitinated proteins in these mice were increased and that most of the identified proteins that were differentially expressed in UBB⁺¹ transgenic mice activity were housekeeping proteins involved in energy metabolism or organization of the cytoskeleton. A relatively high number of these proteins has also been identified in proteomic analyses of AD brain samples and in AD mouse models (Sultana *et al.*, 2007). Please see the Supplementary data for an extended discussion of these proteins. From these results we conclude that many of the proteins listed in Table 1 that are changed due to chronic impaired proteasome activity, are ubiquitously expressed throughout the brain and are implicated to have either significant metabolic functions or play a role in the organization of the cytoskeleton.

Relevance to Alzheimer's Disease

Alzheimer's disease is a multifactorial disease, and many different mouse models have been created to capture specific pathways leading to AD. Proteomic analyses of AD brain and brains of mouse models associated with AD, (i.e. the glycogen synthase kinase-3β (GSK3β) (Tilleman *et al.*, 2002) and tau transgenic mouse (Tilleman *et al.*, 2002), used to study pathogenic mechanisms of tauopathies, the Tg2576 mouse expressing the Swedish mutated form of human β-amyloid precursor protein (Shin *et al.*, 2004) and the ApoE-knockout mouse (Choi *et al.*, 2004)), identified several differentially expressed proteins that were altered in UBB⁺¹ transgenic mice as well (Table 1). Two of the five proteins we identified to be ubiquitinated in UBB⁺¹ transgenic mice are indeed up-regulated in AD brain or in AD mouse models, supporting our hypothesis that a decline of proteasome function correlates with AD-related neuropathology (Fischer *et al.*, 2003). Five out of eight proteins that changed in abundance in UBB⁺¹ transgenic mice showed a similar change in either AD brain or AD mouse models. However, we identified some discrepancy between the studies in AD brain and the β-amyloid or tau transgenic mice (Table 1), with effects on protein abundance in opposite directions. There was more concordance between the UBB⁺¹ transgenic mouse changes and the other transgenic mouse changes than AD brain, suggesting that either the mouse brain responds differently to AD-associated changes, or that the mouse models represent an earlier stage of disease (van Leuven, 2000), compared to the AD brain which is usually representative of the final stages of disease.

The changes in proteomic profiles in AD brain, AD mouse models and our UBB⁺¹ transgenic mice, characterized by a chronic impaired proteasome activity, are consistent with an involvement of a reduced metabolism in the pathophysiology of AD (Swaab, 1991; Salehi and Swaab, 1999). Furthermore, this study underlines the significance of the ubiquitin-proteasome system in neurodegenerative diseases, such as AD (Hol *et al.*,

2006). Interestingly, proteomic analysis of the parkin E3 ubiquitin ligase knock-out mice also showed alterations in a high proportion of proteins related to energy metabolism (Periquet *et al.*, 2005). Significantly, three other studies that reported expression profile changes upon pharmacological proteasome inhibition in cell lines, did not identify any of the protein changes we identified (Jin *et al.*, 2003; Ding *et al.*, 2004; Doll *et al.*, 2007). These data suggest that (1) neurons in the brain responds differently to proteasome inhibition compared to neuronal cell lines, or (2) that a long-term and chronic proteasome inhibition leads to a normalization of the early heat shock response (Hope *et al.*, 2003; Hope *et al.*, 2004; Doll *et al.*, 2007), or (3) that some of the proteomic changes we have observed are indirectly caused by proteasome insufficiency, for instance by compensatory effects on autophagy (Komatsu *et al.*, 2006).

The principal hallmark of AD is cognitive decline, particularly hippocampus-dependent memory, e.g. (Hsiao-Ashe, 2001). The precipitating event that leads to AD-pathology is not known, and likely to be multifactorial (Bertram and Tanzi, 2005). However, increasing evidence suggests that A β is one of the main initiators of neuropathology and cognitive decline (Selkoe, 1991; Hardy and Selkoe, 2002). Early cognitive decline in AD, before the onset of neuropathology, has been suggested to be caused by A β oligomers affecting synaptic transmission (Selkoe, 2002). As another consequence of A β accumulation, a decrease in activity of the UPS has been proposed (Gregori *et al.*, 1997; Song *et al.*, 2003; Oddo *et al.*, 2004; Song and Jung, 2004; Oh *et al.*, 2005; Almeida *et al.*, 2006), although the proteasome has also been reported to be involved in A β production (Christie *et al.*, 1999). Significantly, a recent study showed that over-expression of the ubiquitin hydrolase UCH-L1 rescues A β -mediated synaptic dysfunction and contextual memory (Gong *et al.*, 2006). We show in this paper that a decrease in UPS activity, without A β pathology, also can cause cognitive decline. Line 3413 UBB⁺¹ transgenic mice fail to remember the location of a hidden platform in the Morris watermaze, as well as the spatial context in a fear conditioning paradigm. These findings suggest that optimal activity of the UPS in forebrain neurons such as those of the hippocampus, is required for spatial learning. A large body of data has shown that the formation and storage of long-term memories also require protein synthesis (Flexner *et al.*, 1963; Kelleher *et al.*, 2004; Fonseca *et al.*, 2006). However, in order to produce amnesic effects in rodents, levels of protein synthesis inhibition above 90% are required (Barondes and Cohen, 1967; Routtenberg and Rekart, 2005). Apparently, a balance between protein synthesis and active protein degradation is essential for learning and memory (Fonseca *et al.*, 2006) but the formation of new memories is much more sensitive to the inhibition of protein degradation than to the inhibition of protein synthesis.

Conclusions

The mouse lines we have presented here can be considered as models to study a wide range of neurodegenerative diseases in which a chronic dysfunction of the UPS has been implicated in the pathogenesis. Crossing these mice with, for instance other AD mouse models (Wong *et al.*, 2002) will allow us to investigate the role of inhibition of the UPS in different stages of the disease. Line 3413, which expresses UBB⁺¹ in the striatum (Figure 2) is highly suited for investigation of synergistic action with polyglutamine proteins (De Pril *et al.*, 2004). The involvement of the UPS in ALS can also be studied, as line 8630 expresses UBB⁺¹ in motor neurons in the spinal cord (Figure 2B). The study of synergistic action of UBB⁺¹ and other aberrant proteins may provide clues into the molecular pathology of neurodegenerative diseases. We show in the present paper that cognitive deficits can be caused directly by partial and chronic inhibition of the UPS, at a stage before cellular demise. The proteomic profile of the brains of the UBB⁺¹ transgenic mice show a partial similarity to those of AD brain or of mouse models for AD, suggesting that a decline in UPS activity could underlie some of the pathology observed in neurodegenerative diseases.

Acknowledgements

We would like to thank Gertjan de Fluiter, Miranda Cozijnsen, Gavin Adema, Lotte Vis and Christiaan Levelt (Netherlands Institute for Neuroscience) for animal care. Mark Mayford (University of California at San Diego) kindly provided the CamKIIα vector. We thank Rob de Vos (University of Twente) for neuropathological stainings and Wilma Verweij for the correction of language. We are grateful to Melly Oitzl (Leiden University), Jan de Bruin and Ruud Joosten for assistance with the watermaze. Michel Hofman assisted with statistical analysis and Joop van Heerikhuize helped with the RIA and microscopy. We thank Rinus Westdorp and Ruud van der Blom for the design and construction of testing apparatus. We are grateful to Rob Benne and the Department of Biochemistry (Amsterdam Medical Center) for the use of equipment. We thank Femke de Vrij and Nico Dantuma for insightful discussions. This research was supported by the NWO GPD 970-10-029 and 903-51-192, EU 5th framework QLRT 1999-02238, Van Leersum Fund, ISAO/IARF grants 01504 and 06502, Platform Alternatieven voor Dierproeven Grant PAD 98.19 and Hersenstichting Nederland 12F04.01, H00.06 and 13F05.11.

Supplementary Information

Supplementary Figures

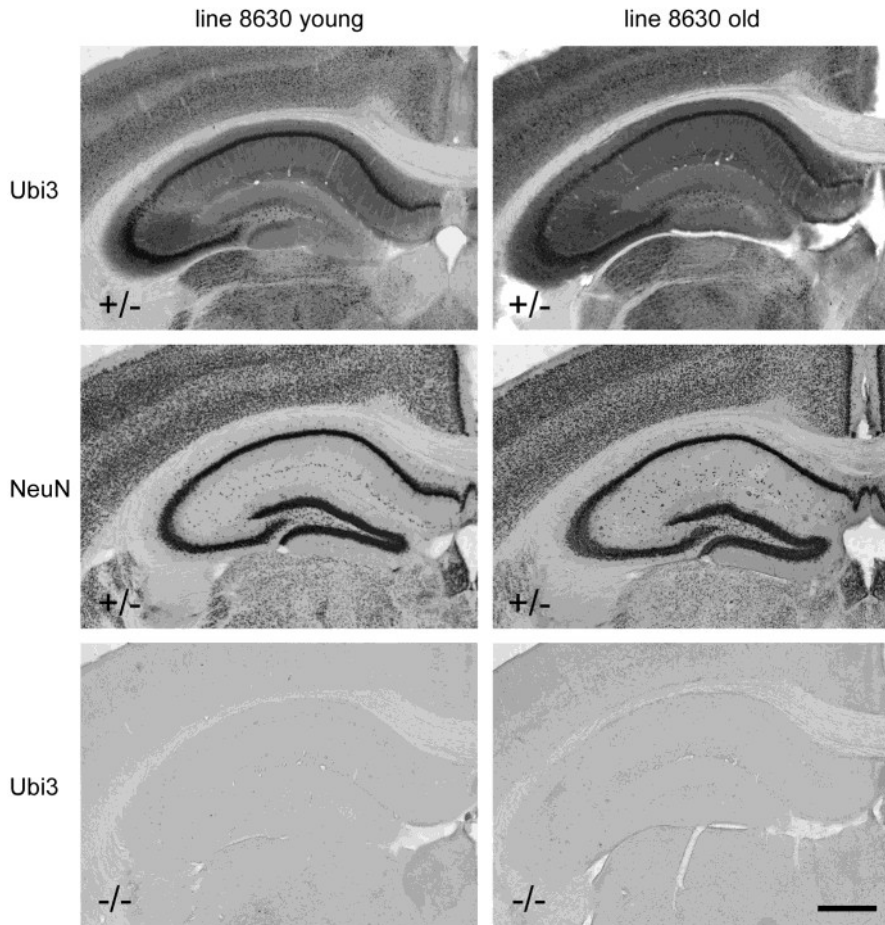


Figure S1 *UBB⁺¹ transgene expression in line 8630.* Coronal vibratome sections of line 8630 transgenic mice were stained with Ubi3 antibody against UBB⁺¹, or with the neuronal marker NeuN. The hippocampal formation at AP-1.6 relative to bregma is shown of young (128 days) and old (512 days) male 8630 heterozygous (+/-) transgenic mice. No increase in UBB⁺¹ protein accumulation or massive neuronal loss is observed during aging. Wild-type (-/-) littermates do not show UBB⁺¹ immunoreactivity, as expected. Scale bar: 0.5 mm.

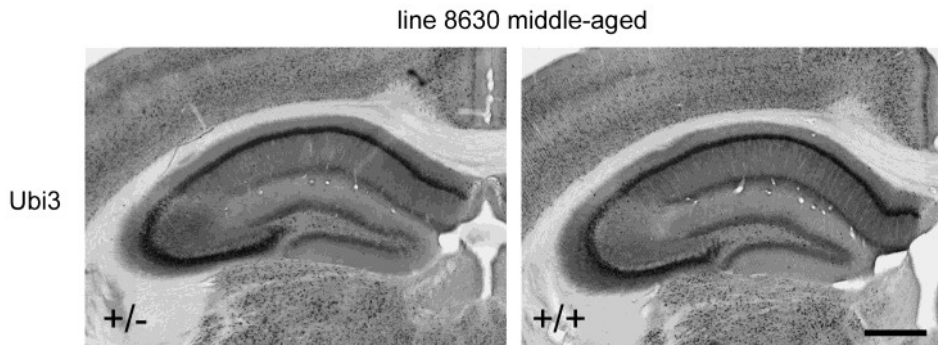


Figure S2 UBB^{+1} expression in homozygous line 8630 transgenic mice. Differences in UBB^{+1} expression levels or brain morphology between heterozygous (+/-) and homozygous (+/+) 8630 transgenic mice were not observed, exemplified here for middle-aged (345 days) male 8630 transgenic mice. Coronal vibratome sections of line 8630 transgenic mice were stained with Ubi3 antibody against UBB^{+1} . Scale bar: 0.5 mm.

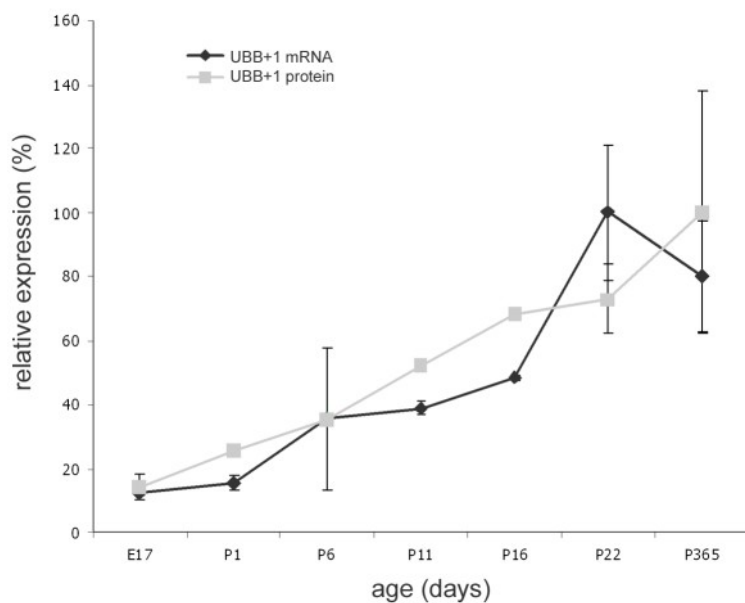


Figure S3 UBB^{+1} mRNA and protein expression in line 3413 transgenic mice. UBB^{+1} mRNA and protein expression in line 3413 transgenic mice relative to the age of the mouse. mRNA levels were determined by RT-QPCR, protein levels were determined by radioimmunoassay. Expression level is relative to the maximal level of expression observed (%).

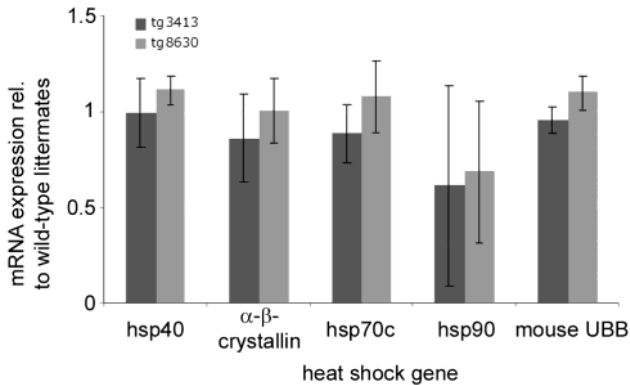


Figure S4 Gene expression analysis in UBB⁺¹ transgenic mice. Gene expression analysis of four heat-shock proteins and mouse UBB in UBB⁺¹ transgenic mice. Total RNA was isolated from cortex of transgenic mice (n=3) of both line 3413, line 8630 and their respective non-transgenic littermates. RT-quantitative PCR was performed to assess gene expression, normalizing for rS27a and EF1 α (Table S3). Paired statistics did not show a significant effect of genotype ($p>0.05$). Data is plotted as ratio of transgenic over wild-type.

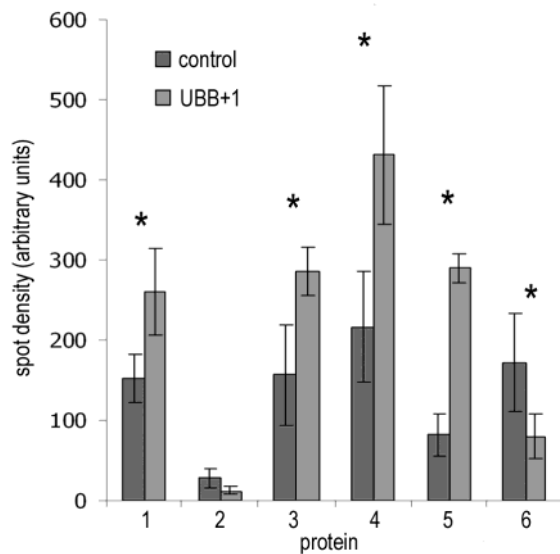


Figure S5 Densitometric analysis. Densitometric analysis of the proteins that showed quantitative differences between UBB⁺¹ transgenics (n=3) and wild-type mice (n=3). Asterisks indicate significant changes ($p<0.05$, t-test). 1: Nucleoside-diphosphate kinase B, 2: Dihydropyrimidinase related protein-2, 3: Dihydrolipoamide dehydrogenase, 4: Glutamine synthetase, 5: Parvalbumin alpha, 6: Mu-crystallin homolog.

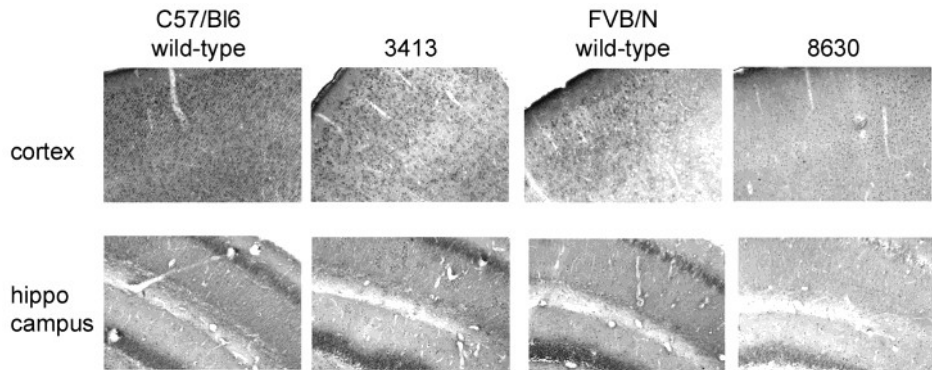


Figure S6 *Alpha-enolase expression in the mouse cortex of UBB^{+1} transgenic mice.* α -enolase expression in the mouse cortex of UBB^{+1} transgenic mice and non-transgenic littermates. Immunohistochemical staining of brain sections of mice with an antibody against α -enolase. The top panel shows images of the cortex and the lower panel shows part of the hippocampus. All four animals show comparable distribution of α -enolase in areas studied.

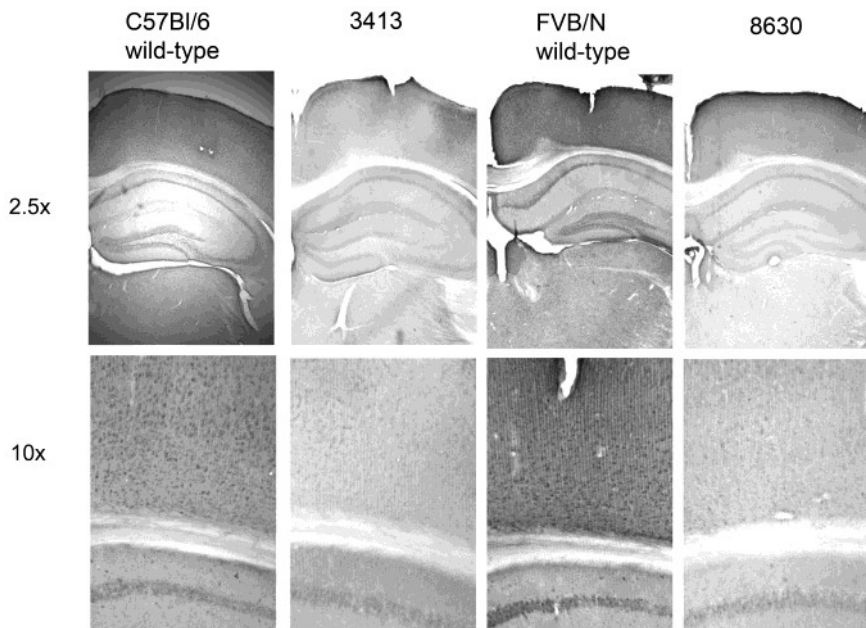


Figure S7 *Malate dehydrogenase expression in the mouse cortex of UBB^{+1} transgenic mice.* Malate dehydrogenase expression in the mouse cortex of UBB^{+1} transgenic mice and non-transgenic littermates. Immunohistochemical staining of brain sections of mice with an antibody against malate dehydrogenase, two magnifications are shown.

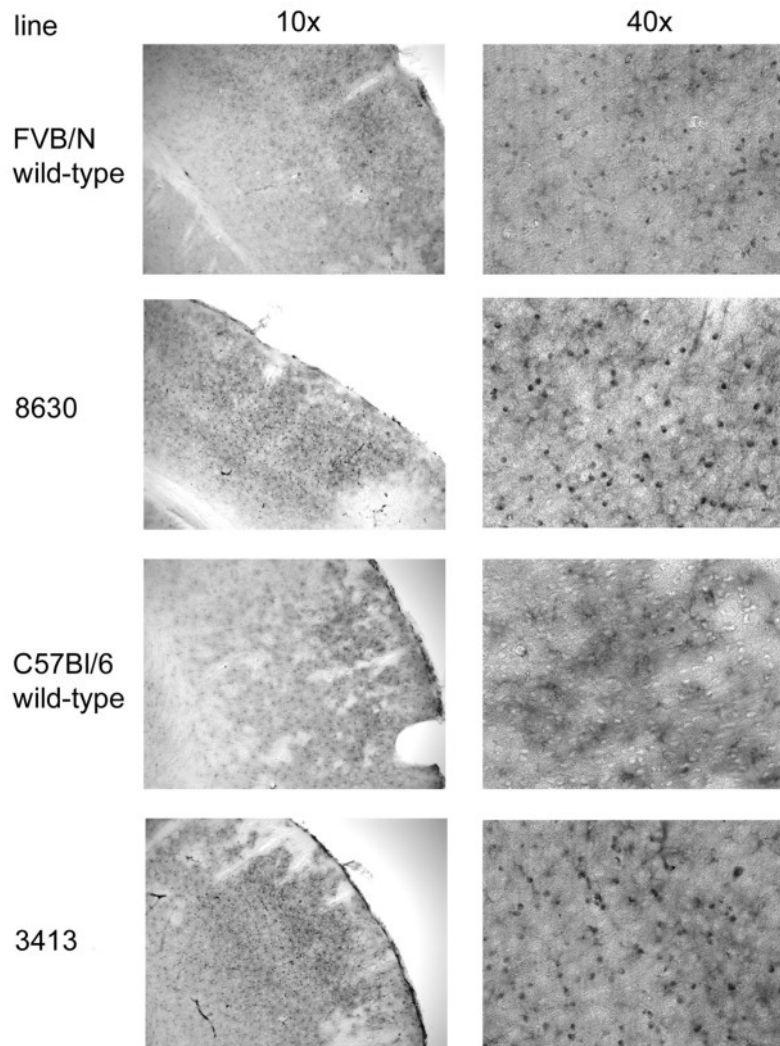


Figure S8 Glutamine synthetase expression in the mouse cortex of UBB⁺¹ transgenic mice. Glutamine synthetase expression in the mouse cortex of UBB⁺¹ transgenic mice and non-transgenic littermates (wild-type). Two magnifications are shown. An increase in glutamine synthetase distribution can be observed in small neuron-like cells in the cortex of transgenic mice.

Supplementary Tables

Table S1 Identified proteins that are up or down regulated or post-translationally modified in the cortex of UBB⁺¹ transgenic mice. Spot numbers correspond to the numbers in Figure 6. Peptide sequences sequenced and associated MASCOT scores are shown. Please note that some protein spots on 2D gels yielded several peptides. For each peptide sequenced, both the theoretical and experimental molecular weight are reported. Ms sc.; MASCOT score.

nº	Protein Name	SWISS PROT	Th. MW (Da)	Th. pI	Th. MW pept.	Exptl. MW pept.	Peptide Sequence	Ms Sc.
1	Alpha enolase	P17182	47009	6.36	1405.71	1405.99	GNPTVEVDLYTAK	46
2	Malate dehydrogenase, mitochondrial [Precursor]	P08249	35596	8.82	1792.08	1792.79	VAVLGASGGIGQPL SLLK	72
3	Glyceraldehyde 3-phosphate dehydrogenase	P16858	35678	8.45	1368.74	1369.19	GAAQNIIPASGAAK	38
4	Pyruvate dehydrogenase (Lipoamide) beta	Q9D051	38937	6.41	1263.62	1262.99	VTGADVPMKYAK	35
5	Dihydrolipoamide dehydrogenase, mitochondrial [Precursor]	O08749	54212	7.97				
6	ATP synthase alpha chain, mitochondrial [Precursor]	Q03265	59752	9.22	1025.59	1026.19	AVDSLVPIGR	50
6	ATP synthase alpha chain, mitochondrial [Precursor]	Q03265	59752	9.22	1315.73	1314.59	TSIAIDTIINQK	58
7	Protein disulfide isomerase [Precursor]	P09103	57143	4.79				
7	Tubulin alpha-2 chain	P05213	50165	4.94				
8	Nucleoside-diphosphate kinase B	Q01768	17363	6.97				
9	Glutamine synthetase	P15105	42145	6.47				
10	Tubulin alpha-1 chain	P02551	50135	4.94	1823.98	1823.79	VGINYQPPTVVPGG DLAK	35
11	Profilin II	Q9JJV2	14901	6.78	1353.69	1352.79	EGFFTNGLTLGAK	38
11	Profilin II	Q9JJV2	14901	6.78	1433.69	1433.99	SQGGEPTYVAVGR	58

Table S1 Identified proteins that are up or down regulated or post-translationally modified in the cortex of UBB⁺¹ transgenic mice (continued).

nº	Protein Name	SWISS PROT	Th. MW (Da)	Th. pI	Th. MW pept.	Exptl. MW pept.	Peptide Sequence	Ms sc.
12	LIM and SH3 protein 1	Q61792	29994	8.33	1417.72	1417.19	GFSVVADTPELQR	43
13	Guanine nucleotide-binding protein beta subunit 4	P29387	37354	5.59				
14	Dihydropyrimidinase related protein-2	O08553	62170	5.95				
15	Parvalbumin alpha	P32848	11799	5.02	1379.68	1379.39	IGVEEFSTLVAES	14
16	Mu-crystallin homolog	O54983	33523	5.44	1078.54	1078.99	FASTVQGDVR	37
16	Mu-crystallin homolog	O54983	33523	5.44	931.53	930.59	TAAVSAIATK	38

Table S2 Summary of UBB⁺¹ transgenic mice and control mice used for proteomics

nº	Line	Background	Transgene	Promoter	Sex (m/f)	Age (days)
1	3413	C57BL/6	-	-	f	145
2	3413	C57BL/6	UBB ⁺¹	CamKIIα	f	145
3	3413	C57BL/6	-	-	m	153
4	3413	C57BL/6	UBB ⁺¹	CamKIIα	f	163
5	8630	FVB/N	-	-	f	138
6	8630	FVB/N	UBB ⁺¹	Thy-1.2	f	138
7	8630	FVB/N	-	-	f	205
8	8630	FVB/N	UBB ⁺¹	Thy-1.2	f	205
9	8630	FVB/N	-	-	f	526
10	8630	FVB/N	UBB ⁺¹	Thy-1.2	f	645

Table S3 PCR primers

Target	QPCR Efficiency	Forward Primer	Reverse Primer
UBB	1.97	TACCGGCAAGACCATCACC	GGATGCCTCTTTATCCTGGAT
BGH poly A	1.95	GCCTTCTAGTTGCCAGCCAT	AGTGGGAGTGGCACCTTCC
EF1 α	1.99	CTGGATGCTGCCATCAAA	GGCGCTTTCCTCTGAAGAA
Ube2d2	1.98	GAGCAGCATTCACCAAAACC	AACAGCAACCAACACCTTGC
rS27a	1.96	AAGGTGGATGAAAATGGCAA	CCATGAAAACCTCCAGCACCA
hsp40	1.67	GCCCTTGCTTGGGTGTAGTG	TCACCCCTCCACGTACAGATC
α β -crystallin	1.85	TCGGAGAGCACCTGTTGGAG	GAGGGTGGCCGAAGGTAGA
hsp70c	1.87	TTGAATGCTGACCTGTTCCGT	TGTGACTTGTCCAGCTTGGC
hsp90	2.46	TGAGGAACCTGGTATCTTGCA	GTGTTCTGTGGATCTCCAGACTG
3413	genotyping	GGTGAGTACTCCCTCTCAAAAGC	CTGCAGTTGGACCTGGAGTGGA
8630	genotyping	CTTAGGCAGTGTCACTCCCTAAG	TCAGACGCAGGACCAGGTGCA

Supplementary Results

Expression of α -enolase, malate dehydrogenase and glutamine synthetase in UBB $^{+1}$ transgenic mouse brain

The localization in the brain of three proteins identified by differential proteomics was verified by immunohistochemistry in order to validate the proteomics data. Antibodies against alpha enolase (#6880-1004, Biotrend Chemikalien GmbH, Koln, Germany; 1:250), malate dehydrogenase (#200-601-145, Rockland Immunochemicals, Gilbertsville, PA, USA; 1:1000) and glutamine synthetase (#MAB302, Chemicon, Temecula, CA; 1:250) were used on brain sections of transgenic and wild-type littermate mice.

Figure S6 shows the distribution of α -enolase in neurons of the hippocampus (upper and lower panel) and the cortex (central panel) of UBB $^{+1}$ transgenic and wild-type control mice from lines 3413 having a CamKII α promoter and 8630 having a Thy1.2 promoter. The protein is localized in the cytoplasm of neurons in both hippocampus and cortex. We could not observe any obvious differences in amount or distribution of α -enolase between UBB $^{+1}$ mice versus controls. This confirms our 2D data where we observed a basic shift of the protein and could not detect a significant difference in the amount of alpha enolase. Thus, the glycolytic enzyme alpha enolase is present at similar levels and distribution pattern in neurons in cortex and hippocampus of both UBB $^{+1}$ transgenic and control mice. However, from our 2D gel profile we can conclude that α -enolase has been post-translationally modified in UBB $^{+1}$ transgenic mice, which could have implications for its functioning.

Malate dehydrogenase is expressed uniformly throughout the cortex, with high expression levels in neurons (Figure S7). Staining of malate dehydrogenase appeared to be reduced in the cortex of both line 3413 and line 8630 UBB⁺¹ transgenic mice. On 2D-gels, we observed that this protein was ubiquitinated. It is not unlikely that the ubiquitination affects the conformation of the protein or accessibility of the antibody to its epitope, resulting in an apparent decrease in staining.

Glutamine synthetase, an enzyme involved in the glutamate-glutamine cycle, is under normal circumstances expressed in astrocytes. This is confirmed by immunohistochemical stainings of cortex and hippocampus of UBB⁺¹ transgenic and control mice, where we found the enzyme to be mainly distributed in astrocytic cells (Figure S8). From the analysis of silver stained gels (Figure 6 and Table 1 spot #9) it appears that the levels of glutamine synthetase are increased in UBB⁺¹ transgenic mice. This increase on 2D-gels is confirmed by an increase in immunoreactivity that we observed in certain cortical regions of UBB⁺¹ transgenic mice (Figure S8). Here, the enzyme seemed to be also localized in small neuronal like cells (as compared to larger pyramidal cells). Unfortunately, we were not able to determine the developmental subtype of these cells in cortex of UBB⁺¹ transgenic mice by immunohistochemistry, therefore, we cannot exclude that they might also be glial cells.

Supplementary Discussion

Table 1 in the main body of Chapter 3 and Table S1 summarize the 16 identified proteins that are either up or down regulated by at least a factor of 1.5 or modified in the cerebral cortex of UBB⁺¹ transgenic mice. Spot #7 contained two proteins: protein disulfide isomerase (PDI) and tubulin alpha-2 chain. Since we could not distinguish between the two proteins in one spot, we did not indicate the fold of decrease in Table 1 (the *total* spot is decreased by a factor of 1.7). Spot #10 only gave one positive hit, but with an ion score of 35, indicating identity or extensive homology ($p < 0.05$) to tubulin alpha-1 chain. Spot #13 had an ion score of 26, indicating a peptide with significant homology to guanine nucleotide-binding protein beta subunit 4. We verified the expression of three of these proteins by immunocytochemistry in mouse brain (different individuals from the proteomics experiments, but from the same age-groups), and showed a down-regulation of staining of malate dehydrogenase and an up-regulation of staining of glutamine synthetase in UBB⁺¹ transgenic mice of both line 3413 and line 8630 (Figures S6, S7 and S8 and Results in the Supplementary data). A number of these proteins have been reported previously as proteasome substrates, although two (PDI, glutamine synthetase) of these may undergo ubiquitin-independent proteolysis by the proteasome (Grune *et al.*, 2003).

Energy / metabolism

Nine of the identified proteins were metabolic enzymes of which six are involved in energy metabolism. These are α -enolase (glycolysis), malate dehydrogenase (tricarboxylic acid cycle), glyceraldehyde 3-phosphate dehydrogenase (glycolysis), pyruvate dehydrogenase (lipoamide) beta (glycolysis, tricarboxylic acid cycle, glucose metabolism), ATP synthase alpha chain (ATP-proton interconversion) and dihydrolipoamide dehydrogenase (glycolysis). The latter also plays a role in electron transport, as does protein disulfide isomerase. PDI is an endoplasmic reticulum enzyme that catalyses the rearrangement of disulfide bonds in various proteins to form the native structures. Alterations in energy metabolism are also a known event in AD; a reduced glucose metabolism has previously been observed in AD brain (Messier and Gagnon, 1996; Mielke *et al.*, 1996) and there are indications that alterations in glucose metabolism induce AD-like tau hyperphosphorylation (Planell *et al.*, 2004). Glutamine synthetase, a metabolic enzyme also identified in AD brain and in the GSK3 β transgenic mouse (Table 1), has been implicated in neurodegeneration in several studies. This astrocyte-specific enzyme catalyzes the amidation of glutamate to form the non-neurotoxic amino acid glutamine. A decline in activity could therefore contribute to a reduced clearance of glutamate leading to glutamate excitotoxicity. It was shown in AD brain that glutamine synthetase activity was decreased relative to age-matched control brain (Smith *et al.*, 1991; Hensley *et al.*, 1995). Impairment of its metabolic functioning could be due to oxidative modification as was proposed by Castegna *et al.* (Castegna *et al.*, 2002) and is also supported by studies suggesting a role for β -amyloid in the generation of free radical peptides, thereby inactivating the enzyme (Hensley *et al.*, 1994; Aksenov *et al.*, 1997). Additionally, it was demonstrated in AD brain that there is a loss of glutamine synthetase from perisynaptic regions of the neuropil and from astrocytic endfeet, which could possibly potentiate glutamate excitotoxicity and ammonia neurotoxicity (Robinson, 2000; Robinson, 2001). Interestingly, glutamine synthetase was found to be expressed by neurons in the Alzheimer brain (Robinson, 2000). Immunocytochemical staining showed that glutamine synthetase was up-regulated by neuron-like cells in the UBB $^{+1}$ transgenic mouse cortex (Figure S8 in Supplementary data). Moreover, glutamine synthetase is up-regulated in GSK-3 β transgenic mice (Tilleman *et al.*, 2002). These data suggest that the up-regulation of glutamine synthetase expression could be a transient phenomenon, that is lost in full-blown AD. We also identified the enzyme nucleoside-diphosphate kinase (NDK) B to be increased in expression in UBB $^{+1}$ transgenic mice cortex. In brains of GSK3 β transgenic mice and tau transgenic mice the isozyme NDK A was also up-regulated (Tilleman *et al.*, 2002; Tilleman *et al.*, 2002) (Table 1). NDK provides nucleoside triphosphates for cellular reactions like synthesis of nucleic acids, lipids, polysaccharides and proteins, G-protein-mediated signal transduction and microtubule polymerisation. Levels of NDK A were however significantly decreased in AD and Down syndrome, as well as the specific activity of the enzyme, suggesting that a decreased activity

are more indicative of a late stage of disease pathology (Kim *et al.*, 2002). Additionally, it was proposed that oxidation of the enzyme could be the reason for this significant decrease of activity, as its activity was shown to be regulated by oxidative modifications (Song *et al.*, 2000). Interestingly, recent data implicate mitochondrial trafficking in one of the down-stream effects of UBB⁺¹ (Tan *et al.*, 2007), suggesting a common denominator for the changes observed on metabolic proteins (Hoglinger *et al.*, 2003).

Cytoskeleton

Furthermore, we identified changes in four proteins in UBB⁺¹ transgenic mice cortex, which are involved in cytoskeletal function. The strong linkage of tau, a microtubule-associated protein with AD and other neurodegenerative diseases provides additional weight to this category of proteins (Goedert *et al.*, 1988; Hutton *et al.*, 1998). These represent the alpha-1 and -2 chain of tubulin, the major constituent of microtubules and two actin binding proteins, profilin II which can affect the structure of the cytoskeleton and is also involved in signal transduction and LIM, and SH3 protein 1 which has a role in the regulation of dynamic actin-based cytoskeletal activities (Chew *et al.*, 2000). Dihydro-pyrimidinase related protein-2 (DRP-2) is also a protein that has an effect on the cytoskeleton. This signal transduction protein is involved in neurite outgrowth and axonal guidance (Hamajima *et al.*, 1996; Quinn *et al.*, 1999), it mediates growth cone collapse through a signalling cascade involving G-protein (Goshima *et al.*, 1995) and it is suggested to play a role in regulating the dynamics of microtubules (Gu and Ihara, 2000). Another signal transduction protein we identified is guanine nucleotide-binding protein beta subunit 4, a subunit of the heterotrimeric G-protein complex, which is involved in various trans-membrane signalling systems. Involvement of DRP-2 in AD comes from Yoshida *et al.* (Yoshida *et al.*, 1998) who found in AD cortex the protein to be associated with neurofibrillary tangles consisting of paired helical filaments. They suggest that neurons containing neurofibrillary tangles are depleted of cytoplasmic DRP-2 because of its entrapment by paired helical filaments. By others it was shown that this neurofibrillary tangle-associated DRP-2 is highly phosphorylated (Gu *et al.*, 2000) and phosphorylation at these sites might play a role in regulation of its activity (i.e. neurite extension) and might therefore be involved in the formation of degenerating neurites.

Others

Two remaining proteins we identified could not be assigned to any of the above categories. These are parvalbumin alpha, a calcium ion binding protein and mu crystallin, a protein involved in sensory organ development (Mouse Genome Informatics, Gene Ontology Classifications).

CHAPTER IV

Low levels of mutant ubiquitin are degraded
by the proteasome in vivo

Submitted manuscript

Paula van Tijn, Marian C. Verhage,
Barbara Hobo, Fred W. van Leeuwen, David F. Fischer

Abstract

The ubiquitin-proteasome system fulfils a pivotal role in regulating intracellular protein turnover. Impairment of this system is implicated in the pathogenesis of neurodegenerative diseases characterized by ubiquitin-containing proteinaceous deposits. UBB⁺¹, a mutant ubiquitin, is one of the proteins accumulating in the neuropathological hallmarks of tauopathies, including Alzheimer's disease, and polyglutamine diseases. *In vitro*, UBB⁺¹ properties shift from a proteasomal ubiquitin-fusion degradation substrate at low expression levels to a proteasome inhibitor at high expression levels. In this study we report on a novel transgenic mouse line expressing low levels of neuronal UBB⁺¹. In these mice, the UBB⁺¹ protein is scarcely detectable in the neuronal cell population. Accumulation of UBB⁺¹ only commences after intracranial infusion of the proteasome inhibitors lactacystin or MG262, showing that at these low expression levels the UBB⁺¹ protein is a substrate for proteasomal degradation *in vivo*. In addition, accumulation of the protein serves as a reporter for proteasome inhibition. These findings strengthen our proposition that in healthy brain, UBB⁺¹ is continuously degraded and disease-related UBB⁺¹ accumulation serves as an endogenous marker for proteasomal dysfunction. This novel transgenic line can give more insight into the intrinsic properties of UBB⁺¹ and its role in neurodegenerative disease.

Introduction

The ubiquitin-proteasome system (UPS) is the main intracellular pathway for regulated protein turnover and essential for maintaining cellular homeostasis (reviewed by (Glickman and Ciechanover, 2002)). Besides functioning as a protein quality control mechanism by degrading aberrant and misfolded proteins, ubiquitin (Ub) modification of proteins also regulates many other processes, including cell-cycle progression, endocytosis and intracellular signaling (reviewed by (Welchman *et al.*, 2005; Mukhopadhyay and Riezman, 2007)). Substrates are tagged for proteasomal degradation by covalent binding of the C-terminal glycine of a Ub moiety to an internal lysine residue in a substrate. Additional Ub moieties are successively attached to the substrate-bound Ub forming a poly-Ub chain (Pickart, 2004). Ubiquitinated substrates with a chain of four or more lysine-48 linked ubiquitins are selectively targeted for degradation by the 26S proteasome (Thrower *et al.*, 2000), a multi-subunit proteolytic complex composed of a barrel-shaped 20S core particle and two 19S regulatory complexes. The 19S particle, which forms a cap-like structure on the 20S core, is essential for substrate recognition, deubiquitination, unfolding and subsequent translocation into the 20S catalytic core. Three different proteolytic activities are present in the 20S particle; chymotrypsin-like, trypsin-like and peptidyl-glutamyl-peptide hydrolyzing (PGPH) activity residing in the β_5 , β_2 and β_1 subunits re-

spectively (reviewed by (Wolf and Hilt, 2004)).

Impairment of the UPS is implicated to play a role in the pathogenesis of a broad array of diseases, including neurodegeneration. This is exemplified by the presence of ubiquitin-positive pathology in many neurodegenerative disorders such as Alzheimer's disease and Parkinson's disease (Ciechanover and Brundin, 2003; van Tijn *et al.*, 2008). Another indication of involvement of the UPS in neurodegeneration is the disease-specific accumulation of a mutant Ub (UBB^{+1}) in tauopathies, including Alzheimer's disease, and polyglutamine diseases such as Huntington's disease and spinocerebellar ataxia-3 (van Leeuwen *et al.*, 1998; Fischer *et al.*, 2003; De Pril *et al.*, 2004). UBB^{+1} is generated by a di-nucleotide deletion in the Ub mRNA which results in a mutant protein with a 19 amino acid C-terminal extension. The UBB^{+1} protein lacks the C-terminal glycine essential for substrate ubiquitination, however UBB^{+1} is a substrate for ubiquitination itself and targeted for degradation by the proteasome (Lam *et al.*, 2000). *In vitro*, degradation of UBB^{+1} occurs only at low expression levels; accumulation of UBB^{+1} commences after exceeding a threshold level, leading to dose-dependent inhibition of the UPS (van Tijn *et al.*, 2007). High expression levels of UBB^{+1} also result in cell cycle arrest, apoptotic-like cell death, expression of heat shock proteins (Hsp) and resistance to oxidative stress (De Vrij *et al.*, 2001; Lindsten *et al.*, 2002; Hope *et al.*, 2003). In human disease, accumulation of the UBB^{+1} protein in the disease-specific neuropathological hallmarks is proposed to be an endogenous reporter for UPS dysfunction (Fischer *et al.*, 2003; Hol *et al.*, 2005).

We previously reported on two UBB^{+1} transgenic mouse lines (lines 3413 and 8630) expressing high levels of neuronal UBB^{+1} , ranging from 50-67% of wildtype Ub mRNA levels (Chapter 3). In the 3413 transgenic mice, UBB^{+1} protein accumulation resulted in a significant decrease of chymotryptic proteasome activity ultimately leading to proteome changes and deficits in spatial reference memory (Chapter 3). As UBB^{+1} shifts from UPS substrate to inhibitor with increasing levels of expression *in vitro*, it is essential to know if these properties are conserved *in vivo* to extrapolate these findings to human disease. To this end, we investigated in the present study the effect of low-level UBB^{+1} expression *in vivo*. We generated a UBB^{+1} transgenic mouse line (line 6663) with neuronal UBB^{+1} expression at relatively low levels compared to the previously reported UBB^{+1} transgenic lines and studied the intrinsic properties of low-level UBB^{+1} expression *in vivo*.

Materials and Methods

Generation of transgenic mice

The murine Ca(2+)/Calmodulin-dependent Protein Kinase II alpha (CamKII α) promoter (Mayford *et al.*, 1996) was used to drive UBB^{+1} expression. The UBB^{+1} cDNA, encoded by the first ubiquitin open reading frame and the C-terminus in the +1 reading frame (van

Leeuwen *et al.*, 1998) was cloned with a flanking 5' intron (Choi *et al.*, 1991) and 3' polyadenylation site (bovine growth hormone) in the CamKIIα cassette by NotI. Before injection, the insert was excised from the plasmid, purified from gel by electro-elution and ethanol precipitated. The construct was injected into fertilized oocytes of FVB/N mice. The line was maintained on its genetic background by breeding hemizygous mice to wild-type mice. From F2 onwards Mendelian ratios were observed in the offspring. Mice were kept in group housing on a 12/12 h light-dark cycle with food and water ad libitum in specific pathogen free conditions (Nicklas *et al.*, 2002). All mice were genotyped on DNA isolated from ear-snips using the QIAamp DNA mini kit (Qiagen), primers being GGTGAGTACTCCCTCTCAAAAGC (forward) and CTGCAGTTGGACCTGGGAGT-GGA (reverse). The copy-number of the transgene (10 copies) was determined by Southern blotting and analysed on a Storm 860 phosphorimager (Molecular Dynamics). All animal experiments were performed conforming to national animal welfare law and under guidance of the animal welfare committee of the Royal Netherlands Academy of Arts and Sciences.

RNA isolation and qPCR

Mice (n=4 per group; 2 male, 2 female) were euthanized by carbon dioxide asphyxiation, the brain was immediately dissected and hemispheres were frozen in liquid nitrogen. RNA was isolated using Trizol (Invitrogen) and an Ultraturrax homogenizer and stored at -20° C. cDNA was synthesized from 2 µg of RNA using superscript II (Invitrogen). Real-time quantitative PCR was performed with SYBR-green mastermix (Applied Biosystems) on an ABI5700 (Applied Biosystems) as described previously (Hope *et al.*, 2003). The primer-set for the *ubiquitin-B* (*UBB*) target recognizes both the endogenous *UBB* mRNA and the transgene (forward: TACCGGCAAGACCATCACC, reverse: GGATGCCTT-CTTTATCCTGGAT, efficiency 1.97), the bovine growth hormone polyA set recognizes the CamKIIα transgene (forward: GCCTTCTAGTTGCCAGCCAT, reverse: AGTGG-GAGTGGCACCTTCC, efficiency 1.95), three house-keeping genes were used as normalizers (*EF1α*, *Ube2d2* and *rS27a* (Warrington *et al.*, 2000; Lee *et al.*, 2002)). Statistics were performed with Mann-Whitney U-test in SPSS 11 for Mac.

Radioimmunoassay

Mice were euthanized by carbon dioxide asphyxiation, the brain was immediately dissected and hemispheres were frozen in liquid nitrogen. A hemisphere was homogenized in suspension buffer: 100 mM NaCl, 50 mM Tris pH7.6, 1 mM EDTA pH8.0, 0.1% Triton-X-100, 10 mM DTT and protease inhibitors (Complete, Roche), samples were stored at -80°C. Total protein concentration was determined by means of a Bradford assay. UBB⁺¹

protein levels were measured in a radioimmunoassay (RIA) as described previously (Hol *et al.*, 2003) with Ub3 peptide (YADLREDPDRQ) and Ub3 antiserum (bleeding date 05/08/97, final dilution 1:24000, (Fischer *et al.*, 2003)). The final UBB⁺¹ protein concentration in the transgenic mice was corrected for background levels in wild-type mice. For the 6663 transgenic mice; n=8 (5 males, 3 females) and for wildtype mice; n=6 (4 males, 2 females).

Implantation of osmotic pumps

Proteasome inhibitors lactacystin (BIOMOL International LP, UK) and MG262 ((Z-Leu-Leu-Leu-B(OH)₂) Boston Biochem Inc., Cambridge, MA) were dissolved in DMSO and diluted to their final concentration in Ringer's solution (Fresenius Kabi). 100 µl of dilution was applied to an osmotic minipump (Alzet 1003D, 3 day run-time, 1 µl/h, Alzet, CA). Osmotic minipumps were primed overnight at 37°C in 0.9% NaCl solution. Mice were anesthetized with 10 ml/kg FFM (0.0787 mg/ml fentanyl citrate, 2.5 mg/ml fluanisone, 0.625 mg/ml Midazolam in H₂O). The skull was exposed and stereotactic coordinates for infusion of proteasome inhibitors were read against bregma (-2.3 mm anterior-posterior; -1.5 mm lateral) (Paxinos and Franklin, 2001). A hole was drilled through the skull and the dura was punctured. A canula, 2.5 mm long with a sharp tip (Brain Infusion Kit II, Alzet) was implanted in the brain and glued to the skull with cyanoacrylate adhesive (Loctite 415). Polyvinylchloride tubing was used to connect the canula to the osmotic pump placed subcutaneously in a pocket under the skin in the flank of the mouse. The skin was sutured and mice were administered 0.05 mg/kg buprenorphine (Shering-Plough) intra-muscularly as an analgesic and 20 ml/kg 0.9% NaCl subcutaneously to prevent dehydration. Mice were kept at 37°C until they were recovered, and subsequently housed individually to prevent opening of the sutures. All experimental mice implanted with an osmotic pump were female, wild-type female littermates were used as controls.

Immunohistochemistry

Animals were given deep pentobarbital anaesthesia (intra-peritoneal) and were perfused intra-cardially with phosphate-buffered saline, pH7.4, followed by phosphate-buffered saline containing 4% paraformaldehyde. The brain was removed and cut on a vibratome (Leica VT1000S) in 50 µm coronal sections. Sections were immuno-histochemically stained overnight as described previously (Chapter 3) at 4°C using the peroxidase-anti-peroxidase method (Sternberger *et al.*, 1970) with rabbit polyclonal anti-UBB⁺¹ antibody (Ub3; bleeding date 05/08/97, 1:1000 (Fischer *et al.*, 2003)), polyclonal anti-ubiquitin antibodies (#Z0458, DAKO, 1:1000 and #U5379, Sigma, 1:200) or a monoclonal anti-polyubiquitin conjugate antibody (LB112, 1:3, (Iwatsubo *et al.*, 1996)). Staining was visu-

alized with 3,3'-diaminobenzidine solution using nickel intensification. Images were made using a Zeiss Axioplan 2 or Wild Makroskop M420 imaging microscope and an Evolution MP digital camera (MediaCybernetics, Silver Spring, MD), analyzed with Image-Pro Plus software (version 5.1, MediaCybernetics).

Results

Generation of transgenic mice expressing low levels of UBB⁺¹

We have generated a transgenic mouse line postnatally expressing low-levels of human UBB⁺¹ in the brain under the neuronal CamKII α promoter on a FVB/N background (line 6663). The relative expression levels of UBB⁺¹ mRNA versus endogenous ubiquitin-B (UBB) mRNA were measured in adult mouse brain with real-time quantitative PCR using primers directed against UBB, recognizing both the endogenous UBB mRNA and the transgene, and a bovine growth hormone polyadenylation primer set recognizing the CamKII α transgene. The expression level of the UBB⁺¹ mRNA in the 6663 line amounted to

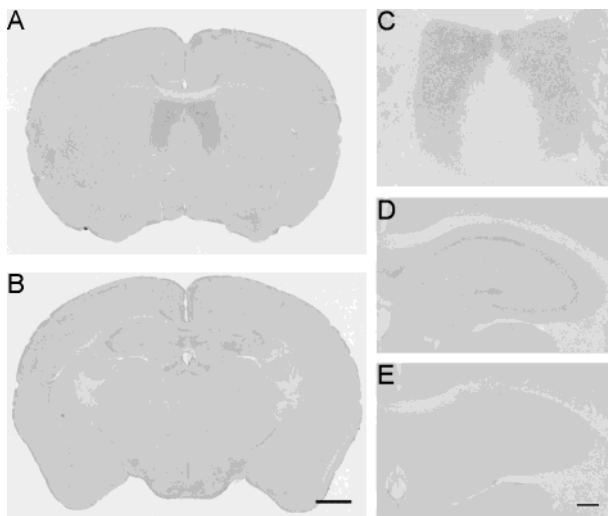


Figure 1 Expression of UBB⁺¹ in transgenic line 6663. A-D. Expression pattern of the UBB⁺¹ protein in the low-level expression transgenic line 6663. Coronal 50 μ m vibratome sections of a 9-month-old 6663 transgenic male were stained with an anti-UBB⁺¹ antibody. Minor UBB⁺¹ reactivity is present in the brain mainly in neurons in the lateral septal area (A) and faintly in the pyramidal cell layer of the hippocampus (B). Magnifications of the lateral septal area and hippocampus are shown in (C) and (D). E. Wild-type littermate FVB/N control mice do not show any hippocampal UBB⁺¹ reactivity when stained with anti-UBB⁺¹. Bar = 1 mm (A-B), bar = 250 μ m (C-E).

17% of the endogenous UBB mRNA ($n=4$ per group). Line 6663 UBB⁺¹ heterozygous mice did not show any overt behavioral abnormalities and lifespan was not reduced compared to wild-type control mice. The gross morphology of the brain also did not differ between UBB⁺¹ 6663 transgenic and FVB/N wild-type mice.

The expression pattern of the CamKIIα promoter is confined to neurons, located mainly in the hippocampus, neocortex, striatum and forebrain (Mayford *et al.*, 1996). The previously described UBB⁺¹ transgenic line 3413 with high levels of UBB⁺¹ expression from the same CamKIIα expression vector as line 6663 indeed showed neuronal UBB⁺¹ protein expression in these brain areas (Chapter 3). Immunohistochemical analysis of the 6663 mice using an antibody directed against the C-terminal +1 extension of UBB⁺¹ only showed very weak staining of UBB⁺¹ positive neurons (fig. 1A-D), located mainly in the lateral septal area (fig. 1A, C) and also in the hippocampal pyramidal cell body layers (fig. 1B, D). Control mice did not show any UBB⁺¹ reactivity (exemplified in fig. 1E). The UBB⁺¹ protein could also be detected in brain homogenates of 6663 transgenic mice by radioimmunoassay ($n=8$ transgenic; $n=6$ wildtype). UBB⁺¹ protein was present in a concentration of 116 ng/g total protein content in the 6663 transgenic mice, a concentration relatively low when compared to the levels of UBB⁺¹ protein in the previously described UBB⁺¹ high expression line 3413 (1080 ng/g total protein content, (Chapter 3)).

Low concentrations of lactacystin transiently inhibit the UPS and induce UBB⁺¹ accumulation

In vitro, UBB⁺¹ is ubiquitinated and degraded by the UPS at low expression levels (Lindsten *et al.*, 2002; van Tijn *et al.*, 2007). Therefore, we investigated whether the low UBB⁺¹ protein expression levels in 6663 transgenic mice were attributable to proteasomal degradation of UBB⁺¹ *in vivo*. We monitored UBB⁺¹ protein levels in 6663 transgenic mice after exogenous inhibition of the UPS; an overview of the results is given in Table 1. Proteasome inhibition was achieved by intra-cranially administering UPS inhibitors using an Alzet osmotic mini-pump placed subcutaneously in the flank of the animal connected with an infusion probe placed unilaterally in the hippocampus.

We implanted the osmotic pump and infusion probe on day 1 and infused wild-type and 6663 transgenic mice with the irreversible proteasome inhibitor lactacystin (0.166 mM) for three consecutive days. Mice were sacrificed directly after the 3-day infusion of lactacystin (day 3) or seven days after the infusion had ended (day 10). Accumulation of UBB⁺¹ was detected using an anti-UBB⁺¹ antibody on 50 µm coronal vibratome sections. Lactacystin treatment resulted in moderate accumulation of UBB⁺¹ in 6663 transgenic mice at day 3, located mainly in hippocampal neurons around the infusion site spreading slightly to the CA1 area of the contralateral hippocampus (fig. 2A), with a small area void of staining where the infusion needle was placed. The intensity of the UBB⁺¹ staining var-

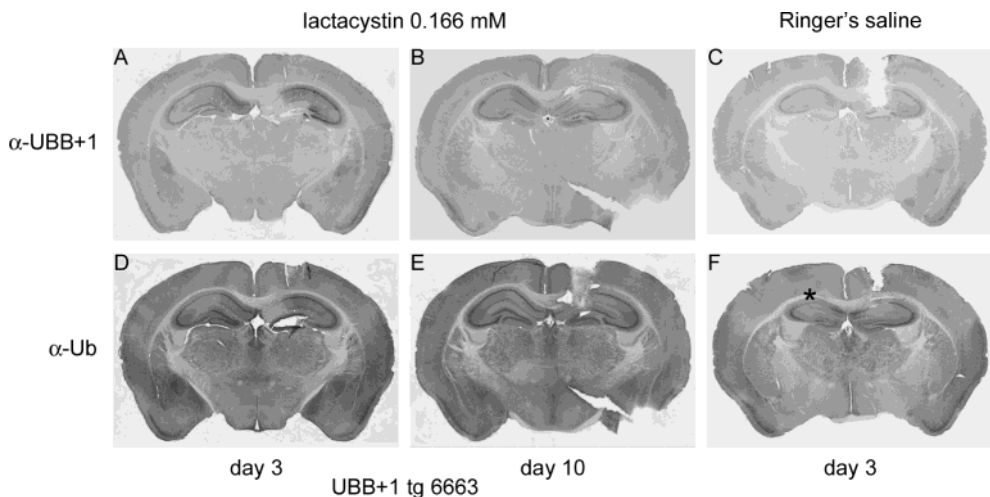


Figure 2 Low concentrations of lactacystin induce reversible UBB⁺¹ accumulation. A, D. Hippocampal infusion of the irreversible inhibitor lactacystin (0.166 mM) for three days in 6663 transgenic mice gives rise to clear accumulation of the UBB⁺¹ protein, mainly in the ipsilateral hippocampus (A). In the same animal, Ub positive cells are dispersed throughout the brain, only minor additional accumulation of Ub is present at the infusion site (D). The Ub reactivity is slightly decreased around the infusion site, marked by an asterisk. B, E. Mice were perfused one week after the 0.166 mM lactacystin infusion into the hippocampus ended (day 10). UBB⁺¹ 6663 transgenic mice do not show accumulation of UBB⁺¹ (B) or Ub (E) at this timepoint. C, F. Infusion of Ringer's saline in the hippocampus of 6663 UBB⁺¹ transgenic mice for 3 days does not give rise to additional accumulation of UBB⁺¹ (C) or of Ub (F). The Ub reactivity is slightly decreased in the contralateral CA2/3 area, marked by an asterisk. The infusion needle was placed in the right hippocampus.

ied slightly between mice ($n=4$), in one animal no increase in UBB⁺¹ expression was seen. Accumulation of endogenous Ub was used as a general marker for UPS dysfunction. Ub-positive cells were present in a dispersed pattern throughout the brain. In the transgenic mice, only minor additional accumulation of Ub was present at day 3 (fig. 2D). However, these Ub levels increased to a much lesser extent compared to the UBB⁺¹ levels; a decrease in expression was observed directly around the probe site (fig. 2D, decreased expression marked by an asterisk). In the wild-type control group, only two out of five mice showed a slightly higher hippocampal Ub expression after infusion of lactacystin ($n=5$, results not shown).

As a control for the proteasome inhibitor we unilaterally infused physiological saline (Ringer's solution) into the hippocampus. After infusion of Ringer's, no increase in UBB⁺¹ reactivity could be detected in the 6663 transgenic mice ($n=7$, fig. 2C), showing that the accumulation of UBB⁺¹ after infusion of lactacystin is specific for UPS inhibitor

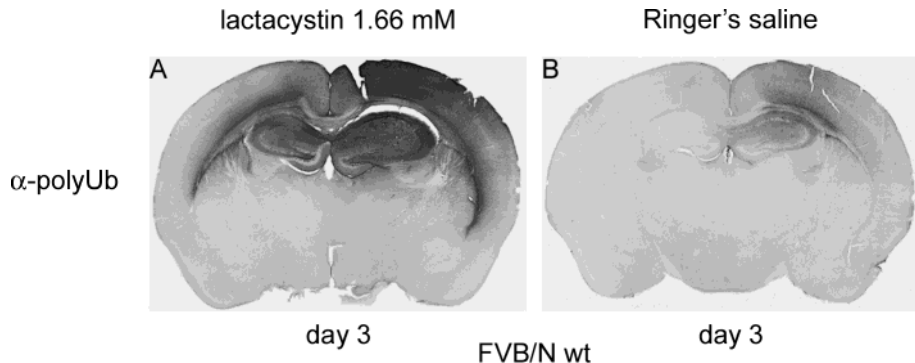


Figure 3 *Poly-ubiquitin chain accumulation after infusion of high concentrations of lactacystin.* A, B. Infusion of high concentrations of lactacystin (1.66 mM) in FVB/N wild-type mice leads to massive accumulation of poly-ubiquitinated proteins at day 3 in the ipsilateral hippocampus and cortex spreading to the contralateral side, shown by staining with an antibody directed against poly-ubiquitin chains (A). Infusion of Ringer's saline leads to only minor accumulation of poly-ubiquitinated proteins in wild-type mice at day 3 (B).

infusion. As wild-type mice do not endogenously express human UBB⁺¹, UBB⁺¹ positive staining was completely absent in these mice in all experimental conditions (n=4, result not shown). Additional accumulation of Ub around the infusion site compared to the contralateral hippocampus was absent at day 3 in all wild-type (result not shown) and 6663 transgenic mice (fig. 2F). In some cases, Ub expression was even slightly decreased in the CA2/3 area of the contralateral hippocampus (fig. 2F, marked by an asterisk).

Considering the fact that lactacystin is an irreversible inhibitor of the UPS (Fenteany *et al.*, 1995), we expected that the UPS inhibition at day 3 would persist up to day 10. Contrary to our expectations, the additional accumulation of UBB⁺¹ observed at day 3 in the 6663 transgenic mice had almost fully disappeared by day 10 (n=3, fig. 2B). Correspondingly, no clear accumulation of Ub was visible at day 10 in the 6663 transgenic mice (fig. 2E) or in the wild-type mice (n= 2, data not shown). The absence of both Ub and UBB⁺¹ accumulation at day 10 suggests that in this setup UPS inhibition induced by 0.166 mM lactacystin was reversed from day 3 to day 10 and thus might not have been complete. Again, Ringer's saline infusion was used a control. Similar to the results obtained at day 3, infusion of Ringer's for 3 days did not induce accumulation of Ub or UBB⁺¹ in a wild-type or a 6663 transgenic mouse at day 10 (results not shown).

Table 1 Results of UPS inhibitor infusion in wild-type and line 6663 transgenic mice (summary)

Condition		n	Ubiquitin staining	UBB ⁺¹ staining	Comments
Ringer's	day 3	wt	4	~	not present
		tg	7	~	~
	day 7/10	wt	5	~	not present
		tg	3	~	~
lactacystin 0.166mM	day 3	wt	5	↑ minor (in 2 out of 5 mice)	not present
		tg	4	↑ minor (in 3 out of 4 mice)	↑ clear in ipsil. hippocampus (3 out of 4 mice) ↑ variable in contral. CA1/DG and cortex
	day 10	wt	2	~ (only few darker cells)	not present
		tg	3	~	reversed inhibition of lacta.
lactacystin 1.66mM	day 3	wt	1	↑ large directly at infusion site ↓ in a large ring around infusion site	not present
		tg	4	↓ in a large ring around infusion site ↑ around ring (in 3 out of 4 mice) cells with abnormal morphology (clear in 1 mouse)	↑ very clear in contral. hippocampus and cortical/thalamic areas near probe (2 mice strong effect, 2 mice moderate effect)
	day 7	wt	2	↓ in a large ring around infusion site ↑ around ring (clear in 1 out of 2 mice)	not present
		tg	3	↓ in a large ring around infusion site ↑ around ring	↑ variable from modest to strong (1 mouse strong effect, 2 mice moderate effect)
MG262 1.66mM	day 3	wt	2	~ / ↑ minimal	not present
		tg	3	↑ moderate in ipsil. DG and cortex	↑ in ipsil. hippocampus
	day 7	wt	3	↑ in ipsil. to contral. hippocampus cells with abnormal morphology	not present
		tg	2	↑ in ipsil. to contral. hippocampus cells with abnormal morphology	↑ in ipsil. to contral. hippocampus absent around infusion site

~ unaltered; ↑ increased; ↓ decreased; Ub: ubiquitin; wt: wild-type; tg: transgenic; ipsil.: ipsilateral, contral.: contralateral, DG: dentate gyrus, lacta.: lactacystin

High concentrations of lactacystin irreversibly inhibit the UPS

The unexpected reversal of lactacystin-induced UPS inhibition over time might be attributed to the concentration of the inhibitor; hence, we also infused a ten-fold higher concentration of lactacystin (1.66 mM). Infusion of 1.66 mM lactacystin lead to widespread accumulation of poly-ubiquitinated proteins in a wild-type mice after three days of continuous infusion, visualized by increased reactivity for poly-ubiquitin chains (LB112, (Iwatsubo *et al.*, 1996)), indicating substantial UPS inhibition (fig. 3A). This large increase in the levels of poly-ubiquitinated proteins was not present after infusion of

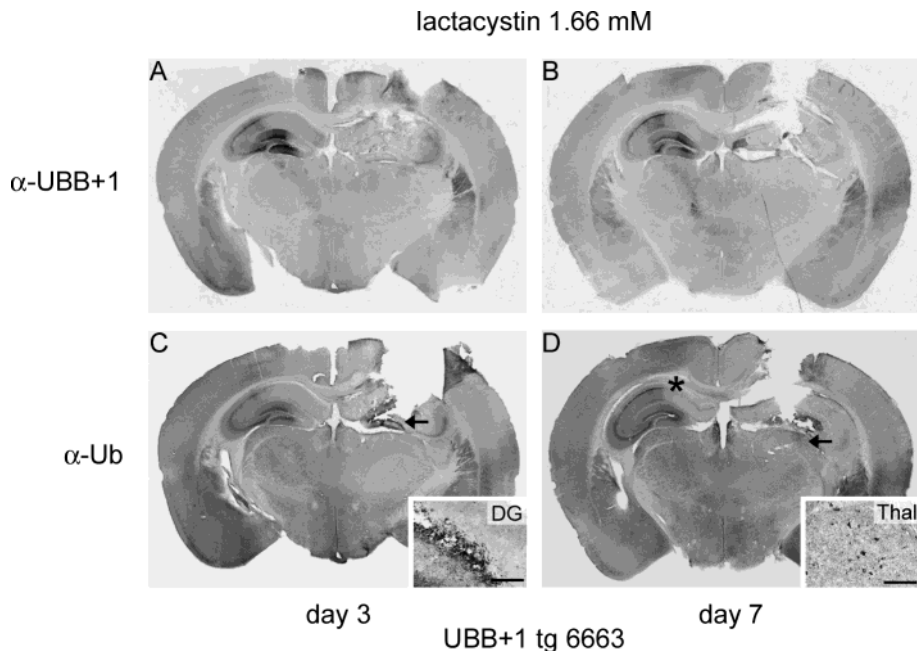


Figure 4 *High concentrations of lactacystin induce irreversible UBB⁺¹ accumulation.* A, C. Treatment of 6663 transgenic mice with a high dose of lactacystin (1.66 mM) induces a clear accumulation of the UBB⁺¹ protein at day 3, mainly in the contralateral hippocampus spreading to adjacent thalamic areas (A). A decrease in Ub expression was found in a large circular area around the infusion site, bordered by a rim of intensely stained cells (C). Magnification of area left of the arrow: some Ub positive cells with abnormal morphology are visible around the infusion site in the dentate gyrus (DG) in this animal (C, inset; bar = 100 µm). B, D. The UBB⁺¹ accumulation present at day 3 persists up to day 7. The staining pattern of UBB⁺¹, mainly in the contralateral hippocampus, is similar to day 3 (B). At day 7, the staining pattern of Ub resembles day 3 as well, however no irregular shaped cells are present in the hippocampus. Decreased Ub staining in the contralateral dentate gyrus is marked by an asterisk (D). Magnification of area left of the arrow: a few cells with abnormal morphology can be seen in the thalamic area (Thal) (D, inset; bar = 100 µm).

Ringer's solution in comparable conditions (fig. 3B). Staining for Ub showed a somewhat different pattern; positive cells disappeared in a large ring around the infusion site bordered by darker stained Ub-positive cells in the transgenic mice (n=4, fig. 4C). In one animal, many Ub accumulating cells showing abnormal morphology appeared in the hippocampus, surrounding the infusion site (fig. 4C, inset). However, 1.66 mM lactacystin also caused extensive necrotic-like damage to the tissue of the ipsilateral hippocampus (fig. 4A, 4C). At day 3, considerable accumulation of UBB⁺¹ was present in the 6663 transgenic mice, mainly in the contralateral hippocampus and also in several additional ipsi- and contralateral brain regions at some distance from the infusion site, e.g. cerebral cortex and thalamic areas (fig. 4A). Here, UBB⁺¹ accumulation was more prominent and widespread compared to the lower concentration of lactacystin, indicating a dose-dependent effect of lactacystin on the accumulation of UBB⁺¹. In contrast to the 0.166 mM lactacystin infusion, infusion of a ten-fold higher concentration of lactacystin (1.66 mM) induced UBB⁺¹ accumulation which remained present for four days after the 3-day infusion of lactacystin ended (day 7). This response varied from modest (not shown) to substantial UBB⁺¹ accumulation (n=3, fig. 4B). Also, the elevated Ub levels in these transgenic mice (fig. 4D) and in wild-type control mice (n=2, result not shown) persisted up to day 7 in ipsilateral areas spreading to the contralateral hemisphere. A few abnormally shaped cells were present in the ipsilateral thalamic area (fig. 4D, inset). The results obtained for UBB⁺¹ and Ub at day 7 showed relatively high variability between animals. Unfortunately, tissue damage also increased over time, making it difficult to accurately compare protein expression patterns at day 3 and day 7. These results show that high concentrations of the proteasome inhibitor lactacystin result in irreversible UPS inhibition leading to UBB⁺¹ accumulation which persists over time.

MG262 causes UBB⁺¹ accumulation in vivo

In vitro, accumulation of UBB⁺¹ induced by a reversible UPS inhibitor can be (partially) reversed after washout of the inhibitor (van Tijn *et al.*, 2007). To confirm these results *in vivo*, we infused the reversible inhibitor MG262 for three days (1.66 mM) and perfused the mice directly (day 3) or 4 days after ending administration (day 7), allowing reversal of MG262 induced UPS inhibition. Hippocampal administration of MG262 in 6663 transgenic mice caused only slight Ub accumulation day 3, resulting in darker cells in e.g. the cortex and dentate gyrus (n=3, fig. 5C). Only a minimal increase in Ub was present in the wild-type mice at day 3 (n=2, not shown). As MG262 is a reversible inhibitor, we expected that washout of MG262 would lead to a decrease in Ub levels. However, the Ub accumulation was increased in the wild-type (n=3, not shown) as well as the 6663 transgenic mice (n=2) at day 7 (fig. 5D). Ub wild-type accumulated in a circular border around a necrotic-like Ub negative area, spreading to contralateral CA1 and DG areas (fig. 5D).

Many dark cells with abnormal morphology were present directly around probe site, in between the damaged tissue (fig. 5D, inset). These results suggest sustained UPS inhibition over time even after washout of MG262. Furthermore, MG262 infusion in 6663 transgenic mice caused ipsilateral accumulation of UBB⁺¹ at day 3 (n=3, fig. 5A) and this accumulation remained present up to four days after ending the MG262 administration (n=2, fig. 5B). We also observed that the UBB⁺¹ accumulation spread to the contralateral CA1 area at day 7 (fig. 5B). The combined results for Ub and UBB⁺¹, as summarized in Table 1, suggest that using this setup UPS inhibition induced by MG262 was not only sustained after a period without continuous inhibitor treatment, but also was more widespread.

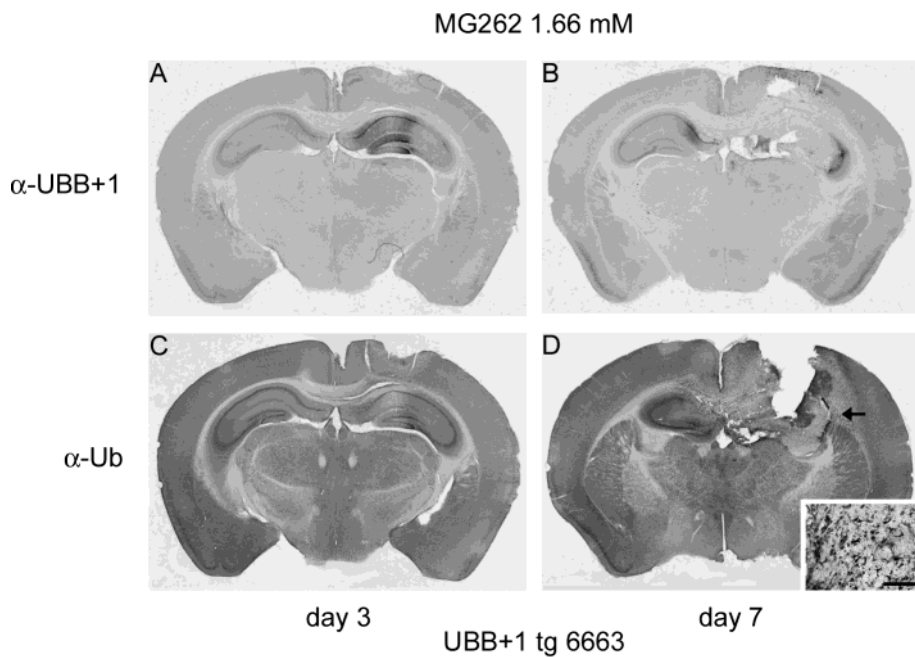


Figure 5 UBB⁺¹ accumulates irreversibly after UPS inhibition by MG262. A, C. After treatment with 1.66 mM MG262, many UBB⁺¹ positive cells are clearly visible in the ipsilateral hippocampus at day 3 (A). In the same 6663 transgenic animal, Ub accumulates slightly in the 6663 transgenic mice in cells mainly in the ipsilateral dentate gyrus. The area directly around the infusion needle is devoid of staining (C). B, D. After 4 days of MG262 washout (day 7), UBB⁺¹ is absent in the area directly around the probe site, accompanied by substantial tissue loss. UBB⁺¹ accumulates in a ring-like shape around the necrotic area dispersing to the outer parts of the ipsilateral hippocampus and into the contralateral CA1 and dentate gyrus areas. (B). A similar staining pattern could be observed for the Ub protein (D). Magnification of area left of the arrow: cells with abnormal morphology are present in the vicinity of the infusion site (D, inset; bar = 100 μ m).

UBB⁺¹ does not accumulate during aging

Proteasome function has been reported to decline during ageing in various tissue types, including in nervous tissue in rat (Keller *et al.*, 2000), and also in several brain regions in aged mice (Zeng *et al.*, 2005). We investigated if this reported decline in proteasome activity would result in an increase in UBB⁺¹ protein levels in the brains of the 6663 transgenic mice, as we showed in this study that UBB⁺¹ readily accumulates after exogenous proteasome inhibition (fig 2A, 4A and 5A). We examined all brain regions where UBB⁺¹ protein expression could be expected due to the CamKII α promoter expression pattern, including hippocampus, cortex, striatum and forebrain (Mayford *et al.*, 1996). However, we did not find an increase in the levels of neuronal UBB⁺¹ in any brain region studied in 6663 transgenic mice up to 18 months of age (exemplified by the microphotographs of the hippocampus in fig. 6A-C).

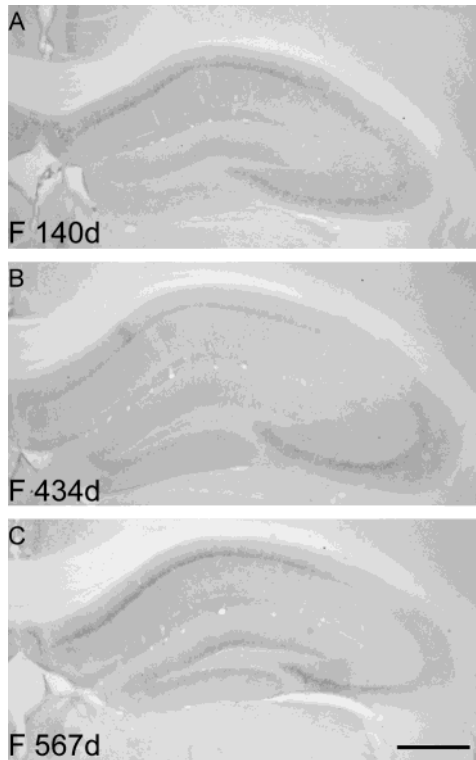


Figure 6 *UBB⁺¹ does not accumulate during aging.* A-C. Expression pattern of hippocampal UBB⁺¹ protein in 6663 transgenic mice during aging. Female 6663 transgenic mice of 140 days old (A), 434 days old (B) and 567 days old (C) were stained with anti-UBB⁺¹ antibody. Scale bar for A-C = 500 μ m.

Discussion

In this study, we generated and characterized a transgenic line with low-levels of neuronal UBB⁺¹ expression (line 6663). In human, UBB⁺¹ accumulates not only in the ubiquitin-positive neuropathological hallmarks of tauopathies (van Leeuwen *et al.*, 1998; Fischer *et al.*, 2003; van Leeuwen *et al.*, 2006), polyglutamine diseases (De Pril *et al.*, 2004) but also in non-neuronal diseases, including alcoholic liver disease (McPhaul *et al.*, 2002) and inclusion-body myositis (Fratta *et al.*, 2004). We show here that the UBB⁺¹ protein is barely detectable in line 6663 UBB⁺¹ transgenic mice. This suggests that the UBB⁺¹ protein is efficiently degraded *in vivo*, similar to our earlier observations *in vitro* showing proteasomal degradation of UBB⁺¹ at low expression levels (Fischer *et al.*, 2003; van Tijn *et al.*, 2007). Indeed, UBB⁺¹ accumulated in the 6663 transgenic mice only after inhibition of the proteasome by intracranial infusion of the irreversible proteasome inhibitor lactacystin or the reversible inhibitor MG262 (results summarized in Table 1). These data confirm that at low-levels of expression, UBB⁺¹ is normally degraded by the neuronal UPS *in vivo*. This strengthens our hypothesis that accumulation of UBB⁺¹ in human neuropathology indicates a dysfunctional UPS (Fischer *et al.*, 2003; Hol *et al.*, 2005).

Strikingly, we found that 0.166 mM lactacystin-induced UPS inhibition had disappeared one week after the completion of the infusion, as shown by the absence of Ub and UBB⁺¹ accumulation, even though lactacystin derived proteasome inhibition is considered to be irreversible (Fenteany *et al.*, 1995). Lactacystin is a potent naturally occurring proteasome inhibitor (reviewed by (Kisselev and Goldberg, 2001) of which the spontaneous derivative *clasto*-lactacystin β-lactone covalently binds to the active site threonine of the β5 subunit in the 20S core particle (Groll and Huber, 2004). The lactone has the highest affinity for the chymotryptic activity, although it also inhibits the trypsin-like (β2) and PGPH (β1) activities, the latter being a reversible process (Fenteany *et al.*, 1995). However, due to the relative minor contribution of the reduction of PGPH activity to lactacystin induced proteasome inhibition (Fenteany *et al.*, 1995), this reversibility is not likely to cause the loss of UPS inhibition in our setup. The reversed inhibition can possibly be attributed to restoration of proteasome activity over time via slow hydrolysis of the β-lactone-proteasome adduct in aqueous solutions by the formation of the inactive lactacystin analogue *clasto*-lactacystin dihydroxy acid (Dick *et al.*, 1996; Kisselev and Goldberg, 2001). Infusion of a higher concentration of lactacystin might overcome this latent reversibility of the inhibitor. Indeed, we show here that UPS inhibition induced by a 10-fold higher concentration of lactacystin (1.66 mM) was irreversible over time. Another possibility is that the natural turnover of 20S core subunits influences the effectiveness of the inhibitor. In chicken skeletal muscle it was shown that the 20S subunits are constitutively turned over, with ~55% of the β5 subunits being newly synthesized over 120 hours (Hayter *et al.*, 2005). It is thus conceivable that the lactone-modified β5 subunit in the

core proteasome is replaced over time via intrinsic turnover of β 5 subunits followed by degradation of the lactacystin-modified β 5 subunit. Newly incorporated β 5 subunits will hold full proteolytic activity, and so reverse the lactacystin induced UPS inhibition.

In this study we also found sustained, and even increased, proteasome inhibition four days after MG262 infusion ended, although MG262 is considered to be a reversible inhibitor. MG262 belongs to the peptidyl boronic acid proteasome inhibitors (Adams *et al.*, 1998), a class of highly potent inhibitors. This class of inhibitors shows a slow dissociation rate of the boronate-proteasome adducts, leading to slow kinetics of inhibition reversal (reviewed in (Kisselev and Goldberg, 2001)). This slow on/off rate could very well explain the sustained UPS inhibition over time by MG262 we observed in our setup. Peptide boronates are highly specific towards inhibiting proteasome activity and are metabolically stable, making them excellent targets for drug development. The peptide boronate derivate PS-341, (Velcade, Millenium Pharmaceuticals), is indeed an FDA approved clinical drug to treat relapsed multiple myeloma, acting on e.g. cell cycle progression and tumor angiogenesis (Adams, 2004). We indeed also show in this study the long-lasting effects of MG262 treatment *in vivo*. The possibility that reversal of proteasome inhibition was unachievable in our setup using osmotic mini-pumps was negated, as proteasome inhibition by 0.166 mM lactacystin did reverse over time.

It was previously shown that infusion of saline into mice cerebral cortex resulted in necrosis of the cortical tissue surrounding the probe site (Jablonska *et al.*, 1993). We did not discern this in our study; infusion of Ringer's saline did not lead to tissue damage or substantial inhibition of the UPS, shown by the absence of UBB⁺¹ or Ub accumulation. The minor accumulation of poly-ubiquitinated proteins found after Ringer's infusion (fig. 3B) could point to an activation of the intracellular stress response due to the probe implantation, leading to an upregulation of Hsp expression. Indeed, increased Hsp70 expression has previously been reported to occur after traumatic brain injury in rodents, e.g. (Brown *et al.*, 1989; Chen *et al.*, 1998) and human (Dutcher *et al.*, 1998; Seidberg *et al.*, 2003). Also in our experiments, upregulation of Hsp70 immunoreactivity was present around the infusion site (not shown). Induction of the heatshock response can be regulated via the UPS, with the ubiquitin-ligase enzyme CHIP mediating e.g. heatshock mediated substrate ubiquitination (Qian *et al.*, 2006). Implantation of the infusion probe could thus lead to a local stress response in the hippocampus, ultimately increasing the level of poly-ubiquitinated substrates.

In contrast to Ringer's infusion, high concentrations of lactacystin and prolonged exposure to MG262 did result in substantial tissue damage in the ipsilateral hippocampus. Lactacystin is known to exhibit dose-dependent toxic effects and ultimately induces apoptosis in several neuronal cell types, including rat cerebellar granule cells (Pasquini *et al.*, 2000), rat dopaminergic cells e.g. (Rideout *et al.*, 2001; McNaught *et al.*, 2002; Fornai *et al.*, 2003) and rat and mouse primary cortical neurons (Qiu *et al.*, 2000; Yew *et al.*, 2005).

These toxic properties possibly account for the increased tissue necrosis after infusion of high concentrations of lactacystin as opposed to low concentrations, as well as the increase in tissue damage after prolonged duration of the exposure. This substantial tissue damage likely abolishes UBB⁺¹ accumulation in the ipsilateral hippocampus, explaining why the majority of UBB⁺¹ accumulation resides in the contralateral hippocampus after inhibition with high concentrations of lactacystin. The observed UBB⁺¹ accumulation does appear to be more widespread than the Ub accumulation following UPS inhibition, indicating that UBB⁺¹ might be a more sensitive marker for UPS dysfunction than Ub in the 6663 transgenic mice.

Many studies report an age-dependent decline in UPS activity in various cell types including nervous tissue, accompanied by an increased amount of oxidized proteins (reviewed by (Carrard *et al.*, 2002; Keller *et al.*, 2002)). More specifically, an age-related decrease of tryptic, chymotryptic and PGPH proteolytic activities was found in aging rat spinal cord (Keller *et al.*, 2000), hippocampus and cortex (Keller *et al.*, 2000) and also in several brain regions in aged mice (Zeng *et al.*, 2005). We expected that this endogenous long-term decline in proteasome activity might be reflected in accumulation of UBB⁺¹ in aged 6663 transgenic mice, as we found massive accumulation of the protein after short-term UPS inhibition with exogenous administered UPS inhibitors. However, we did not observe an alterations in UBB⁺¹ immunoreactivity up to 18 months of age. This implicates that turnover of UBB⁺¹ protein is unimpaired, and that a decline of proteasome activity might not be present. More likely, the levels of UBB⁺¹ expression are at such a low level that a partial decrease of UPS activity (~40%, (Zeng *et al.*, 2005)) is not directly reflected in accumulation of UBB⁺¹. It must be noted that this decrease in proteolytic activity is measured in brain homogenates (Zeng *et al.*, 2005), including all brain-derived cell types, and might not accurately reflect the activity decline in individual neurons, the only cell type which expresses UBB⁺¹.

Our results show that in the 6663 transgenic mice, the UBB⁺¹ protein is degraded by the neuronal UPS *in vivo*. This observation validates our previous results obtained in neuronal cell lines and primary cultures showing that UBB⁺¹ is a ubiquitin fusion degradation substrate for proteasomal degradation at low expression levels (Lindsten *et al.*, 2002; van Tijn *et al.*, 2007). It also supports the hypothesis that in human, the UBB⁺¹ protein is normally degraded and accumulates only when the UPS is compromised, as seen in the disease-specific hallmarks of tauopathies and polyglutamine diseases (Fischer *et al.*, 2003). This novel transgenic line expressing low-levels of UBB⁺¹ can serve as a model system to further elucidate the properties of UBB⁺¹ and to study its role in neurodegenerative disease.

Acknowledgements

We would like to thank Gertjan de Fluiter, Marian Verhage, Gavin Adema, Lotte Vis and Christiaan Levelt (Netherlands Institute for Neuroscience, Amsterdam, The Netherlands) for the animal care and Joop van Heerikhuize (Netherlands Institute for Neuroscience, Amsterdam, The Netherlands) for assistance with the radioimmunoassay experiments and microscopy. Dr. T. Iwatsubo (Department of Neuropathology and Neuroscience, University of Tokyo, Japan) kindly provided us with the LB112 anti-polyubiquitin-chain antibody. This research was supported by the ISAO 01504, Hersenstichting Nederland 12F04.01 and H00.06, Jan Dekker en Ludgardine Bouwman Stichting 04-22 and NWO GPD 970-10-029 and 903-51-192.

CHAPTER V

Alzheimer-associated mutant ubiquitin
impairs spatial reference memory

In preparation

Paula van Tijn, Barbara Hobo, Marian C. Verhage,
Melly S. Oitzl, Fred W. van Leeuwen, David F. Fischer

Abstract

UBB⁺¹ is a mutant ubiquitin which accumulates in the hallmarks of tauopathies, including Alzheimer's disease. Transgenic mice expressing high levels of neuronal UBB⁺¹ exhibit moderately decreased proteasome activity and spatial reference memory deficits at 9 months of age. In the present study, we characterized the behavioral phenotype of male UBB⁺¹ transgenic mice at different ages. We found that UBB⁺¹ transgenic mice showed an age-related functional decline similar to wild-type litter mates, without displaying gross neurological abnormalities or alterations in procedural (motor-) learning and motor coordination at 3, 9, 15 and 21-24 months of age. At 15 months of age, spatial learning was not affected during the acquisition of the Morris watermaze. However, spatial reference memory during the probe trial was initially impaired in the transgenic mice, this deficit was eliminated after intense training. We conclude that the previously reported spatial reference memory deficits of UBB⁺¹ transgenic mice persist, but do not aggravate during aging. In addition, our results demonstrate that spatial reference memory formation depends on intact forebrain proteasome activity.

Introduction

The ubiquitin-proteasome system (UPS) is the main regulated pathway for intracellular protein turnover and is essential for maintaining cellular homeostasis. Substrate proteins are selectively targeted for proteolytic degradation by covalent attachment of a chain of ubiquitin moieties, ultimately resulting in degradation of the substrate by the 26S proteasome (Glickman and Ciechanover, 2002). Besides tagging proteins for degradation, protein modification with one or more ubiquitins is involved in many other cellular processes e.g. endocytosis, DNA repair and transcriptional regulation (Welchman *et al.*, 2005; Mukhopadhyay and Riezman, 2007). In the adult nervous system, the UPS also plays an important role in synaptic plasticity and learning and memory formation (DiAntonio and Hicke, 2004). This was first found in *Aplysia*, where the deubiquitinating enzyme Ap-Uch as well as 26S proteasome function proved critical for inducing long-term facilitation (Hegde *et al.*, 1997; Chain *et al.*, 1999). In rat, inhibiting hippocampal proteasome activity blocks long-term memory formation in an inhibitory avoidance task (Lopez Salon *et al.*, 2001). More recently, a role in cognitive function for deubiquitinating enzymes belonging to the class of ubiquitin C-terminal hydrolases is also described in mouse; Uch-11 is essential for normal synaptic function (Gong *et al.*, 2006) and both Uch-11 and Uch-13 are required for memory formation (Wood *et al.*, 2005; Gong *et al.*, 2006). Also in several other genetically manipulated mouse models with defective components of the UPS, learning and memory is affected (reviewed by (van Tijn *et al.*, 2008)).

As ubiquitin-dependent protein degradation plays an important role in neuronal devel-

opment, as well as in maintenance of the adult nervous system, it is not surprising that malfunctioning of the UPS is implicated in the pathogenesis of neurodegenerative disease. This is reflected by the ubiquitin-positive protein aggregates present in the hallmarks of many neurological disorders, including Alzheimer's disease (AD) and Parkinson's disease (PD) (Ciechanover and Brundin, 2003). In addition, mutations in UPS related enzymes are proposed to be causative for forms of familial PD (Kitada *et al.*, 1998; Leroy *et al.*, 1998) and several disease-related proteins, including amyloid- β and tau in AD, can diminish proteasomal activity (Gregori *et al.*, 1995; Keck *et al.*, 2003; Lopez Salon *et al.*, 2003). Another indication for UPS involvement in disease pathogenesis is the accumulation of a mutant ubiquitin (UBB^{+1}) in the neuropathological hallmarks of tauopathies, including AD, and in Huntington's disease (van Leeuwen *et al.*, 1998; Fischer *et al.*, 2003; De Pril *et al.*, 2004). We previously reported that UBB^{+1} is a ubiquitin-fusion degradation substrate for proteasomal degradation (Lindsten *et al.*, 2002). However, after exceeding a threshold level of expression, UBB^{+1} acts as inhibitor of the 26S proteasome (van Tijn *et al.*, 2007). We therefore proposed that accumulation of UBB^{+1} in human brain is an endogenous marker for proteasomal dysfunction (Fischer *et al.*, 2003).

We recently developed UBB^{+1} transgenic mouse lines with varying levels of neuronal UBB^{+1} expression to further study the properties of UBB^{+1} *in vivo* (Chapter 3). In the transgenic line 3413, high levels of postnatal UBB^{+1} expression led to neuronal accumulation of the UBB^{+1} protein mainly in the cerebral cortex, hippocampus and striatum and resulted in a chronic low-level reduction of cortical chymotryptic proteasome activity *in vivo*, leading to the accumulation of ubiquitinated proteins (Chapter 3). In addition, these mice exhibited cognitive defects in spatial memory at 9 months of age; male 3413 transgenic mice showed intact spatial learning, but were significantly impaired in spatial memory retention in the Morris watermaze task. Also in a fear conditioning paradigm, 9-months-old 3413 transgenic mice exhibited decreased context-related memory, whereas cued memory was unaffected (Chapter 3).

In the present study, we further characterized the effects of chronic low-level neuronal UPS inhibition on gross neurological functioning, motor coordination and procedural motor learning in male UBB^{+1} 3413 transgenic mice and their wild-type littermates, aged 3, 9, 15 and 21-24 months. To study the persistence of the recently reported explicit memory dysfunction in these mice at 9 months of age, we assessed spatial learning and memory in the Morris watermaze paradigm at the age of 15 months.

Materials and Methods

Transgenic mice

The previously described transgenic UBB^{+1} mouse line 3413 (Chapter 3) expresses human

UBB⁺¹ cDNA under control of the murine CamKIIα promoter and was maintained on a C57/Bl6 background by breeding hemizygous mice males to wild-type mice females. Mice were genotyped on DNA isolated from ear-snips (Chapter 3) and kept in group housing on a 12/12 h light-dark cycle with food and water ad libitum in specific pathogen free conditions (Nicklas *et al.*, 2002). Behavioral experiments were performed in the light phase. Mice were housed solitarily one week before behavioral testing commenced. All experimental mice used in the present study were male, the experimenter was blind to the genotype of the mice. Animal experiments were performed conforming to national animal welfare law and under guidance of the animal welfare committee of the Royal Netherlands Academy of Arts and Sciences.

General neurological behavior assessment

General neurological reflexes were tested (Rogers *et al.*, 1997) using the righting reflex, by observing if a mouse returned to a normal posture standing on four paws after being flipped over onto its backside (scored as present/not present). The corneal reflex was measured by observing an eye-lid blinking response after gently touching the cornea with the tip of a cotton swab (scored as present/not present). The reaching reflex was measured by lifting the mouse by the base of the tail to approximately 15 cm above a firm surface. The ability to extend the forelimbs reaching towards the surface was scored (present/not present) (Rogers *et al.*, 1997). Neuromuscular strength was measured with a hanging wire test by placing a mouse on a stainless steel wire cage grid suspended approximately 30 cm in the air above soft bedding material. After the mouse firmly gripped the cage wires, the cage lid was slowly turned upside down and the latency to fall (s) was recorded, with a maximum duration of 60 s (protocol described in (Crawley, 1999)). To monitor hind limb escape extension mice were lifted by the base of the tail and the hind limb response, normally extension in an outward v-shape, was scored (present/not present) (as described in (Lewis *et al.*, 2000).

Rotarod

An accelerating rotarod (model 47600, Ugo Basile Biological Research Apparatus, Italy) was used to measure motor-learning and coordination. The rotarod had a grooved rotating beam (diameter 3 cm) raised 16 cm above a platform, which was divided into five sections for five mice to be tested simultaneously. When falling from the rotating beam, the latency to fall (s) was recorded electronically. Mice were allowed to familiarize with the beam for two 180 s trials with the rod rotating at a constant speed of 4 rpm on day 0. Starting the next day, mice were subjected to four 300 s trials per day for three consecutive days (days 1-3) with an intertrial interval of ~15 min. Over the 300 s, the rotating

beam accelerated from 4 rpm to 40 rpm. Mice remaining on the beam during the full 300 s of the task were taken from the rotarod and given the maximum score. Mice were trained for another three consecutive days following the same protocol one week later (days 8–10). The 3 and 15 months old mice were first subjected to watermaze training before being tested on the rotarod. Analysis of the data was done using WinDAS 2004 software (v 3.0.145, Ugo Basile, Italy).

Watermaze

Mice were handled for four days before the experiment commenced. The watermaze consisted of a circular pool of 1.22 m in diameter filled with water at $26 \pm 1^\circ\text{C}$, made opaque by addition of white non-toxic latex paint. Training was performed as described previously in Chapter 3. Briefly, training commenced with a 120 s free-swim trial on day 1. Hidden platform training was conducted for four consecutive days (4 trials per day, ~30 min inter-trial interval). Mice were allowed to search for a hidden circular platform (11 cm diameter) for 60 s. The platform location remained constant during the trials (NW), the inlet position was chosen pseudorandomly (N, E, S, W) every trial. Memory retention was tested three days after acquisition training in a 60 s probe trial, in which the hidden platform was removed. Inlet position was chosen in the opposite quadrant of the former platform position. Directly following the first probe trial a visual platform test was performed, with both the platform location and the inlet location pseudorandomised. Visual training consisted of three consecutive trials wherein the animals had to locate a clearly visible platform. Mice not able to find the visual platform were excluded from the final analysis (2 transgenic, 3 wild-type mice). A second series of acquisition trials, followed by a second probe trial, commenced three weeks after the first probe trial, following the same procedures as during the first acquisition phase. Directly following the second probe trial a third four-day acquisition phase commenced, followed by a third probe trial. The testing series were concluded by performing a second visual platform test following the third probe trial, similar to the first visual platform test. All trials were monitored by a camera, and recorded and analyzed using a computerized tracking system (Ethovision, Noldus, The Netherlands).

Data analysis

Analysis of bodyweight and hanging wire latencies were assessed with a Student's t-test or Mann-Whitney when the data was not normally distributed. Effects of age and genotype interactions on bodyweight and hanging wire latencies were analyzed with univariate ANOVA. For rotarod data analysis, the latencies to fall were averaged for every subject over the four trials per testing day. Latencies for wild-type vs. transgenic mice were com-

pared per day with a Students t-test. To analyze the overall genotype and learning effects, a repeated measures ANOVA was performed with averaged day latencies for all six training days as a repeated within-subjects measure and genotype as a between-subjects factor. Additionally, repeated measures ANOVA was performed separately for days 1-3 and days 8-10.

For analysis of the watermaze acquisition trials, the latencies to find the hidden platform location were averaged per acquisition day. Swimming speed was averaged over all four days of acquisition. For the probe trials, swimming speed was calculated separately. In all cases, swimming speed did not significantly differ between transgenic and wild-type mice. Statistical analysis was performed by planned comparisons between wild-type and transgenic mice per day for the acquisition and visual tasks using a Students t-test. For learning effects during the acquisition phase and visual tasks, repeated measures ANOVA was performed with day as repeated within-subject measure and genotype as a between-subjects factor. For the probe trial scores (percentage of time spent in each quadrant), the time spent per quadrants was tested per quadrant per genotype against the expected value of 25% with a non-parametric one-sample Wilcoxon signed ranks test. All results are expressed as mean +/- S.E.M. and were considered significant when $p < 0.05$. Statistical analysis was performed using SPSS for Windows (version 12.0.1).

Results

General neurological phenotype assessment

UBB⁺¹ transgenic mice over-express an aberrant form of ubiquitin in forebrain neurons, mainly located in the hippocampus, cortex and striatum (Chapter 3). These mice do not suffer from overt neuropathology in the form of tangles, amyloid plaques or activated neuroglia (Chapter 3). In this study, we examined if the 3413 UBB⁺¹ transgenic mice showed gross phenotypic abnormalities in spontaneous home-cage behavior, including hyperactivity, anxiety and aggression. We did not detect any overt deviation from normal behavior in the 3413 transgenic mice up to 24 months of age. Body weight increased significantly during aging ($p < 0.001$), however without differing between male wild-type and 3413 transgenic mice at any age (Table 1). The righting reflex was present in the wild-type as well as the 3413 transgenic mice at all ages tested (Table 1). Also the reaching reflex and the corneal reflex were present and comparable in wild-type and 3413 transgenic mice at all ages (Table 1). To test the neuromuscular function we examined the escape extension. Normally, when lifted by the tail, the hind limbs of the mouse extend in an outward “v-shape” (Lewis *et al.*, 2000). Correct escape extension of the hind limbs was present up to 15 months of age without differences between the wild-type and transgenic mice. In the 21-24 month old mice, all the 3413 transgenic mice and the majority of the

Table 1 Results of general neurological tests

Test	3 months		9 months		15 months		24 months	
	wt	tg	wt	tg	wt	tg	wt	tg
n	11	7	14	7	10	8	7	8
weight (g) ^a	27.5±0.5	27.3±1.0	35.6±1.4	33.9±0.6	39.8±1.9	41.1±1.8	43.4±2.5	41.7±1.8
righting reflex	+	+	+	+	+	+	+	+
forelimb placing	+	+	+	+	+	+	+	+
eye lid reflex	+	+	+	+	+	+	+	+
escape ext.	outward	outward	outward	outward	outward	outward	poor	poor
hanging wire (s) ^a	60.0	60.0	50.6±5.6	60.0	36.5±7.1	37.1±9.1	17.3±7.4	24.5±9.0

^a data are represented as average ± S.E.M.; +: present

wild-type mice (86%) displayed poor escape extension, keeping the hind limbs close to their body (Table 1). Neuromuscular strength was assessed with the hanging wire test (Crawley, 1999). The latency to fall (with a maximum of 60 s) did not significantly differ between the wild-type and transgenic mice at any age, although a general decrease in performance was observed during aging ($p<0.001$). Also, no significant genotype or age*genotype interactions were present (Table 1).

Motor coordination and motor-learning

An accelerating rotarod task was used to assess motor coordination and motor-learning skills. We tested naïve male 3413 transgenic and age-matched wild-type mice at the ages of 3, 9, and 15 months. The first training-week consisted of four trials per day during three consecutive days (days 1-3) to assess basic motor skills and procedural motor-learning capacities. A second comparable training session took place one week later (days 8-10). At the age of 3 months, both wild-type ($n=9$) and 3413 transgenic mice ($n=6$) performed equally well (fig. 1A). Repeated measures ANOVA over all training days revealed a significant effect of training day ($p=0.014$), indicating that both wild-type and 3413 transgenic mice improved their motor skills, without showing an effect of genotype or day*genotype interaction. When the first and second training week (days 1-3 and days 8-10) were analyzed as separate cohorts, during days 1-3 not only a significant effect of day was present ($p<0.01$), but also a significant interaction of day*genotype ($p=0.049$). This interaction between day and genotype was not significant for days 8-10.

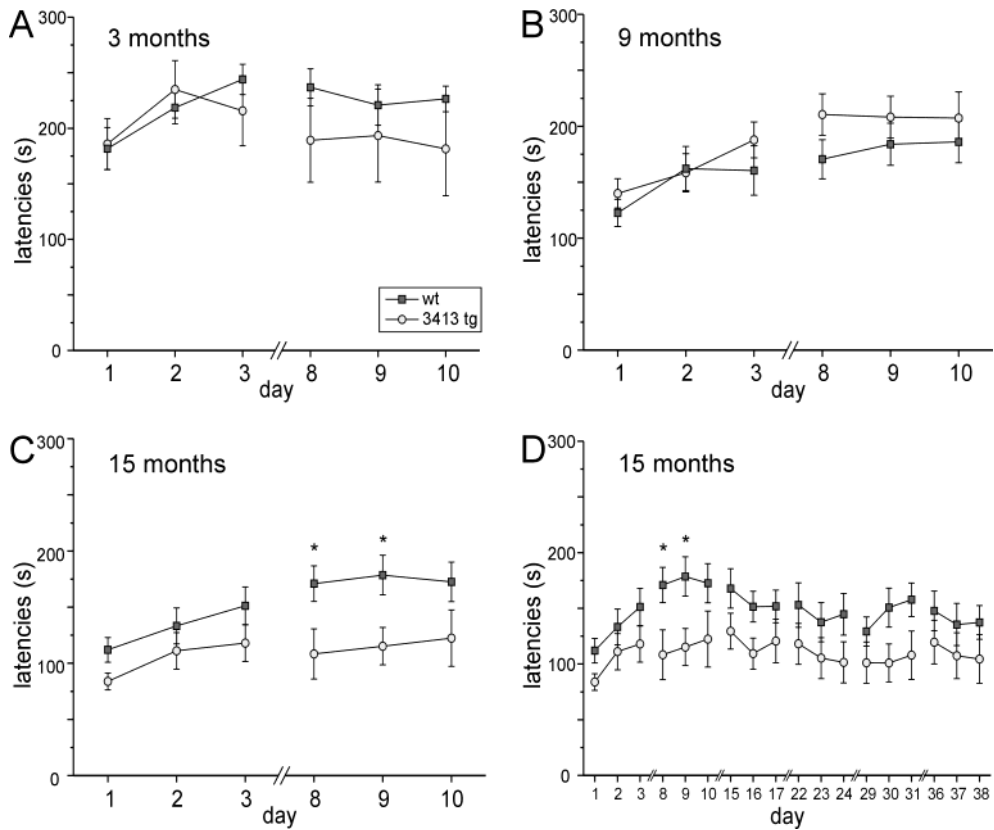


Figure 1 3413 transgenic mice exhibit normal rotarod performance. Motor coordination and motor-learning were tested on an accelerating rotarod in naive 3413 transgenic mice and wild-type control mice at 3, 9 and 15 months of age. Latency to fall (s) from the rod were recorded electronically, with a maximum of 300 s. A-B: At 3 months of age (A) and at 9 months of age (B) motor skills are comparable between wild-type and transgenic mice. C: At 15 months of age, the 3413 transgenic mice perform significantly less than wild-type mice on training day 8 ($p=0.032$) and day 9 ($p=0.021$). D: When the training period is extended for the 15 months old mice, no additional significant differences between wild-type and 3413 transgenic mice are present up to day 38. All data are averages \pm S.E.M. * $p<0.05$.

At 9 months of age, the average latencies to fall did not differ at any day between 3413 transgenic mice ($n=12$) and wild-type mice ($n=13$) (fig. 1B). A significant effect of training day was present over days 1-10 as well as over days 1-3 ($p<0.001$). This effect of training day was not present over days 8-10, indicating that the mice had reached a plateau performance on this task after the first week of training. No additional significant effects were present, further confirming that 3413 transgenic and wild-type mice performed equally well at this age.

At 15 months of age, the 3413 transgenic mice performed significantly inferior to age-matched wild-type mice on day 8 and day 9 in the second week of training ($p=0.032$, $p=0.021$ respectively, fig. 1C). A learning effect was present over days 1-3 and over all training days (effect of day; $p<0.001$), without an effect of genotype or day*genotype interaction. However, repeated measures ANOVA for days 8-10 showed a significant effect of genotype ($p=0.038$), without an effect of training day. These data suggest that at 15 months of age, the motor-learning skills of 3413 transgenic and wild-type mice were identical, but the plateau performance levels were significantly lower in the UBB⁺¹ transgenic mice. To investigate if this decreased motor performance persisted over time, we extended rotarod training to a total of 18 days (3 training days per week, 6 weeks total). The results, depicted in figure 1D, show that the performance of the 3413 transgenic mice remained inferior to wild-type mice, even after saturated learning (fig. 1D). However, this effect did not reach significance for any individual timepoint after day 9, nor did repeated measures ANOVA for days 1-18 reveal a significant effect of genotype or day*genotype interaction.

Spatial learning and memory

We recently reported that 3413 transgenic mice exhibit spatial reference memory deficits in the Morris watermaze and in a fear conditioning paradigm at 9 months of age (Chapter 3). Here, we analyzed if spatial reference memory further declined during aging. Therefore, we tested naïve 3413 transgenic mice ($n=8$) and wild-type littermates ($n=10$) in the watermaze at 15 months of age. The hidden platform position remained constant in the NW quadrant during acquisition. During acquisition days 1-4, transgenic and wild-type mice performed indistinguishable on a day-by-day basis, without significant effects of day, genotype or interaction between these factors (fig. 2A). The absence of an effect of day suggested that both wild-type and transgenic mice did not learn the task properly. The results of the 60 s probe trial to assess spatial memory retention indeed demonstrated that neither group showed a significant preference for the NW quadrant (fig. 2B), the transgenic mice even spent significantly less time in the former platform quadrant NW ($p=0.008$ for NW, fig. 2B). The average distance to the former platform position did not differ significantly between wild-type and transgenic mice (fig. 3A, probe trial 1). In the visual task, directly following the probe trial, both groups performed also sub-optimal, as no learning effect was present (fig. 4A). Although the 3413 transgenic mice tended to perform less than the wild-type mice, this effect was not statistically significant.

Aged C57Bl/6 mice show declined spatial reference memory, expressed as a reduced preference for the former platform quadrant than young mice (Bach *et al.*, 1999; von Bohlen und Halbach *et al.*, 2006). This could possibly account for the poor performance displayed by the wild-type and transgenic mice at 15 months of age after one week of acqui-

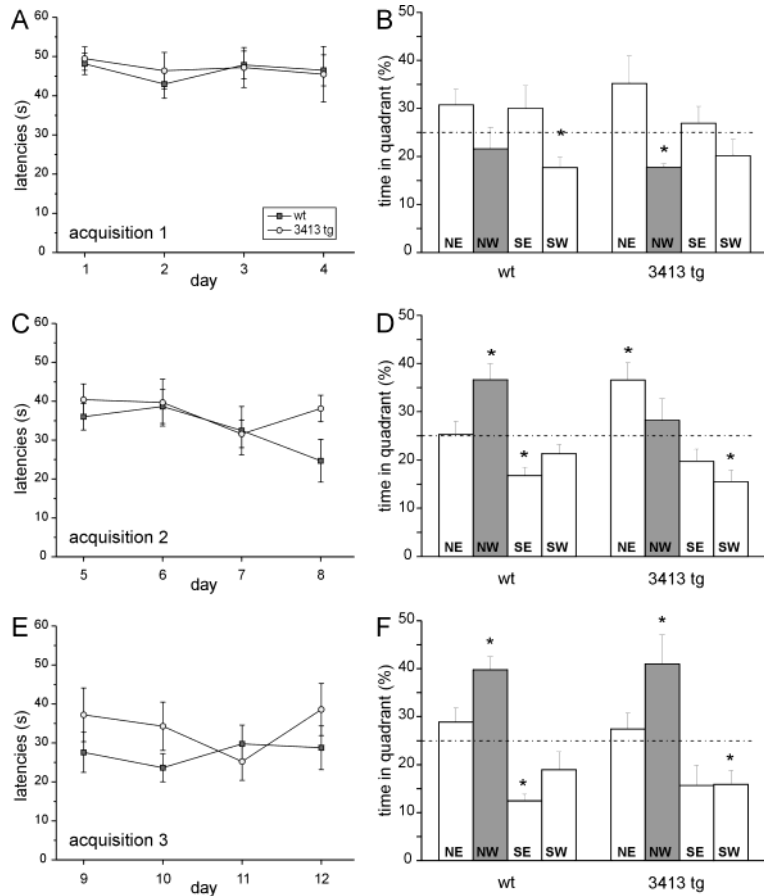


Figure 2 3413 transgenic mice show impaired performance in the Morris watermaze. Spatial performance at 15 months of age was assessed in the Morris watermaze. A: Mean escape latencies (s) to find the hidden platform in the NW quadrant do not differ between wild-type and 3413 transgenic mice during days 1-4 of acquisition. B: The mean time spent in every quadrant of the maze is plotted as percentage of the total time of the 60 s probe trial after the first week of acquisition training. Neither the wild-type mice or the 3413 transgenic mice significantly prefer the former platform quadrant NW. C: Mean escape latencies (s) to find the hidden platform are plotted for the second week of acquisition training, with the wild-type and transgenic mice performing equally well during the second acquisition phase. D: The percentage of time spent in each quadrant of the maze during the second probe trial. The wild-type mice show a significant preference for the former platform quadrant NW during the second 60 s probe trial, whereas the 3413 transgenic mice do not show a preference for the NW quadrant. E: Mean escape latencies (s) to find the hidden platform plotted for the third week of acquisition, no significant differences are present between wild-type and 3413 transgenic mice. F: The percentage of time spent in each quadrant of the maze during the third probe trial, both the wild-type and 3413 transgenic mice show a significant preference for the former platform quadrant NW. All data are averages \pm S.E.M. * p<0.05.

sition. Therefore, we extended the training period to improve acquisition of the watermaze task. Three weeks after the first probe trial, two additional sessions of acquisition trials (days 5-8 and days 9-12) were conducted in a similar fashion as days 1-4, each followed by a probe trial. During this prolonged acquisition, mice showed decreasing escape latencies over all acquisition days (days 1-12, effect of day, $p<0.01$), however this effect did not reach significance if the acquisition sessions were analyzed separately for days 5-8 (fig. 2C) or days 9-12 (fig. 2E). Furthermore, no effects of genotype or day*genotype interactions were present or significant differences between the groups on a day-by day basis.

In the second probe trial, following the first week of extended acquisition, wild-type mice demonstrated a significant preference for the NW quadrant during the probe trial ($p=0.01$, fig. 2D), indicating the establishment of spatial reference memory. Also, the time spent in the opposite quadrant (SE) was significantly lower than the expected 25% chance level ($p=0.002$, fig. 2D). In contrast, the 3413 transgenic mice did not prefer the former hidden platform location in the NW quadrant, but rather showed a significant preference for the NE quadrant ($p=0.016$, fig. 2D). This effect was also observed as a trend in the transgenic mice during the first probe trial. The average distance to the former platform position was lower for the wild-type mice, however this effect was not significant ($p=0.109$, fig. 3, probe trial 2). These results indicated that the wild-type mice were capable of remembering the hidden platform position after four days of extended acquisition, whereas the transgenic mice were not, although the 3413 transgenic mice did have an increased preference for this quadrant compared to the first probe trial. In the final probe trial following acquisition days 9-12, both the wild-type and transgenic mice showed a

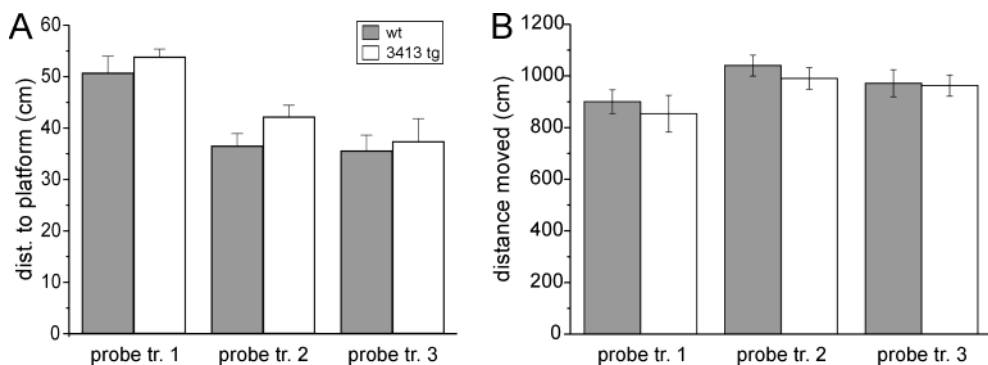


Figure 3 *Distance to the former platform position and average distance moved.* A: The mean distance (cm) to the former platform position in the NW quadrant is plotted per probe trial. B: The average total distance moved (cm) is plotted for probe trial 1 to 3. For each trial, the distances do not differ significantly between wild-type and 3413 transgenic mice. All data are averages \pm S.E.M.

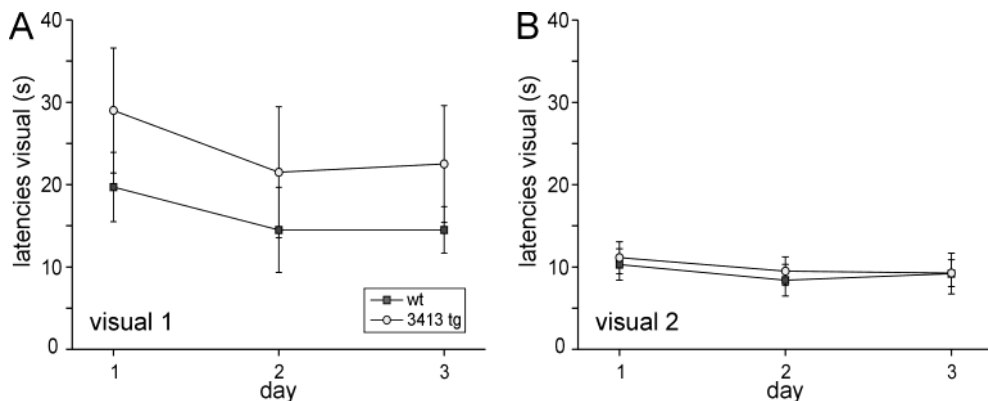


Figure 4 Performance in the visual platform trials is normal for 3413 transgenic mice. A: The mean escape latencies (s) to find the visual platform during the first visual task (following probe trial 1) do not significantly differ for any trial between the wild-type and 3413 transgenic mice. B: The mean escape latencies (s) during the second visual trial (following probe trial 3) are decreased compared to the first visual task, and do not differ between wild-type and 3413 transgenic mice. All data are averages \pm S.E.M.

significant preference for the former platform quadrant NW ($p=0.004$ and $p=0.031$ for wild-type and transgenic mice respectively, fig. 2F). The distance to the former platform position did not differ between the groups (fig. 3, probe trial 3). The observed minor motor-deficit on the rotarod task in the transgenic mice at the age of 15 months (fig. 1C, day 8 and 9) might also affect the swimming performance of these mice in the watermaze. However, swimming speed (not shown) and average distance moved (fig. 3B) did not differ significantly between the transgenic and wild-type mice during any of the probe trials. These results indicated that the 3413 transgenic mice eventually were capable of optimal performance on the watermaze task after prolonged training. Finally, a second visual test was performed, in which both groups performed equally well and improved their performance compared to the first visual test (fig. 4B).

Discussion

In this study we examined neurological functions, coordinated movement and cognitive performance in 3413 UBB⁺¹ transgenic mice. At 15 months of age, UBB⁺¹ transgenic mice display a delay in the formation of hippocampus-related spatial reference memory in the Morris watermaze task. Initial deficits were compensated for by intense training. This observation corroborates our previous results showing impaired hippocampus-dependent spatial memory at 9 months of age (Chapter 3). This cognitive deficit is not accompanied by an overt neurological phenotype. Also, procedural motor-learning and motor skills are

unimpaired in the 3413 transgenic mice at the ages of 3, 9 and 15 months. The lack of an obvious aggravation of the cognitive phenotype during aging is corroborated by the apparent equal levels of expression of the UBB⁺¹ transgene during aging of the mouse (Chapter 3).

We measured motor skills with an accelerating rotarod, a test suitable to assess motor-learning and coordination in mice (Rustay *et al.*, 2003). The cerebellum plays a central role in general motor coordination (Hikosaka *et al.*, 2002), and in rotarod performance in C57Bl/6 mice (Goddyn *et al.*, 2006). Additional brain regions, e.g. the striatum and motor cortex, are also implicated in rotarod motor-learning in mice (Costa *et al.*, 2004). In the 3413 transgenic line, UBB⁺¹ is expressed under the CamKIIα promoter, giving rise to UBB⁺¹ protein expression in neurons mainly in the hippocampus, cortex and the striatum. However, the cerebellum and brainstem are devoid of UBB⁺¹ (Chapter 3). Therefore, we did not expect to observe severe motor deficits. Indeed, rotarod performance was not significantly decreased in the 3413 transgenic mice at 3 or 9 months. At 15 months, the performance of the transgenic mice appeared to be modestly decreased compared to wild-type mice, although this effect reached significance only on day 8 and 9. We did detect a general age-related decline in performance, a similar effect was observed in other rotarod studies conducted in C57Bl/6 mice (Fetsko *et al.*, 2005; Serradj and Jamon, 2007).

We did not observe a clear aggravated decline in watermaze performance of the UBB⁺¹ transgenic mice between 9 and 15 months of age. However, a direct comparison of data was not feasible due to the extended acquisition required for the wild-type control mice to learn the task at 15 months of age compared to 9 months of age. This decreased performance in aged wild-type mice corresponds to results obtained in other studies showing an age-dependent decline in spatial memory in C57Bl/6 mice (Bach *et al.*, 1999; von Bohlen und Halbach *et al.*, 2006). Another confounding factor was the preference for the NE quadrant displayed by the 3413 transgenic mice during the first two probe trials. Possible factors contributing to this erroneous behavior could be unanticipated additional visual, auditory or olfactory cues in the testing area during the probe trials which preferentially affected the transgenic mice. It has been reported previously that extended training improves spatial memory retention in mice (e.g. (Nicolle *et al.*, 2003)). In genetically manipulated mice, showing a spatial memory deficit on earlier probe trials, extended training can ultimately result in performance indistinguishable from wild-type mice (Gordon *et al.*, 1996; Costa *et al.*, 2003). We also corroborate in our study that extended training improved spatial memory in the wild-type mice and further training restored the performance of the transgenic mice to wild-type levels during the third probe trial. The transgenic mice did not perform inferior to the wild-type mice during acquisition of the task, indicating that spatial learning is intact. This is also supported by the observation that throughout probe trial 1 to probe trial 3, the percentage of time spent in the NW target quadrant increased in the wild-type mice as well as the 3413 transgenic mice.

Cognitive decline is the most salient and earliest clinical feature of AD (Walsh and Selkoe, 2004), and is also manifest in a substantial percentage of PD patients (Emre, 2003). This is reflected in many transgenic mouse models for AD, wherein AD-related neuropathology is accompanied by a decline in cognitive function, including deficits in spatial reference memory (Hsiao-Ashe, 2001). Transgenic models of PD are mainly characterized by dopaminergic changes in the brain, motor dysfunction and decline in procedural memory (Fleming and Chesselet, 2006), however age-dependent cognitive decline has also been described in a PD mouse model carrying a mutation in α -synuclein (Freichel *et al.*, 2007). Our recent findings of hippocampus-dependent explicit memory deficiencies in 9 months-old UBB⁺¹ 3413 transgenic mice (Chapter 3) are extended in the present study to 15 months of age. The UPS inhibitory properties of UBB⁺¹ induced a modest decrease in the chymotryptic activity of the 26S proteasome in cortex homogenates of these mice (Chapter 3), suggesting that a life-long inhibition of the proteasome is related to the inferior cognitive performance. Inhibition of the UPS could thus be an underlying mechanism in AD and PD contributing to the decline of cognitive functions. Indeed, changes in components of the UPS machinery are found in brains of AD and PD patients (Keller *et al.*, 2000; Lopez Salon *et al.*, 2000; McNaught and Jenner, 2001).

However, the molecular mechanisms of the observed behavioral phenotype are not yet unravelled. We did not observe altered levels of (ubiquitinated) synaptic proteins in cortex homogenates of transgenic mice using proteomic analysis in previous experiments (Chapter 3). This does not rule out the possibility that subtle changes in the levels of these relatively low-abundance proteins were not detected using this setup (Garbis *et al.*, 2005). Analyzing expression of (known) UPS substrates locally at the synapse might allow discovering the mechanism responsible for chronic proteasome inhibition-induced memory deficits. Besides proteolytic degradation, local protein synthesis is also required for long-term synaptic modulation (Pfeiffer and Huber, 2006). In rat hippocampal slices, the balance between protein synthesis and protein degradation determines long-term synaptic strength (Fonseca *et al.*, 2006). The low-level neuronal proteasome inhibition in the UBB⁺¹ transgenic mice might disturb this delicate balance, and thus hamper long-term memory formation. Inhibition of the proteasome also impairs protein synthesis in neuronal cell lines (Ding *et al.*, 2006), adding an additional layer of complexity to the mechanism behind UBB⁺¹ mediated cognitive decline.

In conclusion, our results point to a role for the UPS in establishment of spatial reference memory, as proteasome dysfunction induced by UBB⁺¹ expression abrogates this process in UBB⁺¹ transgenic mice. These observations provide further evidence that intact forebrain proteasome function is essential for cognitive function.

Acknowledgements

We would like to thank Gertjan de Fluiter, Gavin Adema and Lotte Vis for animal care. We are grateful to Jan de Bruin and Ruud Joosten for assistance with the watermaze and rotarod. Michel Hofman assisted with statistical analysis. This research was supported by the ISAO 01504, Hersenstichting Nederland 12F04.01 and H00.06, Jan Dekker en Ludgardine Bouwman Stichting 04-22, NWO GPD 970-10-029 and 903-51-192, and NWO-Aspasia 015.01.076 to Melly Oitzl.

CHAPTER VI

Mutant ubiquitin decreases amyloid- β deposition
in a transgenic mouse model of Alzheimer's disease

Submitted manuscript

Paula van Tijn, Barbara Hobo, Fred W. van Leeuwen, David F. Fischer

Abstract

UBB⁺¹, a mutant ubiquitin, accumulates in the neuropathological hallmarks of Alzheimer's disease (AD) and is an inhibitor of the ubiquitin-proteasome system. A role for this system is implicated in the formation of amyloid- β , the main component of AD plaques. To investigate the effect of chronic proteasome inhibition on amyloid pathology, we crossed UBB⁺¹ transgenic mice, showing modestly decreased proteasome activity, with a double transgenic AD line expressing mutant amyloid precursor protein (APPswe) and presenilin 1 (PS1dE9). We determined plaque load as well as UBB⁺¹ protein levels in 3, 6, 9 and 11 months-old mice. Unexpectedly, we found decreased amyloid- β deposition in APPS1xUBB⁺¹ triple transgenic mice compared to APPS1 mice at 6 months of age, without alterations in UBB⁺¹ protein levels or in the age of onset of pathology. These results suggest a protective effect of modest proteasome inhibition on the pathogenesis of AD.

Introduction

One of the main neuropathological characteristics of Alzheimer's disease (AD) is the deposition of amyloid- β (A β) in extracellular plaques. The A β peptide is generated via β - and γ -secretase mediated proteolytic cleavage of the amyloid precursor protein (APP) (Selkoe, 2001). According to the "amyloid hypothesis", accumulation of A β , especially the aggregate-prone A β 42, is the primary event in AD pathogenesis (Hardy and Selkoe, 2002). Increasing evidence implicates that impairment of the ubiquitin-proteasome system (UPS), the main intracellular regulated proteolytic pathway, plays a role in the pathogenesis of AD (Ciechanover and Brundin, 2003). Proteasome activity and ubiquitination enzymes are decreased in AD brain (Keller *et al.*, 2000; Lopez Salon *et al.*, 2000) and A β can inhibit UPS activity *in vitro* and *in vivo* (Gregori *et al.*, 1995; Oh *et al.*, 2005). Proteasome inhibition also affects APP processing, variably resulting in increased (e.g. (Nunan *et al.*, 2001; Flood *et al.*, 2005)) or decreased A β production (Christie *et al.*, 1999; Kienlen-Campard *et al.*, 2006).

The mutant ubiquitin UBB⁺¹ accumulates in the neuropathological hallmarks of sporadic AD as well as early-onset familial AD (van Leeuwen *et al.*, 1998; van Leeuwen *et al.*, 2006). Normally, UBB⁺¹ is ubiquitinated and directed to the proteasome for proteolytic degradation (Lindsten *et al.*, 2002), therefore disease-related accumulation of UBB⁺¹ protein serves as an endogenous marker for proteasomal dysfunction (Fischer *et al.*, 2003). UBB⁺¹ also acts as UPS inhibitor when expressed at high concentrations (Lindsten *et al.*, 2002; van Tijn *et al.*, 2007). Indeed, in the recently described UBB⁺¹ transgenic line 3413, chymotryptic proteasome activity in the cerebral cortex is decreased to at least ~80% of normal levels, accompanied by accumulation of ubiquitinated proteins

and decreased context-dependent memory (Chapter 3).

In the present study we analyzed the effect of this life-long moderate proteasome inhibition on A β deposition to further elucidate the contribution of UPS inhibition to AD pathogenesis *in vivo*. We therefore crossed an AD transgenic line co-expressing familial AD-linked APP (APPswedish) and presenilin 1 (PSEN1dE9) (hereafter referred to as line APPPS1), showing increased A β 42 production accompanied by dense-core plaque pathology in the brain (Jankowsky *et al.*, 2004), with the UBB $^{+1}$ transgenic line 3413. By analyzing plaque burden and UBB $^{+1}$ levels in APPPS1/UBB $^{+1}$ triple transgenic mice during aging, we aimed to dissect the effects of low-level UPS inhibition on A β accumulation as well as the effects of A β deposition on UBB $^{+1}$ accumulation *in vivo*.

Methods

Transgenic mice

In the present study, we used the UBB $^{+1}$ transgenic mouse line 3413 (Chapter 3), neuronally expressing human *UBB* $^{+1}$ cDNA under control of the murine CamKII α promoter. The double APPSwe/PS1dE9 transgenic line 85 (Jankowsky *et al.*, 2004), backcrossed to C57/Bl6 for at least seven generations, co-expresses chimeric mouse/human APP695 with the Swedish mutation (K594M/N595L) and human PS1dE9 under control of independent mouse prion protein promoters. All animal experiments were performed conforming to national animal welfare law and under guidance of the animal welfare committee of the Royal Netherlands Academy of Arts and Sciences.

Immunohistochemistry

Mice were intracardially perfused with phosphate-buffered saline containing 4% paraformaldehyde. The left hemisphere was sectioned in 50 μ m coronal sections using a Vibratome (Leica VT1000S). Every tenth section was stained overnight with rabbit polyclonal anti-UBB $^{+1}$ antibody (Ubi3, 1:1,000 (Fischer *et al.*, 2003)), as described previously (Chapter 3). An additional series of every tenth section was stained with mouse monoclonal anti-A β antibody 6E10 (1:16,000; Signet 9300-02, Dedham MA).

Image analysis

Photographs were made using a Zeiss Axioskop microscope connected to a Sony XC-77CE b/w CCD camera. Three sections per hemisphere were analyzed, positioned at AP -1.22, -1.82 and -2.30/2.46 relative to bregma (Paxinos and Franklin, 2001). In these sections, cortex, hippocampus and dentate gyrus were outlined by hand and analyzed with

Image-Pro Plus software (version 5.1, MediaCybernetics). An example of area outlines and plaque determination is given in Supplementary fig. 3. UBB⁺¹ levels were determined by measuring integrated optical densities per outlined brain area in the consecutive sections. Differences between groups were analyzed with non-parametric Kruskal-Wallis followed by Mann-Whitney, results were considered significant when $p < 0.05$. Statistical analysis was performed using SPSS for Windows (version 12.0.1).

For detailed information on transgenic lines, experimental design, immunohistochemistry and image analysis, please refer to the Supplementary information.

Results

UBB⁺¹ induced proteasome inhibition decreases A β plaque load

To investigate the effects of chronic low-level proteasome inhibition on the age of onset and severity of A β pathology, we measured the A β plaque load in APPPS1 transgenic

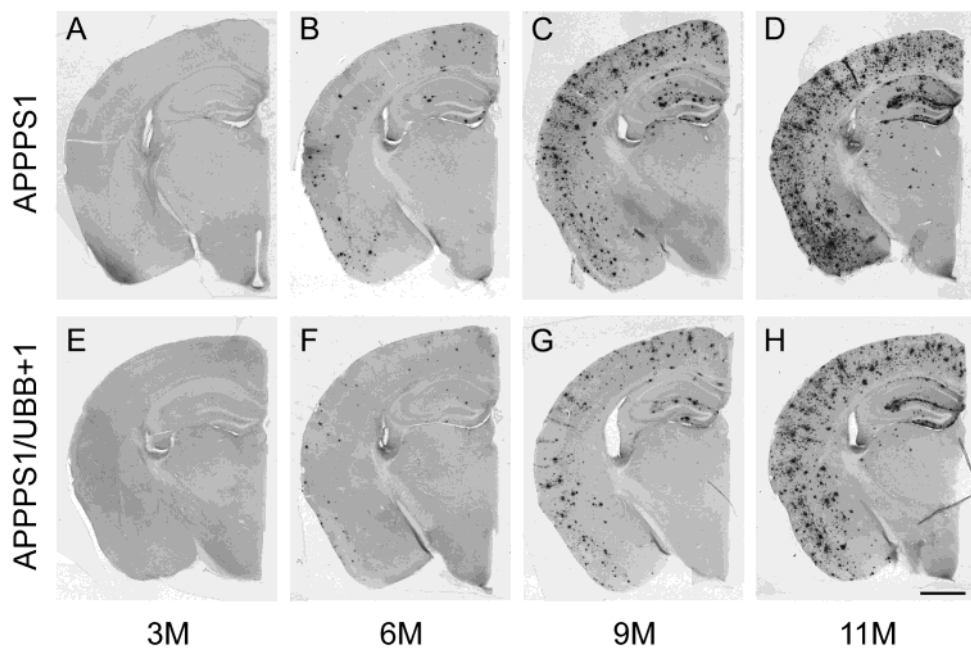


Figure 1 A β deposition in amyloid plaques in APPPS1 transgenic mice. Increasing amyloid deposition during aging in the cortex and hippocampus of APPPS1 (A-D) and APPPS1/UBB⁺¹ (E-H) transgenic mice. The spatial distribution of the A β pathology is similar between the two groups. Representative low-magnification photographs of 50 μ m coronal vibratome sections of 3, 6, 9, and 11-month-old mice, stained with monoclonal anti-amyloid 6E10 antibody, scale bar = 1 mm.

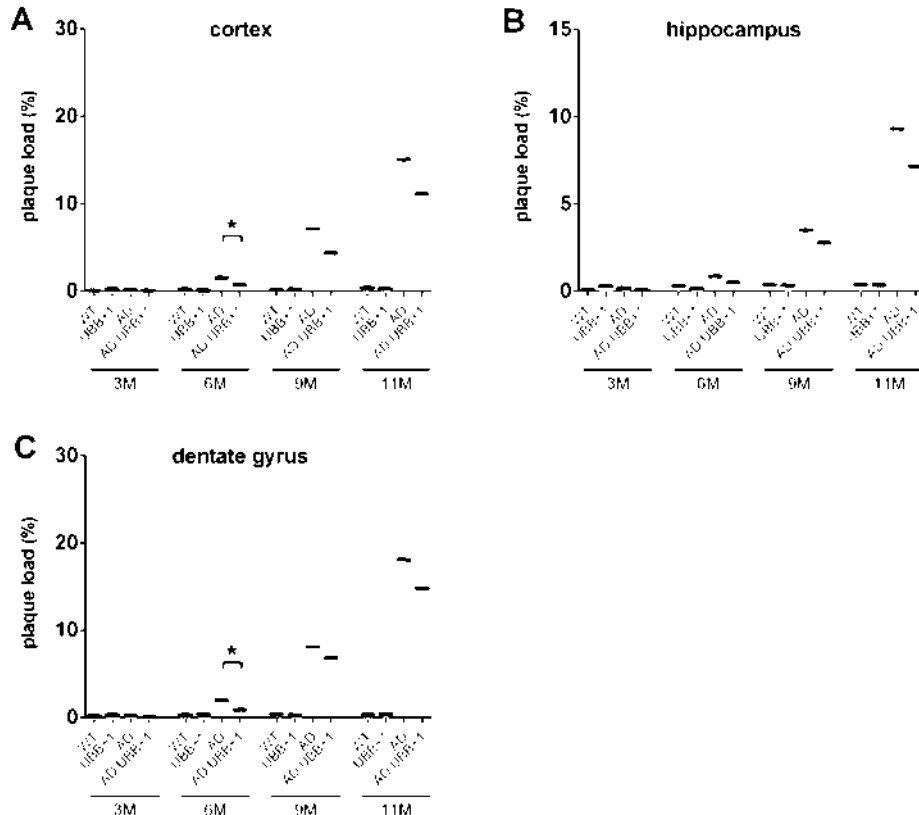


Figure 2 Proteasome inhibition decreases A β plaque load. A β plaque load in wild-type (WT), UBB⁺¹, APPPS1 (AD) and APPPS1/UBB⁺¹ (AD/UBB⁺¹) mice at the age of 3, 6, 9 and 11 months. Plaque load was determined by measuring the percentage covered by amyloid plaques in the sampled area of the cortex (A), hippocampus (B) and dentate gyrus (C). At 6 months of age, the triple transgenic APPPS1/UBB⁺¹ mice show a significantly decreased plaque load in the cortex and dentate gyrus compared to APPPS1 double transgenic mice. Individual cases are plotted, median values per group are indicated by horizontal bars, * p < 0.05.

mice and in triple transgenic APPPS1/UBB⁺¹ mice at 3, 6, 9 and 11 months of age. A β plaques were quantified in the cortex, hippocampus and dentate gyrus using the 6E10 antibody reactive to human A β amino acids 1-16. In these mice, plaques could also be visualized using the A β antibodies 4G8 (A β 17-24) and 6F/3D (A β 8-17) or Congo Red and thioflavin-S (not shown). At the age of 3 months, APPPS1 and APPPS1/UBB⁺¹ transgenic mice showed few small-sized amyloid plaques, located mainly in the cortex (Supplementary fig. 1). From 6 months onward, plaque load increased in both APPPS1 and

APPPS1/UBB⁺¹ mice during aging (fig. 1). We previously reported that UBB⁺¹ transgenic mice do not show overt neuropathology (Chapter 3). Indeed, we did not detect A β pathology in the UBB⁺¹ transgenic mice or wild-type control mice at any age (not shown).

Both APPPS1 and APPPS1/UBB⁺¹ mice show an increased plaque load during aging (figs. 1, 2). However, at the age of 6 months, the plaque covered area in the cortex and dentate gyrus was significantly decreased in APPPS1/UBB⁺¹ transgenic mice compared to APPPS1 mice ($p=0.03$ and $p=0.017$ respectively, fig. 2A, 2C). Also at the age of 9 and 11 months, the plaque load was decreased in APPPS1/UBB⁺¹ transgenic mice compared to APPPS1 mice, however at these ages this effect did not reach statistical significance (fig. 2). The decreased A β plaque load in 6-months old APPPS1/UBB⁺¹ mice was not caused by alterations in the volume of the sampled brain areas, which did not differ between wild-type, UBB⁺¹, APPPS1 or APPPS1/UBB⁺¹ mice at this age (Supplementary fig. 2). Also at 9 and 11 months of age, minor variations in the volume of the sampled brain regions could not account for the lower A β accumulation in the APPPS1/UBB⁺¹ mice (Supplementary fig. 2). These results indicate that inhibition of the UPS decreases the deposition of A β in amyloid plaques *in vivo* at the age of 6 months.

Amyloid deposition does not affect proteolytic turnover of UBB⁺¹

A β has been reported to decrease proteasome function in a APPSwe transgenic mouse model of AD (Oh *et al.*, 2005; Almeida *et al.*, 2006). We investigated if A β accumulation

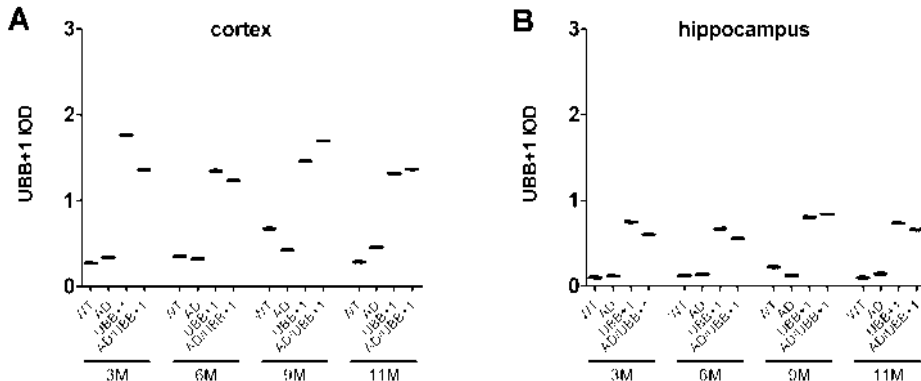


Figure 3 *A β accumulation does not induce UBB⁺¹ accumulation.* UBB⁺¹ levels were measured in the cortex (A) and hippocampus (B) of wild-type (WT), UBB⁺¹, APPPS1 (AD) and APPPS1/UBB⁺¹ (AD/UBB⁺¹) mice at 3, 6, 9 and 11months of age. UBB⁺¹ protein levels were determined by measuring the integrated optical density (IOD) per sampled brain area. No significant differences were present at any age. Individual cases are plotted, median values per group are indicated by horizontal bars.

also affected UPS function in APPPS1/UBB⁺¹ transgenic mice. As UBB⁺¹ is a substrate for proteasomal degradation, proteasome inhibition would lead to increased levels of UBB⁺¹. We determined UBB⁺¹ levels in the same APPPS1/UBB⁺¹ mice used for the plaque load measurements, and compared these levels to UBB⁺¹ levels in single UBB⁺¹ transgenic mice. We previously reported that UBB⁺¹ protein is maximally expressed in from postnatal day 22 onwards (Chapter 3). Indeed, the UBB⁺¹ levels in the cortex and hippocampus remained constant up to 11 months of age (fig. 3). APPPS1 and wild-type mice did not express UBB⁺¹ at any age, as expected (fig. 3). Furthermore, we did not observe any significant differences in the levels of UBB⁺¹ expression between UBB⁺¹ and APPPS1/UBB⁺¹ transgenic mice at any age examined (fig. 3). These results show that in APPPS1/UBB⁺¹ triple transgenic mice, A β accumulation does not induce additional accumulation of UBB⁺¹, suggesting that A β deposition does not lead to further proteasome inhibition in these mice.

Discussion

In the present study, we demonstrate a protective role for decreased proteasome activity in AD pathogenesis *in vivo*. A β deposition was significantly decreased in APPPS1/UBB⁺¹ triple transgenic mice compared to APPPS1 mice, indicating that chronic proteasome inhibition, induced by UBB⁺¹ expression, reduces amyloid pathology. The age of onset of amyloid pathology was unaffected, as A β plaques were detected at 3 months of age in both APPPS1 and APPPS1/UBB⁺¹ transgenic mice. Using different staining methods, others reported detection of plaques in APPPS1 mice at 4 (Garcia-Alloza *et al.*, 2006) or 6 months of age (Jankowsky *et al.*, 2004). In concordance with these two studies, the cerebral cortex and hippocampus were the main brain regions affected by A β deposition.

The precise mechanism by which proteasome inhibition may decrease plaque load remains unclear, as APP processing as well as the clearance of A β peptides could be affected. Neuronal β -secretase cleavage of APP, giving rise to the 99-amino acid C-terminal fragment (β CTF), is predominantly performed by BACE1 (Cai *et al.*, 2001). β CTF is subsequently cleaved by γ -secretase to generate A β 40-42/43. BACE is ubiquitinated and degraded by the proteasome (Qing *et al.*, 2004), although conflicting results show that BACE is not a proteasome substrate (Kienlen-Campard *et al.*, 2006), but rather degraded by the lysosomal pathway (Koh *et al.*, 2005). Nonetheless, neuronal proteasome inhibition significantly decreases β -secretase activity, accompanied by reduced levels of the β -secretase cleavage products β CTF and A β . Possibly, decreased β CTF substrate availability for γ -secretase accounts for the lower A β production (Kienlen-Campard *et al.*, 2006). Administration of BACE1 inhibitor reduces A β production in APPSwexPS1^{M146V} transgenic mice (Hussain *et al.*, 2007) and BACE1 knockout prevents amyloid pathology in several AD transgenic models (e.g. (McConlogue *et al.*, 2007)), indicating that β -secretase

cleavage is the rate-limiting step for A β formation *in vivo*. In APPPS1/UBB⁺¹ transgenic mice, the decreased A β deposition could thus be attributable to a initial decrease in β -secretase activity, due to neuronal proteasome inhibition induced by UBB⁺¹ expression.

Neuronal A β production increases following UPS inhibition when A β is derived from recombinantly expressed β -secretase fragment C99 (Skovronsky *et al.*, 2000; Nunan *et al.*, 2001; Flood *et al.*, 2005; Kienlen-Campard *et al.*, 2006). The seemingly conflicting results we obtained in our study might be attributed to the differential effect of UPS inhibition on the processing of C99 or full-length APP. As C99 is a proteasome substrate, the increase in A β following UPS inhibition is likely caused indirectly by an increased availability of C99 for γ -secretase cleavage (Flood *et al.*, 2005). However, β CTF produced from full-length APP is not a substrate for proteasomal degradation (Kienlen-Campard *et al.*, 2006). In addition, β -secretase cleavage, which is affected by proteasome inhibition, is not required to generate A β from C99. Decreased proteasome activity could also conceivably lead to increased γ -secretase levels, as the essential γ -secretase complex components are degraded by the UPS (Kim *et al.*, 1997; Fraser *et al.*, 1998; Bergman *et al.*, 2004; He *et al.*, 2006; He *et al.*, 2007). However, neuronal γ -secretase activity, acting downstream of β -secretase cleavage, is not regulated by the UPS (Kienlen-Campard *et al.*, 2006). Also, in APPPS1 transgenic mice, γ -secretase activity is most likely not rate-limiting as PSEN1 is overexpressed and the APPSwe mutation leads to potentiation of β -secretase cleavage. Recently it was shown that intraventricular proteasome inhibitor infusion increased intra-neuronal A β levels in 3xTg-AD mice (Tseng *et al.*, 2007), the effect of this acute high-level UPS inhibition on amyloid plaque deposition was however not studied.

A β is reported to reduce chymotryptic proteasome activity *in vitro* (Gregori *et al.*, 1995) and in neuronal cells (Lopez Salon *et al.*, 2003). In neuroblastoma cells, A β induced UPS inhibition and A β toxicity are mediated by the ubiquitin-conjugating enzyme E2-25K (Song *et al.*, 2003). Proteasome activity is decreased in APPSwe transgenic mice (Oh *et al.*, 2005; Almeida *et al.*, 2006) and intraneuronal soluble A β oligomers decrease UPS activity in 3xTg-AD transgenic mice (Tseng *et al.*, 2007). Therefore, we expected a further reduction in proteasome activity in APPPS1/UBB⁺¹ mice compared to single UBB⁺¹ transgenic mice. As UBB⁺¹ is a substrate for proteasomal degradation (Lindsten *et al.*, 2002), we measured UBB⁺¹ levels as reporter for UPS activity. However, we did not observe significant differences in levels of UBB⁺¹, indicating that A β did not affect the proteolytic turnover of UBB⁺¹. It is conceivable that subtle decreases in UPS activity induced by A β are not directly reflected in the UBB⁺¹ levels or that the already present modest UPS inhibition in transgenic line 3413 masks any additional effects of A β on UPS function. Therefore, we cannot discard the possibility that A β accumulation decreases UPS activity in these mice.

Concluding, our results show that neuronal inhibition of the proteasome decreases accumulation of A β in amyloid plaques *in vivo* at 6 months of age. Further research is

necessary to investigate the precise mechanism by which UPS inhibition decreases plaque burden in these mice. It is conceivable that UBB⁺¹ induced proteasome inhibition decreases β -secretase activity, thereby reducing A β formation. Insight in this mechanism can contribute to understanding the role of the UPS in the pathogenesis of AD.

Acknowledgements

Dr. David Borchelt (Department of Neuroscience, McKnight Brain Institute, University of Florida, USA) kindly provided the APPPS1 transgenic line. We thank J.J. van Heerikhuize and C.W. Pool for assistance with the image analysis and M.A. Hofman for statistical advice. This work was funded by the ISAO 01504 and 06502, Hersenstichting Nederland 12F04.01, H00.06, Van Leersum Foundation, Jan Dekker en Ludgardine Bouwman Stichting 04-22 and NWO GPD 970-10-029 and 903-51-192.

Supplementary Information

Supplementary Methods

Transgenic mice

In this study, we used the UBB⁺¹ transgenic mouse line 3413 (Chapter 3), neuronally expressing human *UBB⁺¹* cDNA under control of the murine CamKIIα promoter on a C57/Bl6 background. The double APPSwe/PS1dE9 transgenic line 85, previously described by (Jankowsky *et al.*, 2004), carries a co-integrate of 1) chimeric mouse/human APP695 carrying the Swedish mutation (K594M/N595L) and 2) human PS1 with deletion of exon 9 (Jankowsky *et al.*, 2001), each under control of a mouse prion protein promoter. Line 85 was backcrossed to C57/Bl6 for at least seven generations. Subsequently heterozygous line 85 transgenic mice were crossed to heterozygous line 3413 mice to generate triple transgenic APPSwe/PS1dE9/UBB⁺¹ transgenic mice, the APPSwe/PS1dE9, UBB⁺¹ and wildtype littermates were used as controls. Mice were kept in group housing on a 12/12 h light-dark cycle with food and water ad libitum in specific pathogen free conditions (Nicklas *et al.*, 2002). All animal experiments were performed conforming to national animal welfare law and under guidance of the animal welfare committee of the Royal Netherlands Academy of Arts and Sciences.

Experimental design

Four age groups of transgenic and control mice were compared. For detailed information on number of subjects per group, sex and bodyweight see Supplementary Table 1

Immunohistochemistry

Animals were given intra-peritoneal deep pentobarbital anaesthesia and were sacrificed by intracardial perfusion with phosphate-buffered saline (PBS) pH 7.4, followed by PBS containing 4% paraformaldehyde. The brain was removed and stored in PBS-4% paraformaldehyde at 4°C until further processing. Brains were sectioned over the midline, the left hemisphere was embedded in gelatin and cut in 50 µm coronal sections on a vibratome (Leica VT1000S). To detect and quantify UBB⁺¹ protein levels, every tenth section was immuno-histochemically stained overnight with rabbit polyclonal anti-UBB⁺¹ antibody (Ubi3; bleeding date 05/08/97, 1:1,000 (Fischer *et al.*, 2003)), as described previously (Chapter 3) using the peroxidase-anti-peroxidase method (Sternberger *et al.*, 1970). Staining was visualized with 3,3'-diaminobenzidine solution using nickel intensification (0.2%). An additional series of every tenth section was used to detect and quantify the Aβ plaque load by immuno-histochemically staining the sections overnight with mouse monoclonal anti-Aβ antibody 6E10 (1:16,000; Signet 9300-02, Dedham MA) with 30-min

of pre-treatment with fresh formic acid solution to permeabilize the tissue, sections were further processed using the peroxidase-anti-peroxidase method and 3,3'-diaminobenzidine -Ni color reaction. Stained sections were mounted on glass slides, embedded using Entellan (Merck) and coverslipped.

Image analysis

Photographs in figure 1 and Supplementary figure 1 were made using a Zeiss Axioplan 2 microscope and an Evolution digital camera (MediaCybernetics, Silver Spring, MD). For analysis of plaque load and UBB⁺¹ IOD, photographs were made using a Zeiss Axioskop microscope with Neofluor 2.5x and 5x objectives and a 558,5 nm bandpass filter (type DMZ-12, ITOS), connected to a Sony XC-77CE CCD black and white camera. Three coronal sections per hemisphere were captured, positioned at anterior-posterior -1.22, -1.82 and -2.30/2.46 relative to bregma (Paxinos and Franklin, 2001). In each section, the entire cortex, hippocampus and dentate gyrus were outlined by hand according to Paxinos *et al.* (Paxinos and Franklin, 2001) and analyzed with Image-Pro Plus software (version 5.1, MediaCybernetics). Measurement of sampled area volume (mm³) and Aβ plaque percentage was performed using a custom-made analysis program using Cavalieri's principle of volume estimation (Gundersen and Jensen, 1987). An example of brain area outlines and plaque determination is given in Supplementary figure 3. UBB⁺¹ levels were determined by measuring integrated optical densities per outlined brain area using Image-Pro Plus software. The experimenter was blind to the genotype of the mice. Differences between groups were analyzed with non-parametric Kruskal-Wallis followed by Mann-Whitney, results were considered significant when p<0.05. Statistical analysis was performed using SPSS for Windows (version 12.0.1).

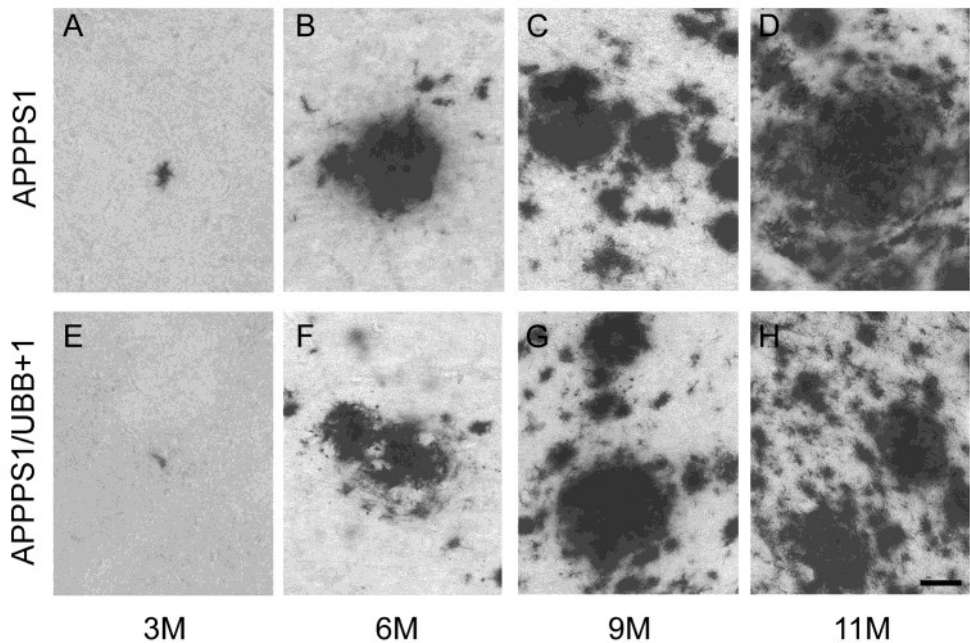
Supplementary Figures

Figure S1 *A β plaques in APPPS1 transgenic mice.* Increasing amyloid deposition in plaques during aging in the cortex of APPPS1 (A-D) and APPPS1/UBB⁺¹ (E-H) transgenic mice. Representative high-magnification photographs of 50 µm coronal vibratome sections of 3, 6, 9, and 11-month-old mice, stained with monoclonal anti-amyloid 6E10 antibody. Photomicrographs are magnifications of photos shown in figure 1 of Chapter 6. Scale bar = 0.025 mm.

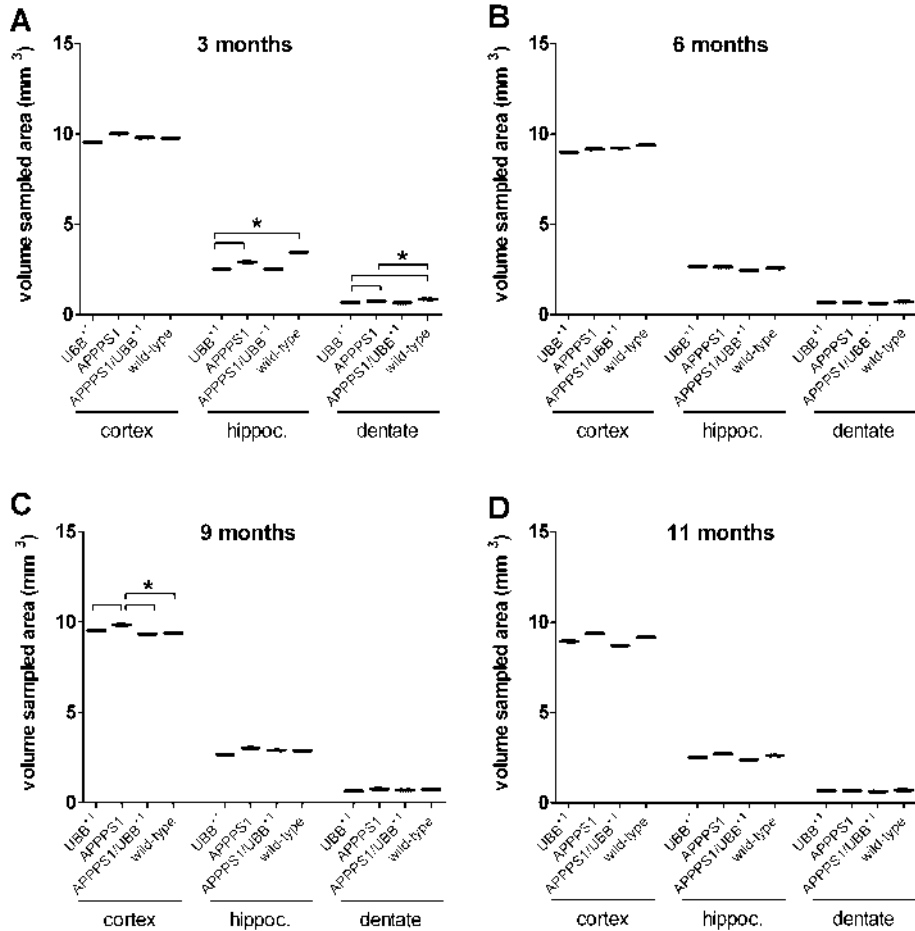


Figure S2 Volume of sampled brain areas is not affected by A β deposition or proteasome inhibition. Volume of the sampled areas (in mm³) of the cortex, hippocampus and dentate gyrus were measured in UBB^{+/+}, APPPS1, APPPS1/UBB^{+/+} and wild-type mice at 3 (A), 6 (B), 9 (C) and 11 (D) months of age. Individual cases are plotted, median values per group are indicated by horizontal bars, * p<0.05.

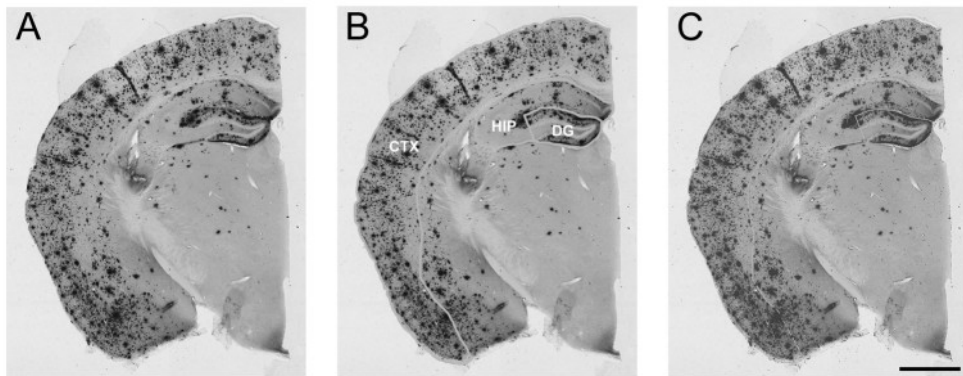


Figure S3 *A β plaque load measurement.* Example of computer automated measurement of the amyloid plaque load in a 11-month old APPPS1 transgenic mouse at -1.82 anterior-posterior from bregma. First, 50 μ m coronal sections were stained with 6E10 anti-amyloid antibody (A). The sampled brain areas, cortex (CTX), hippocampus (HIP) and dentate gyrus (DG), were outlined by hand, outlines are shown in green (B). Overlay in (C) shows the 6E10 stained section overlaid by the computer automated measurement of A β plaque covered area shown in red (C). Scale bar = 1 mm. See color section.

Supplementary Table

Table S1 Summary of the mice used for the A β plaque and UBB⁺¹ analysis

Age	Genotype	n (male;female)	Age (days)	Weight (g)
3 months	wild-type	5 (5;0)	91 \pm 1	30.0 \pm 2.1
	UBB ⁺¹	7 (7;0)	91 \pm 1	31.6 \pm 1.3
	APPPS1	5 (5;0)	91 \pm 3	27.6 \pm 2.7
	APPPS1/UBB ⁺¹	5 (5;0)	90 \pm 2	27.0 \pm 1.1
6 months	wild-type	6 (5;1)	183 \pm 4	33.4 \pm 5.7
	UBB ⁺¹	7 (5;2)	182 \pm 3	31.8 \pm 4.6
	APPPS1	6 (4;2)	182 \pm 3	31.7 \pm 6.8
	APPPS1/UBB ⁺¹	5 (4;1)	180 \pm 2	30.9 \pm 4.0
9 months	wild-type	6 (5;1)	274 \pm 5	38.0 \pm 8.3
	UBB ⁺¹	3 (3;0)	273 \pm 4	36.2 \pm 1.2
	APPPS1	6 (5;1)	275 \pm 2	35.2 \pm 3.8
	APPPS1/UBB ⁺¹	4 (4;0)	267 \pm 1	38.5 \pm 3.6
11 months	wild-type	8 (3;5)	346 \pm 13	35.0 \pm 7.4
	UBB ⁺¹	5 (2;3)	336 \pm 4	33.1 \pm 4.6
	APPPS1	8 (2;6)	355 \pm 10	33.5 \pm 7.4
	APPPS1/UBB ⁺¹	3 (1;2)	337 \pm 4	29.8 \pm 10.2

CHAPTER VII

General Discussion

Partly based upon:

Frameshift proteins in autosomal dominant
forms of Alzheimer disease and other tauopathies

Neurology, 2006; 66(2 Suppl 1): S86-S92

van Leeuwen FW, van Tijn P, Sonnemans MA, Hobo B, Mann DM,
Van Broeckhoven C, Kumar-Singh S, Cras P, Leuba G, Savioz A, Maat-Schieman ML,
Yamaguchi H, Kros JM, Kamphorst W, Hol EM, de Vos RA, Fischer DF

A decade of UBB⁺¹

UBB⁺¹ was discovered over a decade ago as an aberrant protein accumulating in the neuropathological hallmarks of Alzheimer's disease (AD) and Down Syndrome (DS), including in neurofibrillary tangles, neuropil threads and dystrophic neurites (van Leeuwen *et al.*, 1998). UBB⁺¹ is formed by "molecular misreading", a process giving rise to di-nucleotide deletions in messenger RNA (mRNA), preferably in or around GAGAG repetitive motifs (Evans *et al.*, 1994; van Den Hurk *et al.*, 2001). Subsequent translation of these aberrant mRNAs results in proteins showing a frameshift in the alternate +1 open reading frame. In the case of UBB⁺¹, an mRNA ΔGT or ΔCT di-nucleotide deletion close to the C-terminus of the first or third ubiquitin repeat respectively results in translation of the UBB⁺¹ protein, harboring a C-terminal extension of 19 amino acids (van Leeuwen *et al.*, 1998). Molecular misreading has furthermore been shown to occur in amyloid-β precursor protein (APP) mRNA, resulting in a frameshifted APP protein (APP⁺¹). APP⁺¹ also accumulates in the neuropathological hallmarks of AD and DS and often co-localizes with UBB⁺¹ (van Leeuwen *et al.*, 1998). It was initially hypothesized that the rate of molecular misreading increased during aging; UBB⁺¹ and APP⁺¹ proteins were detected only in diseased subjects and aged controls. Hence, molecular misreading was hypothesized to contribute to the early pathology in AD and even be an underlying cause for AD pathology (van Leeuwen *et al.*, 1998). However, later studies by our group and by others revealed that frameshifted UBB and APP mRNA transcripts are present at similar levels in diseased subjects as well as young control subjects (Fischer *et al.*, 2003; Gerez *et al.*, 2005), indicating that molecular misreading is a continuous process during life. The gradual accumulation of +1 proteins is thus more likely attributable to confounding factors allowing accumulation of aberrant proteins during aging or disease progression and not to an increased rate of molecular misreading.

The precise mechanism behind molecular misreading is as yet unknown. It has been suggested that the di-nucleotide deletions originate from RNA polymerase slippage, as well as from post-transcriptional RNA editing (van Leeuwen *et al.*, 2000). Also a failure of RNA quality control could underlie the presence of the +1 transcripts. Normally, aberrant mRNAs are selectively targeted for degradation by the nonsense-mediated mRNA decay (NMD) pathway (reviewed by (Chang *et al.*, 2007). This pathway recognizes mRNAs which contain a (premature) termination codon located more than 50-55 nucleotides upstream of the 3'-outer exon-exon junction, marked by an exon-junction complex (Nagy and Maquat, 1998). In the UBB⁺¹ transcript, no exon-exon boundary is present after the newly formed termination codon, and these transcripts are thus not likely to be targeted for NMD. On the other hand, APP⁺¹ transcripts contain a premature termination codon in exon 9 or 10, far upstream of the outer 3' exon-exon junction at exon 17 and 18. Hypothetically, APP⁺¹ transcripts should be subjected to NMD. The presence of APP⁺¹

protein in diseased patients may thus point to a failing RNA quality control system. Recently, it was hypothesized that UBB⁺¹ and APP⁺¹ proteins could also result from ribosomal frameshifting during translation of intact UBB and APP mRNA. The outcome of this ribosomal frameshifting would be proteins with C-termini similar to UBB⁺¹ and APP⁺¹ (Wills and Atkins, 2006).

Degradation of proteins can be executed by various proteolytic systems, including lysosomal degradation, chaperone-mediated autophagy, and substrate-specific degradation by the ubiquitin-proteasome system (UPS) for protein quality control. The frequency of molecular misreading is very low, occurring in less than 1 in 10⁵ to 10⁶ transcripts (Gerez *et al.*, 2005), and does not differ between AD and DS patients and non-demented control subjects (Fischer *et al.*, 2003; Gerez *et al.*, 2005). Therefore, it is likely that the accumulation of the aberrant proteins in diseased patients can be attributed to a failing protein quality control system. This hypothesis is further supported by the finding that the UBB⁺¹ protein is a natural substrate for proteolytic degradation by the UPS (Lindsten *et al.*, 2002). The decrease in proteasome function associated with aging (Keller *et al.*, 2000) and neurodegenerative disease (reviewed by (Ciechanover and Brundin, 2003)) could underlie the accumulation of the UBB⁺¹ protein. Accordingly, UBB⁺¹ accumulation in disease is postulated to be an endogenous marker for general proteasome dysfunction (Fischer *et al.*, 2003). In the case of APP⁺¹, it is not known if this aberrant protein is normally targeted for proteasomal degradation. However, similar to the wild-type APP cleavage products sAPP α and sAPP β , APP⁺¹ is a secreted protein and accumulates in the cerebrospinal fluid in human (Hol *et al.*, 2003), as well as in a transgenic mouse model neuronally expressing APP⁺¹ (Fischer *et al.*, 2006). Proteasomal degradation takes place in the cytosol as well as the nucleus, and proteasomes are occasionally localized on the cytosolic surface of the endoplasmatic reticulum membrane (Wojcik and DeMartino, 2003). APP⁺¹ is normally trafficked through the endoplasmatic reticulum and Golgi complex (van Dijk *et al.*, 2004) and could there be a target for the proteasomal degradation. However, if APP⁺¹ accumulation is affected by a decrease in protein quality control has not been further studied yet.

Molecular misreading does not only occur in the nervous system; +1 frameshift proteins can also be formed in non-neuronal cells. This was first demonstrated in a transgenic mouse model for molecular misreading expressing multiple copies of the rat vasopressin gene. Frameshifted vasopressin protein was detected in tissues showing high transgene expression, including the epididymis and parotid gland (Van Leeuwen *et al.*, 2000). More recently, UBB⁺¹ accumulation was also detected in the pathological hallmarks of several non-neuronal diseases which show ubiquitin-positive pathology, including muscle disease (Fratta *et al.*, 2004; Olive *et al.*, 2008), alcoholic liver disease (McPhaul *et al.*, 2002) and alpha(1)-antitrypsin deficiency (Wu *et al.*, 2002). These results indicate that UPS dysfunction can be a general underlying cause for UBB⁺¹ accumulation in a variety of diseases.

Processing of UBB⁺¹, a dual proteasome substrate and inhibitor

The precise mechanism by which UBB⁺¹ is processed remains elusive. Ubiquitin is translated as a fusion protein of ubiquitin and a ribosomal protein or as a polyubiquitin precursor protein of three head-to-tail ubiquitin repeats (UBB). To generate monomeric ubiquitin, these precursors are cleaved at the ubiquitin C-terminal glycine by ubiquitin C-terminal hydrolases (UCHs), belonging to the family of deubiquitinating enzymes (DUBs) (Larsen *et al.*, 1998). Lam *et al.* were the first to show that UBB⁺¹ is not proteolytically cleaved by the DUB UCH-D, due to the presence of a 19 amino acid C-terminal extension (Lam *et al.*, 2000). In addition, this *in vitro* study showed that UBB⁺¹ is not actively involved in the ubiquitination of substrate proteins, as it cannot conjugate to the ubiquitin-activating enzyme E1. Conversely, UBB⁺¹ is ubiquitinated itself, and the resulting UBB⁺¹ containing ubiquitin chains are refractory to deubiquitination by isopeptidaseT. This DUB requires an unconjugated C-terminal glycine for deubiquitination, which is not present in UBB⁺¹. This study was also the first to show that ubiquitinated UBB⁺¹ (Ub_x-UBB⁺¹) can inhibit proteasomal substrate degradation in a cell free system (Lam *et al.*, 2000).

These results were corroborated in a neuroblastoma cell line, where high levels of UBB⁺¹ expression resulted in stable levels of UBB⁺¹ protein, ultimately leading to apoptotic-like cell death (De Vrij *et al.*, 2001). UBB⁺¹ also proved to hold seemingly opposing proteasome-related properties; UBB⁺¹ is not only an inhibitor of the UPS, but also a ubiquitin-fusion degradation (UFD) substrate for the proteasomal degradation (Lindsten *et al.*, 2002). Similar to other UFD substrates (Johnson *et al.*, 1995), UBB⁺¹ is ubiquitinated on internal lysine residues K29 and K48. Ubiquitination of UBB⁺¹ at both lysine residues is essential for optimal processing by the proteasome. Intriguingly, enhancement of the UFD degradation signal further strengthens the proteasome inhibitory capacity of UBB⁺¹ (Lindsten *et al.*, 2002). Notably, UBB⁺¹ is the first identified naturally occurring UFD substrate in human. The proteasome substrate properties of UBB⁺¹ also offer an explanation for the resistance to deubiquitination by isopeptidaseT (Lam *et al.*, 2000), as isopeptidaseT shows specific activity toward unanchored ubiquitin chains and does not cleave ubiquitin moieties from substrate proteins (Wilkinson *et al.*, 1995). Confirming previous observations, Lindsten *et al.* also showed that UBB⁺¹ acts as a UPS inhibitor, using a green fluorescent protein (GFP)-reporter cell line for proteasome activity expressing the artificial proteasome substrate Ub^{G76V}-GFP (Lindsten *et al.*, 2002). Ub^{G76V}-GFP is normally degraded by the UPS, however, when the proteasome is inhibited, degradation of Ub^{G76V}-GFP is prevented resulting in green fluorescence (Dantuma *et al.*, 2000). Overexpression of UBB⁺¹ in this cell line resulted in GFP accumulation in the vast majority of transduced cells (Lindsten *et al.*, 2002).

These dual properties of UBB⁺¹ were further studied as described in Chapter 2. Here, we offer an explanation for the dual UPS substrate-inhibitory properties of UBB⁺¹. We demonstrate in HeLa cells that UBB⁺¹ shifts from UPS substrate to proteasome inhibitor depending on the level of expression. UBB⁺¹ is a substrate for proteasomal degradation at low expression levels. Only at high expression levels the protein accumulates and subsequently induces dose-dependent proteasome inhibition. This observation also holds in mouse organotypic cortex slices, a system that reflects a multi-cellular environment wherein neuronal connectivity and neuron-glia interactions are considered to be well preserved (Sundstrom *et al.*, 2005), and which closer resembles the human brain than the previously used HeLa and neuroblastoma cell lines. In these organotypic cultures, the UBB⁺¹ protein is degraded when expressed at relatively low levels using a lentiviral vector (Chapter 2). Higher levels of expression, achieved with adenoviral transduction of UBB⁺¹, lead to accumulation of UBB⁺¹ and inhibition of the UPS.

The levels of expression required to initiate UBB⁺¹ accumulation differ from one physiological setting to another. This is best exemplified by the differential effect of lentiviral UBB⁺¹ transduction on accumulation of the protein in several (neuronal) model systems. Lentiviral UBB⁺¹ transduction induced sufficient expression for UBB⁺¹ to accumulate in the human neuroblastoma cell line SH-SY5Y, as reported in Chapter 2, as well as in mouse primary neuron cultures (Lindsten *et al.*, 2003). On the other hand, in cortex slice cultures obtained from the same mouse strain, lentiviral expression did not give rise to UBB⁺¹ accumulation, shown in Chapter 2. Also after stereotactical injection of lentiviral UBB⁺¹ in the rat hippocampus, UBB⁺¹ protein could not be detected (Fischer *et al.*, 2003). These results indicate that not only the choice of expression vector, but also the physiological context wherein UBB⁺¹ is expressed will influence the expression levels of the protein and thereby determine the UPS-related properties of the protein. Therefore, caution should be taken when these results obtained *in vitro* are translated to the human situation.

UBB⁺¹ induced proteasome inhibition *in vivo*

To closer resemble the human UBB⁺¹ neuropathology by studying the properties of UBB⁺¹ *in vivo*, we developed three transgenic mouse lines expressing varying levels of neuronal UBB⁺¹, as described in Chapters 3 and 4. Using these transgenic lines, the dual UPS substrate/inhibitor properties of UBB⁺¹ as demonstrated *in vitro* could be corroborated *in vivo*. Indeed, when expressed at low levels (17% of endogenous UBB mRNA, transgenic line 6663), the UBB⁺¹ protein is degraded by the proteasome. Only after hippocampal inhibition UPS of the using pharmacological proteasome inhibitors, UBB⁺¹ protein accumulation can be observed. UBB⁺¹ is expressed at high levels in the transgenic lines 3413 and 8630 (49% and 67% of endogenous UBB mRNA respectively). In these lines,

Table 1 Lentivirus particles (1.0×10^6 transducing units in 1 μl) were stereotactically injected into the hippocampus of various transgenic mouse lines. Non-transgenic littermates were used as wild-type controls (C57Bl/6 background). Mice were intracardially perfused 10 days post-injection and 50 μm vibratome sections of the brain were stained for GFP with immuno-fluorescence (Fluorescent GFP) and immuno-histochemistry (DAB GFP) with a polyclonal anti-GFP antibody (Chemicon). -: no GFP present; +: GFP positive staining present; NA: no data available.

Mouse Line	Lentiviral Injection	Fluorescent GFP	DAB GFP
Ub ^{G76V} -GFP/2	UBB ⁺¹	-	-
	UBB ^{+1K29,48R}	-	-
UBB ⁺¹ line 3413	Ub ^{G76V} -GFP	-	+
wild-type control	UBB ⁺¹	NA	-
	UBB ^{+1K29,48R}	NA	-
	Ub ^{G76V} -GFP	-	+

UBB⁺¹ accumulates in the neuronal population wherein the transgene is expressed. The relative UBB⁺¹ mRNA expression level in lines 3413 and 8630 is increased by ~3.5-fold compared to line 6663, whereas the difference on UBB⁺¹ protein level is much greater: the expression of UBB⁺¹ in line 8630 is ~14-fold higher than in line 6663. These data also indicate that UBB⁺¹ protein levels are regulated by a post-transcriptional mechanism and that UBB⁺¹ expression must first surpass a threshold level before accumulation commences, similar to the data obtained *in vitro* in Chapter 2. We also investigated if UBB⁺¹ also acts as an inhibitor of the UPS *in vivo* at high expression levels. The chymotryptic proteasome activity, measured in cortex homogenates of 3413 transgenic mice, indeed showed a modest significant decrease compared to wild-type mice. Also in the 8630 transgenic mice, the proteasome activity is decreased, as shown in Chapter 3.

To further explore these UPS inhibitory properties of UBB⁺¹ *in vivo*, we performed stereotactic injections of lentiviral UBB⁺¹ into the hippocampus of mice expressing the Ub^{G76V}-GFP reporter (Lindsten *et al.*, 2003). Conversely, we injected lentiviral Ub^{G76V}-GFP in line 3413 transgenic mice expressing neuronal UBB⁺¹. As a control, we injected lentiviral UBB⁺¹ with a double lysine mutation (UBB^{+1K29,48R}). UBB^{+1K29,48R} cannot be ubiquitinated and is thus not targeted to the proteasome to be degraded. The results of these experiments are summarized in Table 1.

In the Ub^{G76V}-GFP transgenic mice, injection of lentiviral UBB⁺¹ does not cause accumulation of the GFP reporter, suggesting that UBB⁺¹ does not inhibit the proteasome in these mice. However, lentiviral UBB⁺¹ expression is also not sufficient to cause accumulation of UBB⁺¹ protein in these mice (data not shown), indicating that UBB⁺¹ is expressed at low levels and degraded by the proteasome. When the Ub^{G76V}-GFP reporter is injected into UBB⁺¹ transgenic mice, one would expect that the reporter accumulates due

to the UBB⁺¹ induced proteasome inhibition. The results, as shown in Table 1, do not give conformation of decreased proteasome activity in the UBB⁺¹ transgenic mice. Using fluorescent staining techniques, no GFP accumulation was detected. When GFP was assessed with a immuno-histochemical staining, only a few GFP positive cells were detected. These sparsely present cells showed an astrocytic morphology, suggesting that the GFP accumulation was not attributable to UBB⁺¹, as UBB⁺¹ is only expressed in neurons. When the Ub^{G76V}-GFP reporter was injected in wild-type mice, also a few GFP positive cells were detected. Therefore, the GFP accumulation in these mice is most likely caused by the stereotactic injections leading to cellular stress and subsequent accumulation of the reporter, and not to inhibition of the proteasome by UBB⁺¹.

The absence of GFP reporter accumulation in the UBB⁺¹ mice can have several underlying causes. As mentioned above, the expression levels of UBB⁺¹ achieved with lentivirus could be insufficient to induce accumulation of the reporter. Also, the GFP reporter might not be sensitive enough to detect the modest decrease in UPS activity in the 3413 transgenic mice, as the reporter only accumulates at levels over 50% chymotryptic-like proteasome inhibition in cell lines (Dantuma *et al.*, 2000), whereas in the 3413 transgenic line only a ~20% UPS inhibition is observed. A third possibility is that, despite the reported broad tropism of lentivirus and its ability to transduce neuronal cells (Ehrengruber *et al.*, 2001), mostly astrocytes are transduced in the brain. This is further underscored by fact that the few GFP positive cells that were present showed an astrocytic morphology. Neuronal UPS inhibition induced by UBB⁺¹ would then not affect the turnover of astrocytic-expressed GFP reporter.

We further analyzed the inhibitory properties of UBB⁺¹ *in vivo* by crossing the 3413 transgenic line with GFP reporter line Ub^{G76V}-GFP/2 (Lindsten *et al.*, 2003). However, GFP reporter accumulation could not be observed in the double transgenic mice up to 530 days of age, even though UBB⁺¹ was expressed at high levels (fig. 1). One possible explanation could be that the reporter is not expressed in neuronal cells in this specific transgenic line (Ub^{G76V}-GFP/2), in spite of the CMV-β actin promoter, which should in principle ensure high levels of transgene expression in most cell types in the body, including neurons. In primary neurons of a comparable transgenic line (Ub^{G76V}-GFP/1), indeed GFP accumulation is present when proteasome activity is inhibited (Lindsten *et al.*, 2003). In the line used for these experiments, a slight alteration in the transgene expression pattern, caused by differences in the transgenic integration site, could affect the neuronal expression levels of the reporter. Preliminary studies with primary cortical neuron cultures derived from Ub^{G76V}-GFP/2 mice did not give conclusive evidence for expression of the GFP reporter in neuronal cells. Also in cortex slices of these mice, the morphology of GFP accumulating cells responsive to UPS inhibition showed an astrocytic morphology (shown in Chapter 2 and (F.M. de Vrij, unpublished results)). Alternatively, the GFP reporter might not be sensitive enough to detect a modest neuronal UPS inhibition *in vivo*.

This hypothesis is partly underscored by the observation that intracerebral inoculation of Ub^{G76V} -GFP transgenic mice with mouse scrapie, an inhibitor of UPS activity *in vitro*, does lead to accumulation of the Ub^{G76V} -GFP reporter in the brains of these mice, accompanied by intraneuronal ubiquitin deposits (Kristiansen *et al.*, 2007). However, the cell type wherein accumulation of the Ub^{G76V} -GFP reporter is present is not further specified in this study.

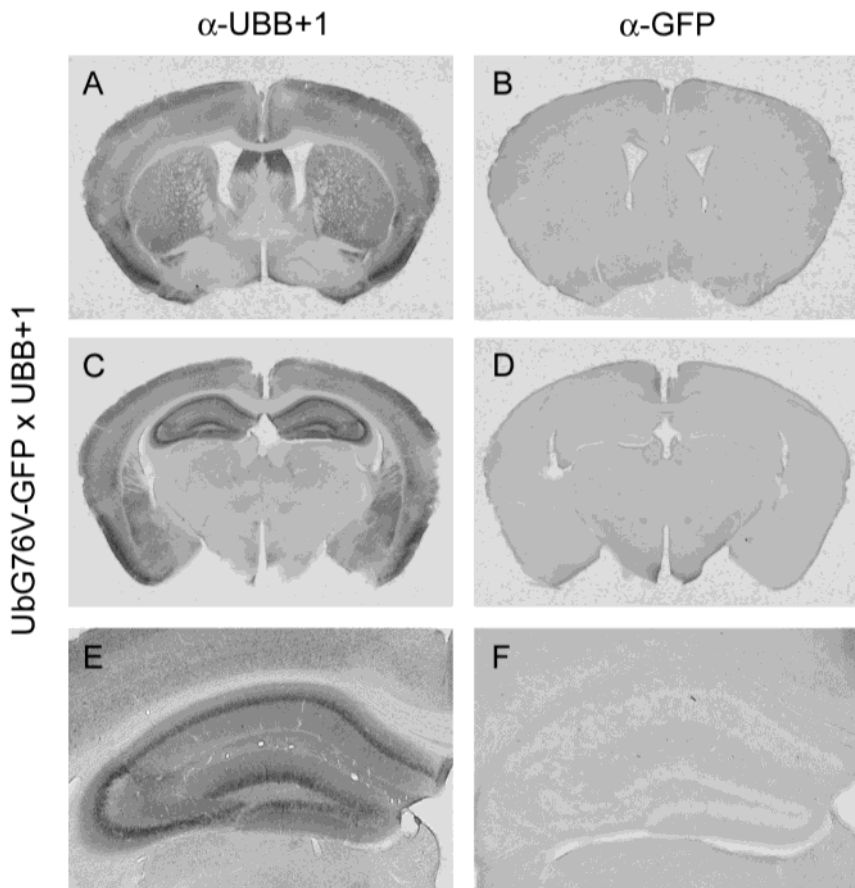


Figure 1 UPS inhibition is not detected in Ub^{G76V} -GFP \times UBB $^{+1}$ transgenic mice. Vibratome sections of a 529 day-old female Ub^{G76V} -GFP \times UBB $^{+1}$ line 3413 double transgenic mouse were immuno-histochemically stained using polyclonal antibodies against UBB $^{+1}$ (Ubi3, (Fischer *et al.*, 2003); left column) or GFP (Chemicon; right column). UBB $^{+1}$ is ubiquitously expressed in neurons in e.g. the cortex, striatum (A) and hippocampus (C, E). In the same animal, no GFP accumulation is present (B, D, F). Panels E and F are enlargements of panels C and D. These results indicate that a decrease in proteasome activity, as reflected by GFP accumulation, cannot be detected in the Ub^{G76V} -GFP \times UBB $^{+1}$ double transgenic mice.

Deubiquitination of UBB⁺¹

The UBB⁺¹ protein is ubiquitinated at two internal lysine residues, at amino acid positions 29 and 48. Ubiquitination at both these lysine residues is required to achieve maximal UBB⁺¹ induced proteasome inhibition, as the UBB⁺¹ double lysine mutant UBB^{+1K29,48R} has completely lost its UPS inhibitory properties (Lindsten *et al.*, 2002). Expression of the single lysine mutants UBB^{+1K29R} or UBB^{+1K48R} also results in decreased proteasomal degradation of UFD substrates, although to a lesser extent than UBB⁺¹. The capacity of the proteasome to degrade N-end rule substrates is not compromised following expression of UBB^{+1K29R} or UBB^{+1K48R}. Therefore, ubiquitination of UBB⁺¹ at both lysines is a prerequisite for maximal UPS inhibition to take place (Lindsten *et al.*, 2002).

As the ubiquitination state of UBB⁺¹ determines its UPS substrate as well as its UPS inhibitory properties, it is of importance to study the mechanisms by which Ub_x-UBB⁺¹ chains can be formed, e.g. by dissecting the nature of the ubiquitination enzymes involved in ubiquitinating UBB⁺¹. One of the E2 enzymes capable of ubiquitinating UBB⁺¹ is the ubiquitin-conjugating enzyme E2-25K/Hip-2. This E2 enzyme is capable of attaching preformed K48-linked ubiquitin chains to UBB⁺¹ *in vitro* (Lam *et al.*, 2000) and can ubiquitinate UBB⁺¹ in a rat neuroblastoma cell line (Song *et al.*, 2003). Possible additional involvement of specific ubiquitin E3 ligating enzymes or of the ubiquitin chain elongation factor E4 in the ubiquitination of UBB⁺¹ has so far not been studied.

However, the ubiquitination state of a substrate protein is governed by a tight balance between ubiquitination and deubiquitination. Deubiquitination is exerted by DUBs, a class of enzymes capable of cleaving ubiquitin moieties from a range of targets, including from ubiquitin chains and substrate proteins (reviewed by (Nijman *et al.*, 2005)). Aside from deubiquitinating target substrates, DUBs can also be active at the proteasome., e.g. to edit the length of the ubiquitin chain of the proteasome bound substrate (Lam *et al.*, 1997) or to delay substrate degradation (Hanna *et al.*, 2006). Also several 19S subunits show deubiquitinating activity themselves, including the Rpn11 subunit mediating ubiquitin chain release from substrates (Verma *et al.*, 2002; Yao and Cohen, 2002).

To further study the mechanisms behind the ubiquitination of UBB⁺¹, we aimed to identify the DUB involved in the deubiquitination of UBB⁺¹. We hypothesized that this DUB (or class of DUBs) would be able to cleave ubiquitin moieties from the ubiquitin chains attached to lysines K29 and K48 of UBB⁺¹, thereby decreasing the total amount of Ub_x-UBB⁺¹. Only when fully ubiquitinated, UBB⁺¹ is directed to the 26S proteasome and will subsequently cause UPS inhibition. By reducing the levels of Ub_x-UBB⁺¹, one could potentially alleviate the UPS inhibiting properties of UBB⁺¹ and possibly reverse the adverse affects of UBB⁺¹ expression. We anticipated to reveal the DUB(s) involved in this process using a DUB RNAi library screen (Brummelkamp *et al.*, 2003). This library contains a total of 200 vectors expressing short hairpin RNAs (shRNAs) targeting a total of

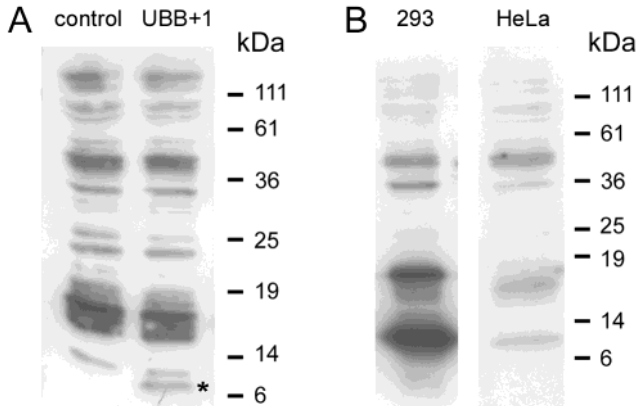


Figure 2 *UBB⁺¹* protein expression after transient transfection in HeLa Ub^{G76V}-GFP cells. A: After transient transfection of HeLa Ub^{G76V}-GFP cells with UBB⁺¹, Western blot analysis of cell lysates reveals a quantifiable band representing monomeric UBB⁺¹ (*, right lane). All other staining appears to be non-specific as it is also present in the cell transduced with empty vector (left lane). B: Western blot analysis of cell lysates of HeLa Ub^{G76V}-GFP reporter cells or 293 cells transiently transfected with UBB⁺¹ shows lower levels of UBB⁺¹ expression in HeLa cells than in 293 cells. Similar protein amounts are loaded for the 293 cells and HeLa cells, confirmed by Western blot for β -actin (not shown). UBB⁺¹ is detected with anti-UBB⁺¹ Ubi3 antibody.

50 human DUBs, with per DUB four pooled shRNA vectors targeting individual sequences (Brummelkamp *et al.*, 2003; Nijman *et al.*, 2005).

We used two complementary approaches to dissect the effect of knockdown of a DUB involved in deubiquitination of UBB⁺¹. After co-transfection of UBB⁺¹ and the knockdown library in a HeLa cell line expressing the Ub^{G76V}-GFP reporter, we measured Ub_x-UBB⁺¹ levels as well as UBB⁺¹ induced UPS inhibition. In the first approach, we set out to analyze the levels of Ub_x-UBB⁺¹ by Western blot using an antibody directed against the +1 C-terminus of UBB⁺¹. However, using this technique, only the levels of monomeric, free UBB⁺¹ could be accurately determined. The ratio of Ub_x-UBB⁺¹ to monomeric UBB⁺¹, potentially more informative of the level of UBB⁺¹ deubiquitination, could not be determined due to non-specific staining by the antibody at higher molecular weights (fig. 2A). Also, the expression levels of UBB⁺¹ after transient transfection were quite low in the HeLa Ub^{G76V}-GFP reporter cell line (compared to expression levels in e.g. 293 cells) and therefore difficult to detect (fig. 2B). The levels of monomeric ubiquitin were analyzed for 14 DUB knockdown vector pools by densitometry. The integrated optical density (IODs) of experimental samples co-transduced with UBB⁺¹ and a DUB knockdown pool were compared to those of controls, in which UBB⁺¹ was co-transduced with empty knockdown vector, using independent sample t-testing (fig. 3). No significant changes

were observed in any DUB knockdown pool.

In addition to the previously described approach using Western blot, we also attempted to identify a UBB⁺¹-associated DUB by measuring UBB⁺¹ induced UPS inhibition in the HeLa Ub^{G76V}-GFP reporter cell line. Theoretically, knockdown of a DUB which deubiquitinates UBB⁺¹ gives rise to higher levels of Ub_x-UBB⁺¹, which subsequently lead to increased UPS inhibition. This would be reflected in increased GFP accumulation in the Ub^{G76V}-GFP reporter cell line. We measured the percentage of GFP positive cells after co-transfection of UBB⁺¹ and the DUB knockdown vectors using flow cytometry. In this setup, we could not find a DUB which significantly increased the amount of GFP positive cells. Surprisingly, knockdown of 5 DUBs, encoding UCH-25, USP-9X, IsopeptidaseT-T, UCH-26 and USP-45, showed a significant decrease in the percentage of GFP fluorescent cells, indicating that knockdown of these specific DUBs decreased the UPS inhibitory capacity of UBB⁺¹ (fig. 4).

One of the underlying causes for this decrease in GFP fluorescence may be that these DUBs are involved in the deubiquitination of the Ub^{G76V}-GFP reporter, as Ub^{G76V}-GFP is ubiquitinated itself to be targeted to the proteasome (Dantuma *et al.*, 2000). When expression of these specific DUBs is decreased, ubiquitinated Ub^{G76V}-GFP levels increase. The ubiquitinated Ub^{G76V}-GFP is subsequently transported to the proteasome and degraded. Consequently, the total levels of GFP reporter in the cell are decreased and UPS

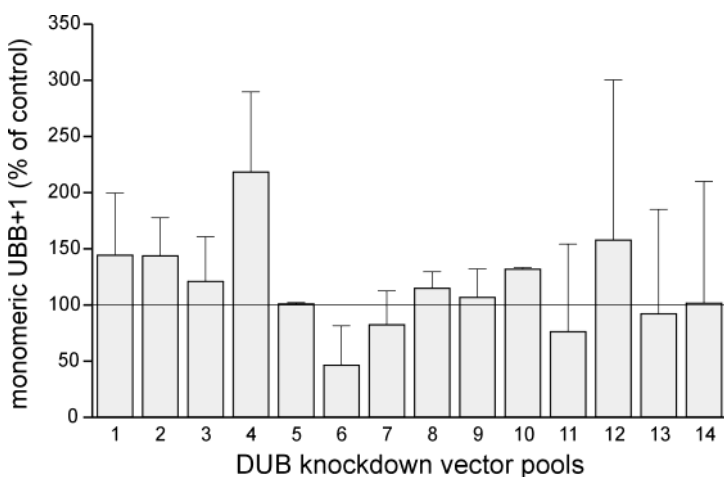


Figure 3 Effect of DUB knockdown on the levels of monomeric UBB⁺¹. The effect of DUB knockdown on levels of monomeric UBB⁺¹ was assessed by Western blot analysis. No significant effects of DUB knockdown on the levels of monomeric UBB⁺¹ are present. Control levels of monomeric UBB⁺¹ (measured by co-transduction of UBB⁺¹ with empty knockdown vector) are set at 100%. Experiment was performed in biological duplicate.

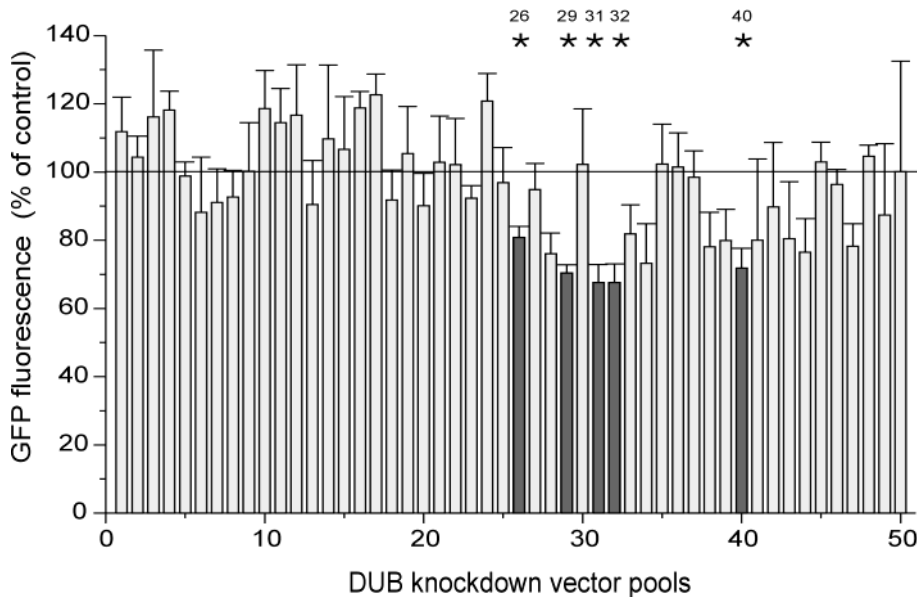


Figure 4 Effect of DUB knockdown on UBB⁺¹ induced proteasome inhibition. The effect of DUB knockdown on UBB⁺¹ induced proteasome inhibition was measured by quantification of the percentage green fluorescent cells in a HeLa Ub^{G76V}-GFP reporter cell line after transient transfection of UBB⁺¹. All DUBs are compared to the negative control (set at 100%). Knockdown of 5 DUBs results in significantly lower GFP fluorescence (*p<0.05). 26. UCH-25; 29. USP-9X; 31. IsopeptidaseT-T; 32. UCH-26; 40. USP-45. Experiment was performed in triplicate.

inhibition by UBB⁺¹ expression will result in lower levels of GFP fluorescence. In addition, Ub^{G76V}-GFP as well as UBB⁺¹ are UFD substrates for proteasomal degradation (Dantuma *et al.*, 2000; Lindsten *et al.*, 2002). Therefore, these two substrates might compete for common DUBs, which makes it difficult to accurately determine a DUB specific for UBB⁺¹. Another disadvantage of this setup, using UPS activity as a readout, is that a possible effect of DUB knockdown on the ubiquitination state of UBB⁺¹ first has to be translated to altered GFP fluorescence to be detected. This extra detection step might render this setup not sensitive enough to detect a target DUB for UBB⁺¹.

RNAi-mediated knockdown of a UBB⁺¹-associated DUB potentially enhances the toxicity of UBB⁺¹ by increasing the levels of Ub_x-UBB⁺¹. By decreasing the expression of one of the proteasome associated DUBs, also the turnover rate of UBB⁺¹ could be modified. Therefore, the ultimate effect of knockdown of a UBB⁺¹-modifying DUB is difficult to predict. For example, knockdown of a DUB editing the ubiquitin chain at the proteasome could increase degradation of UBB⁺¹ by reducing substrate rescue. On the other

hand, inhibiting release of the complete ubiquitin chain from UBB⁺¹ could prevent degradation of UBB⁺¹ and exert a detrimental effect by increasing the amount of Ub_x-UBB⁺¹ leading to proteasome inhibition and cellular toxicity. Further complicating the interpretation of the obtained results are the possible indirect effects of DUB knockdown on the levels of monomeric UBB⁺¹ via Ub_x-UBB⁺¹ induced proteasome inhibition. The knockdown of a DUB which deubiquitinates UBB⁺¹ can lead to a decrease of monomeric UBB⁺¹ and an increase of Ub_x-UBB⁺¹. Subsequently, these high levels of Ub_x-UBB⁺¹ will increase proteasome inhibition. UPS inhibition then in turn leads to an increase of monomeric UBB⁺¹ via a yet unknown mechanism (Lindsten *et al.*, 2002; Fischer *et al.*, 2003). Therefore, the overall effect of DUB knockdown on monomeric UBB⁺¹ levels is hard to dissect, as it depends on the function of the DUB within the UPS and on the relative contribution of above described indirect effects.

With both readouts of this focused RNAi screen, we could not identify a target DUB which is involved in deubiquitination of UBB⁺¹. The aforementioned drawbacks in the experimental setup could contribute to this result. Therefore, we cannot rule out the possibility that one of these 50 DUBs does affect UBB⁺¹ ubiquitination. Another possibility is that the DUB responsible for deubiquitination of UBB⁺¹ is not expressed in this library of 50 knockdown pools, as at the present moment approximately 100 human DUBs are known (Nijman *et al.*, 2005).

Proteasome inhibition and cognitive function

Post-translational modification of substrate proteins by ubiquitination is essential for cell viability, and more specific, plays an important role in intact neuronal function. During neuronal development, ubiquitin-mediated proteolysis is involved in axonal growth and axon guidance, growth cone formation and regulation of synaptic number and size to ensure correct formation of CNS connectivity (Hegde and Upadhyaya, 2007). In the adult nervous system, neuronal homeostasis is sustained via ubiquitin-dependent turnover of a broad range of substrate proteins. In addition, the UPS plays an important role in maintenance of established synaptic connections and development of new synapses. Regulation of synaptic plasticity relies in part on proteasome-mediated degradation of substrate proteins in the pre-synapse as well as the post-synapse. Therefore, UPS activity directly influences synaptic strength and transmission, two processes underlying learning and memory formation (reviewed by (DiAntonio and Hicke, 2004; Yi and Ehlers, 2007)). It is thus believed that protein modification by the UPS is likely to be involved in cognitive function.

Our results, as described in Chapter 3 and Chapter 5, indeed confirm that intact forebrain proteasome activity is required for optimal cognitive performance; in 3413 UBB⁺¹ transgenic mice, endogenous, life-long modest inhibition of the proteasome underlies a

decrease in cognitive ability. Notably, hippocampus-dependent spatial memory was affected in the Morris watermaze and in context-dependent Pavlovian fear conditioning, whereas spatial learning was unaffected. Also procedural (motor-) learning, as assessed in a rotarod paradigm, was not decreased due to UBB⁺¹ induced proteasome inhibition, indicating that chronic low-level UPS inhibition in these mice only affects a specific subset of memory-related processes. In other mouse models, a variety of other UPS alterations also induce deficits in cognition, as reviewed in Chapter 1. The molecular mechanism by which proteasome dysfunction in the UBB⁺¹ transgenic mice leads to spatial memory deficits is not fully understood. Our results suggest that high levels of UBB⁺¹ expression in the hippocampus are causative for the cognitive dysfunction in hippocampus-related memory tasks. In line with these observations, cognitive processes involving brain regions in which UBB⁺¹ expression is absent or only present at low levels, appear to be intact. These include motor learning and motor coordination, which are mainly mediated by the cerebellum (Hikosaka *et al.*, 2002; Goddyn *et al.*, 2006), an area devoid of UBB⁺¹ expression. Cued fear conditioning is also unaffected in the UBB⁺¹ transgenic mice. The amygdala, the brain region responsible for cued conditioning (Maren, 2001), indeed shows relatively low levels of UBB⁺¹ expression.

A caveat when interpreting these behavioral data is the fact that proteasome inhibition as well as the concomitant accumulation of ubiquitinated proteins was measured in cortex homogenates. It is possible that this inhibition is absent in other brain regions in spite of high levels of UBB⁺¹ expression, e.g. in the hippocampus. It is also conceivable that the extent of UPS inhibition is not directly correlated to the levels of UBB⁺¹ protein expression and therefore varies between different regions in the brain. To directly correlate the UPS inhibition to cognitive function, it would be sensible to also determine UPS activity in the hippocampus. This could be performed by measuring the turnover of small fluorogenic proteasome substrates, in a similar fashion as the previous measurements on cortex samples, described in Chapter 3. These fluorogenic substrates have as disadvantage that they readily diffuse into the 20S proteasome core and therefore also do not require ubiquitination to be targeted to the 26S proteasome. An alternative method to measure UPS activity would be monitoring the turnover of well-defined endogenous substrates of the UPS. In this case, the proteasome has to be fully assembled to degrade these substrates. One of these substrates is Ub₅DHFR, which can be ubiquitinated *in vitro* with a defined K48-linked ubiquitin chain (Lam *et al.*, 2005). Preliminary experiments measuring proteolytic activity in partially purified proteasomes of 3413 transgenic mice using Ub₅DHFR however gave inconclusive results. Proteasome activity can also be measured using activity-based small molecule proteasome-probes which directly reflect the activity of all individual proteolytic subunits of the proteasome (Berkers *et al.*, 2005) or by measuring the end-product of a dysfunctional UPS, i.e. the accumulation of K48-linked polyubiquitin chains (Bennett *et al.*, 2007). The latter can be performed using a mass-spectrometry

based assay which renders it possible to define the amount of polyubiquitin in mouse brain samples, as shown in a HD transgenic mouse model (Bennett *et al.*, 2007). As an alternative approach to correlate UPS inhibition to cognitive deficits in the 3413 transgenic mice, cortex-dependent memory could be examined by performing cortex-dependent behavioral tasks, e.g. examining fear extinction which depends on basal lateral amygdala function and medial pre-frontal cortex, although also hippocampal function might play a role in this process (reviewed by (Myers and Davis, 2007)).

One of the molecular mechanisms behind the UBB⁺¹ induced memory deficit could be a decrease in synaptic plasticity. One of the best studied cellular mechanisms that may underlie learning and memory is long-term potentiation (LTP). LTP reflects activity-dependent strengthening of neuronal synaptic connections (synaptic plasticity) and can be evoked by high frequency stimulation of afferent fibres. Indeed, recent evidence strongly suggests that LTP may underlie hippocampal-dependent learning and memory processes (Martin and Morris, 2002; Pastalkova *et al.*, 2006; Whitlock *et al.*, 2006). We therefore investigated synaptic plasticity in male 3413 UBB⁺¹ transgenic mice and wild-type littermates at the ages of 3, 6 and 9 months. The hippocampus is one of the main brain regions involved in memory formation (Martin and Morris, 2002) and hippocampus-dependent spatial memory is affected in UBB⁺¹ transgenic mice. Therefore, we chose to specifically examine hippocampus-dependent LTP. Hippocampal slices were stimulated using electrodes placed in the Schaffer collaterals to induce LTP and extracellular field excitatory post-synaptic potentials (fEPSPs) were recorded at synapses in the CA1 region (fig. 5A). In this region, UBB⁺¹ protein is highly expressed in the 3413 transgenic mice (fig. 5B).

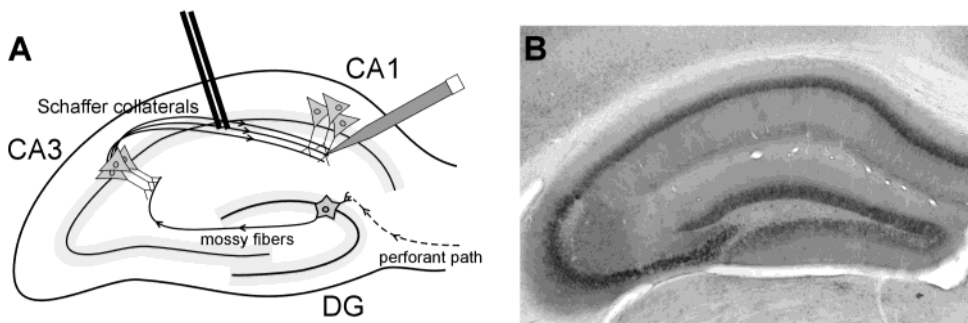


Figure 5 Schematic overview of electrophysiological measurements in UBB⁺¹ transgenic mice. A: Schematic overview of the fEPSP recording-setup in the mouse hippocampus. The stimulation electrode is placed in the Schaffer collaterals to stimulate action potentials. The recording electrode is positioned in the CA1 region of the hippocampus to record extracellular field potentials. B: Expression pattern of UBB⁺¹ protein in the hippocampus of a ~300 day old male 3413 UBB⁺¹ transgenic mouse visualized with anti-UBB⁺¹ antibody (Ubi3) immunostaining on a 50µm coronal vibratome section.

First, baseline synaptic properties were examined by determining the maximal slope and amplitude of the fEPSPs (fig. 6A), S value of the input-output graphs (fig. 6B) and the stimulation intensity needed to reach half maximal values for the slope as well as the amplitude (fig. 6C). Results show that the maximal slope and amplitude did not differ between wild-type and UBB⁺¹ transgenic mice at any age. The S value of the input-output curve was significantly altered for the slope in the 3 months old mice ($p=0.046$), this ef-

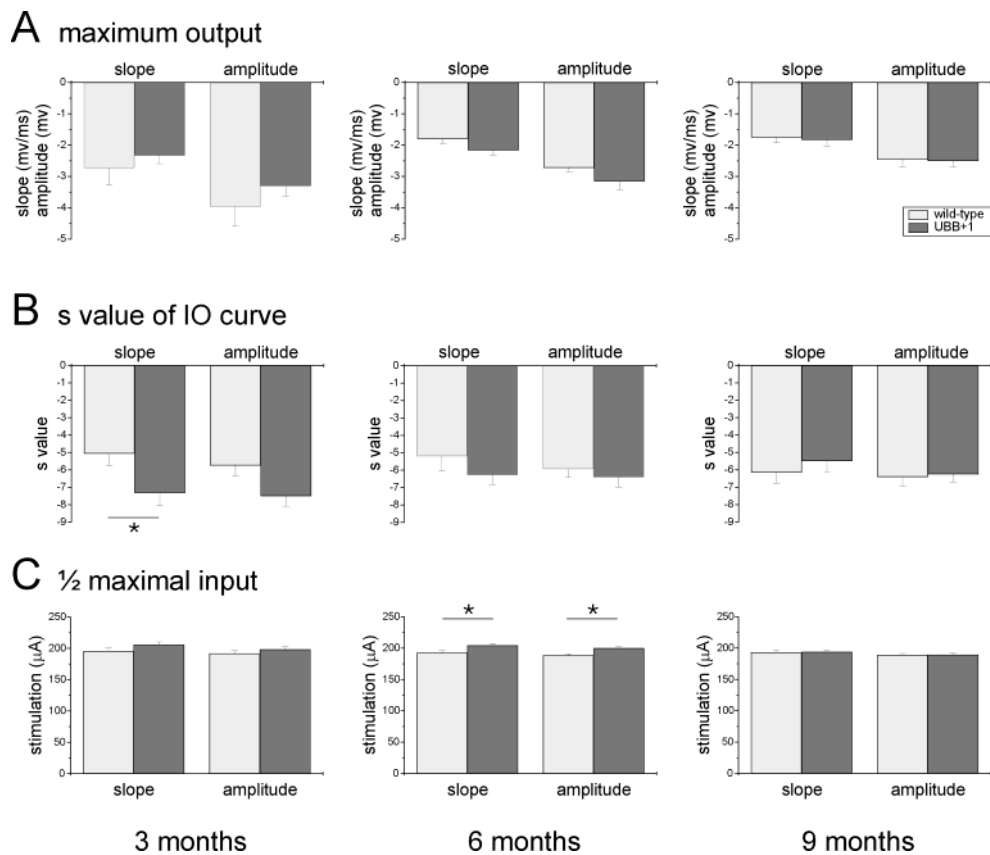


Figure 6 *Altered electrophysiological baseline properties in UBB⁺¹ transgenic mice.* Baseline electrophysiological properties in slices from the CA1 hippocampal area of 3413 UBB⁺¹ transgenic mice were examined at 3, 6 and 9 months of age. Input-output characteristics were examined by recording hippocampal field potentials (fEPSPs) A: Maximal output (slope and amplitude) after stimulation are plotted. No significant differences are observed. B: S-value of the input-output curve is determined. At 3 months of age, the S-value in the UBB⁺¹ transgenic mice is significantly decreased compared to wild-type mice C: half maximal stimulation input in UBB⁺¹ transgenic mice and wild-type littermates. At 6 months of age, UBB⁺¹ transgenic mice show a significant increase in half maximal stimulation intensity. This effect is not sustained at 9 months of age, * $p<0.05$.

fect was not present at 6 and 9 months of age.

The half maximum stimulation intensities were comparable between wild-type and transgenic mice at the ages of 3 and 9 months. However, at 6 months of age, the stimula-

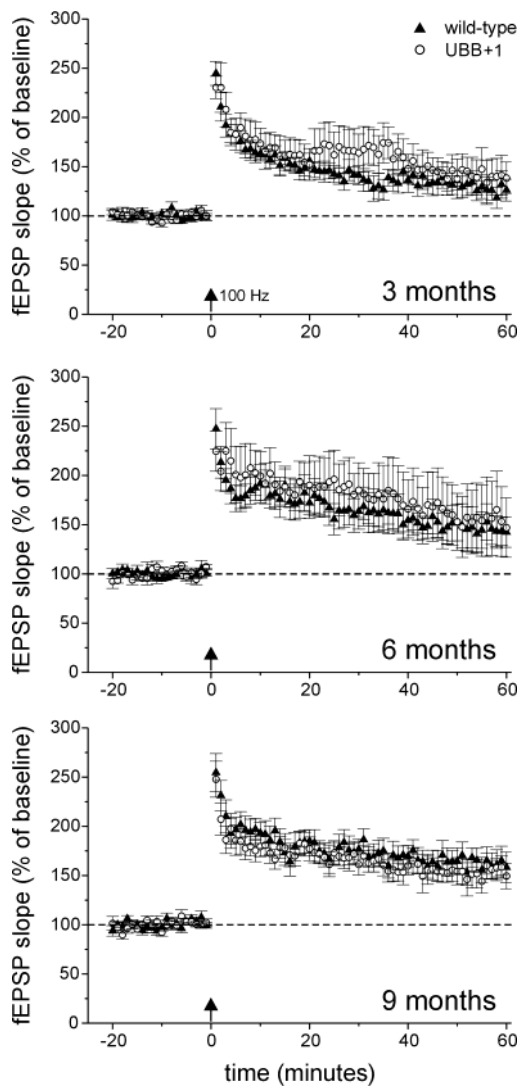


Figure 7 Hippocampal LTP is unaffected in UBB^{+1} transgenic mice. LTP (measured by fEPSP recordings in the hippocampus) was measured following a single 100 Hz stimulation at time point 0 and expressed as percentage of pre-stimulation baseline values. Induction of LTP as well as average LTP levels at the end of the recording after 60 minutes are not significantly different in UBB^{+1} 3413 transgenic mice (open circles) compared to wild-type mice (closed triangles) at 3, 6 and 9 months of age.

tion intensities needed to reach the half maximal values of the the slope and amplitude were significantly higher in the UBB^{+1} transgenic mice than in the wild-type mice ($p=0.020$ and $p=0.006$ respectively). In these mice, a higher stimulation intensity is needed in the transgenic mice to evoke a similar response as in the wild-type mice, indicating that the basal network connectivity is affected. However, this effect is not present at 9 months of age, therefore we cannot correlate this defect with the observed behavioral changes in the 3413 transgenic mice. Possible explanations for the changes in the basal synaptic responses observed at 6 months of age could include pre-synaptic deficits in neurotransmitter release, post-synaptic neurotransmitter uptake problems or other more basal structural changes in the neuronal network. However, additional studies on baseline synaptic transmission (mEPSCs, evoked AMPA receptor mediated synaptic responses) are required to fully investigate whether the mutation affects baseline synaptic transmission.

Then, baseline synaptic responses were recorded for 20 minutes to confirm stability of the recorded field potential. Next, high frequent stimulation (100 pulses @ 100 Hz) was delivered to induce LTP. When induction of hippocampal LTP was measured, results showed that LTP was not affected in the transgenic mice at the ages of 3, 6 and 9 months (fig. 7). Also the levels of LTP at 60 minutes after initial stimulation were comparable between transgenic and wild-type mice (fig. 7). Therefore, the spatial memory deficits in the 3413 transgenic mice at 9 months of age cannot be directly correlated to a decrease in LTP in the CA1 region of the hippocampus.

It could be that more subtle changes in synaptic plasticity underlie the observed memory deficits. In order to examine this, multiple stimulation paradigms should be applied to

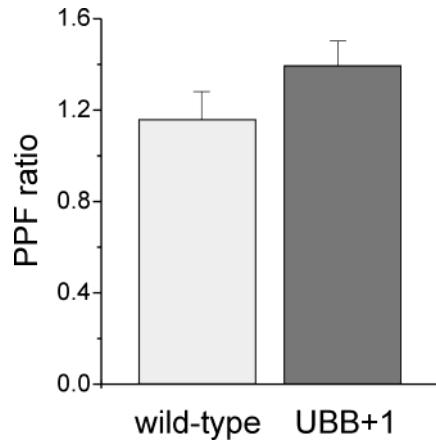


Figure 8 Hippocampal PPF is unaffected in UBB^{+1} transgenic mice. Comparison of the PPF ratio (ratio of the second to the first fEPSP) at the Shaffer-CA1 pyramidal cell synapses between wild-type mice and UBB^{+1} transgenic mice is not significantly different between the wild-type mice and UBB^{+1} transgenic mice.

examine whether the synaptic response function (threshold to evoke LTP or long-term depression (LTD)) is altered as a consequence of UBB⁺¹ expression (Mayford *et al.*, 1995). It is also possible that alterations in synaptic plasticity in other regions of the brain, for example the hippocampal dentate gyrus or the cortex, underlie the observed memory deficits. Preliminary results indeed show decreased LTP in the dentate gyrus of 3413 transgenic mice (van Leeuwen, Dennissen *et al.*, unpublished observations). An alternative approach would be to assess pre-synaptic function. Paired pulse facilitation (PPF) is a transient form of short term plasticity in which the evoked post-synaptic response to a second stimulation pulse is larger than the response to the shortly preceding pulse. PPF originates at the pre-synaptic side of the synaptic cleft (Zucker and Regehr, 2002). To examine pre-synaptic function in UBB⁺¹ transgenic mice, we performed PPF in the hippocampus of wild-type and transgenic mice. Preliminary results on 9-months-old mice show that PPF, expressed by the PPF ratio, is enhanced in the UBB⁺¹ transgenic mice (fig. 8). This effect is however not significant, which could in part be attributed to the low number of mice tested per genotype (n=3). Further experiments should be performed using a larger number of mice, to examine if these results are persistent. If so, the abnormal (enhanced) PPF ratio is indicative of defects in short-term synaptic plasticity in the UBB⁺¹ transgenic mice. Increases in PPF point to an increased neurotransmitter release in response to the second stimulus, caused by abnormal pre-synaptic accumulation of intracellular Ca²⁺ (Zucker and Regehr, 2002).

Although no direct effect of UBB⁺¹ induced UPS inhibition was detected on LTP in the CA1 region by means of electrophysiological measurements, UPS inhibition could still affect levels of substrate proteins at the synapse normally degraded by the proteasome. It has been shown that regulation of many synaptic proteins is dependent on proteasome activity levels in the post-synaptic density (e.g. (Ehlers, 2003; Yi and Ehlers, 2005)). No alterations were observed in levels of (ubiquitinated) synaptic proteins in cortex homogenates of UBB⁺¹ transgenic mice using proteomic analysis in previous experiments, as shown in Chapter 3. However, it is conceivable that subtle changes in the levels of these relatively low-abundance proteins were not detected using this proteomics approach. Additional studies on the protein expression levels of these substrates in brain sections of 3413 transgenic mice could give further clues to the mechanism behind the memory deficits.

In several other mouse models with genetic manipulation of the UPS, cognitive deficits are found, as summarized in Chapter 1. These deficits are not always accompanied by LTP deficits, similar to the 3413 transgenic mice. Mice deficient for the DUB Uchl3, exhibit decreased hippocampus dependent memory without decreases in LTP or PPF (Wood *et al.*, 2005). In mice lacking the DUB Usp14, differences in short-term synaptic plasticity point to disturbed pre-synaptic function. These mice did not show differences in LTP compared to wild-type littermates, comparable to the 3413 transgenic mice (Wilson *et al.*,

2002). Also other groups have shown that lower short-term synaptic plasticity can lead to context-dependent memory defects, without the need for LTP deficits (e.g. (Silva *et al.*, 1996)). The modest spatial memory deficits in the 3413 UBB⁺¹ transgenic mice, induced by inhibition of the UPS, could therefore have several underlying causes. With our current knowledge on the hippocampal electrophysiological properties of 3413 transgenic mice, deficiencies in basal synaptic transmission in combination with altered pre-synaptic function is one of the most promising candidates.

Cognitive decline is one of the most prominent and earliest clinical features of AD (Walsh and Selkoe, 2004). If UBB⁺¹ accumulation observed in the neuropathological hallmarks of AD patients can also directly affect cognitive function in human, analogous to the results we obtained in the UBB⁺¹ mouse model, is not known. However, inhibition of the UPS in general could be an underlying mechanism in AD contributing to the decline of cognitive functions. Indeed, changes in components of the UPS machinery are found in AD brain (Keller *et al.*, 2000; Lopez Salon *et al.*, 2000) and several AD-related proteins, including amyloid- β and tau, can diminish proteasomal activity (Gregori *et al.*, 1995; Keck *et al.*, 2003; Lopez Salon *et al.*, 2003).

Role of UBB⁺¹ in human pathology

Accumulation of the UBB⁺¹ protein was first discovered to occur in the neuropathological hallmarks of AD and DS (van Leeuwen *et al.*, 1998). Subsequently, UBB⁺¹ was found to be present in a broad selection of tauopathies, also including Pick disease (PiD) and fronto-temporal dementia (FTD) (Fischer *et al.*, 2003). UBB⁺¹ also is present in the ubiquitin-positive neuronal intranuclear inclusions in polyglutamine disease, including Huntington's Disease (HD) and spinocerebellar ataxia type-3 (SCA-3) (De Pril *et al.*, 2004). As the UPS is compromised in many of these neurodegenerative disorders, as reviewed in Chapter 1 of this thesis, the co-localization of UBB⁺¹ with ubiquitin positive pathology in these tauopathies led to the hypothesis that UBB⁺¹ accumulation serves as an endogenous marker for a decreased UPS function (Fischer *et al.*, 2003).

However, not all neurodegenerative diseases characterized by intracellular ubiquitin aggregates also show UBB⁺¹ accumulation. One of the most prominent examples hereof is Parkinson's Disease (PD), a movement disorder neuropathologically characterized by α -synuclein containing Lewy bodies. In PD, as well as in other synucleinopathies, UBB⁺¹ accumulation is absent (van Leeuwen *et al.*, 1998; Fischer *et al.*, 2003; Zouambia *et al.*, 2008). The differential presence of UBB⁺¹ in tauopathies and synucleinopathies might be attributed to the different roles the UPS plays in the aetiology of these diseases. First of all, ubiquitin-positive pathology in the intraneuronal tangles can be found in all cases of AD (Selkoe, 2001), in contrast to PD, where the ubiquitin containing Lewy bodies and Lewy neurites are present in the majority of cases, but are only sporadically found in cases

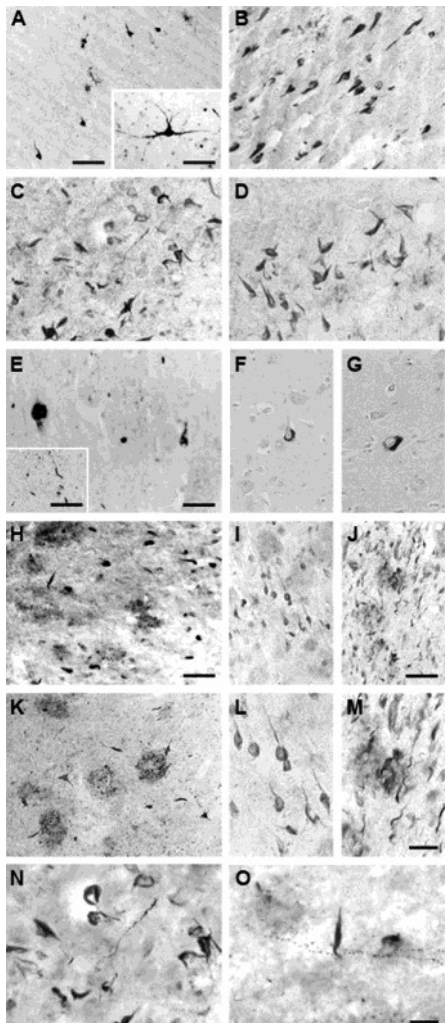


Figure 9 APP^{+1} and UBB^{+1} protein expression in various forms of AD. Expression of APP^{+1} (left row, A-K) and UBB^{+1} (right row, B-M) in 50 μ m thick vibratome and 6 μ m thick paraffin (E-G) sections of the hippocampus in various forms of AD. A, B: Sporadic form of AD. Insert in (A) shows an APP^{+1} positive neuron with beaded neurites in a young DS patient. These neurites are also present in the absence of any form of AD type of neuropathology and are also present in autosomal dominant cases of AD. C, D: Flemish type FAD (APP A692G). Note the beaded neurite. E to G: HCHWA-D type FAD (APP E693Q). Insert shows APP^{+1} positive dystrophic neurites. H to M: PSEN1 forms of FAD (PSEN1 I143T in H, I, K, L and PSEN1 Y115C in J, M). L and M are enlargements of I and J respectively. K: APP^{+1} is present in dystrophic neurites forming a neuritic plaque. N, O: Beaded neurites in autosomal dominant cases of AD, composed of a stack of five images. N is an Enlargement of C, O is an enlargement of H. Bar = 50 μ m (except in I, J, N, and O, bar = 25 μ m). Figure adapted from (van Leeuwen *et al.*, 2006).

of early-onset autosomal-recessive PD caused by a genetic mutation in the parkin gene (Savitt *et al.*, 2006). This points to a general role for the UPS in the pathogenesis of AD, whereas PD can also develop without the UPS being compromised. As UBB⁺¹ accumulation is an endogenous marker for decreased activity of the UPS, in AD it is conceivable that the general activity of the UPS is decreased and thus leads to UBB⁺¹ accumulation (Fischer *et al.*, 2003; Hol *et al.*, 2005). In PD, a partial, transient decrease in UPS activity might underlie the disease phenotype (Fornai *et al.*, 2005), although a general decrease in proteasome composition and activity has been shown in several studies using human PD patient material (McNaught *et al.*, 2006). This transient decrease of UPS function might initiate the accumulation of several proteins, including α -synuclein, however might not be sufficient to cause UBB⁺¹ to accumulate (Hol *et al.*, 2005). Another possibility is that in PD, a specific subset of proteins is not targeted to the UPS correctly and thus accumulate in the ubiquitin-positive aggregates. In support of this hypothesis, two genes causative of familial PD encode enzymes involved in ubiquitination (parkin) (Kitada *et al.*, 1998) and deubiquitination (UCHL1) (Leroy *et al.*, 1998) of substrate proteins. These affected components of the ubiquitin-proteasome machinery may thus induce accumulation of specific -ubiquitinated- substrate proteins, but not affect the turnover of UBB⁺¹ to such extent that UBB⁺¹ will accumulate (Hol *et al.*, 2005).

To find further evidence for a specific role of UBB⁺¹ in tauopathies, we next investigated if +1 proteins were also present in the ubiquitin-positive neuropathological hallmarks in early onset familial Alzheimer's disease (FAD) (van Leeuwen *et al.*, 2006). Although the majority of the AD cases are sporadic, at least three genes are recognized in which inherited autosomal mutations are causative for FAD. These genes include the APP and presenilin 1 and 2 (PSEN1 and PSEN2) genes (Van Broeckhoven, 1998). FAD is neuropathologically indistinguishable from sporadic AD, both characterized by extracellular amyloid- β (A β) plaques and intraneuronal tangles. To identify +1 protein accumulation in FAD, we performed an immuno-histochemical study on 50 μ m vibratome and 6 μ m paraffin sections of human brain material collected from FAD patients with a wide variety of APP and PS1 FAD mutations. APP⁺¹ as well as UBB⁺¹ could be clearly detected in a sporadic case of AD (fig. 9A-B), as reported previously (van Leeuwen *et al.*, 1998). In FAD, APP⁺¹ and UBB⁺¹ proteins were detected in the neuropathological hallmarks (neurofibrillary tangles and neuritic plaques) of patients carrying Flemish (fig. 9C-D) and Dutch type APP mutations (fig. 9E-G) and in various PSEN1 mutations (fig. 9H-M). In addition to the presence of the +1 frameshift proteins in FAD, we also found UBB⁺¹ and APP⁺¹ in other tauopathies, such as Pick Disease (PiD) and progressive supranuclear palsy (PSP) (fig. 10). We hypothesized that, as the presence of +1 proteins coincides with neuritic pathology in FAD individuals and other tauopathies (e.g. PiD and PSP), +1 proteins might contribute to the pathogenesis of FAD in concert with other mechanisms of neurodegeneration (van Leeuwen *et al.*, 2006).

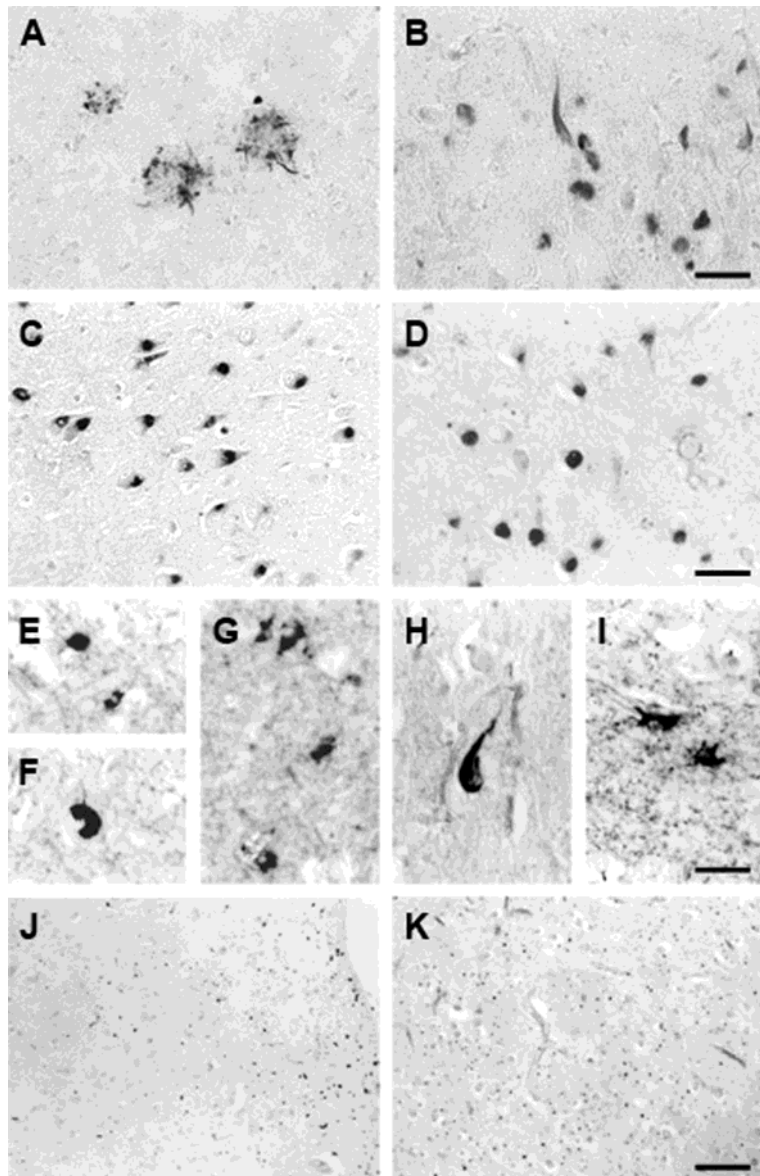


Figure 10 *APP^{+I} and UBB^{+I} protein expression in tauopathies.* Immunocytochemical localization of APP^{+I} (left row) and UBB^{+I} (right row) in various tauopathies. A, B: FTD cases. C, D: PiD, pyramidal cells of the CA1 region; note discrete localization outside nucleus. E-I: PSP, note reaction in globose tangles (\blacktriangle) and in tufted astrocytes (in G, at bottom, and I). J, K: Argyrophilic grain disease. Bar = 50 μ m (A and B), 25 μ m (C–I), and 60 μ m (J and K). Figure adapted from (van Leeuwen *et al.*, 2006).

We further studied the relation between FAD and UBB⁺¹ using a mouse model for AD, described in Chapter 6 of this thesis. We double crossed the 3413 UBB⁺¹ transgenic mouse line with an FAD mouse model expressing mutant APP (APPswe) and mutant PS1 (PS1dE9) (Jankowsky *et al.*, 2004) and analyzed the effect of UBB⁺¹ on amyloid deposition as well as the effect of APPswe and PS1dE9 expression on the levels of UBB⁺¹ accumulation. We demonstrated that amyloid- β deposition was significantly decreased in APPPS1xUBB⁺¹ triple transgenic mice compared to APPPS1 mice at 6 months of age, without alterations in UBB⁺¹ protein levels or in the age of onset of pathology. Similar results were observed in mice aged 9 months, however, results did not reach significance at this age, possibly due to the low number of mice that were available for analysis per genotype.

The results obtained in this study using triple transgenic mice imply that neuronal UBB⁺¹ expression and the consequent modest proteasome inhibition have a protective effect on the neuropathogenesis of AD. In this model, UBB⁺¹ expression does not contribute to AD disease pathogenesis as was suggested for human FAD patients (van Leeuwen *et al.*, 2006). Various different causes could underlie these seemingly opposing results. In the 3413 transgenic line, the level of UBB⁺¹ mRNA and protein expression increases up to postnatal day 22 and is expressed at high levels onwards, as shown in Chapter 3. This in contrast to human, where UBB⁺¹ mRNA is expressed at low levels during life and accumulation of the protein is only observed in aged or diseased subjects. In the 3413 transgenic mouse line, the highly expressed UBB⁺¹ protein acts actively as an inhibitor of proteasome activity instead of being foremost a marker for UPS inhibition as observed in human (Fischer *et al.*, 2003). The life-long modest inhibition of the UPS in the 3413 transgenic line could very well modify the effect of UBB⁺¹ on plaque deposition as UPS inhibition is known to affect several steps of A β processing, as described in Chapter 6. In addition, the time course of AD neuropathogenesis differs between the APPPS1 mouse model and human FAD. In APPPS1 mice, the first neuropathology can already be detected by 3 months of age, increasing up to 12 months of age. Recently, it was reported that in this mouse model of AD, the formation of new plaques is a very rapid process, with amyloid plaque formation occurring within 24 hours (Meyer-Luehmann *et al.*, 2008), whereas in human, the buildup of neuropathology is believed to be a gradual process taking several years. In human FAD patients, the neuropathology is indistinguishable from sporadic AD pathology, including the presence of amyloid pathology and neurofibrillary tangles, consisting of intraneuronal paired helical filaments (PHF) composed of hyperphosphorylated tau. However, tau pathology is absent in the APPPS1 mouse model (Jankowsky *et al.*, 2004), similar to other transgenic mouse models harboring FAD mutations in APP or APP and PS1 (McGowan *et al.*, 2006; Eriksen and Janus, 2007). It could be conceivable that the lack of intraneuronal tau influences the effect of UBB⁺¹ on amyloid deposition in the APPPS1 transgenic line. Further questions on the mechanism by which UBB⁺¹ could alle-

viate amyloid pathology arise when the localization of the involved proteins is taken into account; UBB⁺¹ and tau are intercellular proteins, whereas amyloid deposition in senile plaques is extracellular. In the UBB⁺¹xAPP^{S1} triple transgenic mice (see Chapter 6), further studies on the precise localization of these proteins might further elucidate the mechanism by which UBB⁺¹ can decrease plaque load. It could be possible that UPS inhibition by UBB⁺¹ influences the levels of intracellular A β , which is believed to be an important mediator of AD pathogenesis (LaFerla *et al.*, 2007). Furthermore, it has been reported that over-expression of DUBs (USP2 and USP21) results in increased amyloid beta secretion (patent application US26281699A1).

All the circumstances stated above could by themselves or combined underlie the differential effects of UBB⁺¹ protein accumulation on A β deposition in human FAD and a murine FAD model. However, it is also very well possible that the presence of UBB⁺¹ in human FAD patients is purely an effect of the disruption of intracellular homeostasis without directly contributing to disease pathogenesis. It could be that, once accumulated, UBB⁺¹ does have an additive effect on already present UPS dysfunction in FAD as well as other neurodegenerative diseases.

Concluding remarks

The etiology of many neurodegenerative diseases is multifactorial and the (relative) contribution of the genetic, cellular and environmental factors influencing disease progression is still unclear. Over the last two decades, increasing empirical evidence has established a central role for the UPS in the maintenance of intracellular homeostasis (Goldberg, 2005). In parallel, a decline in UPS activity has been recognized as a pivotal factor involved in the pathogenesis of many neurodegenerative disorders, including AD and HD (Ciechanover and Brundin, 2003). The results as reported in this thesis support the observation that intracellular protein degradation, mediated by the UPS, is essential for intact cellular function. Impairment of this system can directly lead to accumulation of ubiquitinated substrate proteins and eventually cause a decline in cognitive function, thereby contributing to disease progression.

The intrinsic properties of the mutant ubiquitin UBB⁺¹, accumulating in the ubiquitin-positive pathological hallmarks of a specific subset of neurodegenerative disorders, can provide us further insight in the role of UPS dysfunction in these diseases. As the UPS substrate UBB⁺¹ accumulates only when proteasomal activity is compromised, its presence in the neuropathological hallmarks of e.g. AD presents additional evidence that decreased UPS function can be one of the underlying factors contributing to disease progression. In this respect, the newly developed transgenic mouse lines expressing high levels of UBB⁺¹ provide us with useful models to study the effects of chronic low-level endogenous proteasome inhibition *in vivo*. By employing these transgenic lines in future experiments,

we can obtain more understanding of the role of UPS function in a multitude of physiological parameters in health and disease.

References

References

- Adams, J. (2004). "The development of proteasome inhibitors as anticancer drugs." *Cancer Cell* 5(5): 417-21.
- Adams, J., Behnke, M., Chen, S., Cruickshank, A.A., Dick, L.R., Grenier, L., Klunder, J.M., Ma, Y.T., Plumondon, L. and Stein, R.L. (1998). "Potent and selective inhibitors of the proteasome: dipeptidyl boronic acids." *Bioorg Med Chem Lett* 8(4): 333-8.
- Aksenov, M.Y., Aksenova, M.V., Carney, J.M. and Butterfield, D.A. (1997). "Oxidative modification of glutamine synthetase by amyloid beta peptide." *Free Radic Res* 27(3): 267-81.
- Albrecht, U., Sutcliffe, J.S., Cattanach, B.M., Beechey, C.V., Armstrong, D., Eichele, G. and Beaudet, A.L. (1997). "Imprinted expression of the murine Angelman syndrome gene, Ube3a, in hippocampal and Purkinje neurons." *Nat Genet* 17(1): 75-8.
- Almeida, C.G., Takahashi, R.H. and Gouras, G.K. (2006). "Beta-amyloid accumulation impairs multivesicular body sorting by inhibiting the ubiquitin-proteasome system." *J Neurosci* 26(16): 4277-88.
- Amerik, A.Y. and Hochstrasser, M. (2004). "Mechanism and function of deubiquitinating enzymes." *Biochim Biophys Acta* 1695(1-3): 189-207.
- Anderson, C., Crimmins, S., Wilson, J.A., Korbel, G.A., Ploegh, H.L. and Wilson, S.M. (2005). "Loss of Usp14 results in reduced levels of ubiquitin in ataxia mice." *J Neurochem* 95(3): 724-31.
- Arrasate, M., Mitra, S., Schweitzer, E.S., Segal, M.R. and Finkbeiner, S. (2004). "Inclusion body formation reduces levels of mutant huntingtin and the risk of neuronal death." *Nature* 431(7010): 805-10.
- Bach, M.E., Barad, M., Son, H., Zhuo, M., Lu, Y.F., Shih, R., Mansuy, I., Hawkins, R.D. and Kandel, E.R. (1999). "Age-related defects in spatial memory are correlated with defects in the late phase of hippocampal long-term potentiation in vitro and are attenuated by drugs that enhance the cAMP signaling pathway." *Proc Natl Acad Sci U S A* 96(9): 5280-5.
- Barondes, S.H. and Cohen, H.D. (1967). "Delayed and sustained effect of acetoxy cycloheximide on memory in mice." *Proc Natl Acad Sci U S A* 58(1): 157-64.
- Beal, F. and Lang, A. (2006). "The proteasomal inhibition model of Parkinson's disease: "Boon or bust""? *Ann Neurol* 60(2): 158-61.
- Bence, N.F., Sampat, R.M. and Kopito, R.R. (2001). "Impairment of the ubiquitin-proteasome system by protein aggregation." *Science* 292(5521): 1552-5.
- Bennett, E.J., Bence, N.F., Jayakumar, R. and Kopito, R.R. (2005). "Global impairment of the ubiquitin-proteasome system by nuclear or cytoplasmic protein aggregates precedes inclusion body formation." *Mol Cell* 17(3): 351-65.
- Bennett, E.J., Shaler, T.A., Woodman, B., Ryu, K.Y., Zaitseva, T.S., Becker, C.H., Bates, G.P., Schulman, H. and Kopito, R.R. (2007). "Global changes to the ubiquitin system in Huntington's disease." *Nature* 448(7154): 704-8.
- Bergman, A., Hansson, E.M., Pursglove, S.E., Farmery, M.R., Lannfelt, L., Lendahl, U., Lundkvist, J. and Naslund, J. (2004). "Pen-2 is sequestered in the endoplasmic reticulum and subjected to ubiquitylation and proteasome-mediated degradation in the absence of presenilin." *J Biol Chem* 279(16): 16744-53.
- Berke, S.J., Chai, Y., Marrs, G.L., Wen, H. and Paulson, H.L. (2005). "Defining the role of ubiquitin-interacting motifs in the polyglutamine disease protein, ataxin-3." *J Biol Chem* 280(36): 32026-34.
- Berkers, C.R., Verdoes, M., Lichtman, E., Fiebiger, E., Kessler, B.M., Anderson, K.C., Ploegh, H.L., Ovaa, H. and Galardy, P.J. (2005). "Activity probe for *in vivo* profiling of the specificity of proteasome inhibitor bortezomib." *Nat Methods* 2(5): 357-62.
- Bertram, L. and Tanzi, R.E. (2005). "The genetic epidemiology of neurodegenerative disease." *J Clin Invest* 115(6): 1449-57.
- Bett, J.S., Goellner, G.M., Woodman, B., Pratt, G., Rechsteiner, M. and Bates, G.P. (2006). "Proteasome impairment does not contribute to pathogenesis in R6/2 Huntington's disease mice: exclusion of proteasome activator REGgamma as a therapeutic target." *Hum Mol Genet* 15(1): 33-44.
- Bi, X., Yong, A.P., Zhou, J., Ribak, C.E. and Lynch, G. (2001). "Rapid induction of intraneuronal neurofibrillary tangles in apolipoprotein E-deficient mice." *Proc Natl Acad Sci USA* 98(15): 8832-37.
- Borodovsky, A., Kessler, B.M., Casagrande, R., Overkleef, H.S., Wilkinson, K.D. and Ploegh, H.L. (2001). "A novel active site-directed probe specific for deubiquitylating enzymes reveals proteasome association of USP14." *Embo J* 20(18): 5187-96.

REFERENCES

- Bowman, A.B., Yoo, S.Y., Dantuma, N.P. and Zoghbi, H.Y. (2005). "Neuronal dysfunction in a polyglutamine disease model occurs in the absence of ubiquitin-proteasome system impairment and inversely correlates with the degree of nuclear inclusion formation." *Hum Mol Genet* 14(5): 679-91.
- Braak, H., Del Tredici, K., Rub, U., de Vos, R.A., Jansen Steur, E.N. and Braak, E. (2003). "Staging of brain pathology related to sporadic Parkinson's disease." *Neurobiol Aging* 24(2): 197-211.
- Bradford, M.M. (1976). "A rapid and sensitive method for the quantitation of microgram quantities of protein utilizing the principle of protein-dye binding." *Anal Biochem* 72: 248-54.
- Brown, I.R., Rush, S. and Ivy, G.O. (1989). "Induction of a heat shock gene at the site of tissue injury in the rat brain." *Neuron* 2(6): 1559-64.
- Brummelkamp, T.R., Nijman, S.M., Dirac, A.M. and Bernards, R. (2003). "Loss of the cylindromatosis tumour suppressor inhibits apoptosis by activating NF-kappaB." *Nature* 424(6950): 797-801.
- Burnett, B., Li, F. and Pittman, R.N. (2003). "The polyglutamine neurodegenerative protein ataxin-3 binds polyubiquitylated proteins and has ubiquitin protease activity." *Hum Mol Genet* 12(23): 3195-205.
- Burnett, B.G. and Pittman, R.N. (2005). "The polyglutamine neurodegenerative protein ataxin 3 regulates aggresome formation." *Proc Natl Acad Sci U S A* 102(12): 4330-5.
- Burt, A.M. (1980). "Morphologic abnormalities in the postnatal differentiation of CA1 pyramidal cells and granule cells in the hippocampal formation of the ataxic mouse." *Anat Rec* 196(1): 61-9.
- Cai, H., Wang, Y., McCarthy, D., Wen, H., Borchelt, D.R., Price, D.L. and Wong, P.C. (2001). "BACE1 is the major beta-secretase for generation of Abeta peptides by neurons." *Nat Neurosci* 4(3): 233-4.
- Campbell, D.S. and Holt, C.E. (2001). "Chemotropic responses of retinal growth cones mediated by rapid local protein synthesis and degradation." *Neuron* 32(6): 1013-26.
- Caroni, P. (1997). "Overexpression of growth-associated proteins in the neurons of adult transgenic mice." *J Neurosci Methods* 71: 3-9.
- Carrard, G., Bulteau, A.L., Petropoulos, I. and Friguet, B. (2002). "Impairment of proteasome structure and function in aging." *Int J Biochem Cell Biol* 34(11): 1461-74.
- Castegna, A., Aksenov, M., Aksenova, M., Thongboonkerd, V., Klein, J.B., Pierce, W.M., Booze, R., Markesberry, W.R. and Butterfield, D.A. (2002). "Proteomic identification of oxidatively modified proteins in Alzheimer's disease brain. Part I: creatine kinase BB, glutamine synthase, and ubiquitin carboxy-terminal hydrolase L-1." *Free Radic Biol Med* 33(4): 562-71.
- Castegna, A., Aksenov, M., Thongboonkerd, V., Klein, J.B., Pierce, W.M., Booze, R., Markesberry, W.R. and Butterfield, D.A. (2002). "Proteomic identification of oxidatively modified proteins in Alzheimer's disease brain. Part II: dihydropyrimidinase-related protein 2, alpha-enolase and heat shock cognate 71." *J Neurochem* 82(6): 1524-32.
- Castegna, A., Thongboonkerd, V., Klein, J.B., Lynn, B., Markesberry, W.R. and Butterfield, D.A. (2003). "Proteomic identification of nitrated proteins in Alzheimer's disease brain." *J Neurochem* 85(6): 1394-401.
- Cemal, C.K., Carroll, C.J., Lawrence, L., Lowrie, M.B., Ruddle, P., Al-Mahdawi, S., King, R.H., Pook, M.A., Huxley, C. and Chamberlain, S. (2002). "YAC transgenic mice carrying pathological alleles of the MJD1 locus exhibit a mild and slowly progressive cerebellar deficit." *Hum Mol Genet* 11(9): 1075-94.
- Chain, D.G., Casadio, A., Schacher, S., Hegde, A.N., Valbrun, M., Yamamoto, N., Goldberg, A.L., Bartsch, D., Kandel, E.R. and Schwartz, J.H. (1999). "Mechanisms for generating the autonomous cAMP-dependent protein kinase required for long-term facilitation in Aplysia." *Neuron* 22(1): 147-56.
- Chang, Y.F., Imam, J.S. and Wilkinson, M.F. (2007). "The nonsense-mediated decay RNA surveillance pathway." *Annu Rev Biochem* 76: 51-74.
- Chen, M., Clark, R.S., Kochanek, P.M., Chen, J., Schiding, J.K., Stetler, R.A., Simon, R.P. and Graham, S.H. (1998). "72-kDa heat shock protein and mRNA expression after controlled cortical impact injury with hypoxemia in rats." *J Neurotrauma* 15(3): 171-81.
- Cheron, G., Servais, L., Wagstaff, J. and Dan, B. (2005). "Fast cerebellar oscillation associated with ataxia in a mouse model of Angelman syndrome." *Neuroscience* 130(3): 631-7.
- Chew, C.S., Parente, J.A., Jr., Chen, X., Chaponnier, C. and Cameron, R.S. (2000). "The LIM and SH3 domain-containing protein, lasp-1, may link the cAMP signaling pathway with dynamic membrane restructuring activities in ion transporting epithelia." *J Cell Sci* 113 (Pt 11): 2035-45.

- Choi, J., Forster, M.J., McDonald, S.R., Weintraub, S.T., Carroll, C.A. and Gracy, R.W. (2004). "Proteomic identification of specific oxidized proteins in ApoE-knockout mice: relevance to alzheimer's disease." *Free Radic Biol Med* 36(9): 1155-62.
- Choi, J., Levey, A.I., Weintraub, S.T., Rees, H.D., Gearing, M., Chin, L.S. and Li, L. (2004). "Oxidative modifications and down-regulation of ubiquitin carboxyl-terminal hydrolase L1 associated with idiopathic Parkinson's and Alzheimer's diseases." *J Biol Chem* 279(13): 13256-64.
- Choi, T., Huang, M., Gorman, C. and Jaenisch, R. (1991). "A generic intron increases gene expression in transgenic mice." *Mol Cell Biol* 11(6): 3070-74.
- Christie, G., Markwell, R.E., Gray, C.W., Smith, L., Godfrey, F., Mansfield, F., Wadsworth, H., King, R., McLaughlin, M., Cooper, D.G., Ward, R.V., Howlett, D.R., Hartmann, T., Lichtenthaler, S.F., Beyreuther, K., Underwood, J., Gribble, S.K., Cappai, R., Masters, C.L., Tamaoka, A., Gardner, R.L., Rivett, A.J., Karran, E.H. and Allsop, D. (1999). "Alzheimer's disease: correlation of the suppression of beta-amyloid peptide secretion from cultured cells with inhibition of the chymotrypsin-like activity of the proteasome." *J Neurochem* 73(1): 195-204.
- Chung, K.K., Zhang, Y., Lim, K.L., Tanaka, Y., Huang, H., Gao, J., Ross, C.A., Dawson, V.L. and Dawson, T.M. (2001). "Parkin ubiquitinates the alpha-synuclein-interacting protein, synphilin-1: implications for Lewy-body formation in Parkinson disease." *Nat Med* 7(10): 1144-50.
- Ciechanover, A. and Brundin, P. (2003). "The ubiquitin proteasome system in neurodegenerative diseases: sometimes the chicken, sometimes the egg." *Neuron* 40(2): 427-46.
- Ciechanover, A., Heller, H., Elias, S., Haas, A.L. and Hershko, A. (1980). "ATP-dependent conjugation of reticulocytote proteins with the polypeptide required for protein degradation." *Proc Natl Acad Sci U S A* 77(3): 1365-8.
- Colas, D., Wagstaff, J., Fort, P., Salvert, D. and Sarda, N. (2005). "Sleep disturbances in Ube3a maternal-deficient mice modeling Angelman syndrome." *Neurobiol Dis* 20(2): 471-8.
- Coleman, P., Federoff, H. and Kurlan, R. (2004). "A focus on the synapse for neuroprotection in Alzheimer disease and other dementias." *Neurology* 63(7): 1155-62.
- Costa, R.M., Cohen, D. and Nicolelis, M.A. (2004). "Differential corticostriatal plasticity during fast and slow motor skill learning in mice." *Curr Biol* 14(13): 1124-34.
- Costa, R.M., Honjo, T. and Silva, A.J. (2003). "Learning and memory deficits in Notch mutant mice." *Curr Biol* 13(15): 1348-54.
- Crawley, J.N. (1999). "Behavioral phenotyping of transgenic and knockout mice: experimental design and evaluation of general health, sensory functions, motor abilities, and specific behavioral tests." *Brain Res* 835(1): 18-26.
- Crawley, J.N., Belknap, J.K., Collins, A., Crabbe, J.C., Frankel, W., Henderson, N., Hitzemann, R.J., Maxson, S.C., Miner, L.L., Silva, A.J., Wehner, J.M., Wynshaw-Boris, A. and Paylor, R. (1997). "Behavioral phenotypes of inbred mouse strains: implications and recommendations for molecular studies." *Psychopharmacology (Berl)* 132(2): 107-24.
- Crimmins, S., Jin, Y., Wheeler, C., Huffman, A.K., Chapman, C., Dobrunz, L.E., Levey, A., Roth, K.A., Wilson, J.A. and Wilson, S.M. (2006). "Transgenic rescue of ataxia mice with neuronal-specific expression of ubiquitin-specific protease 14." *J Neurosci* 26(44): 11423-31.
- Cripps, D., Thomas, S.N., Jeng, Y., Yang, F., Davies, P. and Yang, A.J. (2006). "Alzheimer disease-specific conformation of hyperphosphorylated paired helical filament-Tau is polyubiquitinated through Lys-48, Lys-11, and Lys-6 ubiquitin conjugation." *J Biol Chem* 281(16): 10825-38.
- Cyr, D.M., Hohfeld, J. and Patterson, C. (2002). "Protein quality control: U-box-containing E3 ubiquitin ligases join the fold." *Trends Biochem Sci* 27(7): 368-75.
- D'Amato, C.J. and Hicks, S.P. (1965). "Neuropathologic alterations in the ataxia (paralytic) mouse." *Arch Pathol* 80(6): 604-12.
- Dahlmann, B., Ruppert, T., Kuehn, L., Merforth, S. and Kloetzel, P.M. (2000). "Different proteasome subtypes in a single tissue exhibit different enzymatic properties." *J Mol Biol* 303(5): 643-53.
- Dai, Q., Zhang, C., Wu, Y., McDonough, H., Whaley, R.A., Godfrey, V., Li, H.H., Madamanchi, N., Xu, W., Neckers, L., Cyr, D. and Patterson, C. (2003). "CHIP activates HSF1 and confers protection against apoptosis and cellular stress." *Embo J* 22(20): 5446-58.
- Dantuma, N.P., Lindsten, K., Glas, R., Jellne, M. and Masucci, M.G. (2000). "Short-lived green fluorescent proteins for quantifying ubiquitin/proteasome-dependent proteolysis in living cells." *Nat Biotechnol* 18(5): 538-43.

REFERENCES

- David, D.C., Ittner, L.M., Gehrig, P., Nergenau, D., Shepherd, C., Halliday, G. and Gotz, J. (2006). "Beta-amyloid treatment of two complementary P301L tau-expressing Alzheimer's disease models reveals similar deregulated cellular processes." *Proteomics* 6(24): 6566-77.
- David, D.C., Layfield, R., Serpell, L., Narain, Y., Goedert, M. and Spillantini, M.G. (2002). "Proteasomal degradation of tau protein." *J Neurochem* 83(1): 176-85.
- Day, I.N. and Thompson, R.J. (1984). "Levels of immunoreactive aldolase C, creatine kinase-BB, neuronal and non-neuronal enolase, and 14-3-3 protein in circulating human blood cells." *Clin Chim Acta* 136(2-3): 219-28.
- De Pril, R., Fischer, D.F., Maat-Schieman, M.L., Hobo, B., De Vos, R.A., Brunt, E.R., Hol, E.M., Roos, R.A. and Van Leeuwen, F.W. (2004). "Accumulation of aberrant ubiquitin induces aggregate formation and cell death in polyglutamine diseases." *Hum Mol Genet* 13(16): 1803-13.
- de Pril, R., Fischer, D.F., Roos, R.A. and van Leeuwen, F.W. (2007). "Ubiquitin-conjugating enzyme E2-25K increases aggregate formation and cell death in polyglutamine diseases." *Mol Cell Neurosci* 34 (1): 10-9.
- de Vrij, F.M., Fischer, D.F., van Leeuwen, F.W. and Hol, E.M. (2004). "Protein quality control in Alzheimer's disease by the ubiquitin proteasome system." *Prog Neurobiol* 74(5): 249-70.
- De Vrij, F.M., Sluijs, J.A., Gregori, L., Fischer, D.F., Hermens, W.T., Goldgaber, D., Verhaagen, J., Van Leeuwen, F.W. and Hol, E.M. (2001). "Mutant ubiquitin expressed in Alzheimer's disease causes neuronal death." *Faseb J* 15(14): 2680-8.
- Deveraux, Q., Ustrell, V., Pickart, C. and Rechsteiner, M. (1994). "A 26 S protease subunit that binds ubiquitin conjugates." *J Biol Chem* 269(10): 7059-61.
- DiAntonio, A. and Hicke, L. (2004). "Ubiquitin-dependent regulation of the synapse." *Annu Rev Neurosci* 27: 223-46.
- Diaz-Hernandez, M., Hernandez, F., Martin-Aparicio, E., Gomez-Ramos, P., Moran, M.A., Castano, J.G., Ferrer, I., Avila, J. and Lucas, J.J. (2003). "Neuronal induction of the immunoproteasome in Huntington's disease." *J Neurosci* 23(37): 11653-61.
- Diaz-Hernandez, M., Valera, A.G., Moran, M.A., Gomez-Ramos, P., Alvarez-Castelao, B., Castano, J.G., Hernandez, F. and Lucas, J.J. (2006). "Inhibition of 26S proteasome activity by huntingtin filaments but not inclusion bodies isolated from mouse and human brain." *J Neurochem* 98(5): 1585-96.
- Dick, L.R., Cruikshank, A.A., Grenier, L., Melandri, F.D., Nunes, S.L. and Stein, R.L. (1996). "Mechanistic studies on the inactivation of the proteasome by lactacystin: a central role for clasto-lactacystin beta-lactone." *J Biol Chem* 271(13): 7273-6.
- Dickey, C.A., Yue, M., Lin, W.L., Dickson, D.W., Dunmore, J.H., Lee, W.C., Zehr, C., West, G., Cao, S., Clark, A.M., Caldwell, G.A., Caldwell, K.A., Eckman, C., Patterson, C., Hutton, M. and Petrucelli, L. (2006). "Deletion of the ubiquitin ligase CHIP leads to the accumulation, but not the aggregation, of both endogenous phospho- and caspase-3-cleaved tau species." *J Neurosci* 26(26): 6985-96.
- Ding, Q., Bruce-Keller, A.J., Chen, Q. and Keller, J.N. (2004). "Analysis of gene expression in neural cells subject to chronic proteasome inhibition." *Free Radic Biol Med* 36(4): 445-55.
- Ding, Q., Dimayuga, E., Markesberry, W.R. and Keller, J.N. (2006). "Proteasome inhibition induces reversible impairments in protein synthesis." *Faseb J* 20(8): 1055-63.
- Ding, Q., Dimayuga, E., Martin, S., Bruce-Keller, A.J., Nukala, V., Cuervo, A.M. and Keller, J.N. (2003). "Characterization of chronic low-level proteasome inhibition on neural homeostasis." *J Neurochem* 86(2): 489-97.
- Ding, Q., Markesberry, W.R., Chen, Q., Li, F. and Keller, J.N. (2005). "Ribosome dysfunction is an early event in Alzheimer's disease." *J Neurosci* 25(40): 9171-5.
- Ding, Q., Martin, S., Dimayuga, E., Bruce-Keller, A.J. and Keller, J.N. (2006). "LMP2 knock-out mice have reduced proteasome activities and increased levels of oxidatively damaged proteins." *Antioxid Redox Signal* 8(1-2): 130-5.
- Ding, W.X., Ni, H.M., Gao, W., Yoshimori, T., Stoltz, D.B., Ron, D. and Yin, X.M. (2007). "Linking of autophagy to ubiquitin-proteasome system is important for the regulation of endoplasmic reticulum stress and cell viability." *Am J Pathol* 171(2): 513-24.
- Doll, D., Sarikas, A., Krajcik, R. and Zolk, O. (2007). "Proteomic expression analysis of cardiomyocytes subjected to proteasome inhibition." *Biochem Biophys Res Commun* 353(2): 436-42.

- Donaldson, K.M., Li, W., Ching, K.A., Batalov, S., Tsai, C.C. and Joazeiro, C.A. (2003). "Ubiquitin-mediated sequestration of normal cellular proteins into polyglutamine aggregates." *Proc Natl Acad Sci U S A* 100(15): 8892-7.
- Drews, O., Wildgruber, R., Zong, C., Sukop, U., Nissum, M., Weber, G., Gomes, A.V. and Ping, P. (2007). "Mammalian proteasome subpopulations with distinct molecular compositions and proteolytic activities." *Mol Cell Proteomics* 6(11): 2021-31.
- Dutcher, S.A., Underwood, B.D., Walker, P.D., Diaz, F.G. and Michael, D.B. (1998). "Patterns of heat-shock protein 70 biosynthesis following human traumatic brain injury." *J Neurotrauma* 15(6): 411-20.
- Ehlers, M.D. (2003). "Activity level controls postsynaptic composition and signaling via the ubiquitin-proteasome system." *Nat Neurosci* 6(3): 231-42.
- Ehrengreuber, M.U., Hennou, S., Bueler, H., Naim, H.Y., Deglon, N. and Lundstrom, K. (2001). "Gene transfer into neurons from hippocampal slices: comparison of recombinant Semliki Forest Virus, adenovirus, adeno-associated virus, lentivirus, and measles virus." *Mol Cell Neurosci* 17(5): 855-71.
- Elsasser, S. and Finley, D. (2005). "Delivery of ubiquitinated substrates to protein-unfolding machines." *Nat Cell Biol* 7(8): 742-9.
- Emre, M. (2003). "Dementia associated with Parkinson's disease." *Lancet Neurol* 2(4): 229-37.
- Eriksen, J.L. and Janus, C.G. (2007). "Plaques, tangles, and memory loss in mouse models of neurodegeneration." *Behav Genet* 37(1): 79-100.
- Evans, D.A., van der Kleij, A.A., Sonnemans, M.A., Burbach, J.P. and van Leeuwen, F.W. (1994). "Frameshift mutations at two hotspots in vasopressin transcripts in post-mitotic neurons." *Proc Natl Acad Sci U S A* 91(13): 6059-63.
- Fallaux, F.J., Kranenburg, O., Cramer, S.J., Houweling, A., Van Ormondt, H., Hoeben, R.C. and Van Der Eb, A.J. (1996). "Characterization of 911: a new helper cell line for the titration and propagation of early region 1-deleted adenoviral vectors." *Hum Gene Ther* 7(2): 215-22.
- Feng, G., Mellor, R.H., Bernstein, M., Keller-Peck, C., Nguyen, Q.T., Wallace, M., Nerbonne, J.M., Lichtman, J.W. and Sanes, J.R. (2000). "Imaging Neuronal Subsets in Transgenic Mice Expressing Multiple Spectral Variants of GFP." *Neuron* 28(1): 41-51.
- Fenteany, G., Standaert, R.F., Lane, W.S., Choi, S., Corey, E.J. and Schreiber, S.L. (1995). "Inhibition of proteasome activities and subunit-specific amino-terminal threonine modification by lactacystin." *Science* 268(5211): 726-31.
- Fetsko, L.A., Xu, R. and Wang, Y. (2005). "Effects of age and dopamine D2L receptor-deficiency on motor and learning functions." *Neurobiol Aging* 26(4): 521-30.
- Fiebiger, E., Story, C., Ploegh, H.L. and Tortorella, D. (2002). "Visualization of the ER-to-cytosol dislocation reaction of a type I membrane protein." *Embo J* 21(5): 1041-53.
- Finley, D., Ciechanover, A. and Varshavsky, A. (1984). "Thermolability of ubiquitin-activating enzyme from the mammalian cell cycle mutant ts85." *Cell* 37(1): 43-55.
- Fischer, D.F., De Vos, R.A., Van Dijk, R., De Vrij, F.M., Proper, E.A., Sonnemans, M.A., Verhage, M.C., Sluijs, J.A., Hobo, B., Zouambia, M., Steur, E.N., Kamphorst, W., Hol, E.M. and Van Leeuwen, F.W. (2003). "Disease-specific accumulation of mutant ubiquitin as a marker for proteasomal dysfunction in the brain." *Easeb J* 17(14): 2014-24.
- Fischer, D.F., Hol, E.M., Hobo, B. and van Leeuwen, F.W. (2006). "Alzheimer-associated APP+1 transgenic mice: frameshift beta-amyloid precursor protein is secreted in cerebrospinal fluid without inducing neuropathology." *Neurobiol Aging* 27(10): 1445-50.
- Fischer, D.F., van Tijn, P., Verhage, M.C., Hobo, B., Hol, E.M. and van Leeuwen, F.W. (2004). Mouse models for proteasome insufficiency: aberrant ubiquitin as a tool in the study of neurodegenerative disease. *Neuroscience Meeting*. San Diego CA, 23-27 October 2004, Society for Neuroscience.
- Fleming, S.M. and Chesselet, M.F. (2006). "Behavioral phenotypes and pharmacology in genetic mouse models of Parkinsonism." *Behav Pharmacol* 17(5-6): 383-91.
- Fleming, S.M., Fernagut, P.O. and Chesselet, M.F. (2005). "Genetic mouse models of parkinsonism: strengths and limitations." *NeuroRx* 2(3): 495-503.
- Flexner, J.B., Flexner, L.B. and Stellar, E. (1963). "Memory in mice as affected by intracerebral puromycin." *Science* 141: 57-9.

REFERENCES

- Flood, F., Murphy, S., Cowburn, R.F., Lannfelt, L., Walker, B. and Johnston, J.A. (2005). "Proteasome-mediated effects on amyloid precursor protein processing at the gamma-secretase site." *Biochem J* 385(Pt 2): 545-50.
- Fonseca, R., Vabulas, R.M., Hartl, F.U., Bonhoeffer, T. and Nagerl, U.V. (2006). "A balance of protein synthesis and proteasome-dependent degradation determines the maintenance of LTP." *Neuron* 52 (2): 239-45.
- Fornai, F., Lenzi, P., Gesi, M., Ferrucci, M., Lazzeri, G., Busceti, C.L., Ruffoli, R., Soldani, P., Ruggieri, S., Alessandri, M.G. and Paparelli, A. (2003). "Fine structure and biochemical mechanisms underlying nigrostriatal inclusions and cell death after proteasome inhibition." *J Neurosci* 23(26): 8955-66.
- Fornai, F., Schluter, O.M., Lenzi, P., Gesi, M., Ruffoli, R., Ferrucci, M., Lazzeri, G., Busceti, C.L., Pontarelli, F., Battaglia, G., Pellegrini, A., Nicoletti, F., Ruggieri, S., Paparelli, A. and Sudhof, T.C. (2005). "Parkinson-like syndrome induced by continuous MPTP infusion: convergent roles of the ubiquitin-proteasome system and alpha-synuclein." *Proc Natl Acad Sci U S A* 102(9): 3413-8.
- Fraser, P.E., Levesque, G., Yu, G., Mills, L.R., Thirlwell, J., Frantseva, M., Gandy, S.E., Seeger, M., Carlen, P.L. and St George-Hyslop, P. (1998). "Presenilin 1 is actively degraded by the 26S proteasome." *Neurobiol Aging* 19(1 Suppl): S19-21.
- Frasier, M., Walzer, M., McCarthy, L., Magnuson, D., Lee, J.M., Haas, C., Kahle, P. and Wolozin, B. (2005). "Tau phosphorylation increases in symptomatic mice overexpressing A30P alpha-synuclein." *Exp Neurol* 192(2): 274-87.
- Fratta, P., Engel, W.K., Van Leeuwen, F.W., Hol, E.M., Vattemi, G. and Askanas, V. (2004). "Mutant ubiquitin UBB+1 is accumulated in sporadic inclusion-body myositis muscle fibers." *Neurology* 63 (6): 1114-7.
- Freichel, C., Neumann, M., Ballard, T., Muller, V., Woolley, M., Ozmen, L., Borroni, E., Kretzschmar, H.A., Haass, C., Spooren, W. and Kahle, P.J. (2007). "Age-dependent cognitive decline and amygdala pathology in alpha-synuclein transgenic mice." *Neurobiol Aging* 28(9): 1421-35.
- Gaczynska, M., Rock, K.L., Spies, T. and Goldberg, A.L. (1994). "Peptidase activities of proteasomes are differentially regulated by the major histocompatibility complex-encoded genes for LMP2 and LMP7." *Proc Natl Acad Sci U S A* 91(20): 9213-7.
- Garbis, S., Lubec, G. and Fountoulakis, M. (2005). "Limitations of current proteomics technologies." *J Chromatogr A* 1077(1): 1-18.
- Garcia-Alloza, M., Robbins, E.M., Zhang-Nunes, S.X., Purcell, S.M., Betensky, R.A., Raju, S., Prada, C., Greenberg, S.M., Bacsik, B.J. and Frosch, M.P. (2006). "Characterization of amyloid deposition in the APPswe/PS1dE9 mouse model of Alzheimer disease." *Neurobiol Dis* 24(3): 516-24.
- Gerez, L., de Haan, A., Hol, E.M., Fischer, D.F., van Leeuwen, F.W., van Steeg, H. and Benne, R. (2005). "Molecular misreading: the frequency of dinucleotide deletions in neuronal mRNAs for beta-amyloid precursor protein and ubiquitin B." *Neurobiol Aging* 26(2): 145-55.
- Gilchrist, C.A., Gray, D.A., Stieber, A., Gonatas, N.K. and Kopito, R.R. (2005). "Effect of ubiquitin expression on neuropathogenesis in a mouse model of familial amyotrophic lateral sclerosis." *Neuropathol Appl Neurobiol* 31(1): 20-33.
- Gillardon, F., Kloss, A., Berg, M., Neumann, M., Mechtler, K., Hengerer, B. and Dahlmann, B. (2007). "The 20S proteasome isolated from Alzheimer's disease brain shows post-translational modifications but unchanged proteolytic activity." *J Neurochem* 101(6): 1483-90.
- Glickman, M.H. and Ciechanover, A. (2002). "The ubiquitin-proteasome proteolytic pathway: destruction for the sake of construction." *Physiol Rev* 82(2): 373-428.
- Goddyn, H., Leo, S., Meert, T. and D'Hooge, R. (2006). "Differences in behavioural test battery performance between mice with hippocampal and cerebellar lesions." *Behav Brain Res* 173(1): 138-47.
- Goedert, M., Wischik, C.M., Crowther, R.A., Walker, J.E. and Klug, A. (1988). "Cloning and sequencing of the cDNA encoding a core protein of the paired helical filament of Alzheimer disease: identification as the microtubule-associated protein tau." *Proc Natl Acad Sci U S A* 85(11): 4051-5.
- Goldberg, A.L. (2005). "Nobel committee tags ubiquitin for distinction." *Neuron* 45(3): 339-44.
- Goldberg, M.S., Fleming, S.M., Palacino, J.J., Cepeda, C., Lam, H.A., Bhatnagar, A., Meloni, E.G., Wu, N., Ackerson, L.C., Klapstein, G.J., Gajendiran, M., Roth, B.L., Chesselet, M.F., Maidment, N.T., Levine, M.S. and Shen, J. (2003). "Parkin-deficient mice exhibit nigrostriatal deficits but not loss of dopaminergic neurons." *J Biol Chem* 278(44): 43628-35.

- Goldstein, G., Scheid, M., Hammerling, U., Schlesinger, D.H., Niall, H.D. and Boyse, E.A. (1975). "Isolation of a polypeptide that has lymphocyte-differentiating properties and is probably represented universally in living cells." *Proc Natl Acad Sci U S A* 72(1): 11-5.
- Gong, B., Cao, Z., Zheng, P., Vitolo, O.V., Liu, S., Staniszewski, A., Moolman, D., Zhang, H., Shelanski, M. and Arancio, O. (2006). "Ubiquitin hydrolase Uch-L1 rescues beta-amyloid-induced decreases in synaptic function and contextual memory." *Cell* 126(4): 775-88.
- Gordon, J.A., Cioffi, D., Silva, A.J. and Stryker, M.P. (1996). "Deficient plasticity in the primary visual cortex of alpha-calcium/calmodulin-dependent protein kinase II mutant mice." *Neuron* 17(3): 491-9.
- Goshima, Y., Nakamura, F., Strittmatter, P. and Strittmatter, S.M. (1995). "Collapsin-induced growth cone collapse mediated by an intracellular protein related to UNC-33." *Nature* 376(6540): 509-14.
- Goti, D., Katzen, S.M., Mez, J., Kurtis, N., Kiluk, J., Ben-Haim, L., Jenkins, N.A., Copeland, N.G., Kakinaka, A., Sharp, A.H., Ross, C.A., Mouton, P.R. and Colomer, V. (2004). "A mutant ataxin-3 putative-cleavage fragment in brains of Machado-Joseph disease patients and transgenic mice is cytotoxic above a critical concentration." *J Neurosci* 24(45): 10266-79.
- Gray, D.A., Tsirigotis, M., Brun, J., Tang, M., Zhang, M., Beyers, M. and Woulfe, J. (2004). "Protective effects of mutant ubiquitin in transgenic mice." *Ann N Y Acad Sci* 1019: 215-8.
- Gregori, L., Fuchs, C., Figueiredo-Pereira, M.E., Van Nostrand, W.E. and Goldgaber, D. (1995). "Amyloid beta-protein inhibits ubiquitin-dependent protein degradation in vitro." *J Biol Chem* 270(34): 19702-8.
- Gregori, L., Hainfeld, J.F., Simon, M.N. and Goldgaber, D. (1997). "Binding of amyloid beta protein to the 20 S proteasome." *J Biol Chem* 272(1): 58-62.
- Groll, M. and Huber, R. (2004). "Inhibitors of the eukaryotic 20S proteasome core particle: a structural approach." *Biochim Biophys Acta* 1695(1-3): 33-44.
- Grune, T., Merker, K., Sandig, G. and Davies, K.J. (2003). "Selective degradation of oxidatively modified protein substrates by the proteasome." *Biochem Biophys Res Commun* 305(3): 709-18.
- Gu, Y., Hamajima, N. and Ihara, Y. (2000). "Neurofibrillary tangle-associated collapsin response mediator protein-2 (CRMP-2) is highly phosphorylated on Thr-509, Ser-518, and Ser-522." *Biochemistry* 39(15): 4267-75.
- Gu, Y. and Ihara, Y. (2000). "Evidence that collapsin response mediator protein-2 is involved in the dynamics of microtubules." *J Biol Chem* 275(24): 17917-20.
- Gundersen, H.J. and Jensen, E.B. (1987). "The efficiency of systematic sampling in stereology and its prediction." *J Microsc* 147(Pt 3): 229-63.
- Haacke, A., Broadley, S.A., Boteva, R., Tsvetkov, N., Hartl, F.U. and Breuer, P. (2006). "Proteolytic cleavage of polyglutamine-expanded ataxin-3 is critical for aggregation and sequestration of non-expanded ataxin-3." *Hum Mol Genet* 15(4): 555-68.
- Haglund, K., Di Fiore, P.P. and Dikic, I. (2003). "Distinct monoubiquitin signals in receptor endocytosis." *Trends Biochem Sci* 28(11): 598-603.
- Hamajima, N., Matsuda, K., Sakata, S., Tamaki, N., Sasaki, M. and Nonaka, M. (1996). "A novel gene family defined by human dihydropyrimidinase and three related proteins with differential tissue distribution." *Gene* 180(1-2): 157-63.
- Hanna, J., Hathaway, N.A., Tone, Y., Crosas, B., Elsasser, S., Kirkpatrick, D.S., Leggett, D.S., Gygi, S.P., King, R.W. and Finley, D. (2006). "Deubiquitinating enzyme Ubp6 functions noncatalytically to delay proteasomal degradation." *Cell* 127(1): 99-111.
- Hara, T., Nakamura, K., Matsui, M., Yamamoto, A., Nakahara, Y., Suzuki-Migishima, R., Yokoyama, M., Mishima, K., Saito, I., Okano, H. and Mizushima, N. (2006). "Suppression of basal autophagy in neural cells causes neurodegenerative disease in mice." *Nature* 441(7095): 885-9.
- Hardy, J. and Selkoe, D.J. (2002). "The amyloid hypothesis of Alzheimer's disease: progress and problems on the road to therapeutics." *Science* 297(5580): 353-6.
- Hayter, J.R., Doherty, M.K., Whitehead, C., McCormack, H., Gaskell, S.J. and Beynon, R.J. (2005). "The subunit structure and dynamics of the 20S proteasome in chicken skeletal muscle." *Mol Cell Proteomics* 4(9): 1370-81.
- He, G., Qing, H., Cai, F., Kwok, C., Xu, H., Yu, G., Bernstein, A. and Song, W. (2006). "Ubiquitin-proteasome pathway mediates degradation of APH-1." *J Neurochem* 99(5): 1403-12.
- He, G., Qing, H., Tong, Y., Cai, F., Ishiura, S. and Song, W. (2007). "Degradation of nicastrin involves both proteasome and lysosome." *J Neurochem* 101(4): 982-92.

REFERENCES

- He, L., Lu, X.Y., Jolly, A.F., Eldridge, A.G., Watson, S.J., Jackson, P.K., Barsh, G.S. and Gunn, T.M. (2003). "Spongiform degeneration in mahoganyd mutant mice." *Science* 299(5607): 710-2.
- Hegde, A.N., Inokuchi, K., Pei, W., Casadio, A., Ghirardi, M., Chain, D.G., Martin, K.C., Kandel, E.R. and Schwartz, J.H. (1997). "Ubiquitin C-terminal hydrolase is an immediate-early gene essential for long-term facilitation in Aplysia." *Cell* 89(1): 115-26.
- Hegde, A.N. and Upadhyay, S.C. (2007). "The ubiquitin-proteasome pathway in health and disease of the nervous system." *Trends Neurosci* 30(11): 587-95.
- Hendil, K.B., Kristensen, P. and Uerkvitz, W. (1995). "Human proteasomes analysed with monoclonal antibodies." *Biochem J* 305 (Pt 1): 245-52.
- Hensley, K., Carney, J.M., Mattson, M.P., Aksenova, M., Harris, M., Wu, J.F., Floyd, R.A. and Butterfield, D.A. (1994). "A model for beta-amyloid aggregation and neurotoxicity based on free radical generation by the peptide: relevance to Alzheimer disease." *Proc Natl Acad Sci U S A* 91(8): 3270-4.
- Hensley, K., Hall, N., Subramaniam, R., Cole, P., Harris, M., Aksenova, M., Gabbita, S.P., Wu, J.F., Carney, J.M. and et al. (1995). "Brain regional correspondence between Alzheimer's disease histopathology and biomarkers of protein oxidation." *J Neurochem* 65(5): 2146-56.
- Hermens, W.T., Giger, R.J., Holtmaat, A.J., Dijkhuizen, P.A., Houweling, D.A. and Verhaagen, J. (1997). "Transient gene transfer to neurons and glia: analysis of adenoviral vector performance in the CNS and PNS." *J Neurosci Methods* 71(1): 85-98.
- Hershko, A. and Ciechanover, A. (1998). "The ubiquitin system." *Annu Rev Biochem* 67: 425-79.
- Hershko, A., Ciechanover, A., Heller, H., Haas, A.L. and Rose, I.A. (1980). "Proposed role of ATP in protein breakdown: conjugation of protein with multiple chains of the polypeptide of ATP-dependent proteolysis." *Proc Natl Acad Sci U S A* 77(4): 1783-6.
- Hikosaka, O., Nakamura, K., Sakai, K. and Nakahara, H. (2002). "Central mechanisms of motor skill learning." *Curr Opin Neurobiol* 12(2): 217-22.
- Hoglinger, G.U., Carrard, G., Michel, P.P., Medja, F., Lombes, A., Ruberg, M., Friguet, B. and Hirsch, E.C. (2003). "Dysfunction of mitochondrial complex I and the proteasome: interactions between two biochemical deficits in a cellular model of Parkinson's disease." *J Neurochem* 86(5): 1297-307.
- Hol, E.M., Fischer, D.F., Ovaa, H. and Scheper, W. (2006). "Ubiquitin proteasome system as a pharmacological target in neurodegeneration." *Expert Rev Neurother* 6(9): 1337-47.
- Hol, E.M., Van Dijk, R., Gerez, L., Sluijs, J.A., Hobo, B., Tonk, M.T., De Haan, A., Kamphorst, W., Fischer, D.F., Benne, R. and Van Leeuwen, F.W. (2003). "Frameshifted {beta}-Amyloid Precursor Protein (APP+1) Is a Secretory Protein, and the Level of APP+1 in Cerebrospinal Fluid Is Linked to Alzheimer Pathology." *J Biol Chem* 278(41): 39637-43.
- Hol, E.M., van Leeuwen, F.W. and Fischer, D.F. (2005). "The proteasome in Alzheimer's disease and Parkinson's disease: lessons from ubiquitin B(+1)." *Trends Mol Med* 11(11): 488-95.
- Hope, A.D., de Silva, R., Fischer, D.F., Hol, E.M., van Leeuwen, F.W. and Lees, A.J. (2003). "Alzheimer's associated variant ubiquitin causes inhibition of the 26S proteasome and chaperone expression." *J Neurochem* 86(2): 394-404.
- Hope, A.D., Lashley, T., Lees, A.J. and De Silva, R. (2004). "Failure in heat-shock protein expression in response to UBB(+1) protein in progressive supranuclear palsy in humans." *Neurosci Lett* 359(1-2): 94-8.
- Hoppe, T. (2005). "Multiubiquitylation by E4 enzymes: 'one size' doesn't fit all." *Trends Biochem Sci* 30 (4): 183-7.
- Hsiao-Ashe, K. (2001). "Learning and memory in transgenic mice modeling Alzheimer's disease." *Learn Mem* 8(6): 301-8.
- Hussain, I., Hawkins, J., Harrison, D., Hille, C., Wayne, G., Cutler, L., Buck, T., Walter, D., Demont, E., Howes, C., Naylor, A., Jeffrey, P., Gonzalez, M.I., Dingwall, C., Michel, A., Redshaw, S. and Davis, J.B. (2007). "Oral administration of a potent and selective non-peptidic BACE-1 inhibitor decreases beta-cleavage of amyloid precursor protein and amyloid-beta production in vivo." *J Neurochem* 100(3): 802-9.

- Hutton, M., Lendon, C.L., Rizzu, P., Baker, M., Froelich, S., Houlden, H., Pickering-Brown, S., Chakraverty, S., Isaacs, A., Grover, A., Hackett, J., Adamson, J., Lincoln, S., Dickson, D., Davies, P., Petersen, R.C., Stevens, M., de Graaff, E., Wauters, E., van Baren, J., Hillebrand, M., Joosse, M., Kwon, J.M., Nowotny, P., Heutink, P. and et al. (1998). "Association of missense and 5'-splice-site mutations in tau with the inherited dementia FTDP-17." *Nature* 393(6686): 702-05.
- Hyun, D.H., Lee, M.H., Halliwell, B. and Jenner, P. (2002). "Proteasomal dysfunction induced by 4-hydroxy-2,3-trans-nonenal, an end-product of lipid peroxidation: a mechanism contributing to neurodegeneration?" *J Neurochem* 83(2): 360-70.
- Ichihara, N., Wu, J., Chui, D.H., Yamazaki, K., Wakabayashi, T. and Kikuchi, T. (1995). "Axonal degeneration promotes abnormal accumulation of amyloid beta-protein in ascending gracile tract of gracile axonal dystrophy (GAD) mouse." *Brain Res* 695(2): 173-8.
- Ichikawa, Y., Goto, J., Hattori, M., Toyoda, A., Ishii, K., Jeong, S.Y., Hashida, H., Masuda, N., Ogata, K., Kasai, F., Hirai, M., Maciel, P., Rouleau, G.A., Sakaki, Y. and Kanazawa, I. (2001). "The genomic structure and expression of MJD, the Machado-Joseph disease gene." *J Hum Genet* 46(7): 413-22.
- Ikeda, H., Yamaguchi, M., Sugai, S., Aze, Y., Narumiya, S. and Kakizuka, A. (1996). "Expanded polyglutamine in the Machado-Joseph disease protein induces cell death in vitro and in vivo." *Nat Genet* 13(2): 196-202.
- Imai, Y., Soda, M., Hatakeyama, S., Akagi, T., Hashikawa, T., Nakayama, K.I. and Takahashi, R. (2002). "CHIP is associated with Parkin, a gene responsible for familial Parkinson's disease, and enhances its ubiquitin ligase activity." *Mol Cell* 10(1): 55-67.
- Imai, Y., Soda, M., Inoue, H., Hattori, N., Mizuno, Y. and Takahashi, R. (2001). "An unfolded putative transmembrane polypeptide, which can lead to endoplasmic reticulum stress, is a substrate of Parkin." *Cell* 105(7): 891-902.
- Itier, J.M., Ibanez, P., Mena, M.A., Abbas, N., Cohen-Salmon, C., Bohme, G.A., Laville, M., Pratt, J., Corti, O., Pradier, L., Ret, G., Joubert, C., Periquet, M., Araujo, F., Negroni, J., Casarejos, M.J., Canals, S., Solano, R., Serrano, A., Gallego, E., Sanchez, M., Denefle, P., Benavides, J., Tremp, G., Rooney, T.A., Brice, A. and Garcia de Yebenes, J. (2003). "Parkin gene inactivation alters behaviour and dopamine neurotransmission in the mouse." *Hum Mol Genet* 12(18): 2277-91.
- Iwatsubo, T., Yamaguchi, H., Fujimuro, M., Yokosawa, H., Ihara, Y., Trojanowski, J.Q. and Lee, V.M. (1996). "Purification and characterization of Lewy bodies from the brains of patients with diffuse Lewy body disease." *Am J Pathol* 148(5): 1517-29.
- Jablonska, B., Gierdalski, M., Kublik, A., Skangiel-Kramska, J. and Kossut, M. (1993). "Effects of implantation of Alzet 1007D osmotic minipumps upon 2-deoxyglucose uptake in the cerebral cortex of mice." *Acta Neurobiol Exp (Wars)* 53(4): 577-80.
- Jana, N.R., Zemskov, E.A., Wang, G. and Nukina, N. (2001). "Altered proteasomal function due to the expression of polyglutamine-expanded truncated N-terminal huntingtin induces apoptosis by caspase activation through mitochondrial cytochrome c release." *Hum Mol Genet* 10(10): 1049-59.
- Jankowsky, J.L., Fadale, D.J., Anderson, J., Xu, G.M., Gonzales, V., Jenkins, N.A., Copeland, N.G., Lee, M.K., Younkin, L.H., Wagner, S.L., Younkin, S.G. and Borchelt, D.R. (2004). "Mutant presenilins specifically elevate the levels of the 42 residue beta-amyloid peptide in vivo: evidence for augmentation of a 42-specific gamma secretase." *Hum Mol Genet* 13(2): 159-70.
- Jankowsky, J.L., Slunt, H.H., Ratovitski, T., Jenkins, N.A., Copeland, N.G. and Borchelt, D.R. (2001). "Co-expression of multiple transgenes in mouse CNS: a comparison of strategies." *Biomol Eng* 17(6): 157-65.
- Jiang, Y.H., Armstrong, D., Albrecht, U., Atkins, C.M., Noebels, J.L., Eichele, G., Sweatt, J.D. and Beaudet, A.L. (1998). "Mutation of the Angelman ubiquitin ligase in mice causes increased cytoplasmic p53 and deficits of contextual learning and long-term potentiation." *Neuron* 21(4): 799-811.
- Jin, B.F., He, K., Wang, H.X., Wang, J., Zhou, T., Lan, Y., Hu, M.R., Wei, K.H., Yang, S.C., Shen, B.F. and Zhang, X.M. (2003). "Proteomic analysis of ubiquitin-proteasome effects: insight into the function of eukaryotic initiation factor 5A." *Oncogene* 22(31): 4819-30.
- Jin, J., Li, X., Gygi, S.P. and Harper, J.W. (2007). "Dual E1 activation systems for ubiquitin differentially regulate E2 enzyme charging." *Nature* 447(7148): 1135-8.
- Johnson, E.S., Ma, P.C., Ota, I.M. and Varshavsky, A. (1995). "A proteolytic pathway that recognizes ubiquitin as a degradation signal." *J Biol Chem* 270(29): 17442-56.

REFERENCES

- Johnston, J.A., Ward, C.L. and Kopito, R.R. (1998). "Aggresomes: a cellular response to misfolded proteins." *J Cell Biol* 143(7): 1883-98.
- Jones, N. and Shenk, T. (1979). "An adenovirus type 5 early gene function regulates expression of other early viral genes." *Proc Natl Acad Sci U S A* 76(8): 3665-9.
- Kalchman, M.A., Graham, R.K., Xia, G., Koide, H.B., Hodgson, J.G., Graham, K.C., Goldberg, Y.P., Gietz, R.D., Pickart, C.M. and Hayden, M.R. (1996). "Huntingtin is ubiquitinated and interacts with a specific ubiquitin-conjugating enzyme." *J Biol Chem* 271(32): 19385-94.
- Kawaguchi, Y., Okamoto, T., Taniwaki, M., Aizawa, M., Inoue, M., Katayama, S., Kawakami, H., Nakamura, S., Nishimura, M., Akiguchi, I. and et al. (1994). "CAG expansions in a novel gene for Machado-Joseph disease at chromosome 14q32.1." *Nat Genet* 8(3): 221-8.
- Keck, S., Nitsch, R., Grune, T. and Ullrich, O. (2003). "Proteasome inhibition by paired helical filament-tau in brains of patients with Alzheimer's disease." *J Neurochem* 85(1): 115-22.
- Kelleher, R.J., 3rd, Govindarajan, A. and Tonegawa, S. (2004). "Translational Regulatory Mechanisms in Persistent Forms of Synaptic Plasticity." *Neuron* 44(1): 59-73.
- Keller, J.N., Gee, J. and Ding, Q. (2002). "The proteasome in brain aging." *Ageing Res Rev* 1(2): 279-93.
- Keller, J.N., Hanni, K.B. and Markesberry, W.R. (2000). "Impaired proteasome function in Alzheimer's disease." *J Neurochem* 75(1): 436-9.
- Keller, J.N., Hanni, K.B. and Markesberry, W.R. (2000). "Possible involvement of proteasome inhibition in aging: implications for oxidative stress." *Mech Ageing Dev* 113(1): 61-70.
- Keller, J.N., Huang, F.F. and Markesberry, W.R. (2000). "Decreased levels of proteasome activity and proteasome expression in aging spinal cord." *Neuroscience* 98(1): 149-56.
- Kessler, B.M., Tortorella, D., Altun, M., Kisseelev, A.F., Fiebiger, E., Hekking, B.G., Ploegh, H.L. and Overkleef, H.S. (2001). "Extended peptide-based inhibitors efficiently target the proteasome and reveal overlapping specificities of the catalytic beta-subunits." *Chem Biol* 8(9): 913-29.
- Kienlen-Campard, P., Feyt, C., Huysseune, S., de Diesbach, P., N'Kuli, F., Courtoy, P.J. and Octave, J.N. (2006). "Lactacystin decreases amyloid-beta peptide production by inhibiting beta-secretase activity." *J Neurosci Res* 84(6): 1311-22.
- Kim, S.H., Fountoulakis, M., Cairns, N.J. and Lubec, G. (2002). "Human brain nucleoside diphosphate kinase activity is decreased in Alzheimer's disease and Down syndrome." *Biochem Biophys Res Commun* 296(4): 970-5.
- Kim, T.W., Pettingell, W.H., Hallmark, O.G., Moir, R.D., Wasco, W. and Tanzi, R.E. (1997). "Endoproteolytic cleavage and proteasomal degradation of presenilin 2 in transfected cells." *J Biol Chem* 272(17): 11006-10.
- Kishino, T., Lalande, M. and Wagstaff, J. (1997). "UBE3A/E6-AP mutations cause Angelman syndrome." *Nat Genet* 15(1): 70-3.
- Kisseelev, A.F. and Goldberg, A.L. (2001). "Proteasome inhibitors: from research tools to drug candidates." *Chem Biol* 8(8): 739-58.
- Kitada, T., Asakawa, S., Hattori, N., Matsumine, H., Yamamura, Y., Minoshima, S., Yokochi, M., Mizuno, Y. and Shimizu, N. (1998). "Mutations in the parkin gene cause autosomal recessive juvenile parkinsonism." *Nature* 392(6676): 605-8.
- Ko, H.S., von Coelln, R., Sriram, S.R., Kim, S.W., Chung, K.K., Pletnikova, O., Troncoso, J., Johnson, B., Saffary, R., Goh, E.L., Song, H., Park, B.J., Kim, M.J., Kim, S., Dawson, V.L. and Dawson, T.M. (2005). "Accumulation of the authentic parkin substrate aminoacyl-tRNA synthetase cofactor, p38/JTV-1, leads to catecholaminergic cell death." *J Neurosci* 25(35): 7968-78.
- Koegl, M., Hoppe, T., Schlenker, S., Ulrich, H.D., Mayer, T.U. and Jentsch, S. (1999). "A novel ubiquitination factor, E4, is involved in multiubiquitin chain assembly." *Cell* 96(5): 635-44.
- Koeppen, A.H. (2005). "The pathogenesis of spinocerebellar ataxia." *Cerebellum* 4(1): 62-73.
- Koh, Y.H., von Arnim, C.A., Hyman, B.T., Tanzi, R.E. and Tesco, G. (2005). "BACE is degraded via the lysosomal pathway." *J Biol Chem* 280(37): 32499-504.
- Komatsu, M., Waguri, S., Chiba, T., Murata, S., Iwata, J., Tanida, I., Ueno, T., Koike, M., Uchiyama, Y., Kominami, E. and Tanaka, K. (2006). "Loss of autophagy in the central nervous system causes neurodegeneration in mice." *Nature* 441(7095): 880-4.
- Kopito, R.R. (2000). "Aggresomes, inclusion bodies and protein aggregation." *Trends Cell Biol* 10(12): 524-30.

- Koyano, S., Iwabuchi, K., Yagishita, S., Kuroiwa, Y. and Uchihara, T. (2002). "Paradoxical absence of nuclear inclusion in cerebellar Purkinje cells of hereditary ataxias linked to CAG expansion." *J Neurol Neurosurg Psychiatry* 73(4): 450-2.
- Kristiansen, M., Deriziotis, P., Dimcheff, D.E., Jackson, G.S., Ovaa, H., Naumann, H., Clarke, A.R., van Leeuwen, F.W., Menendez-Benito, V., Dantuma, N.P., Portis, J.L., Collinge, J. and Tabrizi, S.J. (2007). "Disease-associated prion protein oligomers inhibit the 26S proteasome." *Mol Cell* 26(2): 175-88.
- Kumarapeli, A.R., Horak, K.M., Glasford, J.W., Li, J., Chen, Q., Liu, J., Zheng, H. and Wang, X. (2005). "A novel transgenic mouse model reveals deregulation of the ubiquitin-proteasome system in the heart by doxorubicin." *Faseb J* 19(14): 2051-3.
- Kurihara, L.J., Kikuchi, T., Wada, K. and Tilghman, S.M. (2001). "Loss of Uch-L1 and Uch-L3 leads to neurodegeneration, posterior paralysis and dysphagia." *Hum Mol Genet* 10(18): 1963-70.
- Kurihara, L.J., Semenova, E., Levorse, J.M. and Tilghman, S.M. (2000). "Expression and functional analysis of Uch-L3 during mouse development." *Mol Cell Biol* 20(7): 2498-504.
- Kwon, J. and Wada, K. (2006). The *GAD* mouse: a window into UPS-related neurodegeneration and the function of the deubiquitinating enzyme UCH-L1. *The Proteasome in Neurodegeneration*. L. Stefanis and J. N. Keller. New York, Springer: 185-98.
- LaFerla, F.M., Green, K.N. and Oddo, S. (2007). "Intracellular amyloid-beta in Alzheimer's disease." *Nat Rev Neurosci* 8(7): 499-509.
- Lam, Y.A., Huang, J.W. and Showole, O. (2005). "The synthesis and proteasomal degradation of a model substrate Ub5DHFR." *Methods Enzymol* 398: 379-90.
- Lam, Y.A., Lawson, T.G., Velayutham, M., Zweier, J.L. and Pickart, C.M. (2002). "A proteasomal ATPase subunit recognizes the polyubiquitin degradation signal." *Nature* 416(6882): 763-7.
- Lam, Y.A., Pickart, C.M., Alban, A., Landon, M., Jamieson, C., Ramage, R., Mayer, R.J. and Layfield, R. (2000). "Inhibition of the ubiquitin-proteasome system in Alzheimer's disease." *Proc Natl Acad Sci U S A* 97(18): 9902-6.
- Lam, Y.A., Xu, W., DeMartino, G.N. and Cohen, R.E. (1997). "Editing of ubiquitin conjugates by an isopeptidase in the 26S proteasome." *Nature* 385(6618): 737-40.
- Larsen, C.N., Krantz, B.A. and Wilkinson, K.D. (1998). "Substrate specificity of deubiquitinating enzymes: ubiquitin C-terminal hydrolases." *Biochemistry* 37(10): 3358-68.
- Larsen, C.N., Price, J.S. and Wilkinson, K.D. (1996). "Substrate binding and catalysis by ubiquitin C-terminal hydrolases: identification of two active site residues." *Biochemistry* 35(21): 6735-44.
- Le Saux, F., Besson, M.J. and Maurin, Y. (2002). "Abnormal postnatal ontogeny of the locus coeruleus in the epileptic mutant mouse quaking." *Brain Res Dev Brain Res* 136(2): 197-205.
- Lee, P.D., Sladek, R., Greenwood, C.M. and Hudson, T.J. (2002). "Control genes and variability: absence of ubiquitous reference transcripts in diverse Mammalian expression studies." *Genome Res* 12(2): 292-7.
- Lee, V.M., Goedert, M. and Trojanowski, J.Q. (2001). "Neurodegenerative tauopathies." *Annu Rev Neurosci* 24: 1121-59.
- Leggett, D.S., Hanna, J., Borodovsky, A., Crosas, B., Schmidt, M., Baker, R.T., Walz, T., Ploegh, H. and Finley, D. (2002). "Multiple associated proteins regulate proteasome structure and function." *Mol Cell* 10(3): 495-507.
- Leroy, E., Boyer, R., Auburger, G., Leube, B., Ulm, G., Mezey, E., Harta, G., Brownstein, M.J., Jonnalagada, S., Chernova, T., Dehejia, A., Lavedan, C., Gasser, T., Steinbach, P.J., Wilkinson, K.D. and Polymeropoulos, M.H. (1998). "The ubiquitin pathway in Parkinson's disease." *Nature* 395(6701): 451-2.
- Lewis, J., McGowan, E., Rockwood, J., Melrose, H., Nacharaju, P., Van Slegtenhorst, M., Gwinn-Hardy, K., Paul Murphy, M., Baker, M., Yu, X., Duff, K., Hardy, J., Corral, A., Lin, W.L., Yen, S.H., Dickson, D.W., Davies, P. and Hutton, M. (2000). "Neurofibrillary tangles, amyotrophy and progressive motor disturbance in mice expressing mutant (P301L) tau protein." *Nat Genet* 25(4): 402-5.
- Li, K.W., Hornshaw, M.P., Van Der Schors, R.C., Watson, R., Tate, S., Casetta, B., Jimenez, C.R., Gouwenberg, Y., Gundelfinger, E.D., Smalla, K.H. and Smit, A.B. (2004). "Proteomics analysis of rat brain postsynaptic density: Implications of the diverse protein functional groups for the integration of synaptic physiology." *J Biol Chem* 279(2): 987-1002.

REFERENCES

- Li, W., Tu, D., Brunger, A.T. and Ye, Y. (2007). "A ubiquitin ligase transfers preformed polyubiquitin chains from a conjugating enzyme to a substrate." *Nature* 446(7133): 333-7.
- Li, Z., Arnaud, L., Rockwell, P. and Figueiredo-Pereira, M.E. (2004). "A single amino acid substitution in a proteasome subunit triggers aggregation of ubiquitinated proteins in stressed neuronal cells." *J Neurochem* 90(1): 19-28.
- Lim, K.L., Chew, K.C., Tan, J.M., Wang, C., Chung, K.K., Zhang, Y., Tanaka, Y., Smith, W., Engeler, S., Ross, C.A., Dawson, V.L. and Dawson, T.M. (2005). "Parkin mediates nonclassical, proteasomal-independent ubiquitination of synphilin-1: implications for Lewy body formation." *J Neurosci* 25(8): 2002-9.
- Lindsten, K. and Dantuma, N.P. (2003). "Monitoring the ubiquitin/proteasome system in conformational diseases." *Ageing Res Rev* 2(4): 433-49.
- Lindsten, K., de Vrij, F.M., Verhoef, L.G., Fischer, D.F., van Leeuwen, F.W., Hol, E.M., Masucci, M.G. and Dantuma, N.P. (2002). "Mutant ubiquitin found in neurodegenerative disorders is a ubiquitin fusion degradation substrate that blocks proteasomal degradation." *J Cell Biol* 157(3): 417-27.
- Lindsten, K., Menendez-Benito, V., Masucci, M.G. and Dantuma, N.P. (2003). "A transgenic mouse model of the ubiquitin/proteasome system." *Nat Biotechnol* 21(8): 897-902.
- Liu, Y., Fallon, L., Lashuel, H.A., Liu, Z. and Lansbury, P.T. (2002). "The UCH-L1 Gene Encodes Two Opposing Enzymatic Activities that Affect alpha-Synuclein Degradation and Parkinson's Disease Susceptibility." *Cell* 111(2): 209-18.
- Lockhart, P.J., O'Farrell, C.A. and Farrer, M.J. (2004). "It's a double knock-out! The quaking mouse is a spontaneous deletion of parkin and parkin co-regulated gene (PACRG)." *Mov Disord* 19(1): 101-4.
- Lopez Salon, M., Morelli, L., Castano, E.M., Soto, E.F. and Pasquini, J.M. (2000). "Defective ubiquitination of cerebral proteins in Alzheimer's disease." *J Neurosci Res* 62(2): 302-10.
- Lopez Salon, M., Pasquini, L., Besio Moreno, M., Pasquini, J.M. and Soto, E. (2003). "Relationship between beta-amyloid degradation and the 26S proteasome in neural cells." *Exp Neurol* 180(2): 131-43.
- Luker, G.D., Pica, C.M., Song, J., Luker, K.E. and Piwnica-Worms, D. (2003). "Imaging 26S proteasome activity and inhibition in living mice." *Nat Med* 9(7): 969-73.
- Ma, J. and Lindquist, S. (2002). "Conversion of PrP to a self-perpetuating PrPSc-like conformation in the cytosol." *Science* 298(5599): 1785-8.
- Ma, J., Wollmann, R. and Lindquist, S. (2002). "Neurotoxicity and neurodegeneration when PrP accumulates in the cytosol." *Science* 298(5599): 1781-5.
- Mani, A. and Gelmann, E.P. (2005). "The ubiquitin-proteasome pathway and its role in cancer." *J Clin Oncol* 23(21): 4776-89.
- Maren, S. (2001). "Neurobiology of Pavlovian fear conditioning." *Annu Rev Neurosci* 24(1): 897-931.
- Martin, S., Gee, J.R., Bruce-Keller, A.J. and Keller, J.N. (2004). "Loss of an individual proteasome sub-unit alters motor function but not cognitive function or ambulation in mice." *Neurosci Lett* 357(1): 76-8.
- Martin, S.J. and Morris, R.G. (2002). "New life in an old idea: the synaptic plasticity and memory hypothesis revisited." *Hippocampus* 12(5): 609-36.
- Matsumoto, M., Yada, M., Hatakeyama, S., Ishimoto, H., Tanimura, T., Tsuji, S., Kakizuka, A., Kitagawa, M. and Nakayama, K.I. (2004). "Molecular clearance of ataxin-3 is regulated by a mammalian E4." *Embo J* 23(3): 659-69.
- Mayford, M., Bach, M.E., Huang, Y.Y., Wang, L., Hawkins, R.D. and Kandel, E.R. (1996). "Control of memory formation through regulated expression of a CaMKII transgene." *Science* 274(5293): 1678-83.
- Mayford, M., Wang, J., Kandel, E.R. and O'Dell, T.J. (1995). "CaMKII regulates the frequency-response function of hippocampal synapses for the production of both LTD and LTP." *Cell* 81(6): 891-904.
- McConlogue, L., Buttini, M., Anderson, J.P., Brigham, E.F., Chen, K.S., Freedman, S.B., Games, D., Johnson-Wood, K., Lee, M., Zeller, M., Liu, W., Motter, R. and Sinha, S. (2007). "Partial reduction of BACE1 has dramatic effects on Alzheimer plaque and synaptic pathology in APP Transgenic Mice." *J Biol Chem* 282(36): 26326-34.
- McGowan, E., Eriksen, J. and Hutton, M. (2006). "A decade of modeling Alzheimer's disease in transgenic mice." *Trends Genet* 22(5): 281-9.

- McNaught, K.S., Belizaire, R., Isaacson, O., Jenner, P. and Olanow, C.W. (2003). "Altered proteasomal function in sporadic Parkinson's disease." *Exp Neurol* 179(1): 38-46.
- McNaught, K.S., Belizaire, R., Jenner, P., Olanow, C.W. and Isaacson, O. (2002). "Selective loss of 20S proteasome alpha-subunits in the substantia nigra pars compacta in Parkinson's disease." *Neurosci Lett* 326(3): 155-8.
- McNaught, K.S., Bjorklund, L.M., Belizaire, R., Isaacson, O., Jenner, P. and Olanow, C.W. (2002). "Proteasome inhibition causes nigral degeneration with inclusion bodies in rats." *Neuroreport* 13 (11): 1437-41.
- McNaught, K.S., Jackson, T., JnoBaptiste, R., Kapustin, A. and Olanow, C.W. (2006). "Proteasomal dysfunction in sporadic Parkinson's disease." *Neurology* 66(10 Suppl 4): S37-49.
- McNaught, K.S. and Jenner, P. (2001). "Proteasomal function is impaired in substantia nigra in Parkinson's disease." *Neurosci Lett* 297(3): 191-4.
- McNaught, K.S., Mytilineou, C., JnobaPbistre, R., Yabut, J., Shashidharan, P., Jennert, P. and Olanow, C.W. (2002). "Impairment of the ubiquitin-proteasome system causes dopaminergic cell death and inclusion body formation in ventral mesencephalic cultures." *J Neurochem* 81(2): 301-6.
- McNaught, K.S., Perl, D.P., Brownell, A.L. and Olanow, C.W. (2004). "Systemic exposure to proteasome inhibitors causes a progressive model of Parkinson's disease." *Ann Neurol* 56(1): 149-62.
- McPhaul, L.W., Wang, J., Hol, E.M., Sonnemann, M.A., Riley, N., Nguyen, V., Yuan, Q.X., Lue, Y.H., Van Leeuwen, F.W. and French, S.W. (2002). "Molecular misreading of the ubiquitin B gene and hepatic mallory body formation." *Gastroenterology* 122(7): 1878-85.
- Meinnel, T., Serero, A. and Giglione, C. (2006). "Impact of the N-terminal amino acid on targeted protein degradation." *Biol Chem* 387(7): 839-51.
- Menendez-Benito, V., Verhoef, L.G., Masucci, M.G. and Dantuma, N.P. (2005). "Endoplasmic reticulum stress compromises the ubiquitin-proteasome system." *Hum Mol Genet* 14(19): 2787-99.
- Meng, L., Mohan, R., Kwok, B.H., Elofsson, M., Sin, N. and Crews, C.M. (1999). "Epoxomicin, a potent and selective proteasome inhibitor, exhibits in vivo antiinflammatory activity." *Proc Natl Acad Sci U S A* 96(18): 10403-8.
- Messier, C. and Gagnon, M. (1996). "Glucose regulation and cognitive functions: relation to Alzheimer's disease and diabetes." *Behav Brain Res* 75(1-2): 1-11.
- Meusser, B., Hirsch, C., Jarosch, E. and Sommer, T. (2005). "ERAD: the long road to destruction." *Nat Cell Biol* 7(8): 766-72.
- Meyer-Luehmann, M., Spires-Jones, T.L., Prada, C., Garcia-Alloza, M., de Calignon, A., Rozkalne, A., Koenigsknecht-Talbot, J., Holtzman, D.M., Bacska, B.J. and Hyman, B.T. (2008). "Rapid appearance and local toxicity of amyloid-beta plaques in a mouse model of Alzheimer's disease." *Nature* 451(7179): 720-4.
- Mielke, R., Schroder, R., Fink, G.R., Kessler, J., Herholz, K. and Heiss, W.D. (1996). "Regional cerebral glucose metabolism and postmortem pathology in Alzheimer's disease." *Acta Neuropathol (Berl)* 91 (2): 174-9.
- Miller, V.M., Nelson, R.F., Gouvier, C.M., Williams, A., Rodriguez-Lebron, E., Harper, S.Q., Davidson, B.L., Rebagliati, M.R. and Paulson, H.L. (2005). "CHIP suppresses polyglutamine aggregation and toxicity in vitro and in vivo." *J Neurosci* 25(40): 9152-61.
- Miura, K., Kishino, T., Li, E., Webber, H., Dikkes, P., Holmes, G.L. and Wagstaff, J. (2002). "Neurobehavioral and electroencephalographic abnormalities in Ube3a maternal-deficient mice." *Neurobiol Dis* 9(2): 149-59.
- Miwa, H., Kubo, T., Suzuki, A., Nishi, K. and Kondo, T. (2005). "Retrograde dopaminergic neuron degeneration following intrastriatal proteasome inhibition." *Neurosci Lett* 380(1-2): 93-8.
- Moore, D.J. (2006). "Parkin: a multifaceted ubiquitin ligase." *Biochem Soc Trans* 34(Pt 5): 749-53.
- Mori, H., Kondo, J. and Ihara, Y. (1987). "Ubiquitin is a component of paired helical filaments in Alzheimer's disease." *Science* 235(4796): 1641-4.
- Mukhopadhyay, D. and Riezman, H. (2007). "Proteasome-independent functions of ubiquitin in endocytosis and signaling." *Science* 315(5809): 201-5.
- Myat, A., Henry, P., McCabe, V., Flintoft, L., Rotin, D. and Tear, G. (2002). "Drosophila Nedd4, a ubiquitin ligase, is recruited by Commissureless to control cell surface levels of the roundabout receptor." *Neuron* 35(3): 447-59.
- Myers, K.M. and Davis, M. (2007). "Mechanisms of fear extinction." *Mol Psychiatry* 12(2): 120-50.

REFERENCES

- Myung, J., Kim, K.B. and Crews, C.M. (2001). "The ubiquitin-proteasome pathway and proteasome inhibitors." *Med Res Rev* 21(4): 245-73.
- Nagle, G.T., de Jong-Brink, M., Painter, S.D. and Li, K.W. (2001). "Structure, localization and potential role of a novel molluscan trypsin inhibitor in Lymnaea." *Eur J Biochem* 268(5): 1213-21.
- Nagy, E. and Maquat, L.E. (1998). "A rule for termination-codon position within intron-containing genes: when nonsense affects RNA abundance." *Trends Biochem Sci* 23(6): 198-9.
- Naldini, L., Blomer, U., Gallay, P., Ory, D., Mulligan, R., Gage, F.H., Verma, I.M. and Trono, D. (1996). "In vivo gene delivery and stable transduction of nondividing cells by a lentiviral vector." *Science* 272(5259): 263-7.
- Nalepa, G., Rolfe, M. and Harper, J.W. (2006). "Drug discovery in the ubiquitin-proteasome system." *Nat Rev Drug Discov* 5(7): 596-613.
- Neefjes, J. and Dantuma, N.P. (2004). "Fluorescent probes for proteolysis: tools for drug discovery." *Nat Rev Drug Discov* 3(1): 58-69.
- Nicklas, W., Baneux, P., Boot, R., Decelle, T., Deeney, A.A., Fumanelli, M. and Illgen-Wilcke, B. (2002). "Recommendations for the health monitoring of rodent and rabbit colonies in breeding and experimental units." *Lab Anim* 36(1): 20-42.
- Nicolle, M.M., Prescott, S. and Bizon, J.L. (2003). "Emergence of a cue strategy preference on the water maze task in aged C57B6 x SJL F1 hybrid mice." *Learn Mem* 10(6): 520-4.
- Nijman, S.M., Huang, T.T., Dirac, A.M., Brummelkamp, T.R., Kerkhoven, R.M., D'Andrea, A.D. and Bernards, R. (2005). "The Deubiquitinating Enzyme USP1 Regulates the Fanconi Anemia Pathway." *Mol Cell* 17(3): 331-9.
- Nijman, S.M., Luna-Vargas, M.P., Velds, A., Brummelkamp, T.R., Dirac, A.M., Sixma, T.K. and Bernards, R. (2005). "A genomic and functional inventory of deubiquitinating enzymes." *Cell* 123(5): 773-86.
- Nikulina, E.M., Skrinskaya, J.A., Avgustinovich, D.F. and Popova, N.K. (1995). "Dopaminergic brain system in the quaking mutant mouse." *Pharmacol Biochem Behav* 50(3): 333-7.
- Nixon, R.A. (2006). "Autophagy in neurodegenerative disease: friend, foe or turncoat?" *Trends Neurosci* 29(9): 528-35.
- Nunan, J., Shearman, M.S., Checler, F., Cappai, R., Evin, G., Beyreuther, K., Masters, C.L. and Small, D.H. (2001). "The C-terminal fragment of the Alzheimer's disease amyloid protein precursor is degraded by a proteasome-dependent mechanism distinct from gamma-secretase." *Eur J Biochem* 268(20): 5329-36.
- Oddo, S., Billings, L., Kesslak, J.P., Cribbs, D.H. and LaFerla, F.M. (2004). "Abeta Immunotherapy Leads to Clearance of Early, but Not Late, Hyperphosphorylated Tau Aggregates via the Proteasome." *Neuron* 43(3): 321-32.
- Oh, S., Hong, H.S., Hwang, E., Sim, H.J., Lee, W., Shin, S.J. and Mook-Jung, I. (2005). "Amyloid peptide attenuates the proteasome activity in neuronal cells." *Mech Ageing Dev* 126(12): 1292-9.
- Okada, K., Wangpoengtrakul, C., Osawa, T., Toyokuni, S., Tanaka, K. and Uchida, K. (1999). "4-Hydroxy-2-nonenal-mediated impairment of intracellular proteolysis during oxidative stress. Identification of proteasomes as target molecules." *J Biol Chem* 274(34): 23787-93.
- Olive, M., van Leeuwen, F.W., Janue, A., Moreno, D., Torrejon-Escribano, B. and Ferrer, I. (2008). "Expression of mutant ubiquitin (UBB(+1)) and p62 in myotilinopathies and desminopathies." *Neuropathol Appl Neurobiol* 34(1): 76-87.
- Osaka, H., Wang, Y.L., Takada, K., Takizawa, S., Setsuie, R., Li, H., Sato, Y., Nishikawa, K., Sun, Y.J., Sakurai, M., Harada, T., Hara, Y., Kimura, I., Chiba, S., Namikawa, K., Kiyama, H., Noda, M., Aoki, S. and Wada, K. (2003). "Ubiquitin carboxy-terminal hydrolase L1 binds to and stabilizes monoubiquitin in neuron." *Hum Mol Genet* 12(16): 1945-58.
- Palacino, J.J., Sagi, D., Goldberg, M.S., Krauss, S., Motz, C., Wacker, M., Klose, J. and Shen, J. (2004). "Mitochondrial dysfunction and oxidative damage in parkin-deficient mice." *J Biol Chem* 279(18): 18614-22.
- Pandey, U.B., Nie, Z., Batlevi, Y., McCray, B.A., Ritson, G.P., Nedelsky, N.B., Schwartz, S.L., DiProspero, N.A., Knight, M.A., Schuldiner, O., Padmanabhan, R., Hild, M., Berry, D.L., Garza, D., Hubbert, C.C., Yao, T.P., Baehrecke, E.H. and Taylor, J.P. (2007). "HDAC6 rescues neurodegeneration and provides an essential link between autophagy and the UPS." *Nature* 447(7146): 859-63.

- Pasquini, L.A., Besio Moreno, M., Adamo, A.M., Pasquini, J.M. and Soto, E.F. (2000). "Lactacystin, a specific inhibitor of the proteasome, induces apoptosis and activates caspase-3 in cultured cerebellar granule cells." *J Neurosci Res* 59(5): 601-11.
- Pastalkova, E., Serrano, P., Pinkhasova, D., Wallace, E., Fenton, A.A. and Sacktor, T.C. (2006). "Storage of spatial information by the maintenance mechanism of LTP." *Science* 313(5790): 1141-4.
- Paxinos, G. and Franklin, K.B.J. (2001). *The mouse brain in stereotaxic coordinates*. San Diego, CA, Academic Press.
- Pelzer, C., Kassner, I., Matentzoglu, K., Singh, R.K., Wollscheid, H.P., Scheffner, M., Schmidtke, G. and Groettrup, M. (2007). "UBE1L2, a novel E1 enzyme specific for ubiquitin." *J Biol Chem* 282(32): 23010-4.
- Perez, F.A. and Palmiter, R.D. (2005). "Parkin-deficient mice are not a robust model of parkinsonism." *Proc Natl Acad Sci U S A* 102(6): 2174-9.
- Periquet, M., Corti, O., Jacquier, S. and Brice, A. (2005). "Proteomic analysis of parkin knockout mice: alterations in energy metabolism, protein handling and synaptic function." *J Neurochem* 95(5): 1259-76.
- Perry, G., Friedman, R., Shaw, G. and Chau, V. (1987). "Ubiquitin is detected in neurofibrillary tangles and senile plaque neurites of Alzheimer disease brains." *Proc Natl Acad Sci U S A* 84(9): 3033-6.
- Petrucelli, L., Dickson, D., Kehoe, K., Taylor, J., Snyder, H., Grover, A., De Lucia, M., McGowan, E., Lewis, J., Prihar, G., Kim, J., Dillmann, W.H., Browne, S.E., Hall, A., Voellmy, R., Tsuboi, Y., Dawson, T.M., Wolozin, B., Hardy, J. and Hutton, M. (2004). "CHIP and Hsp70 regulate tau ubiquitination, degradation and aggregation." *Hum Mol Genet* 13(7): 703-14.
- Petrucelli, L., O'Farrell, C., Lockhart, P.J., Baptista, M., Kehoe, K., Vink, L., Choi, P., Wolozin, B., Farmer, M., Hardy, J. and Cookson, M.R. (2002). "Parkin protects against the toxicity associated with mutant alpha-synuclein: proteasome dysfunction selectively affects catecholaminergic neurons." *Neuron* 36(6): 1007-19.
- Pfeiffer, B.E. and Huber, K.M. (2006). "Current advances in local protein synthesis and synaptic plasticity." *J Neurosci* 26(27): 7147-50.
- Pickart, C.M. (2001). "Mechanisms Underlying Ubiquitination." *Annu Rev Biochem* 70: 503-33.
- Pickart, C.M. (2004). "Back to the future with ubiquitin." *Cell* 116(2): 181-90.
- Pickart, C.M. and Cohen, R.E. (2004). "Proteasomes and their kin: proteases in the machine age." *Nat Rev Mol Cell Biol* 5(3): 177-87.
- Pines, J. and Lindon, C. (2005). "Proteolysis: anytime, any place, anywhere?" *Nat Cell Biol* 7(8): 731-5.
- Planeil, E., Miyasaka, T., Launey, T., Chui, D.H., Tanemura, K., Sato, S., Murayama, O., Ishiguro, K., Tatebayashi, Y. and Takashima, A. (2004). "Alterations in glucose metabolism induce hypothermia leading to tau hyperphosphorylation through differential inhibition of kinase and phosphatase activities: implications for Alzheimer's disease." *J Neurosci* 24(10): 2401-11.
- Ponelies, N., Hirsch, T., Krehmeier, U., Denz, C., Patel, M.B. and Majetschak, M. (2005). "Cytosolic ubiquitin and ubiquitylation rates in human peripheral blood mononuclear cells during sepsis." *Shock* 24(1): 20-5.
- Puttaraparthi, K., Wojcik, C., Rajendran, B., DeMartino, G.N. and Elliott, J.L. (2003). "Aggregate formation in the spinal cord of mutant SOD1 transgenic mice is reversible and mediated by proteasomes." *J Neurochem* 87(4): 851-60.
- Qian, S.B., McDonough, H., Boellmann, F., Cyr, D.M. and Patterson, C. (2006). "CHIP-mediated stress recovery by sequential ubiquitination of substrates and Hsp70." *Nature* 440(7083): 551-5.
- Qing, H., Zhou, W., Christensen, M.A., Sun, X., Tong, Y. and Song, W. (2004). "Degradation of BACE by the ubiquitin-proteasome pathway." *Faseb J* 18(13): 1571-3.
- Qiu, J.H., Asai, A., Chi, S., Saito, N., Hamada, H. and Kirino, T. (2000). "Proteasome inhibitors induce cytochrome c-caspase-3-like protease-mediated apoptosis in cultured cortical neurons." *J Neurosci* 20(1): 259-65.
- Quinn, C.C., Gray, G.E. and Hockfield, S. (1999). "A family of proteins implicated in axon guidance and outgrowth." *J Neurobiol* 41(1): 158-64.
- Rajkumar, S.V., Richardson, P.G., Hideshima, T. and Anderson, K.C. (2005). "Proteasome inhibition as a novel therapeutic target in human cancer." *J Clin Oncol* 23(3): 630-9.
- Rattan, S.I. (1996). "Synthesis, modifications, and turnover of proteins during aging." *Exp Gerontol* 31(1-2): 33-47.

REFERENCES

- Reddy, S.K., Rape, M., Margansky, W.A. and Kirschner, M.W. (2007). "Ubiquitination by the anaphase-promoting complex drives spindle checkpoint inactivation." *Nature* 446(7138): 921-5.
- Rideout, H.J., Larsen, K.E., Sulzer, D. and Stefanis, L. (2001). "Proteasomal inhibition leads to formation of ubiquitin/alpha-synuclein-immunoreactive inclusions in PC12 cells." *J Neurochem* 78(4): 899-908.
- Robinson, S.R. (2000). "Neuronal expression of glutamine synthetase in Alzheimer's disease indicates a profound impairment of metabolic interactions with astrocytes." *Neurochem Int* 36(4-5): 471-82.
- Robinson, S.R. (2001). "Changes in the cellular distribution of glutamine synthetase in Alzheimer's disease." *J Neurosci Res* 66(5): 972-80.
- Rogers, D.C., Fisher, E.M., Brown, S.D., Peters, J., Hunter, A.J. and Martin, J.E. (1997). "Behavioral and functional analysis of mouse phenotype: SHIRPA, a proposed protocol for comprehensive phenotype assessment." *Mamm Genome* 8(10): 711-3.
- Routtenberg, A. and Rekart, J.L. (2005). "Post-translational protein modification as the substrate for long-lasting memory." *Trends Neurosci* 28(1): 12-9.
- Rustay, N.R., Wahlsten, D. and Crabbe, J.C. (2003). "Influence of task parameters on rotarod performance and sensitivity to ethanol in mice." *Behav Brain Res* 141(2): 237-49.
- Ryu, K.Y., Maehr, R., Gilchrist, C.A., Long, M.A., Bouley, D.M., Mueller, B., Ploegh, H.L. and Kopito, R.R. (2007). "The mouse polyubiquitin gene UbC is essential for fetal liver development, cell-cycle progression and stress tolerance." *Embo J* 26(11): 2693-706.
- Saigoh, K., Wang, Y.L., Suh, J.G., Yamanishi, T., Sakai, Y., Kiyosawa, H., Harada, T., Ichihara, N., Wakanishi, S., Kikuchi, T. and Wada, K. (1999). "Intragenic deletion in the gene encoding ubiquitin carboxy-terminal hydrolase in gad mice." *Nat Genet* 23(1): 47-51.
- Salehi, A. and Swaab, D.F. (1999). "Diminished neuronal metabolic activity in Alzheimer's disease." *J Neural Transm* 106(9/10): 955-86.
- Savitt, J.M., Dawson, V.L. and Dawson, T.M. (2006). "Diagnosis and treatment of Parkinson disease: molecules to medicine." *J Clin Invest* 116(7): 1744-54.
- Scheper, W. and Hol, E.M. (2005). "Protein quality control in Alzheimer's disease: a fatal saviour." *Curr Drug Targets CNS Neurol Disord* 4(3): 283-92.
- Schmidt, T., Landwehrmeyer, G.B., Schmitt, I., Trottier, Y., Auburger, G., Laccone, F., Klockgether, T., Volpel, M., Epplen, J.T., Schols, L. and Riess, O. (1998). "An isoform of ataxin-3 accumulates in the nucleus of neuronal cells in affected brain regions of SCA3 patients." *Brain Pathol* 8(4): 669-79.
- Schonberger, S.J., Edgar, P.F., Kydd, R., Faull, R.L. and Cooper, G.J. (2001). "Proteomic analysis of the brain in Alzheimer's disease: Molecular phenotype of a complex disease process." *Proteomics* 1(12): 1519-28.
- Schwartz, D.C. and Hochstrasser, M. (2003). "A superfamily of protein tags: ubiquitin, SUMO and related modifiers." *Trends Biochem Sci* 28(6): 321-8.
- Seidberg, N.A., Clark, R.S., Zhang, X., Lai, Y., Chen, M., Graham, S.H., Kochanek, P.M., Watkins, S.C. and Marion, D.W. (2003). "Alterations in inducible 72-kDa heat shock protein and the chaperone cofactor BAG-1 in human brain after head injury." *J Neurochem* 84(3): 514-21.
- Selkoe, D.J. (1991). "The molecular pathology of Alzheimer's disease." *Neuron* 6(4): 487-98.
- Selkoe, D.J. (2001). "Alzheimer's disease: genes, proteins, and therapy." *Physiol Rev* 81(2): 741-66.
- Selkoe, D.J. (2002). "Alzheimer's disease is a synaptic failure." *Science* 298(5594): 789-91.
- Semple, C.A. (2003). "The comparative proteomics of ubiquitination in mouse." *Genome Res* 13(6B): 1389-94.
- Seo, H., Sonntag, K.C. and Isacson, O. (2004). "Generalized brain and skin proteasome inhibition in Huntington's disease." *Ann Neurol* 56(3): 319-28.
- Serradj, N. and Jamon, M. (2007). "Age-related changes in the motricity of the inbred mice strains 129/sv and C57BL/6j." *Behav Brain Res* 177(1): 80-9.
- Setsuie, R., Wang, Y.L., Mochizuki, H., Osaka, H., Hayakawa, H., Ichihara, N., Li, H., Furuta, A., Sano, Y., Sun, Y.J., Kwon, J., Kabuta, T., Yoshimi, K., Aoki, S., Mizuno, Y., Noda, M. and Wada, K. (2007). "Dopaminergic neuronal loss in transgenic mice expressing the Parkinson's disease-associated UCH-L1 193M mutant." *Neurochem Int* 50(1): 119-29.
- Shevchenko, A., Wilm, M., Vorm, O. and Mann, M. (1996). "Mass spectrometric sequencing of proteins silver-stained polyacrylamide gels." *Anal Chem* 68(5): 850-8.

- Shimura, H., Schwartz, D., Gygi, S.P. and Kosik, K.S. (2004). "CHIP-Hsc70 complex ubiquitinates phosphorylated tau and enhances cell survival." *J Biol Chem* 279(6): 4869-76.
- Shin, S.J., Lee, S.E., Boo, J.H., Kim, M., Yoon, Y.D., Kim, S.I. and Mook-Jung, I. (2004). "Profiling proteins related to amyloid deposited brain of Tg2576 mice." *Proteomics* 4(11): 3359-68.
- Shringarpure, R., Grune, T., Mehlhase, J. and Davies, K.J. (2003). "Ubiquitin conjugation is not required for the degradation of oxidized proteins by proteasome." *J Biol Chem* 278(1): 311-8.
- Sidman, R.L., Dickie, M.M. and Appel, S.H. (1964). "Mutant Mice (Quaking and Jimpy) with Deficient Myelination in the Central Nervous System." *Science* 144: 309-11.
- Silva, A.J., Rosahl, T.W., Chapman, P.F., Marowitz, Z., Friedman, E., Frankland, P.W., Cestari, V., Cioffi, D., Sudhof, T.C. and Bourachuladze, R. (1996). "Impaired learning in mice with abnormal short-lived plasticity." *Curr Biol* 6(11): 1509-18.
- Silva, A.J., Simpson, E.M., Takahashi, J.S., Lipp, H.-P., Nakanishi, S., Wehner, J.M., Giese, K.P., Tully, T., Abel, T., Chapman, P.F., Fox, K., Grant, S., Itohara, S., Lathe, R., Mayford, M., McNamara, J.O., Morris, R.J., Picciotto, M., Roder, J., Shin, H.-S., Slesinger, P.A., Storm, D.R., Stryker, M.P., Tonegawa, S., Wang, Y. and Wolfer, D.P. (1997). "Mutant mice and neuroscience: recommendations concerning genetic background. Banbury Conference on genetic background in mice." *Neuron* 19(4): 755-59.
- Skovronsky, D.M., Pijak, D.S., Doms, R.W. and Lee, V.M. (2000). "A distinct ER/IC gamma-secretase competes with the proteasome for cleavage of APP." *Biochemistry* 39(4): 810-7.
- Smith, C.D., Carney, J.M., Starke-Reed, P.E., Oliver, C.N., Stadtman, E.R., Floyd, R.A. and Markesberry, W.R. (1991). "Excess brain protein oxidation and enzyme dysfunction in normal aging and in Alzheimer disease." *Proc Natl Acad Sci U S A* 88(23): 10540-3.
- Song, E.J., Kim, Y.S., Chung, J.Y., Kim, E., Chae, S.K. and Lee, K.J. (2000). "Oxidative modification of nucleoside diphosphate kinase and its identification by matrix-assisted laser desorption/ionization time-of-flight mass spectrometry." *Biochemistry* 39(33): 10090-7.
- Song, S. and Jung, Y.K. (2004). "Alzheimer's disease meets the ubiquitin-proteasome system." *Trends Mol Med* 10(11): 565-70.
- Song, S., Kim, S.Y., Hong, Y.M., Jo, D.G., Lee, J.Y., Shim, S.M., Chung, C.W., Seo, S.J., Yoo, Y.J., Koh, J.Y., Lee, M.C., Yates, A.J., Ichijo, H. and Jung, Y.K. (2003). "Essential role of E2-25K/Hip-2 in mediating amyloid-beta neurotoxicity." *Mol Cell* 12(3): 553-63.
- Spence, J., Gali, R.R., Dittmar, G., Sherman, F., Karin, M. and Finley, D. (2000). "Cell cycle-regulated modification of the ribosome by a variant multiubiquitin chain." *Cell* 102(1): 67-76.
- Stack, J.H., Whitney, M., Rodems, S.M. and Pollok, B.A. (2000). "A ubiquitin-based tagging system for controlled modulation of protein stability." *Nat Biotechnol* 18(12): 1298-302.
- Stavreva, D.A., Kawasaki, M., Dundr, M., Koberna, K., Muller, W.G., Tsujimura-Takahashi, T., Komatsu, W., Hayano, T., Isobe, T., Raska, I., Misteli, T., Takahashi, N. and McNally, J.G. (2006). "Potential roles for ubiquitin and the proteasome during ribosome biogenesis." *Mol Cell Biol* 26 (13): 5131-45.
- Stegmeier, F., Rape, M., Draviam, V.M., Nalepa, G., Sowa, M.E., Ang, X.L., McDonald, E.R., 3rd, Li, M.Z., Hannon, G.J., Sorger, P.K., Kirschner, M.W., Harper, J.W. and Elledge, S.J. (2007). "Anaphase initiation is regulated by antagonistic ubiquitination and deubiquitination activities." *Nature* 446(7138): 876-81.
- Sternberger, L.A., Hardy, P.H., Jr., Cuculis, J.J. and Meyer, H.G. (1970). "The unlabeled antibody enzyme method of immunohistochemistry: preparation and properties of soluble antigen-antibody complex (horseradish peroxidase-antihorseradish peroxidase) and its use in identification of spirochetes." *J Histochem Cytochem* 18(5): 315-33.
- Sultana, R., Boyd-Kimball, D., Cai, J., Pierce, W.M., Klein, J.B., Merchant, M. and Butterfield, D.A. (2007). "Proteomics analysis of the Alzheimer's disease hippocampal proteome." *J Alzheimers Dis* 11(2): 153-64.
- Sun, K., Johnson, B.S. and Gunn, T.M. (2007). "Mitochondrial dysfunction precedes neurodegeneration in mahogunin (Mggn1) mutant mice." *Neurobiol Aging* 28(12): 1840-52.
- Sundstrom, L., Morrison, B., 3rd, Bradley, M. and Pringle, A. (2005). "Organotypic cultures as tools for functional screening in the CNS." *Drug Discov Today* 10(14): 993-1000.
- Swaab, D.F. (1991). "Brain aging and Alzheimer's disease, "wear and tear" versus "use it or lose it"." *Neurobiol Aging* 12(4): 317-24.

REFERENCES

- Takada, K., Hibi, N., Tsukada, Y., Shibasaki, T. and Ohkawa, K. (1996). "Ability of ubiquitin radioimmunoassay to discriminate between monoubiquitin and multi-ubiquitin chains." *Biochim Biophys Acta* 1290(3): 282-8.
- Tan, Z., Sun, X., Hou, F.S., Oh, H.W., Hilgenberg, L.G., Hol, E.M., van Leeuwen, F.W., Smith, M.A., O'Dowd, D.K. and Schreiber, S.S. (2007). "Mutant ubiquitin found in Alzheimer's disease causes neuritic beading of mitochondria in association with neuronal degeneration." *Cell Death Differ* 14 (10): 1721-32.
- Taylor, J.P., Tanaka, F., Robitschek, J., Sandoval, C.M., Taye, A., Markovic-Plese, S. and Fischbeck, K.H. (2003). "Aggresomes protect cells by enhancing the degradation of toxic polyglutamine-containing protein." *Hum Mol Genet* 12(7): 749-57.
- Terni, B., Rey, M.J., Boluda, S., Torrejon-Escribano, B., Sabate, M.P., Calopa, M., van Leeuwen, F.W. and Ferrer, I. (2007). "Mutant ubiquitin and p62 immunoreactivity in cases of combined multiple system atrophy and Alzheimer's disease." *Acta Neuropathol (Berl)* 113(4): 403-16.
- Thrower, J.S., Hoffman, L., Rechsteiner, M. and Pickart, C.M. (2000). "Recognition of the polyubiquitin proteolytic signal." *Embo J* 19(1): 94-102.
- Tilleman, K., Stevens, I., Spittaels, K., Haute, C.V., Clerens, S., Van Den Berghe, G., Geerts, H., Van Leuven, F., Vandesande, F. and Moens, L. (2002). "Differential expression of brain proteins in glycogen synthase kinase-3 transgenic mice: A proteomics point of view." *Proteomics* 2(1): 94-104.
- Tilleman, K., Van Den Haute, C., Geerts, H., Leuven Fv, F., Esmans, E.L. and Moens, L. (2002). "Proteomics analysis of the neurodegeneration in the brain of tau transgenic mice." *Proteomics* 2(6): 656-65.
- Tseng, B.P., Green, K.N., Chan, J.L., Blurton-Jones, M. and Laferla, F.M. (2007). "Abeta inhibits the proteasome and enhances amyloid and tau accumulation." *Neurobiol Aging* doi:10.1016/j.neurobiolaging.2007.04.014.
- Tsirigotis, M., Tang, M.Y., Beyers, M., Zhang, M., Woulfe, J. and Gray, D.A. (2006). "Delayed spinocerebellar ataxia in transgenic mice expressing mutant ubiquitin." *Neuropathol Appl Neurobiol* 32(1): 26-39.
- Tsirigotis, M., Thurig, S., Dube, M., Vanderhyden, B.C., Zhang, M. and Gray, D.A. (2001). "Analysis of ubiquitination in vivo using a transgenic mouse model." *Biotechniques* 31(1): 120-6, 28, 30.
- Tsugita, A., Kawakami, T., Uchida, T., Sakai, T., Kamo, M., Matsui, T., Watanabe, Y., Morimasa, T., Hosokawa, K. and Toda, T. (2000). "Proteome analysis of mouse brain: two-dimensional electrophoresis profiles of tissue proteins during the course of aging." *Electrophoresis* 21(9): 1853-71.
- Tsuji, T., Shiozaki, A., Kohno, R., Yoshizato, K. and Shimohama, S. (2002). "Proteomic profiling and neurodegeneration in Alzheimer's disease." *Neurochem Res* 27(10): 1245-53.
- Valera, A.G., Diaz-Hernandez, M., Hernandez, F., Ortega, Z. and Lucas, J.J. (2005). "The ubiquitin-proteasome system in Huntington's disease." *Neuroscientist* 11(6): 583-94.
- Van Broeckhoven, C. (1998). "Alzheimer's disease: identification of genes and genetic risk factors." *Prog Brain Res* 117: 315-25.
- van Den Hurk, W.H., Willems, H.J., Bloemen, M. and Martens, G.J. (2001). "Novel frameshift mutations near short simple repeats." *J Biol Chem* 276(15): 11496-8.
- van Dijk, R., Fischer, D.F., Sluijs, J.A., Sonnemans, M.A., Hobo, B., Mercken, L., Mann, D.M., Hol, E.M. and van Leeuwen, F.W. (2004). "Frame-shifted amyloid precursor protein found in Alzheimer's disease and Down's syndrome increases levels of secreted amyloid beta40." *J Neurochem* 90(3): 712-23.
- Van Kaer, L., Ashton-Rickardt, P.G., Eichelberger, M., Gaczynska, M., Nagashima, K., Rock, K.L., Goldberg, A.L., Doherty, P.C. and Tonegawa, S. (1994). "Altered peptidase and viral-specific T cell response in LMP2 mutant mice." *Immunity* 1(7): 533-41.
- van Leeuwen, F.W., de Kleijn, D.P., van den Hurk, H.H., Neubauer, A., Sonnemans, M.A., Sluijs, J.A., Kooy, S., Ramdjielal, R.D., Salehi, A., Martens, G.J., Grosveld, F.G., Peter, J., Burbach, H. and Hol, E.M. (1998). "Frameshift mutants of beta amyloid precursor protein and ubiquitin-B in Alzheimer's and Down patients." *Science* 279(5348): 242-7.
- van Leeuwen, F.W., Fischer, D.F., Kamel, D., Sluijs, J.A., Sonnemans, M.A., Benne, R., Swaab, D.F., Salehi, A. and Hol, E.M. (2000). "Molecular misreading: a new type of transcript mutation expressed during aging." *Neurobiol Aging* 21(6): 879-91.

- Van Leeuwen, F.W., Hol, E.M., Hermanussen, R.W., Sonnemans, M.A., Moraal, E., Fischer, D.F., Evans, D.A., Chooi, K.F., Burbach, J.P. and Murphy, D. (2000). "Molecular misreading in non-neuronal cells." *Faseb J* 14(11): 1595-602.
- van Leeuwen, F.W., van Tijn, P., Sonnemans, M.A., Hobo, B., Mann, D.M., Van Broeckhoven, C., Kumar-Singh, S., Cras, P., Leuba, G., Savioz, A., Maat-Schieman, M.L., Yamaguchi, H., Kros, J.M., Kamphorst, W., Hol, E.M., de Vos, R.A. and Fischer, D.F. (2006). "Frameshift proteins in autosomal dominant forms of Alzheimer disease and other tauopathies." *Neurology* 66(2 Suppl 1): S86-92.
- van Leuven, F. (2000). "Single and multiple transgenic mice as models for Alzheimer's disease." *Prog Neurobiol* 61(3): 305-12.
- van Tijn, P., de Vrij, F.M., Schuurman, K.G., Dantuma, N.P., Fischer, D.F., van Leeuwen, F.W. and Hol, E.M. (2007). "Dose-dependent inhibition of proteasome activity by a mutant ubiquitin associated with neurodegenerative disease." *J Cell Sci* 120(Pt 9): 1615-23.
- van Tijn, P., Hobo, B., Verhage, M.C., Hol, E.M., van Leeuwen, F.W. and Fischer, D.F. (2005). Partial proteasome inhibition by aberrant ubiquitin impairs learning and memory in transgenic mice. *Neuroscience Meeting* Washington DC, 12-16 November 2005, Society for Neuroscience.
- van Tijn, P., Hol, E.M., van Leeuwen, F.W. and Fischer, D.F. (2008). "The neuronal ubiquitin-proteasome system: Murine models and their neurological phenotype." *Prog Neurobiol* 85(2): 176-93.
- van Woerden, G.M., Harris, K.D., Hojjati, M.R., Gustin, R.M., Qiu, S., de Avila Freire, R., Jiang, Y.H., Elgersma, Y. and Weeber, E.J. (2007). "Rescue of neurological deficits in a mouse model for Angelman syndrome by reduction of alphaCaMKII inhibitory phosphorylation." *Nat Neurosci* 10(3): 280-2.
- Verhoef, L.G., Lindsten, K., Masucci, M.G. and Dantuma, N.P. (2002). "Aggregate formation inhibits proteasomal degradation of polyglutamine proteins." *Hum Mol Genet* 11(22): 2689-700.
- Verma, P., Chierzi, S., Codd, A.M., Campbell, D.S., Meyer, R.L., Holt, C.E. and Fawcett, J.W. (2005). "Axonal protein synthesis and degradation are necessary for efficient growth cone regeneration." *J Neurosci* 25(2): 331-42.
- Verma, R., Aravind, L., Oania, R., McDonald, W.H., Yates, J.R., 3rd, Koonin, E.V. and Deshaies, R.J. (2002). "Role of Rpn11 metalloprotease in deubiquitination and degradation by the 26S proteasome." *Science* 298(5593): 611-5.
- von Bohlen und Halbach, O., Zacher, C., Gass, P. and Unsicker, K. (2006). "Age-related alterations in hippocampal spines and deficiencies in spatial memory in mice." *J Neurosci Res* 83(4): 525-31.
- Von Coelln, R., Thomas, B., Savitt, J.M., Lim, K.L., Sasaki, M., Hess, E.J., Dawson, V.L. and Dawson, T.M. (2004). "Loss of locus coeruleus neurons and reduced startle in parkin null mice." *Proc Natl Acad Sci U S A* 101(29): 10744-9.
- Walsh, D.M. and Selkoe, D.J. (2004). "Deciphering the molecular basis of memory failure in Alzheimer's disease." *Neuron* 44(1): 181-93.
- Wang, Q., Woltjer, R.L., Cimino, P.J., Pan, C., Montine, K.S., Zhang, J. and Montine, T.J. (2005). "Proteomic analysis of neurofibrillary tangles in Alzheimer disease identifies GAPDH as a detergent-insoluble paired helical filament tau binding protein." *Faseb J* 19(7): 869-71.
- Warrick, J.M., Morabito, L.M., Bilen, J., Gordesky-Gold, B., Faust, L.Z., Paulson, H.L. and Bonini, N.M. (2005). "Ataxin-3 suppresses polyglutamine neurodegeneration in Drosophila by a ubiquitin-associated mechanism." *Mol Cell* 18(1): 37-48.
- Warrington, J.A., Nair, A., Mahadevappa, M. and Tsyganskaya, M. (2000). "Comparison of human adult and fetal expression and identification of 535 housekeeping/maintenance genes." *Physiol Genomics* 2: 143-47.
- Watts, R.J., Hooper, E.D. and Luo, L. (2003). "Axon Pruning during Drosophila Metamorphosis. Evidence for Local Degeneration and Requirement of the Ubiquitin-Proteasome System." *Neuron* 38 (6): 871-85.
- Weeber, E.J., Jiang, Y.H., Elgersma, Y., Varga, A.W., Carrasquillo, Y., Brown, S.E., Christian, J.M., Mirnikjoo, B., Silva, A., Beaudet, A.L. and Sweatt, J.D. (2003). "Derangements of hippocampal calcium/calmodulin-dependent protein kinase II in a mouse model for Angelman mental retardation syndrome." *J Neurosci* 23(7): 2634-44.
- Weissman, A.M. (2001). "Themes and variations on ubiquitylation." *Nat Rev Mol Cell Biol* 2(3): 169-78.

REFERENCES

- Welchman, R.L., Gordon, C. and Mayer, R.J. (2005). "Ubiquitin and ubiquitin-like proteins as multifunctional signals." *Nat Rev Mol Cell Biol* 6(8): 599-609.
- Whitlock, J.R., Heynen, A.J., Shuler, M.G. and Bear, M.F. (2006). "Learning induces long-term potentiation in the hippocampus." *Science* 313(5790): 1093-7.
- Wilkinson, K.D., Tashayev, V.L., O'Connor, L.B., Larsen, C.N., Kasperek, E. and Pickart, C.M. (1995). "Metabolism of the polyubiquitin degradation signal: structure, mechanism, and role of isopeptidase T." *Biochemistry* 34(44): 14535-46.
- Wills, N.M. and Atkins, J.F. (2006). "The potential role of ribosomal frameshifting in generating aberrant proteins implicated in neurodegenerative diseases." *Rna* 12(7): 1149-53.
- Wilson, S.M., Bhattacharyya, B., Rachel, R.A., Coppola, V., Tessarollo, L., Householder, D.B., Fletcher, C.F., Miller, R.J., Copeland, N.G. and Jenkins, N.A. (2002). "Synaptic defects in ataxia mice result from a mutation in Usp14, encoding a ubiquitin-specific protease." *Nat Genet* 32(3): 420-5.
- Wojcik, C. and DeMartino, G.N. (2003). "Intracellular localization of proteasomes." *Int J Biochem Cell Biol* 35(5): 579-89.
- Wolf, D.H. and Hilt, W. (2004). "The proteasome: a proteolytic nanomachine of cell regulation and waste disposal." *Biochim Biophys Acta* 1695(1-3): 19-31.
- Wong, P.C., Cai, H., Borchelt, D.R. and Price, D.L. (2002). "Genetically engineered mouse models of neurodegenerative diseases." *Nat Neurosci* 5(7): 633-9.
- Wood, M.A., Kaplan, M.P., Brensinger, C.M., Guo, W. and Abel, T. (2005). "Ubiquitin C-terminal hydrolase L3 (UCHL3) is involved in working memory." *Hippocampus* 15(5): 610-21.
- Wu, J., Ichihara, N., Chui, D.H., Yamazaki, K., Wakabayashi, T. and Kikuchi, T. (1996). "Abnormal ubiquitination of dystrophic axons in central nervous system of gracile axonal dystrophy (GAD) mutant mouse." *Alzheimer's Res* 2(5): 163-68.
- Wu, S.S., de Chadarevian, J.P., McPhaul, L., Riley, N.E., van Leeuwen, F.W. and French, S.W. (2002). "Coexpression and accumulation of ubiquitin +1 and ZZ proteins in livers of children with alpha(1)-antitrypsin deficiency." *Pediatr Dev Pathol* 5(3): 293-8.
- Yamazaki, K., Wakasugi, N., Tomita, T., Kikuchi, T., Mukoyama, M. and Ando, K. (1988). "Gracile axonal dystrophy (GAD), a new neurological mutant in the mouse." *Proc Soc Exp Biol Med* 187(2): 209-15.
- Yao, T. and Cohen, R.E. (2002). "A cryptic protease couples deubiquitination and degradation by the proteasome." *Nature* 419(6905): 403-7.
- Yedidia, Y., Horonchik, L., Tzabari, S., Yanai, A. and Taraboulos, A. (2001). "Proteasomes and ubiquitin are involved in the turnover of the wild-type prion protein." *Embo J* 20(19): 5383-91.
- Yew, E.H., Cheung, N.S., Choy, M.S., Qi, R.Z., Lee, A.Y., Peng, Z.F., Melendez, A.J., Manikandan, J., Koay, E.S., Chiu, L.L., Ng, W.L., Whiteman, M., Kandiah, J. and Halliwell, B. (2005). "Proteasome inhibition by lactacystin in primary neuronal cells induces both potentially neuroprotective and pro-apoptotic transcriptional responses: a microarray analysis." *J Neurochem* 94(4): 943-56.
- Yi, J.J. and Ehlers, M.D. (2005). "Ubiquitin and protein turnover in synapse function." *Neuron* 47(5): 629-32.
- Yi, J.J. and Ehlers, M.D. (2007). "Emerging roles for ubiquitin and protein degradation in neuronal function." *Pharmacol Rev* 59(1): 14-39.
- Yoshida, H., Watanabe, A. and Ihara, Y. (1998). "Collapsin response mediator protein-2 is associated with neurofibrillary tangles in Alzheimer's disease." *J Biol Chem* 273(16): 9761-8.
- Young, P., Deveraux, Q., Beal, R.E., Pickart, C.M. and Rechsteiner, M. (1998). "Characterization of two polyubiquitin binding sites in the 26 S protease subunit 5a." *J Biol Chem* 273(10): 5461-7.
- Zarow, C., Lyness, S.A., Mortimer, J.A. and Chui, H.C. (2003). "Neuronal loss is greater in the locus coeruleus than nucleus basalis and substantia nigra in Alzheimer and Parkinson diseases." *Arch Neurol* 60(3): 337-41.
- Zeng, B.Y., Medhurst, A.D., Jackson, M., Rose, S. and Jenner, P. (2005). "Proteasomal activity in brain differs between species and brain regions and changes with age." *Mech Ageing Dev* 126(6-7): 760-6.
- Zhang, M., Thuring, S., Tsirigotis, M., Wong, P.K., Reuhl, K.R. and Gray, D.A. (2003). "Effects of mutant ubiquitin on ts1 retrovirus-mediated neuropathology." *J Virol* 77(13): 7193-201.

REFERENCES

- Zoghbi, H.Y. and Orr, H.T. (2000). "Glutamine repeats and neurodegeneration." *Annu Rev Neurosci* 23: 217-47.
- Zouamibia, M., Fischer, D.F., Hobo, B., De Vos, R.A., Hol, E.M., Varndell, I.M., Sheppard, P.W. and Van Leeuwen, F.W. (2008). "Proteasome subunit proteins and neuropathology in tauopathies and synucleinopathies: Consequences for proteomic analyses." *Proteomics* 8(6): 1221-36.
- Zucker, R.S. and Regehr, W.G. (2002). "Short-term synaptic plasticity." *Annu Rev Physiol* 64: 355-405.

Color Figures

Color Figures

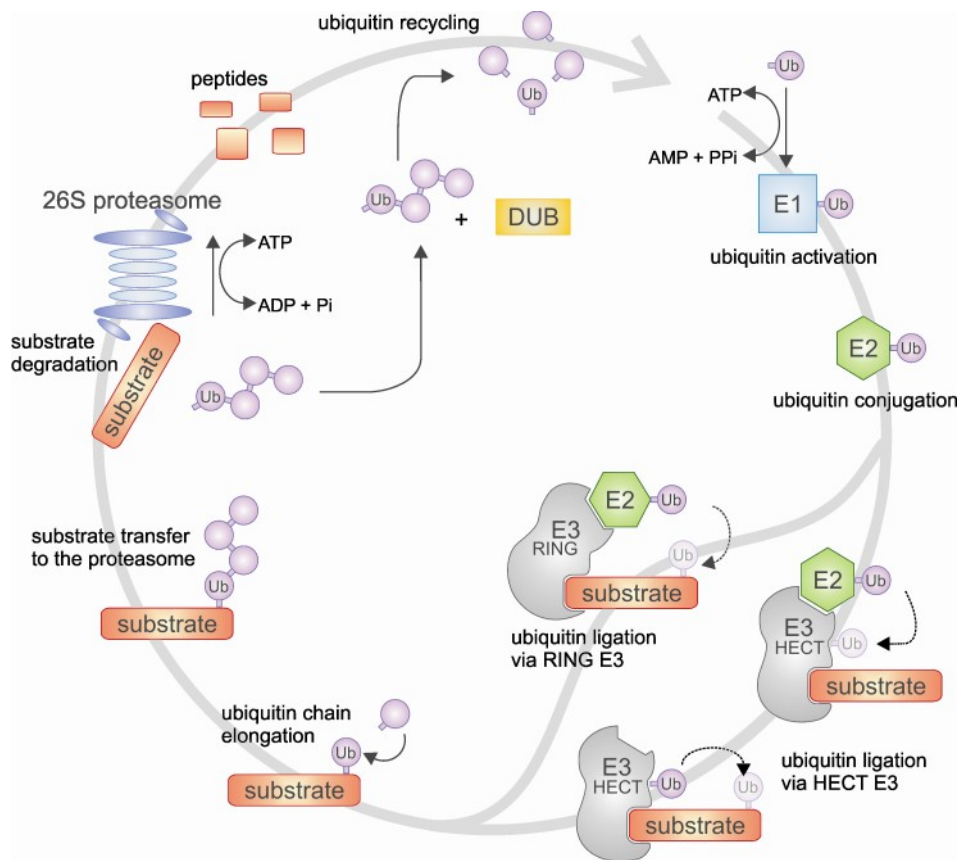


Figure 1 *Ubiquitination cascade and proteasomal degradation.* Ubiquitin (purple sphere) is activated by the E1 ubiquitin activating enzyme and transferred to a ubiquitin carrier, the E2 ubiquitin conjugating enzyme. Protein substrates to be targeted for degradation by the proteasome are recognized by one of the E3 ubiquitin ligase enzymes. In the case of RING-E3 ligases, the ubiquitin is directly transferred from the E3-bound E2 enzyme to a lysine residue in the substrate. For HECT-E3 enzymes, the ubiquitin is first transferred from the E2 to the E3 ligase and is subsequently attached to the substrate. Successive ubiquitin moieties are attached to the substrate-bound ubiquitin, forming a ubiquitin chain. With a K48-linked polyubiquitin chain of four or more ubiquitins the substrate is targeted to the 26S proteasome. Here, the ubiquitin chain is released and the substrate is degraded into small peptides by the 26S proteasome. Finally, the ubiquitin is recycled by release of free monomeric ubiquitin from the ubiquitin chain, an activity mediated by DUBs (Chapter 1).

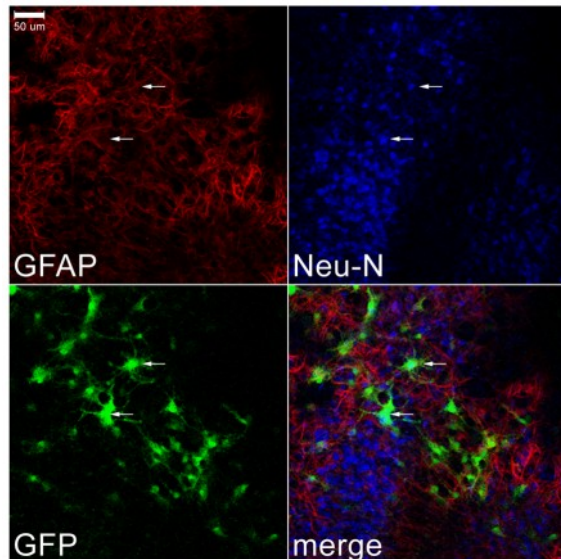


Figure 4 Lentiviral transduction targets a heterogeneous cell population in cortex slice cultures. GFAP (red) and NeuN (blue) double staining on LV-Ub-M-GFP transduced organotypic cortex slice cultures of C57Bl/6 mice revealed mostly GFAP labelled GFP positive glia, but also GFP positive neurons. Arrows indicate transduced neurons, positive for both GFP and NeuN. Bar, 50 μm (Chapter 2).

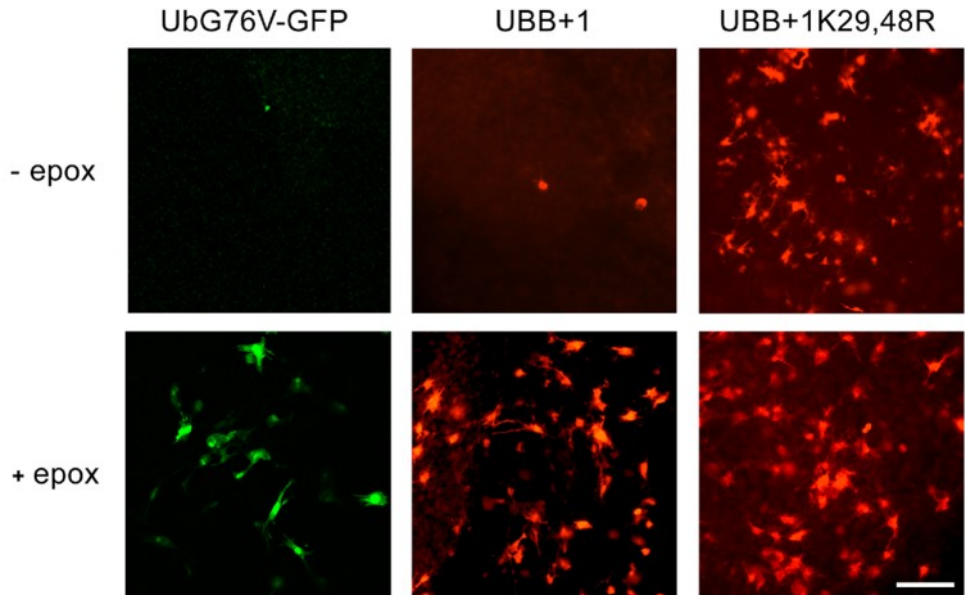


Figure 5 UBB^{+1} is degraded by the proteasome in cortex slice cultures. Organotypic cortex slices of C57Bl/6 mice were transduced with LV-Ub^{G76V}-GFP, LV-UBB⁺¹ or LV-UBB^{+1K29,48R}. Both the UPS reporter protein Ub^{G76V}-GFP (green) and UBB⁺¹ (red) are efficiently degraded by the 26S proteasome and only accumulate after treatment with proteasome inhibitor. The lysine mutant of UBB⁺¹, UBB^{+1K29,48R}, is not degraded by the proteasome and accumulates already without inhibitor treatment; - epox: not treated with epoxomicin, + epox: treated overnight with 1 μ M epoxomicin. Bar, 100 μ m (Chapter 2).

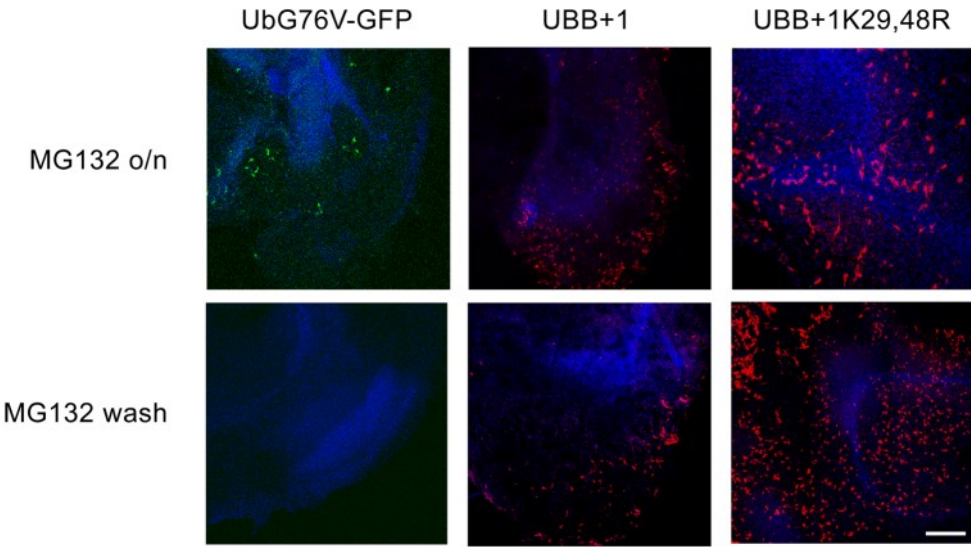


Figure 6 *UBB⁺¹ remains present after washout of inhibitor in cortex slice cultures.* Overnight incubation of cortex cultures transduced with LV-Ub^{G76V}-GFP or LV-UBB⁺¹ with the reversible proteasome inhibitor MG132 (10 μ M) resulted in accumulation of both proteins. Washing out the reversible inhibitor reactivated the proteasome, as shown by the degradation of the proteasome reporter substrate Ub^{G76V}-GFP. However, UBB⁺¹ remained accumulated in a considerable amount of cells after reactivation of the proteasome. Transduction with the LV- UBB^{+1K29,48R} control construct gave rise to accumulation of the UBB⁺¹ protein regardless of proteasome inhibitor treatment. Ub^{G76V}-GFP is depicted in green, UBB⁺¹ in red and the nuclear staining (TO-PRO) in blue. Bar, 500 μ m (Chapter 2).

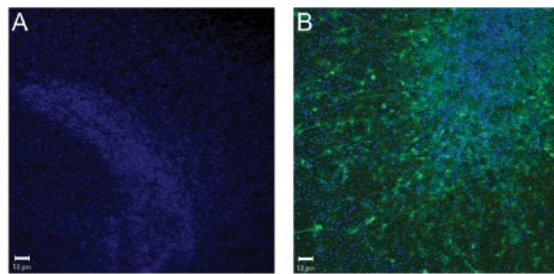


Figure 7 The UPS reporter system in cortex cultures of Ub^{G76V} -GFP transgenic mice. A: Ub^{G76V} -GFP tg organotypic cortex cultures without treatment with proteasome inhibitors. B: Ub^{G76V} -GFP tg cortex cultures treated with 1 μ M epoxomicin. The GFP-reporter substrate only accumulated after proteasome inhibition. Bars, 50 μ m (Chapter 2).

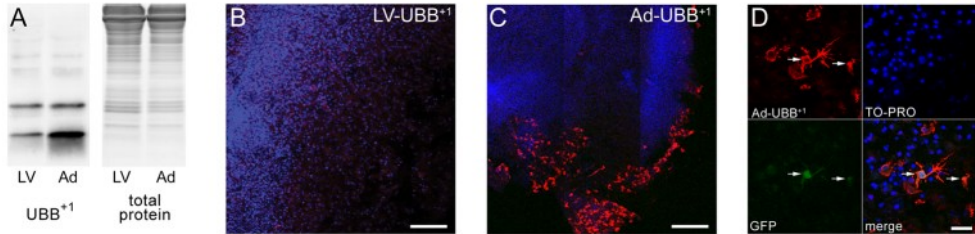


Figure 8 High Ad-UBB⁺¹ expression causes proteasome inhibition in cortex cultures. High levels of UBB⁺¹ expression with Ad-UBB⁺¹ lead to accumulation of UBB⁺¹ without inhibitor treatment. A: Representative Westernblot of HEK293 cell lysates transduced with equal MOI of LV-UBB⁺¹ (left lane) or Ad-UBB⁺¹ (right lane). Equal amounts of protein were loaded per lane, as confirmed by Coomassie staining of total protein load of the same lanes shown on the right. The blot was stained with anti-UBB⁺¹ antibody Ub3 and quantified with Imagepro software (quantification not shown). B, C: Organotypic cortex slice cultures of Ub^{G76V} -GFP tg mice were transduced with LV-UBB⁺¹, which did not induce UBB⁺¹ accumulation (B) or Ad-UBB⁺¹, which did result in many UBB⁺¹ immuno-positive cells (C). D: UBB⁺¹ accumulation after adenoviral transduction lead to accumulation of Ub^{G76V} -GFP (arrows). Bars, 250 μ m (B), 500 μ m (C), 50 μ m (D) (Chapter 2).

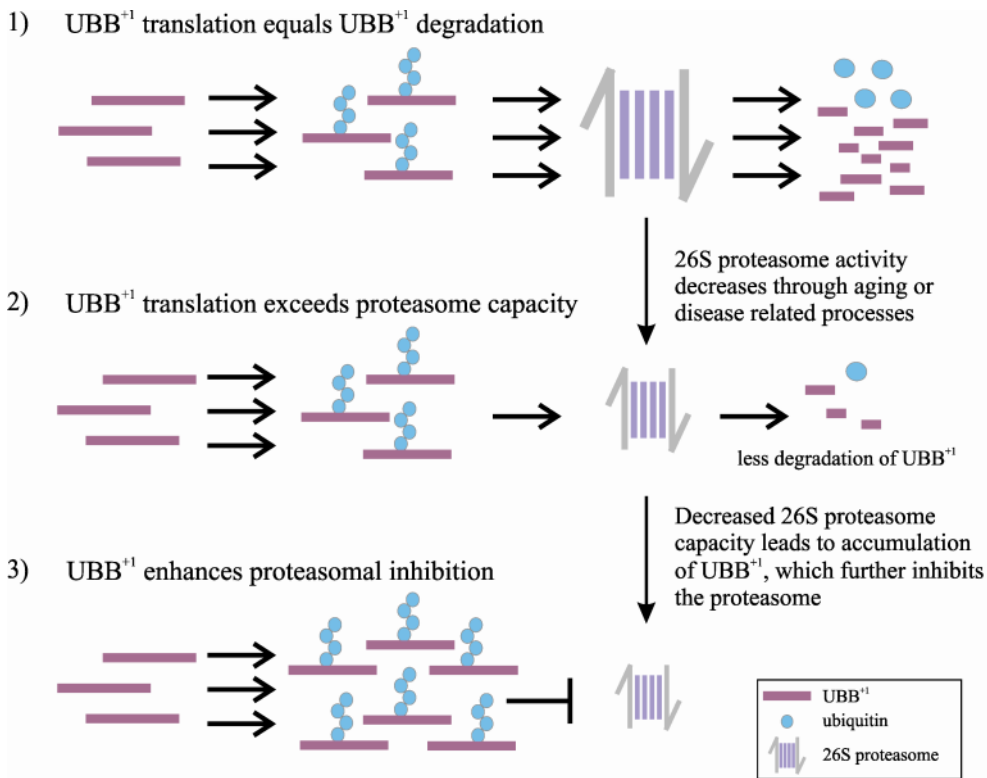


Figure 9 UBB^{+1} properties shift from UPS substrate to inhibitor. (1) UBB^{+1} mRNA and translation levels are constant throughout life (Fischer et al., 2003; Gerez et al., 2005). In non-diseased tissue, the 26S proteasome is capable of degrading all the translated UBB^{+1} and accumulation of UBB^{+1} is not present. (2) Due to various causes such as disease or aging the efficiency of proteasomal degradation can decrease, leading to a diminished degradation of UBB^{+1} . (3) The levels of translated UBB^{+1} exceed the degradation capacity of the proteasome and surpasses the accumulation threshold. Accumulated UBB^{+1} now holds UPS inhibitory properties itself, which can aggravate the initial decrease in UPS activity (Chapter 2).

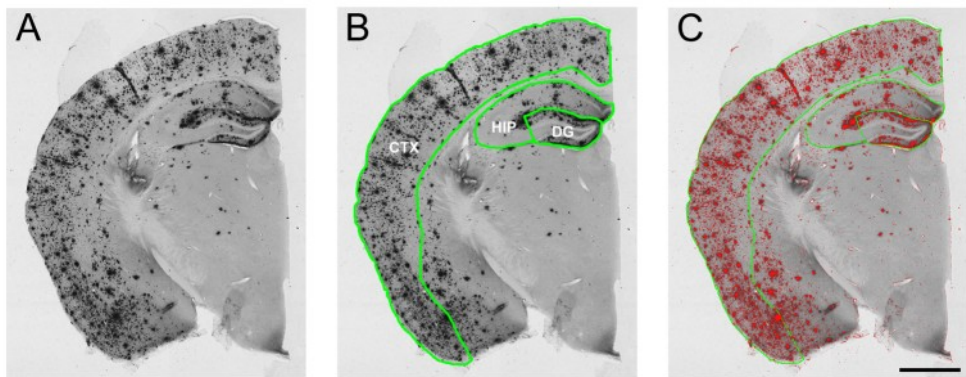


Figure S3 *A β plaque load measurement.* Example of computer automated measurement of the amyloid plaque load in a 11-month old APPPS1 transgenic mouse at -1.82 anterior-posterior from bregma. First, 50 μ m coronal sections were stained with 6E10 anti-amyloid antibody (A). The sampled brain areas, cortex (CTX), hippocampus (HIP) and dentate gyrus (DG), were outlined by hand, outlines are shown in green (B). Overlay in (C) shows the 6E10 stained section overlaid by the computer automated measurement of A β plaque covered area shown in red (C). Scale bar = 1 mm (Chapter 6).

Summary

The ubiquitin-proteasome system (UPS) is the main intracellular regulated pathway for degradation of substrate proteins and, being one of the main cellular protein quality control systems, is essential for cell viability and maintaining proteostasis. Malfunction of this system is implicated to play a role in a broad array of diseases pathologically characterized by ubiquitin-positive deposits. The aberrant ubiquitin UBB⁺¹ is present in the neuro-pathological hallmarks of a subset of these diseases, including Alzheimer's disease and Huntington's disease, providing compelling evidence that UPS malfunction can contribute to the pathological cascade leading to (neuro-) pathology. *In vitro*, UBB⁺¹ acts as a potent inhibitor of the UPS when expressed at high levels. In this thesis, we aimed to further dissect the UPS-related properties of UBB⁺¹. Furthermore, we studied the effects of varying levels of UBB⁺¹ expression, and the concomitant proteasome inhibition *in vivo*, employing novel UBB⁺¹ transgenic mouse models. **Chapter 1** gives a comprehensive overview of the UPS and its role in neurodegenerative disease. In addition, the currently available murine models with altered components of the UPS leading to neurological deficits are reviewed.

The aim of the research described in **Chapter 2** was to further characterize the UPS-related properties of UBB⁺¹. UBB⁺¹ has seemingly opposing properties *in vitro*; UBB⁺¹ is a substrate for proteasomal degradation as well as an inhibitor of the UPS. In this study, we showed that UBB⁺¹ properties shift from proteasome substrate to inhibitor in a dose-dependent manner in cell culture using an inducible UBB⁺¹ expression system. This finding was confirmed in mouse organotypic cortex slice cultures. Based on this study combined with previous findings, we hypothesize that in the human brain, once the level of UBB⁺¹ protein has surpassed a threshold level of expression, UBB⁺¹ induced UPS inhibition can contribute to disease progression. Using the dual UPS proteasome substrate/inhibitory properties, UBB⁺¹ can serve as research tool to study the ubiquitin-proteasome system and to further elucidate the role of aberrations of this pathway in disease.

In **Chapter 3**, the effects of high levels of UBB⁺¹ expression are studied *in vivo*. To this end, two transgenic mouse lines were generated, which postnatally express high levels of UBB⁺¹ under the neuronal CaMKinaseIIα (line 3413) or the Thy1.2 (line 8630) promoter. In both lines, UBB⁺¹ protein expression was present mainly in the cortex and hippocampus. Increased levels of ubiquitinated proteins were detected in the cortex, suggesting inhibition of the UPS. Indeed, chymotryptic proteasome activity was decreased in the cortex of line 3413 mice. Despite this low-level chronic UPS inhibition, these mice did not show an overt neurological phenotype. However, deficits in contextual memory in both Morris watermaze and fear conditioning paradigms were present at the age of 9 months. Furthermore, proteomic analysis of these mice showed a remarkable overlap with changes in the brain proteome reported in Alzheimer's patients and in Alzheimer mouse models. These UBB⁺¹ transgenic mouse models provide new tools to understand how the

UPS is involved in neurodegenerative pathology and memory formation. In addition, these UBB⁺¹ transgenic lines serve as model for life-long neuronal modest UPS inhibition.

Chapter 4 describes the generation and characterization of a transgenic mouse model (line 6663) neuronally expressing low levels of UBB⁺¹. In this mouse line, UBB⁺¹ protein was detected at very low levels. Via intracranial infusion of different classes of proteasome inhibitors into the hippocampus, we showed that UBB⁺¹ protein accumulated only when proteasome inhibitor was administrated. These *in vivo* results confirm our previous *in vitro* data, as presented in Chapter 2, showing that UBB⁺¹ is a substrate for proteasomal degradation at low expression levels and only accumulates after inhibition of the UPS. This transgenic mouse model can serve as a model system to further elucidate the properties of UBB⁺¹ and to study its role in neurodegenerative disease. Furthermore, this mouse model can serve as a reporter line for UPS inhibition associated with disease, employing a natural substrate rather than the widely used artificial fluorescent reporters currently used by the research community.

Chapter 5 describes the effect of low-level UPS inhibition of cognitive function. The UPS plays an important role in synaptic plasticity and learning and memory formation in the adult nervous system. We hypothesized that proteasome inhibition induced by UBB⁺¹ expression would thus lead to a decreased cognitive function. Indeed, we showed that UBB⁺¹ transgenic mice showed a defect in spatial reference memory in the Morris water-maze at 15 months of age. The UBB⁺¹ transgenic mice did not display further gross neurological abnormalities or alterations in procedural (motor-) learning and motor coordination up to 24 months of age. From these results, we conclude that the spatial reference memory deficits detected in UBB⁺¹ transgenic mice at 9 months, as described in Chapter 3, persist, but are not aggravated during aging. In addition, these results demonstrate that intact forebrain proteasome function is essential for maintenance of spatial reference memory formation.

Chapter 6 reports on the effects of UBB⁺¹ induced proteasome inhibition on Alzheimer related neuropathology, i.e. Aβ deposition, as well as the effects of Aβ deposition on UBB⁺¹ accumulation *in vivo*. In a novel triple transgenic mouse model, expressing UBB⁺¹ and familial Alzheimer's disease related mutant APP and PS1, we show that modest neuronal UPS inhibition induced by UBB⁺¹ expression reduced the amyloid plaque burden at the age of 6 months, without alterations in UBB⁺¹ protein levels or in the age of onset of pathology. It is conceivable that APP processing, leading to Aβ formation, is affected by proteasome inhibition, resulting in a decreased plaque burden.

Finally, in **Chapter 7**, the results obtained in the studies described in this thesis are critically discussed and suggestions for future research are provided. Additional preliminary results further elucidate the role of mutant ubiquitin and concomitant proteasome dysfunction in neurodegenerative disease.

SUMMARY

Based on the findings as presented in this thesis, we conclude that accumulation of aberrant ubiquitin and subsequent malfunction of the UPS affects protein degradation *in vitro* and *in vivo*, can lead to spatial memory deficits and interferes with Alzheimer's disease-associated amyloid pathology. The novel transgenic mouse models expressing mutant ubiquitin, as presented in Chapter 3 and Chapter 4, can contribute to dissecting the role of the UPS in a broad range of neurological diseases in future studies.

Samenvatting

De belangrijkste vorm van gereguleerde eiwitafbraak in de cel wordt gemedieerd door het ubiquitine-proteasoom systeem (UPS). Een goed functionerend UPS is voor cellen van vitaal belang, mede door de belangrijke functie die dit systeem vervult in de kwaliteitscontrole van eiwitten die betrokken zijn bij de regulatie van intracellulaire homeostase. Er zijn sterke aanwijzingen dat een afname in de activiteit van het UPS een rol speelt in de pathogenese van neuronale en niet-neuronale ziekten die gekarakteriseerd worden door ubiquitine-bevattende pathologie. In een aantal van deze ziekten, waaronder de ziekte van Alzheimer en de ziekte van Huntington, hoopt een afwijkende vorm van het eiwit ubiquitine (UBB^{+1}) zich op in de neuropathologische kenmerken van deze ziektebeelden. De aanwezigheid van UBB^{+1} hierin bevestigt het idee dat een verstoring van het UPS kan bijdragen aan de pathologische cascade die uiteindelijk resulteert in (neuro-) pathologie. Eerdere studies in gekweekte cellen hebben laten zien dat UBB^{+1} de activiteit van het proteasoom inhibeert bij een hoog expressie niveau. In dit proefschrift wordt verder onderzoek beschreven naar de UPS-gerelateerde eigenschappen van UBB^{+1} *in vitro*. Tevens werden de effecten van verschillende expressie niveaus van UBB^{+1} , en de bijbehorende inhibitie van het proteasoom, *in vivo* bestudeerd. Voor dit doeleinde zijn drie nieuwe transgene muizen lijnen ontwikkeld die UBB^{+1} tot expressie brengen in neuronen.

In **Hoofdstuk 1** wordt een overzicht gegeven van het UPS en wat de mogelijke rol van dit systeem zou kunnen zijn in neurodegeneratieve ziekten. Ook worden de huidige beschikbare muismodellen besproken waarin afwijkingen in het UPS leiden tot een neurologisch fenotype.

Het doel van het onderzoek zoals beschreven in **Hoofdstuk 2** is de karakterisatie van de UPS-gerelateerde eigenschappen van UBB^{+1} . *In vitro* zijn deze eigenschappen ogenschijnlijk tegengesteld; UBB^{+1} is een substraat voor proteasomale afbraak, terwijl het eveneens de activiteit van het proteasoom remt. In deze studie laten we zien, door gebruik te maken van een induceerbaar UBB^{+1} expressie systeem, dat deze eigenschappen van UBB^{+1} dosis-afhankelijk zijn. Bij lage niveaus van expressie wordt UBB^{+1} afgebroken door het proteasoom terwijl bij hoge expressie UBB^{+1} de activiteit van het proteasoom inhibeert. Deze bevindingen in humane celllijnen zijn daarna bevestigd in organotypische kweken van muizen cortex. Op basis van onze eerdere resultaten en de resultaten verkregen in dit onderzoek, volgt de hypothese dat in de humane hersenen, UBB^{+1} het proteasoom alleen remt, en op deze wijze kan bijdragen aan pathogenese, nadat een bepaalde expressie drempel is overschreden. Door de proteasoom substraat/remmer eigenschappen van UBB^{+1} kan de expressie van dit eiwit als experimentele methode dienen in onderzoek naar het UPS, en naar de rol van dit systeem in ziekteprocessen.

In **Hoofdstuk 3** wordt het effect van hoge UBB^{+1} expressie *in vivo* bestudeerd in twee nieuw ontwikkelde transgene muizen lijnen, die postnataal UBB^{+1} tot expressie brengen in

neuronen onder controle van de CaMKinaseII α (lijn 3413) of de Thy1.2 (lijn 8630) promoter. In beide lijnen zijn de cortex en hippocampus de voornaamste hersengebieden waarin het UBB $^{+1}$ eiwit tot expressie komt. In de cortex van de transgene muizen is de concentratie van geubiquitineerde eiwitten verhoogd, wat een aanwijzing is voor inhibitie van het UPS. Dit wordt bevestigd door een kleine verlaging van proteasoom activiteit in cortex homogenaten van lijn 3413 muizen. Ondanks deze inhibitie van het UPS vertonen de UBB $^{+1}$ muizen geen duidelijke kenmerken van neuropathologie noch van een neurologisch fenotype. Daarentegen is er wel een vermindering van het plaats-afhankelijke geheugen aanwezig in UBB $^{+1}$ transgene muizen van 9 maanden oud. De resultaten van de proteoom-analyse van UBB $^{+1}$ muizen laten een opmerkelijke gelijkenis zien met resultaten verkregen in Alzheimer patiënten en Alzheimer muismodellen. De voor deze studie ontwikkelde UBB $^{+1}$ transgene muis modellen kunnen verder bijdragen aan onderzoek naar de rol van het UPS in neurodegeneratie en geheugen processen. Ook zijn deze lijnen een uniek model voor chronische, sub-optimale neuronale UPS activiteit *in vivo*.

Hoofdstuk 4 beschrijft de ontwikkeling en karakterisatie van een UBB $^{+1}$ transgene muizenlijn die het afwijkende ubiquitine eiwit op een laag niveau tot expressie brengt in neuronen (lijn 6663). Het UBB $^{+1}$ eiwit kan slechts zeer beperkt worden gedetecteerd in deze muizen. Alleen na remming van het proteasoom, bereikt door rechtstreekse infusie van verschillende UPS remmers in de hippocampus, hoopt het UBB $^{+1}$ eiwit zich op. Hieruit kan worden geconcludeerd dat *in vivo*, UBB $^{+1}$ wordt afgebroken bij lage expressie niveaus en zich alleen ophoopt na remming van het UPS. Deze resultaten bevestigen de eerdere bevindingen *in vitro*, beschreven in Hoofdstuk 2. Deze UBB $^{+1}$ lijn kan als model worden gebruikt in toekomstig onderzoek naar de eigenschappen van UBB $^{+1}$ en de rol van dit eiwit in neurodegeneratie. Daarnaast kan deze lijn een waardevolle aanvulling zijn als UPS-reporter lijn voor neurodegeneratie-geassocieerde UPS inhibitie, waarbij ophoping van een natuurlijk UPS substraat, UBB $^{+1}$, aangeeft dat het proteasoom geremd is.

In **Hoofdstuk 5** worden de effecten van proteasoom inhibitie op cognitief functioneren beschreven. Het UPS speelt een belangrijke rol in synaptische plasticiteit en in geheugen processen in de volwassen hersenen. In dit onderzoek toetsen wij de hypothese dat proteasoom remming, geïnduceerd door UBB $^{+1}$ expressie, het cognitief vermogen aantast. In de Morris watermaze, een test voor ruimtelijk leren en geheugen, laten lijn 3413 UBB $^{+1}$ transgene muizen een verlies van ruimtelijk geheugen zien op een leeftijd van 15 maanden. Bij deze UBB $^{+1}$ transgene muizen manifesteren zich tot een leeftijd van 24 maanden geen sterke neurologische afwijkingen en motor-leren en -coördinatie zijn onaangestast. Uit dit onderzoek kan worden geconcludeerd dat het verlies van ruimtelijk geheugen, zoals beschreven in Hoofdstuk 3 voor UBB $^{+1}$ muizen van 9 maanden oud, ook op de leeftijd van 15 maanden aanwezig is, zonder te verergeren tijdens veroudering. Tevens bevestigen deze resultaten dat een intacte functie van de voorhersenen noodzakelijk is voor ruimtelijk geheugen.

De *in vivo* effecten van UBB⁺¹ geïnduceerde proteasoom remming op de vorming van Alzheimer-gerelateerde neuropathologie, met name op de vorming van de amyloïde plaques, alsmede het effect van A β depositie op UBB⁺¹ opstapeling worden beschreven in **Hoofdstuk 6**. In een transgeen muismodel, welke UBB⁺¹ en familiaire Alzheimer-gerelateerd mutant APP en PS1 tot expressie brengt, zorgt beperkte neuronale inhibitie van het proteasoom (geïnduceerd door hoge expressie van UBB⁺¹) voor een opmerkelijke en onverwachte reductie in plaque depositie op een leeftijd van 6 maanden. Zowel de stapeling van UBB⁺¹ eiwit als de leeftijd waarop de amyloidopathie start in deze dieren zijn onveranderd. Proteasoom inhibitie zou mogelijk de processing van APP tot A β kunnen verstören, en op deze wijze de hoeveelheid A β plaques kunnen verminderen.

Ten slotte worden in **Hoofdstuk 7** de resultaten zoals verkregen in dit proefschrift bediscussieerd en worden suggesties voor toekomstig onderzoek gegeven. De in dit hoofdstuk gepresenteerde (preliminaire) onderzoeksresultaten verschaffen meer inzicht in de rol van UBB⁺¹ in proteasoom dysfunctie in neurodegeneratieve ziekten.

Op grond van de bevindingen in dit proefschrift kan de conclusie worden getrokken dat stapeling van mutant ubiquitine en de bijbehorende vermindering van proteasoomactiviteit zowel *in vitro* als *in vivo* verstoringen teweeg kunnen brengen in de gereguleerde eiwitafbraak. Tevens leidt langdurige, gedeeltelijke remming van het proteasoom in neuronen tot een afname van het ruimtelijk geheugen en interfereert het met Alzheimer-gecorreleerde neuropathologie. De muismodellen die neuronaal UBB⁺¹ tot expressie brengen, beschreven in Hoofdstuk 3 en Hoofdstuk 4, kunnen in toekomstige studies bijdragen aan een beter begrip van de rol van het UPS in neurodegeneratieve ziekten.

List of Publications

van Leeuwen FW, **van Tijn P**, Sonnemans MA, Hobo B, Mann DM, van Broeckhoven C, Kumar-Singh S, Cras P, Leuba G, Savioz A, Maat-Schieman ML, Yamaguchi H, Kros JM, Kamphorst W, Hol EM, de Vos RA, Fischer DF (2006). "Frameshift proteins in autosomal dominant forms of Alzheimer disease and other tauopathies." Neurology 66(2 Suppl 1): S86-S92.

van Tijn P, de Vrij FM, Schuurman KG, Dantuma NP, Fischer DF, van Leeuwen FW, Hol EM (2007). "Dose-dependent inhibition of proteasome activity by a mutant ubiquitin associated with neurodegenerative disease." J Cell Sci 120(Pt 9): 1615-1623.

van Tijn P, Hol EM, van Leeuwen FW, Fischer DF (2008). "The neuronal ubiquitin-proteasome system: murine models and their neurological phenotype." Prog Neurobiol 85 (2): 176-193.

Fischer DF, van Dijk R, **van Tijn P**, Hobo B, Verhage MC, van der Schors RC, Li KW, van Minnen J, Hol EM, van Leeuwen FW (2008). "Long-term proteasome dysfunction in the mouse brain by expression of aberrant ubiquitin." Neurobiol Aging: in press.

van Tijn P, Verhage MC, Hobo B, van Leeuwen FW, Fischer DF. "Low levels of mutant ubiquitin are degraded by the proteasome in vivo." Submitted.

van Tijn P, Hobo B, van Leeuwen FW, Fischer DF. "Mutant ubiquitin decreases amyloid - β deposition in a transgenic mouse model of Alzheimer's disease." Submitted.

Middeldorp J, Kamphuis W, Sluijs JA, Achoui D, Leenaars C, Feenstra MG, **van Tijn P**, Fischer DF, Berkers C, Ovaa H, Quinlan RA, Hol EM. "Intermediate filament transcription in astrocytes is reduced by proteasome inhibition." Submitted.

Boonen RA, **van Tijn P**, Zivkovic D. "Wnt signaling in Alzheimer's disease; presenilins lead the way." Submitted.

van Tijn P, Hobo B, Verhage MC, Oitzl MS, van Leeuwen FW, Fischer DF. "Alzheimer-associated mutant ubiquitin impairs spatial reference memory." In preparation.

de Pril R, Hobo B, **van Tijn P**, van Leeuwen FW, Fischer DF. "Low level proteasome inhibition by aberrant ubiquitin exacerbates aggregate formation in polyglutamine disorders." In preparation.

Dankwoord

Graag wil ik hier iedereen bedanken die heeft bijgedragen aan de totstandkoming van dit proefschrift.

Dick, bedankt voor al je adviezen tijdens mijn promotietijd, die mij vanuit de “wetenschappelijke puberteit”, zoals jij het zo mooi verwoordde, hebben laten groeien tot een volwassen onderzoekster. Fred, als ontdekker van het UBB⁺¹ eiwit stond jij aan de basis van mijn promotie project. Bedankt voor het mogelijkmaken van dit onderzoek en al je bijdragen aan dit boekje. David, ik heb erg fijn met je samengewerkt en veel van je geleerd de afgelopen zes jaar. Alle praktische adviezen, je waardevolle commentaar op mijn manuscripten en je niet aflatende interesse hebben dit proefschrift gemaakt tot wat het is. Ik hoop zeker dat ik jouw bevlogenheid kan vasthouden in de toekomst! Natuurlijk ook “mijn” studenten Arij, Laura en Gineke en de vele anderen die op uiteenlopende wijze hebben bijgedragen aan de wetenschappelijke inhoud van dit boekje, bedankt.

Voor mijn leuke tijd op het NIH wil ik bij deze alle collega’s ontzettend hartelijk bedanken. Variërend van vele borrels en chocolade-sessies tot jullie pogingen mij de kunst van het achteruit inparkeren bij te brengen... Met name alle (oud-) +1-ers en mollen, het was een fijne tijd. Roomies Elske, YingHui en Martijn, samen begonnen, (bijna) samen klaar; van gezelligheid tot serieuze wetenschappelijke zaken, ik kon altijd mijn ei bij jullie kwijt. Elly, jouw wijze raad en daad gedurende de afgelopen jaren heeft een echte wetenschapster in mij losgemaakt, bedankt voor alles. Barbara, zonder jouw hulp was ik op pagina één blijven steken!

Lieve familie en vrienden, bedankt voor jullie interesse in mijn onderzoek, het aanhoren van mijn verhalen over de wondere wereld van de hersenen, voor jullie niet aflatende aanmoedigingen en alle ontspannende tijden naast het werk. Zonder jullie was dit resultaat er niet geweest.

Paula

Curriculum Vitae

Paula van Tijn werd geboren op 18 november 1979 te Amsterdam. In 1997 behaalde zij haar gymnasium diploma aan het St. Ignatius Gymnasium in Amsterdam. Na het behalen van haar beta-gamma propaedeuse aan de Universiteit van Amsterdam, met als hoofdvak Medische Biologie, vervolgde zij haar studie in deze richting aan dezelfde universiteit.

In 2000 volgde zij een stage bij het Nederlands Instituut voor Neurowetenschappen onder begeleiding van dr. F.W. van Leeuwen, waarin de aanwezigheid van mutant GFAP werd onderzocht in humaan glioom weefsel. In een tweede afstudeerstage werd de rol van mutant ubiquitine onderzocht in gekweekte cellen onder begeleiding van dr. E.M. Hol en dr. F.M. de Vrij, eveneens aan het Nederlands Instituut voor Neurowetenschappen. Daarna schreef zij een scriptie over transgene muismodellen voor de ziekte van Alzheimer, begeleid door dr. P.J. Lucassen van de Universiteit van Amsterdam.

Na het behalen van het doctoraal diploma Medische Biologie in september 2002, kwam zij in dienst bij het Nederlands Instituut voor Neurowetenschappen als onderzoeker in opleiding. De resultaten van dit onderzoek naar de effecten van mutant ubiquitine op proteasoom functie in relatie tot neurodegeneratieve ziekten, onder begeleiding van prof. dr. D.F. Swaab, dr. F.W. van Leeuwen en dr. D.F. Fischer, zijn beschreven in dit proefschrift.

Van juni 2007 tot april 2008 is zij werkzaam geweest als associate scientist bij BioFocus DPI in Leiden. Vanaf april 2008 is de auteur van dit proefschrift werkzaam als postdoctoraal onderzoeker in de groep van dr. D. Zivkovic op het Hubrecht Instituut te Utrecht.